THE UNIVERSITY *of* EDINBURGH

Modulation of tissue glucocorticoid exposure by cleavage of Corticosteroid Binding Globulin in humans

Luke David Boyle

Presented for the degree of Doctor of Philosophy

The University of Edinburgh

2023

Declaration

I hereby declare that this thesis was written by me, and that the data published in this thesis are the result of my own work.

The work in this thesis has not previously been submitted for any other degree or qualification.

Luke D Boyle

Edinburgh, July 2023

Acknowledgements

Firstly I'd like to thank the three wise men, my supervisors Brian Walker, Roland Stimson and Mark Nixon – for the fantastic opportunities and their constant support throughout the PhD. I've learnt a lot from them.

I want to thank our collaborators, who were very generous with their time, and consumables! Geoff Hammond, Lesley Hill and Caroline Underhill in Vancouver, John Lewis in New Zealand and Peter Henriksen at the Edinburgh Heart Centre.

I want to thank all those who helped me deliver my clinical study: Archie Campbell and all the team at Generation Scotland; our sponsor Jo-Anne Robertson in ACCORD; Kareen Darnley, Anna Gill, Sam Simpson, Katie Doverman and the rest of the amazing staff at the WTCRF. Thanks also to Catriona Kyle for showing me the ropes, and last but not least the study participants themselves, who travelled from all over Scotland and made this PhD possible.

A huge thank you to Marisa Magennis, Natalie Homer, Ruth Andrew, Scott Denham and their colleagues at the Mass Spectrometry Core Facility in the Centre for Cardiovascular Science. Thanks also to Lynne Ramage for the pearls of wisdom when I ran into difficulties in the lab.

I'm very grateful to my parents, my sisters Laura and Sophie and brother Christian for their support over the years. And finally, I want to thank my fiancée Amy who has been a constant source of support and encouragement during the write-up, particularly during the pandemic.

Funding acknowledgements

The work presented in this thesis was supported by a grant from the Wellcome Trust.

Contents

Abstract

Corticosteroid Binding Globulin (CBG) binds over 85% of plasma cortisol and modulates free cortisol levels. Observations *in vitro* show that CBG undergoes proteolytic cleavage by neutrophil elastase (NE) at its reactive centre loop (RCL), a mechanism proposed to reduce CBG binding capacity by approximately ten-fold and increase the availability of free cortisol to tissues at sites of inflammation. However, detection of cleaved CBG *in vivo* in human plasma is controversial, and any influence of NE on CBG cleavage has not been tested *in vivo*. The CORtisol NETwork (CORNET) consortium found that genetic variation at a locus spanning *SERPINA1* (encoding alpha-1 antitrypsin, AAT, the endogenous inhibitor of NE) and *SERPINA6* (CBG) contributes to morning total plasma cortisol variation.

We tested the hypotheses that: (i) CBG cleavage occurs in tissues *in vivo*, controlling tissue cortisol delivery; (ii) AAT deficiency increases CBG cleavage and hence free plasma cortisol; (iii) greater cleavage of CBG results in increased tissue cortisol delivery in adipose and in hypothalamic-pituitary-adrenal (HPA) axis negative feedback; and (iv) NE inhibition inhibits NE-mediated CBG cleavage and thus plasma free cortisol *in vivo*.

To test tissue-specific CBG cleavage we recruited 48 men and collected arterialised blood and samples from veins draining abdominal subcutaneous adipose, forearm skeletal muscle, brain and liver. Arterio-venous differences in CBG were calculated, adjusting for blood flow. Net CBG production from the liver was detected in people with obesity and type 2 diabetes, but no *in vivo* cleavage of CBG was observed across the tissues studied.

In recall-by-genotype studies of people who are heterozygous for inactivating mutations in *SERPINA1*, 16 healthy carriers of either of the two most common AAT-deficiency single nucleotide polymorphisms (rs17580 & rs28929474) and 16 age-, sex- and BMI-matched controls were recruited from the Generation Scotland Biobank. Participants underwent placebo-controlled combined receptor antagonist stimulation of the HPA axis ('CRASH') testing using the glucocorticoid receptor antagonist RU486 plus mineralocorticoid receptor antagonist spironolactone, in a double-blind randomised crossover design. No measurable differences in CBG were observed. However, plasma free cortisol fraction was higher in those carrying AAT mutations. Adipose cortisol concentrations were not significantly different but transcripts of glucocorticoid-responsive genes were higher in adipose from AAT-deficient subjects. Plasma cortisol was elevated during CRASH testing in both groups, with the increment versus placebo tending to be lower in AAT-deficient subjects.

Using coronary artery bypass graft (CABG) surgery as a model of acute neutrophil-mediated inflammation, we measured CBG and cortisol in a randomised double-blind parallel group clinical trial of 35 patients administered placebo or elafin, an endogenous NE inhibitor, intravenously immediately before CABG surgery. Plasma CBG concentration and binding capacity fell by >30% following surgery, with corresponding increases in total and free cortisol, with a trend towards higher, rather than lower free cortisol in the elafin-treated group.

In conclusion, these data suggest that AAT deficiency brings about changes consistent with enhanced cleavage of CBG, including enhanced delivery of glucocorticoid to adipose tissue and reduced tonic HPA axis negative feedback. This is consistent with a role for intact CBG in

delivery of cortisol to the central HPA axis and a role for CBG cleavage in releasing cortisol to enhance tissue access in inflamed adipose tissue.

Lay abstract

One of the human body's natural steroid hormones, called cortisol, is produced by the adrenal glands. It plays a key role in our response to stress, fighting infection and inflammation, and controlling metabolism and mood. Having too much or too little cortisol is dangerous, causing the symptoms of Cushing's syndrome and Addison's disease, respectively. It is therefore important that cortisol levels are tightly controlled. Our research group has shown how this control happens not only in the adrenal glands but also within individual tissues - such as brain, liver, muscle and fat - for example when enzymes within the tissue inactivate or regenerate cortisol.

About 85% of cortisol is carried in the bloodstream bound to a protein called Corticosteroid Binding Globulin (CBG). When cortisol is bound to the CBG protein, it cannot enter cells. So it has been suggested that the CBG needs to be cleaved by an enzyme known as Neutrophil Elastase (NE) in order to release cortisol to the tissues. A second enzyme called Alpha-1 Antitrypsin (AAT) is also important in this theory, because AAT is the natural blocker of the NE enzyme. Since NE is present in larger amounts at sites of inflammation, this could amplify the anti-inflammatory effect of cortisol within inflamed tissues. Also, if AAT fails to inhibit NE this might allow exaggerated cleavage of CBG and more cortisol to be delivered to tissues. However, while this theory has been tested in test tubes it has yet to be tested in living humans.

To test this, we first measured CBG in blood samples from the veins draining different tissues of the body, including fat, muscle and liver. We then investigated whether healthy people known (from genetic testing) to have lower AAT levels have exaggerated cleavage of CBG by NE and altered free cortisol levels in their blood and fat tissue. Finally, we investigated whether giving a natural NE inhibitor as a drug has any effect on CBG cleavage or free cortisol levels in patients undergoing surgery.

We found only limited evidence of CBG cleavage in the tissues we studied, but we did find evidence that people with lower AAT levels have a higher free cortisol level in their blood and fat tissue. Giving a NE blocking drug to patients undergoing heart surgery tended to increase free cortisol levels. These results lend support to the theory that CBG cleavage influences cortisol action in particular tissues, and might provide new treatments in future that prevent CBG cleavage and reduce inappropriate cortisol action in fat tissue in people with obesity.

Presentations at conferences

- *Tissue-specific cleavage of Corticosteroid Binding Globulin* in vivo *in humans*

  Poster presentation at the 18th International Congress on Endocrinology, Cape Town, December 2018

- *Subclinical alpha-1 antitrypsin deficiency is associated with increased free cortisol fraction in plasma*

  Oral presentation at the British Endocrine Society Annual Conference, Brighton, November 2019

- *Subclinical Alpha-1 Antitrypsin Deficiency Is Associated with Increased Free Cortisol Fraction in Plasma and Altered Glucocorticoid Delivery to Tissues*

  Accepted for poster presentation at ENDO 2020 (The Endocrine Society Annual Meeting in March 2020 in San Francisco was cancelled due to the COVID-19 pandemic)

- *A single dose of Neutrophil Elastase inhibitor Elafin does not alter CBG cleavage during post-surgical stress in humans* in vivo

  Poster presentation at the European Congress of Endocrinology, Milan, May 2022

Awards

- Society for Endocrinology Best Adrenal and Cardiovascular Oral Communication Prize at the BES Conference, November 2019
- Shortlisted for Presidential Poster Competition at ENDO 2020 (meeting cancelled)

Original articles arising from this thesis

Hill LA, Vassiliada DA, Dimopoulou I, Anderson AJ, **Boyle LD**, Kilgour AHM, Stimson RH, Machado Y, Overall CM, Walker BR, Lewis JG, Hammond GL. Neutrophil elastase-cleaved corticosteroid-binding globulin is absent in human plasma. *J Endocrinol.* 2019 Jan 1;240(1):27-39. PMID: 30452386

Abbreviations

AAT	Alpha-1 antitrypsin
ACCORD	Academic and Clinical Central Office for Research and Development
ACPAs	Citrullinated antigens
ACTH	Adrenocorticotropic Hormone
ADIPOQ	Adiponectin
ALI	Acute lung injury
AMREC	ACCORD Medical Research Ethics Committee
ANOVA	Analysis of variance
ATGL	Adipose Triglyceride Lipase
AUC	Area under the ROC curve
AVP	Vasopressin
BCA	Binding Capacity Assay
BMI	Body mass index
Ca	California
CABG	Coronary artery bypass graft
$CaCl_2$	Calcium chloride
cAMP	Cyclic adenosine monophosphate
CAH	Congenital adrenal hyperplasia
CBG	Corticosteroid Binding Globulin
C/EBPβ	CAAT/enhancer binding protein beta
CH_3COONa	Anhydrous sodium acetate

CNS	Central nervous system
COPD	Chronic obstructive pulmonary disease
CORNET	CORtisol NETwork consortium
CPM	Counts per minute
CRASH	Combined Receptor Antagonist Stimulation test of the Hypothalamic-Pituitary-Adrenal axis
CRF	Clinical Research Facility
CRH	Corticotropin-releasing Hormone
CRHR1	CRH receptor 1
CRP	C-Reactive Protein
CSF	Cerebrospinal fluid
$C_6H_8O_7$	Citric acid
DCC	Dextran coated charcoal
DEPC	Diethylpyrocarbonate
DNA	Deoxyribonucleic acid
D4-cortisol	9,11,12,12-$[^2H]_4$–cortisol
D3-cortisone	9,12,12-$[^2H]_3$-cortisone
D3-cortisol	9,12,12-$[^2H]_3$-cortisol
D8-cortisone	2,2,4,6,6,9,12,12-$[^2H]_8$-cortisone
E	Cortisone
EDTA	Ethylenediaminetetraacetic acid
ELISA	Enzyme-linked immunosorbent assay
EMPIRE	Elafin Myocardial Protection from Ischaemia Reperfusion
Epi-F	Epi-cortisol

eQTL	Expression quantitative trait loci
ER	Endoplasmic reticulum
ERα	Oestrogen receptor alpha
ESI	Electrospray ionisation
F	Cortisol
FA	Formic acid
GC	Glucocorticoid
GH	Growth hormone
GR	Glucocorticoid Receptor
GS	Generation Scotland
GWAMA	Genome Wide Association Meta-Analysis
GWAS	Genome Wide Association Study
HepG2	Human hepatoblastoma cells
HFD	High fat diet
HNF-1β	Hepatic nuclear factor 1-beta
HNF-3α	Hepatic nuclear factor 3-alpha
HOMA-IR	Homeostatic model assessment for insulin resistance
HPA	Hypothalamic-Pituitary-Adrenal
HPLC	High performance liquid chromatography
HRP	Horseradish peroxidase
HSD3B1	3β-hydroxysteroid dehydrogenase
HSL	Hormone-sensitive lipase
HSP-90	90-kDa heat-shock protein
H_2O_2	Hydrogen peroxide

H_2SO_4	Sulphuric acid
H4IIEC3	Rat hepatoma cells
IGF-1	Insulin-like growth factor 1
IL-1β	Interleukin 1 beta
IL-6	Interleukin 6
IL-8	Interleukin 8
KCl	Potassium chloride
LC-MS/MS	Liquid chromatography with tandem mass spectrometry
LCR	Locus control region
LFTs	Liver function tests
LPL	Lipoprotein lipase
MA	Massachusetts
MC2R	Melanocortin type-2 receptor
MR	Mineralocorticoid Receptor
MRI	Magnetic resonance imaging
mRNA	Messenger ribonucleic acid
NaCl	Sodium chloride
NAD	Nicotinamide adenine dinucleotide
$NaHCO_3$	Sodium bicarbonate
NaOH	Sodium hydroxide
Na_2CO_3	Sodium carbonate
NE	Neutrophil elastase
NHS	National Health Service
PBS	Phosphate buffered saline

PCR	Polymerase chain reaction
PEPCK	Phosphoenolpyruvate carboxykinase
PER1	Period Circadian Regulator 1 gene
PIS	Patient Information Sheet
PiZZ	Proteinase inhibitor ZZ genotype
PKA	Protein kinase A
POMC	Pro-opiomelanocortin
PSI	Pound-force per square inch
PVN	Paraventricular nucleus
QMRI	Queen's Medical Research Institute
qPCR	Quantitative Polymerase Chain Reaction
Ra	Rate of appearance
RCL	Reactive centre loop
RI	Rhode Island
RIE	Royal Infirmary of Edinburgh
RT	Reverse transcription
RU486	Mifepristone
SAPALDIA	Swiss study on Air Pollution and Lung Disease in adults
SCN	Suprachiasmatic nucleus
SDR	Steroid displacement reagent
SEM	Standard error of the mean
SERPINA1	Serine protease inhibitor family A member 1
SERPINA6	Serine protease inhibitor family A member 6
SERPINs	Serine protease inhibitors

SLE	Supported liquid extraction
SLPI	Secretory leucocyte protease inhibitor
SNPs	Single nucleotide polymorphisms
StAR	Steroidogenic acute regulatory protein
TBE	Tris/Borate/EDTA buffer
TFTs	Thyroid function tests
TMB	3,3',5,5'-Tetramethylbenzidine
TNF-α	Tumour necrosis factor-alpha
TTR	Tracer:tracee ratio
T2DM	Type 2 diabetes mellitus
UBC	University of British Columbia
uHPLC	Ultra high performance liquid chromatography
UK	United Kingdom
UPL®	Universal Probe Library
USA	United States of America
U&E	Urea and electrolytes
V1bR	AVP 1B receptor
WA	Washington
WGH	Western General Hospital
WI	Wisconsin
WT	Wild-type
WTCRF	Wellcome Trust Clinical Research Facility
Xe	Xenon
9G12	Monoclonal antibody for measurement of RCL-intact CBG concentration

11β-HSD1	11β-hydroxysteroid dehydrogenase type 1
11β-HSD2	11β-hydroxysteroid dehydrogenase type 2
12G2	Monoclonal antibody for measurement of total CBG concentration

List of figures

List of tables

Chapter 1: Introduction

1.1 Glucocorticoid physiology

Glucocorticoids are catabolic steroid hormones secreted by the adrenal cortex in a circadian and stress-associated manner and are regulated by the hypothalamic-pituitary-adrenal (HPA) axis. Glucocorticoids exert their effects primarily by modulating gene expression through intracellular glucocorticoid (GR) as well as mineralocorticoid (MR) receptors, which are widely expressed throughout the body in order to modulate fuel metabolism (particularly in adipose tissue and muscle), cardiovascular homeostasis, mood, memory, and inflammation (Sapolsky et al., 2000; Walker, 2007). Several rapid non-genomic actions have also been reported (Kadmiel and Cidlowski, 2013).

Activation of the HPA axis in response to a stressful stimulus is an adaptive response. Chronic hypercortisolaemia in the absence of stressful stimuli (as in Cushing's syndrome) is maladaptive, and causes obesity, hyperglycaemia, hypertension, depression and memory loss. Additionally, in adrenal insufficiency, replacement with hydrocortisone (i.e. cortisol) or synthetic glucocorticoids (e.g. prednisolone and dexamethasone) has been standard clinical practice for over 60 years, but usually results in supraphysiological glucocorticoid (GC) levels and is associated with adverse cardiometabolic outcomes (Bergthorsdottir et al., 2006).

1.1.1 Structure of glucocorticoids

Glucocorticoids are a sub-family of steroid hormones derived from cholesterol; all steroid hormones have the same core structure which consists of seventeen carbon atoms arranged into four fused rings – three are cyclohexane rings and the other is cyclopentane. The addition of side chain moieties around this structure determines the specific hormone function, and

are labelled α or β according to their positioning above or below the plane. Each ring is labelled A to D; sequential numbering of the carbon atoms around each ring enables identification and standardised naming of each compound. Cortisol is defined structurally by its hydroxyl groups at positions 11 (distinguishing it from cortisone), 21 and at position 17 (distinguishing it from corticosterone), on a pregnane 21-Carbon backbone (Figure 1.1).

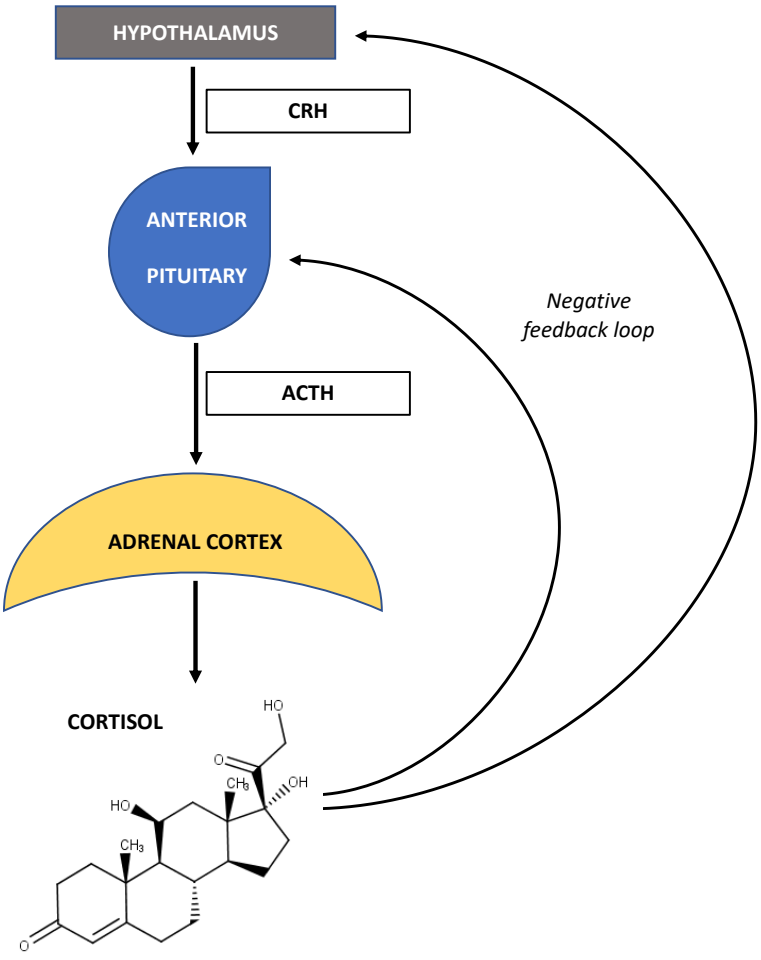

FIGURE 1.1 The Hypothalamic-Pituitary-Adrenal (HPA Axis)

In response to stress, cells in the paraventricular nucleus (PVN) of the hypothalamus produce and release corticotropin-releasing hormone (CRH). From there, CRH is transported to the anterior pituitary gland, where it acts on corticotropes to stimulate the production of proopiomelanocortin (POMC) and the release of adrenocorticotropic releasing hormone (ACTH) into the circulation. ACTH then acts on

cells within the zona fasciculata of the adrenal cortex to stimulate the production and secretion of glucocorticoids (cortisol). When circulating cortisol levels rise, they act on the hypothalamus and anterior pituitary via negative feedback loops to inhibit the release of CRH and ACTH.

1.1.2 The HPA axis

Glucocorticoids are synthesised via a multi-step enzymatic reaction in the *zona fasciculata*, the middle layer, of the adrenal cortex. This process is initiated and tightly controlled by the HPA axis, a negative feedback system enabling fine control of circulating glucocorticoids (Figure 1.1).

The hypothalamus receives afferent signals from neuroendocrine pathways, inflammatory mediators and from the limbic system (Ulrich-Lai and Herman, 2009) controlling the secretion of corticotropin-releasing hormone (CRH). Potentiating the effect of CRH is vasopressin (AVP), which is co-secreted by the parvocellular neurons of the hypothalamic paraventricular nucleus (Gillies et al., 1982; Rivier and Vale, 1983; Sawchenko et al., 1984; Vale et al., 1981). These neuropeptides are released from neuronal terminals at the level of the median eminence into the portal vessels (Antoni, 1986). Via the portal circulation, CRH and AVP reach the anterior pituitary, where they bind to their receptors CRH receptor 1 (CRHR1) and AVP 1B receptor (V1bR) (Antoni et al., 1984; Chalmers et al., 1995) and stimulate release of adrenocorticotrophic hormone (ACTH) from corticotroph cells in the pituitary gland into the general systemic circulation, via activation and processing of pituitary pro-opiomelanocortin (POMC) gene transcription (Vegiopoulos and Herzig, 2007). ACTH then stimulates the adrenal gland to produce and secrete glucocorticoid hormones (Dallman et al., 1987a; Dallman and Jones, 1973). In contrast to peptide hormones (which are presynthesised, stored within the

cytoplasm and released upon activation), glucocorticoids are highly lipophilic and cannot be stored in vesicles within the adrenals, so must be produced *de novo* when required; once synthesised they are released immediately into the blood by diffusion to access target tissues (Spiga et al., 2014).

1.1.2.1 Negative feedback of the HPA axis

Glucocorticoids regulate HPA axis activity, and thus their own production, through several feedback mechanisms (Figure 1.1). They act at the pituitary where they inhibit ACTH release via interference with POMC transcription (Jones et al., 1977) and at the PVN and other sites to inhibit synthesis and release of CRH and AVP (Dallman et al., 1987a; Dallman et al., 1987b; Jones et al., 1977).

1.1.3 Adrenal steroidogenesis

Glucocorticoid steroidogenesis is activated when ACTH binds to its specific cell surface G-protein-coupled receptor, the melanocortin type-2 receptor (MC2R) (Mountjoy et al., 1994). Upon ACTH binding, MC2R undergoes conformational changes that activate adenylyl cyclase, which increases intracellular levels of cyclic adenosine monophosphate (cAMP). Increased cAMP activates downstream signalling pathways, including the protein kinase A (PKA) pathway (Spiga et al., 2014). Activation of PKA induces a rapid synthesis of glucocorticoids within *zona fasciculata* cells via a number of enzymatic reactions (Figure 1.2).

The rate-limiting step in glucocorticoid synthesis is the delivery of cholesterol to mitochondria and transfer across the mitochondrial membrane, a process mediated by the activity of the steroidogenic acute regulatory protein (StAR) (Arakane et al., 1997; Lin et al., 1995; Stocco

and Clark, 1996). Inside the mitochondria, cholesterol is modified by a cascade of enzymes, which ultimately lead to glucocorticoid synthesis (Hum and Miller, 1993). In the initial step of steroid biosynthesis, a 6-carbon residue is removed from the side chain of cholesterol, converting it into pregnenolone. The hydroxyl group at carbon position 3 is subsequently oxidised by 3β-hydroxysteroid dehydrogenase, encoded by *HSD3B1*, forming progesterone.

Pregnenolone and progesterone can follow one of three pathways, depending on their location within the adrenal cortex and thus availability of specific enzymes resulting in the formation of (i) the mineralocorticoid aldosterone, primarily from the outer *zona glomerulosa*, (ii) cortisol from the middle *zona fasciculata* and (iii) androgens from the innermost *zona reticularis*. The production of cortisol necessitates the presence of the 17α-hydroxylase activity of the P450 enzyme, CYP17A1, for the generation of 17α-hydroxypregnenolone or 17α-hydroxyprogesterone from pregnenolone and progesterone respectively. From here further enzymatic reactions involving 21-hydroxylase and 11β-hydroxylase result in the end product cortisol. Failure of one of these pathways, typically through enzyme deficiency, can result in an accumulation of ‘upstream’ intermediate compounds resulting in divergence of the pathway in favour of another end product. For example, the androgen excess seen in congenital adrenal hyperplasia (CAH) is most commonly caused by deficiency of 21-hydroxylase, resulting in 17-hydroxyprogesterone accumulation (Han et al., 2014).

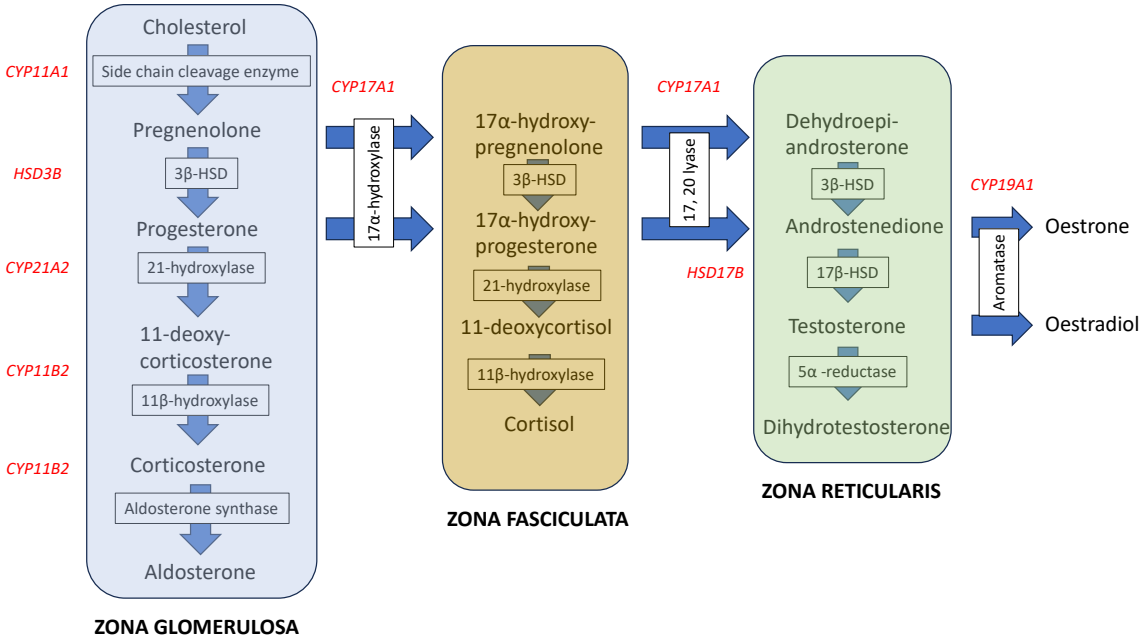

FIGURE 1.2 Adrenal steroidogenesis pathway

The enzyme-mediated biosynthetic pathways that convert cholesterol to glucocorticoids are shown. Steroid names are in black, regions of the adrenal cortex in bold, gene names in red italics and enzyme names are boxed. In the first step, the side chain of cholesterol is cleaved by the cholesterol side-chain cleavage enzyme (CYP11A1) in the zona glomerulosa (blue zone) to generate pregnenolone. For cortisol production from the zona fasciculata (gold zone), pregnenolone is first converted to 17α-hydroxypregnenolone through the actions of the 17α-hydroxylase (CYP17A1) enzyme. Further steroid conversions are by 3β-hydroxysteroid dehydrogenase (HSD3B1), 21-hydroxylase (CYP21A2) and 11β-hydroxylase (CYP11B1) to yield cortisol.

1.1.3.1 Pattern of glucocorticoid release

Cortisol secretion exhibits a natural circadian rhythm with humans having higher concentrations on wakening, falling to a sleep time nadir (Henley and Lightman, 2014). This process is controlled by the suprachiasmatic nucleus (SCN), which receives light signals via the retino-hypothalamic tract, activating a signalling cascade within SCN neurons.

Within the circadian rhythm many additional smaller fluctuations occur throughout the day in an ultradian rhythm, an intrinsic property of the system, and in addition there are responses to factors including environmental changes, eating and stress. These distinct pulses occur at approximately 1-hour intervals, and are made possible by the pulsatile nature of ACTH secretion (Spiga et al., 2011) in combination with the delay in cortisol release after an ACTH peak, giving rise to repetitive 'overshooting' and oscillation (Spiga et al., 2014).

1.1.4 Genomic and non-genomic actions of glucocorticoids

The effects of glucocorticoids are mediated primarily by binding to two specific receptors expressed in target tissues; the glucocorticoid receptor (GR) and mineralocorticoid receptor (MR) are members of the nuclear receptor subfamily 3, group C, the genes for which are located on chromosome 5 (Mangelsdorf et al., 1995). Both remain in the cytoplasm, stabilised by chaperone molecules (Nishi and Kawata, 2006; Wochnik et al., 2005) including the 90-kDa heat-shock protein (HSP-90) (Pratt et al., 2004), until activated. Upon glucocorticoid binding, the chaperone-receptor complex dissociates and the ligand-receptor complex moves to the nucleus and dimerises (Htun et al., 1996), then binds to DNA sequences (glucocorticoid response elements) or other DNA-bound transcription factors to allow trans-activation or trans-repression of target genes (Rhen and Cidlowski, 2005).

MR are much fewer in number than GR, and with higher affinity. MR are therefore saturated at lower concentrations of ligand, while GR occupancy is dynamic across a much wider range. The affinity of cortisol for MR is approximately 10-fold higher than its affinity for GR, thus variations in circulating glucocorticoid levels has a major impact on shifts in the balance

between GR and MR activity (Reul et al., 1990). The high-affinity MR (Kd = 0.5-2 nM) is activated at low glucocorticoid concentrations, so in 'basal' (non-stressed) physiological states when glucocorticoid concentrations are relatively lower (e.g. in the evening and overnight), MR is activated and located in the nucleus, with GR latent in the cytoplasm (Arriza et al., 1987). In contrast, the lower affinity GR (Kd = 10-25 nM) is only activated at high glucocorticoid concentrations – once glucocorticoid levels reach a threshold level (e.g. during a circadian peak or following acute stress) GR translocates into the nucleus and exerts its genomic effects (Conway-Campbell et al., 2007; Kitchener et al., 2004; Spencer et al., 1993). In addition, differences between MR and GR are also found in their distribution throughout the body. While GR is ubiquitously expressed in the periphery, the distribution of MR is more localised to aldosterone-sensitive tissues such as sodium transporting epithelia (found e.g. within the kidney) and specific organs including the heart (Funder, 2005). As in the periphery, GR and MR are not uniformly distributed in the brain. GR is expressed in almost all neurons and glial cells, particularly so in the hippocampus and in parvocellular neurons of the PVN. In contrast, MR is more localised to the hippocampus, pre-frontal cortex and amygdala (Arriza et al., 1988; Van Eekelen and De Kloet, 1992). Both GR and MR are highly expressed in brain areas which regulate the HPA axis, including limbic structures that control PVN activity.

In addition to their genomic effects, which rely on the actions of GR and/or MR within the nucleus, glucocorticoids can also modulate cellular activity much more rapidly (i.e. within seconds to minutes) through a mechanism mediated by G-protein couple membrane-associated receptors. Given the rapidity with which glucocorticoids inhibit the HPA axis, this effect is likely to be mediated by non-genomic mechanisms (Evanson et al., 2010; Groeneweg et al., 2011; Orchinik et al., 1991). In contrast, GR- and MR-mediated negative feedback can

occur over hours or even days (Keller-Wood and Dallman, 1984). *In vivo*, both processes occur simultaneously.

1.1.4.1 Combined Receptor Antagonist Stimulation of the HPA axis

In clinical practice, negative feedback is commonly tested using fixed doses of the selective GR agonist dexamethasone. The results of conventional dynamic testing can often be difficult to interpret, and dexamethasone cannot be used in isolation to assess the contribution of MR to HPA axis negative feedback. An alternative approach to testing negative feedback by endogenous cortisol using GR and MR antagonists in combination, which overcomes the limitations of GR agonists, is therefore desirable. In healthy humans, administration of the GR antagonist mifepristone, also known as RU486, increases plasma cortisol levels during the peak of diurnal variation in cortisol secretion (Bertagna et al., 1984; Kling et al., 1993), and similarly administration of the MR antagonist spironolactone increases plasma cortisol in the evening (Deuschle et al., 1998; Heuser et al., 2000; Young et al., 1998). In view of evidence from rodents indicating that GR and MR interact in mediating the negative feedback signal (Bradbury et al., 1994; Spencer et al., 1998), Mattsson et al devised a new clinical test known as the Combined Receptor Antagonist Stimulation Test of the HPA axis, or 'CRASH', to quantify the negative feedback signal attributable to endogenous cortisol (Mattsson et al., 2009). The CRASH test demonstrated that spironolactone and RU486 alone have modest effects, increasing cortisol by less than 50% in both lean and overweight/obese men. However, combined spironolactone plus RU486 elevated cortisol concentrations substantially, more so in lean than obese men, suggesting impaired negative feedback by endogenous cortisol in obesity (Mattsson et al., 2009). We use the CRASH test to dissect HPA axis negative feedback control in alpha-1 antitrypsin (AAT) deficiency during chapter 4 of this thesis.

1.1.5 Glucocorticoid clearance

Cortisol is irreversibly cleared from the circulation by enzymes including the A-ring reductases, 5α-reductase and 5β-reductase, primarily in the liver to form dihydrocortisol (Nixon et al., 2012). Cortisone is also metabolised by 5β-reductase to form 5β-dihydrocortisone. These metabolites are then reduced further by 3α-hydroxysteroid dehydrogenase and excreted mainly as tetrahydrocortisol (or tetrahydrocortisone), while a proportion are further reduced by 20α/β-hydroxysteroid dehydrogenase to form cortols or cortolones. Cortols are conjugated with either glucuronic acid or sulphate for renal excretion. It is estimated that 50% of secreted cortisol is excreted as α/β-tetrahydrocortisol, 25% as α/β-cortols, 10% as C19 steroids and 10% as cortolic acid. The remainder is excreted in urine as free unconjugated steroids (Tomlinson et al., 2004).

1.1.6 Glucocorticoid bioavailability

In order to exert any of these genomic and non-genomic effects, glucocorticoids must first be delivered to target tissues. In 1956, the first observations were made of a human plasma protein that was capable of binding glucocorticoids (Daughaday, 1956). Often referred to in the early literature as transcortin, this protein is now known as Corticosteroid Binding Globulin (CBG). CBG has a high affinity and specificity for glucocorticoids, but limited capacity. It binds over 85% of plasma cortisol, which may give CBG a key role in controlling cortisol responses by modulating the levels of unbound or 'free' cortisol. This is in contrast to the non-specific carrier protein albumin, which binds all classes of steroids in the circulation with lower affinity but much higher capacity than CBG (Dunn et al., 1981). Despite the low affinity of albumin for steroids, its high plasma concentrations mean it too has an important role in

controlling the 'free fraction' of cortisol in plasma. In accordance with the free hormone hypothesis, i.e. that steroids are only biologically active when unbound (Mendel, 1989), the inference from the plasma proteins CBG and albumin together binding approximately 90-95% of circulating cortisol is that only the remaining 5-10% is 'bioavailable' and free to enter cells (Lin et al., 2010). Both CBG and albumin effectively act both as a reservoir and buffer, protecting against large oscillations in cortisol levels caused by pulsatile circadian and ultradian adrenal secretion (Henley and Lightman, 2011). CBG is fully occupied easily, but where its affinity has been altered by a rare genetic variant, or the protein has been denatured by heat, cortisol binding by albumin may continue to influence excursions in free cortisol concentrations above the saturated threshold (Emptoz-Bonneton et al., 2000; Siiteri et al., 1982).

Within target tissues, glucocorticoid bioavailability is also determined locally by the actions of multiple enzymes capable of metabolizing glucocorticoids within cells. The two most well studied are the 11β-hydroxysteroid dehydrogenase (11β-HSD) enzymes, 11β-HSD1 and 11β-HSD2. 11β-HSD1 acts predominantly as a reductase *in vivo*, converting inactive cortisone to cortisol. This allows tissue-specific regeneration of glucocorticoids independently of HPA axis production, particularly in tissues such as liver, brain, skeletal muscle and adipose (Seckl and Walker, 2001).

Cortisol circulates at around 1000-fold higher concentrations than aldosterone, and also has a greater affinity for MR than aldosterone, its main ligand. 11β-HSD2 is typically expressed in tissues with high MR expression, thereby protecting against MR over-activation by cortisol in target tissues such as the kidney (Edwards et al., 1988; Funder et al., 1988). It acts as a catalyst

for the nicotinamide adenine dinucleotide (NAD^+)-dependent reduction of cortisol to cortisone, thus enabling aldosterone to bind MR in the presence of much higher glucocorticoid concentrations (Stewart et al., 1988).

Dysregulation of either of these enzymes affects cortisol metabolism and clearance, and may manifest clinically; inactivating mutations in 11β-HSD2 can produce the disorder of 'Apparent mineralocorticoid excess' – in this condition MR is activated by glucocorticoids in the absence of inactivation by 11β-HSD2, which leads to elevated local concentrations of cortisol in MR target tissues. This in turn gives rise to sequalae typically associated with aldosterone excess, including sodium and water retention, hypokalaemia and severe hypertension (Stewart et al., 1988; Stewart et al., 1987).

Conversely, dysregulation of 11β-HSD1 effectively causes 'Apparent cortisone reductase deficiency', resulting in relative excess of cortisone compared to cortisol and compensatory activation of the HPA axis. It presents clinically with hirsutism due to adrenal androgen excess (Jamieson et al., 1999; Phillipov et al., 1996).

1.1.6.1 Measurement of 11β-HSD1 activity

Isotopic tracers have enabled whole body 11β-HSD1 activity to be quantified (Anderson et al., 2020), as well as tissue-specific quantification of 11β-HSD1 activity in tissues including adipose (Stimson et al., 2009), brain (Kilgour et al., 2015), liver (Basu et al., 2009; Stimson et al., 2011), skeletal muscle and splanchnic tissues (Basu et al., 2004; Basu et al., 2005; Hughes et al., 2012).

Taking the tracer which features throughout this thesis as an example, by replacing four hydrogen atoms with deuteriums, the stable isotope of cortisol, 9,11,12,12-$[^2H]_4$–cortisol (D4-cortisol) is produced. D4-cortisol behaves chemically and physiologically like endogenous cortisol; only the difference in mass enables distinction and quantification. When the deuterium atom attached to carbon at position 11 is irreversibly removed by dehydrogenation, 9,12,12-$[^2H]_3$-cortisone (D3-cortisone) is generated. Further reduction by 11β-HSD1 then generates 9,12,12-$[^2H]_3$-cortisol (D3-cortisol) (Figure 1.3). The rate of appearance of D3-cortisol on the background of steady influx of D4-cortisol allows the specific reductase activity of 11β-HSD1 to be calculated.

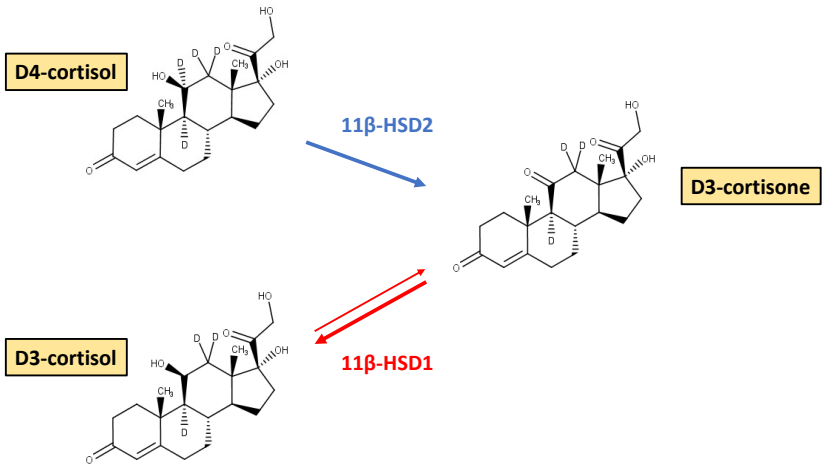

FIGURE 1.3 Stable isotope tracers for measuring cortisol-cortisone interconversion by 11β-HSDs

11β-HSD2 is a unidirectional enzyme catalyzing the dehydrogenase conversion of cortisol to cortisone. 11β-HSD1 is a potentially reversible enzyme catalyzing interconversion of cortisol and cortisone, predominantly in the reductase (cortisone to cortisol) direction. Production of cortisol can be measured by infusing the tracer, D4-cortisol. When D4-cortisol is metabolised by 11β-HSD2, the deuterium in position 11 is irreversibly removed, producing D3-cortisone; when this D3-cortisone is converted back

to cortisol by 11β-HSD1, D3-cortisol is produced. Dilution of D4-cortisol with D3-cortisol therefore indicates specific 11β-HSD1 reductase activity.

1.2 Corticosteroid binding globulin (CBG)

1.2.1 CBG function

The most obvious role of CBG is to transport glucocorticoids and regulate the plasma distribution and levels of free cortisol (Lin et al., 2010; Perogamvros et al., 2012). In normal human physiology, plasma CBG levels are approximately 400 nmol/L (Lewis et al., 2005) and plasma CBG binds 80-90% of circulating cortisol, leaving 10-15% bound to albumin and 5-10% free (Lin et al., 2010; Siiteri et al., 1982). Perturbations in the plasma distribution of cortisol, with an enhanced percentage free fraction, have been observed in patients with CBG variants (discussed in detail in chapter 1.3) that produce a lower affinity for cortisol (Emptoz-Bonneton et al., 2000; Hammond, 2016; Perogamvros et al., 2010). Moreover, in one of several studies of *Serpina6*$^{-/-}$ mice, free corticosterone (the dominant glucocorticoid in rodents) levels were found to be approximately ten-fold higher than in wild-type controls (Petersen et al., 2006), providing a further illustration of the key role that CBG plays in regulating the free fraction of glucocorticoid in the blood circulation; although this is debated by others who have observed normal free corticosterone concentrations at rest and reduced free corticosterone levels in response to stress in *Serpina6*$^{-/-}$ mice compared to wild-type controls (de Medeiros et al., 2016; Minni et al., 2012; Moisan, 2013; Moisan and Castanon, 2016; Richard et al., 2010). However, despite either normal or high GC levels in the free plasma pool, both patients and animals with low or no CBG exhibit features of GC deficiency. Taken together, these findings suggest that CBG has an important role to play in delivering GC to target tissues.

In addition to its primary role in plasma transport, it has been proposed that CBG mediates the targeted delivery of glucocorticoids to sites of inflammation (Hammond et al., 1990a; Hammond et al., 1991). *In vitro* evidence suggests that the targeted delivery of anti-inflammatory glucocorticoids is achieved through cleavage of the CBG reactive centre loop (RCL) by proteases present at sites of inflammation, for example elastase (Hammond et al., 1990a; Pemberton et al., 1988) released by activated neutrophils. Additionally, the steroid binding affinity of CBG decreases during pyrexia (Henley and Lightman, 2011; Mickelson et al., 1981) which might occur during acute inflammation, may therefore increase the free 'bioavailable' fraction of glucocorticoids in plasma. In this proposal CBG essentially acts as a reservoir for glucocorticoids which can be delivered to target tissues and released during inflammation (Henley and Lightman, 2011; Perogamvros et al., 2012). However, this is yet to be proven *in vivo* and forms the main focus of this thesis.

1.2.2 Structure of human CBG

The complex structure of human CBG provides us with further insights as to its key functions. Despite their different functions, serine protease inhibitors (SERPINs) share a common three-dimensional protein structure that consists of three β-sheets and seven or more α-helices. A hallmark of the SERPIN structure is the reactive centre loop (RCL), the essential region of the protein responsible for interactions with target proteases. Through molecular cloning of cDNAs from human liver and lung (Hammond et al., 1987), and the human gene encoding CBG (Underhill and Hammond, 1989), Hammond *et al* deduced the primary structure of the human CBG precursor polypeptide, and discovered that the gene is comprised of five exons over approximately 19 kb, with exons 2 to 5 contributing to the coding sequence. Human CBG

is produced as a 405 amino acid precursor, including a 22 amino acid signal polypeptide that is removed prior to secretion (Hammond et al., 1987). The mature polypeptide of 383 amino acids contains six potential *N*-glycosylation sites that are differentially utilized (Avvakumov et al., 1993), and two cysteine residues which do not disulfide bond; one of these is located within a hydrophobic pocket that contains the steroid binding site (Hammond et al., 1987).

1.2.3 The CBG Steroid Binding Site and Reactive Centre Loop (RCL)

Crystal structures of human CBG provided insights into its structurally and functionally important elements (Gardill et al., 2012; Zhou et al., 2008). These CBG crystal structures, in complex with steroid ligands, identified a single-high affinity steroid-binding site close to the surface of the protein, three β-sheets (sA-sC), ten intervening α-helices (hA-hJ), six *N*-glycosylation sites and a poorly structured RCL that acts as a protease bait domain. β-sheet B and α-helices A and H are particularly important, as they contain residues which hydrogen bond with steroids (Lin et al., 2010); Trp371 within β-strand s5B is essential for steroid binding, as it makes several points of contact with a ligand (Avvakumov and Hammond, 1994b). The binding affinity of a given steroid ligand is determined by its hydrogen bonding capability, which explains why CBG has a higher binding affinity for cortisol than progesterone; the presence of three hydroxyl groups on cortisol (C11, C17 & C21) facilitate a greater number of polar interactions between steroid and CBG residues than occurs when progesterone binds CBG, and only a single direct hydrogen bond is formed via the carbonyl oxygen at C20 (Gardill et al., 2012).

In the cortisol-bound state, the CBG RCL is fully expelled and exposed for targeting by proteases, displaying a ‘stressed’ (S) serpin conformation. Upon cleavage, the CBG RCL fully

inserts into the protein core and displays a 'relaxed' (R) conformation. In what is known as the 'stressed to relaxed' or S-to-R transition, the RCL fully inserts into β-sheet A as a novel strand (s4A), unwinding helix D and irreversibly disrupting the CBG steroid-binding site (Gardill et al., 2012; Zhou et al., 2008). This conformational change brings about an approximately tenfold decrease in CBG binding affinity for cortisol (Hammond et al., 1990a; Pemberton et al., 1988), associated with an increase in thermostability (Zhou et al., 2008).

1.2.4 RCL cleavage by different proteases

There is considerable variability in the RCL length and amino acid sequence of different SERPINs, which almost certainly exists to facilitate interactions with their target proteases. Within the CBG RCL, residues 333-349 are denoted P17-P1 based on their relative distance from the neutrophil elastase cleavage site (P1-P1') of SERPINA1 (AAT) (Lin et al., 2009). Two endogenous proteases specifically cleave the human CBG RCL: neutrophil elastase (NE) (Hammond et al., 1990a; Pemberton et al., 1988) and chymotrypsin (Lewis and Elder, 2014). NE cleaves the CBG RCL between P6 (Val344) and P5 (Thr345), mediating local delivery of cortisol at sites of inflammation (Hammond et al., 1990a; Hammond et al., 1991) (Figure 1.4). Chymotrypsin cleaves the CBG RCL at two sites, one after P4 (Leu346) and the other after P2 (Leu348), but the physiological significance of this remains unknown (Lewis and Elder, 2014).

Given this is a relatively recent discovery, in the context of CBG cleavage it is unknown whether chymotrypsin is worthy of greater or lesser consideration than NE. Whereas the role of NE in neutrophil-mediated inflammation has been described extensively, comparatively little is known about the clinical utility of serum levels of chymotrypsin, synthesised in the pancreas, even in the setting of chronic pancreatitis (Kavutharapu et al., 2012).

In addition to endogenous NE and chymotrypsin, a metalloprotease (LasB) produced by the opportunistic bacterial pathogen, *Pseudomonas aeruginosa*, specifically targets and cleaves the RCL of CBG (Simard et al., 2014). The significance of this is that like NE, LasB would most likely be present at sites of inflammation caused by *P. aeruginosa* infection, and its ability to cleave CBG is thought to promote the release of cortisol at these sites (Hammond, 2016).

Despite the wide variation between the RCLs of CBG (SERPINA6) and closely related SERPINA members, for example alpha-1 antitrypsin (AAT) (SERPINA1), a number of residues are highly conserved. Positions P15-P9 are collectively known as the 'hinge' region, aptly named as these residues provide the mobility for RCL insertion after cleavage. Exactly how amino acid substitutions in the human CBG RCL influence steroid binding before and after its cleavage by NE has been examined in detail (Lin et al., 2009); the steroid binding properties of CBG variants with substitutions at P15 (G335P), P14 (V336R), or P12 (T338P) in the RCL hinge were largely unaffected after elastase cleavage, as insertion of the cleaved RCL was blocked. By contrast, substitutions at P10 (G340P) or P8 (T342P) resulted in a partial loss of cortisol binding after proteolysis, because of an incomplete insertion of the cleaved RCL (Lin et al., 2009).

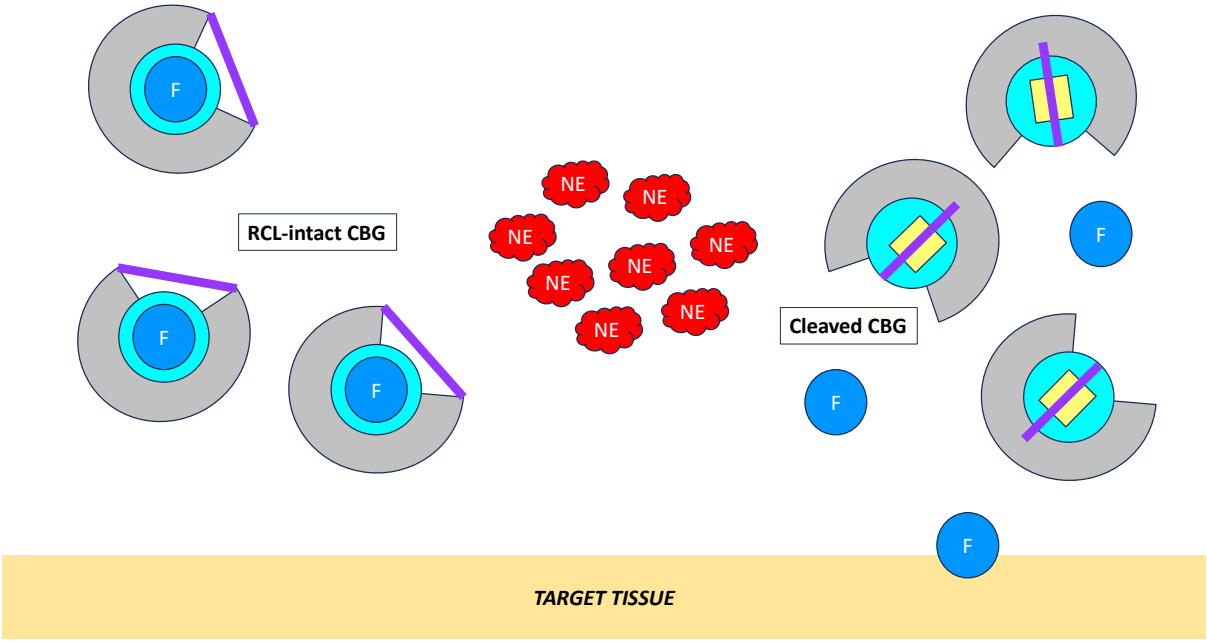

FIGURE 1.4 CBG cleavage by NE mediates delivery of cortisol to target tissues

The stressed form of CBG (grey) has a fully exposed RCL (purple) and binds cortisol (labelled 'F' and shown in blue) with high affinity at its steroid-binding site (shown in turquoise). Following cleavage by NE (illustrated in red), the cleaved RCL is fully inserted into the β-sheet (shown in yellow) at the core of the protein and CBG transitions to the relaxed conformational, low cortisol binding affinity state, thereby releasing cortisol to target tissues and at sites of inflammation.

1.2.5 Impact of RCL cleavage on CBG binding capacity, plasma free GC and tissue GC action

During acute inflammation, the plasma levels and binding capacity of CBG decrease rapidly, caused principally by both down-regulation of hepatic CBG production (Emptoz-Bonneton et al., 1997) and proteolytic cleavage of CBG (Hammond et al., 1990a). Proteolysis of the RCL of CBG by NE (Figure 1.4) appears to happen early during acute inflammation (Hill et al., 2016), releasing CBG-bound cortisol at sites of inflammation (Hammond, 1990; Perogamvros et al., 2012), but this has never been proven *in vivo*. The significance of CBG RCL cleavage by chymotrypsin (Lewis and Elder, 2014), a pancreatic digestive enzyme, has yet to be

elucidated, but NE (and in some cases LasB (Simard et al., 2014)) is present at sites of inflammation and infection, where it would be expected to cleave CBG (Hammond et al., 1990b). It is thought that the decrease in CBG binding capacity caused by RCL cleavage will in turn cause a rapid plasma redistribution of cortisol, with increases in the albumin-bound and unbound 'free' fractions both locally and systemically (Hammond, 2016). As a result, it has been predicted that the local bioavailable concentration of glucocorticoid may increase by three- to four-fold (Chan et al., 2013). The enhanced delivery of anti-inflammatory glucocorticoid to local tissues is thought to suppress cytokine production and activity, limiting cytokine-mediated tissue damage (Brattsand and Linden, 1996; Simon, 2003).

HPA axis negative feedback would be expected to control systemic free cortisol, unless CBG cleavage is a local mechanism occurring only within target tissues where NE is present. However, stress-induced activation of the HPA axis causes plasma cortisol concentrations to rise (Sapolsky et al., 2000), which further amplifies tissue cortisol exposure. Systemically, in response to an inflammatory stressor, any increases in ACTH-driven cortisol production can be expected to overwhelm a reduced CBG binding capacity, further increasing plasma free cortisol (Hammond, 2016). As discussed in chapter 1.2.8.2, the higher cortisol concentrations downregulate CBG production (Smith and Hammond, 1992), likely in tandem with circulating cytokines which repress CBG synthesis, for example interleukin 6 (IL-6) (Bartalena et al., 1993).

CBG binding capacity is also altered by changes in temperature and pH, which are subject to change during infection and inflammation (Cameron et al., 2010; Meyer et al., 2020). During recovery from an inflammatory insult, plasma CBG levels gradually recover, presumably

restoring a normal homeostatic balance of plasma cortisol levels and bioavailability (Hammond, 2016).

Significant decreases in plasma CBG levels have been described most commonly in patients with sepsis (Ho et al., 2010) and septic shock (Bendel et al., 2008; Ho et al., 2006; Meyer et al., 2018; Nenke et al., 2015; Pugeat et al., 1989; Savu et al., 1981), but have also been observed in patients suffering from a variety of other conditions which are also characterised by acute inflammation, including burns (Bernier et al., 1998; Garrel, 1996), multi-trauma (Beishuizen et al., 2001), necrotising pancreatitis (Muller et al., 2007), myocardial infarction (Zouaghi et al., 1985) and those undergoing cardiac surgery (Tinnikov et al., 1996).

Given the identification of LasB, produced by the bacteria *Pseudomonas aeruginosa*, as a protease capable of cleaving the CBG RCL (Simard et al., 2014), and the thought that NE activity may be significantly reduced in (the clinically not uncommon) neutropenic sepsis, attempts are now being made to differentiate between infectious pathogens which could influence CBG cleavage (Nenke et al., 2017a). To date, decreased plasma CBG levels have been found in patients with septic shock caused by bacteria (Pugeat et al., 1989; Savu et al., 1981), fungi (Zouaghi et al., 1983) and parasites (Zouaghi et al., 1984).

The association between plasma CBG levels and inflammation has also been assessed in animals, including pigs (Carroll et al., 2003) and rodents (D'Elia et al., 2005; Dhabhar et al., 1993; Garrel et al., 1993). A recent study of female rats has shown CBG to be an important biomarker of both inflammation onset and severity (Hill et al., 2016).

Studies in CBG deficient mice also support an important role for CBG during inflammation. The observation that C57BL/6 mice are much more sensitive to an acute inflammatory challenge with TNF-alpha than DBA/2J mice enabled mapping of this response to the murine *Serpina6* gene locus (Libert et al., 1999); plasma CBG levels in both male and female C57BL/6 mice had previously been reported to be about 50% lower than those in DBA/2J mice (Jones et al., 1998). These findings were subsequently substantiated in CBG knockout *(Serpina6)*$^{-/-}$ mice (Petersen et al., 2006). The CBG-null mice were much more sensitive to an acute inflammatory challenge than their wild-type counterparts, exhibited an aggravated response to septic shock, had no detectable CBG binding capacity in serum and an approximately tenfold increase in free glucocorticoid levels, consistent with the role of CBG in the regulation of circulating free glucocorticoid levels (Petersen et al., 2006). In further support of this, later studies in different colonies of Sprague-Dawley rats found that plasma CBG deficiencies are associated with a greater sensitivity to an acute inflammatory challenge (Bodnar et al., 2015).

1.2.6 Importance of CBG glycosylation

Like other plasma proteins in the circulation, human CBG is heavily glycosylated – of the six available consensus sites for *N*-glycosylation (Hammond et al., 1987), five per CBG molecule are used, with these *N*-linked oligosaccharides making up close to 30% of its molecular mass (Sumer-Bayraktar et al., 2011). *N*-glycosylation also influences the plasma half-life of CBG, which is estimated to be approximately 10-13 hours (Lewis et al., 2015).

Glycosylation of CBG is important in a number of respects. Firstly, it is essential to the creation of a functional steroid-binding site; recombinant CBG produced from *E. Coli* have approximately tenfold lower steroid-binding affinities than natural CBG, due to lack of *N*-

glycosylation (Chan et al., 2013; Lin et al., 2010). Glycosylation of the Asn238 residue of human CBG is required for high-affinity steroid binding (Avvakumov et al., 1993); lack of an *N*-glycan at this position is believed to negatively impact the correct folding and overall stability of the steroid-binding site (Avvakumov and Hammond, 1994a). Of the CBG glycosylation sites, Asn238 has the least branching, which possibly serves to make the binding site more accessible to steroid ligands (Sumer-Bayraktar et al., 2011).

Secondly, CBG glycosylation may also serve a protective role, restricting the access of proteases to cleavage sites within the RCL. Due to its position N-terminal to the NE cleavage site (Hammond et al., 1990a; Pemberton et al., 1988) and between the two chymotrypsin cleavage sites (Lewis and Elder, 2014), the extent of glycosylation at Asn347 and types of *N*-glycan attached to it may be particularly influential in this regard (Sumer-Bayraktar et al., 2016), although *N*-glycans at other sites also appear to protect CBG from NE or chymotrypsin (Simard et al., 2018).

Some evidence suggests that the composition of CBG carbohydrate chains may vary under different physiological conditions, for example pregnancy (Mitchell et al., 2004), or following treatment with different hormones, including thyroxine, insulin and oestradiol (Mihrshahi et al., 2006). However, whether higher plasma glucose concentrations seen in conditions such as diabetes mellitus have any significant impact on glycosylation of CBG remains unknown.

Importantly, glycosylation is also likely to have significant implications for accurate measurement of CBG; the differential occupancy of *N*-glycosylation sites and types of oligosaccharides attached to them may affect the immunological recognition of surface

epitopes on CBG. This is particularly relevant to monoclonal antibodies directed against non-glycosylated synthetic peptide antigens (discussed further in chapter 1.2.7 below), because *N*-glycosylation of CBG may alter its recognition in immunoassays.

1.2.7 Measurement of CBG in humans

Both the concentration and binding capacity of plasma CBG play important roles in determining the ratio of free and bound steroid, with alterations in either of these modifying the amount of free GC available to target tissues (Perogamvros et al., 2012). Differentiating between CBG concentration and CBG binding capacity is an important distinction because they are measured in different ways. Plasma CBG binding capacity was first determined using a radio-ligand saturation assay (Hammond and Lähteenmäki, 1983), which remains the 'gold standard' method for measurement of CBG binding capacity, adopted throughout this thesis.

More recently, ELISAs have been introduced that rely on the use of polyclonal antibodies as the immobilization reagent and monoclonal antibodies that recognize specific epitopes on the surface of CBG for its detection (Lewis and Elder, 2011; Lewis et al., 2003). One of these ELISAs employs a monoclonal antibody (12G2) that detects an epitope outside the RCL and so is unperturbed by structural changes caused by RCL proteolysis (Lewis et al., 2003), thus providing a measurement of total CBG concentration (Figure 1.5). Comparisons between plasma CBG values obtained using this ELISA and a cortisol-binding capacity assay have been used to identify CBG variants with abnormal steroid-binding activity (Hill et al., 2012; Simard et al., 2015). Another (second) ELISA has been developed based on the use of a detection monoclonal antibody (9G12) raised against a synthetic polypeptide that does span the RCL, and its epitope is lost when the RCL is cleaved by NE (Lewis and Elder, 2011), thus this ELISA

provides a measure of RCL-intact (uncleaved) CBG. When plasma CBG levels measured using these two different ELISAs have been compared in healthy individuals (Lewis and Elder, 2011, 2013; Nenke et al., 2016c) and patients (Nenke et al., 2016a; Nenke et al., 2016b; Nenke et al., 2017a), discrepancies in values have been interpreted as evidence for the presence of CBG with a NE-cleaved RCL and low affinity for cortisol in the circulation, but direct evidence for this is lacking.

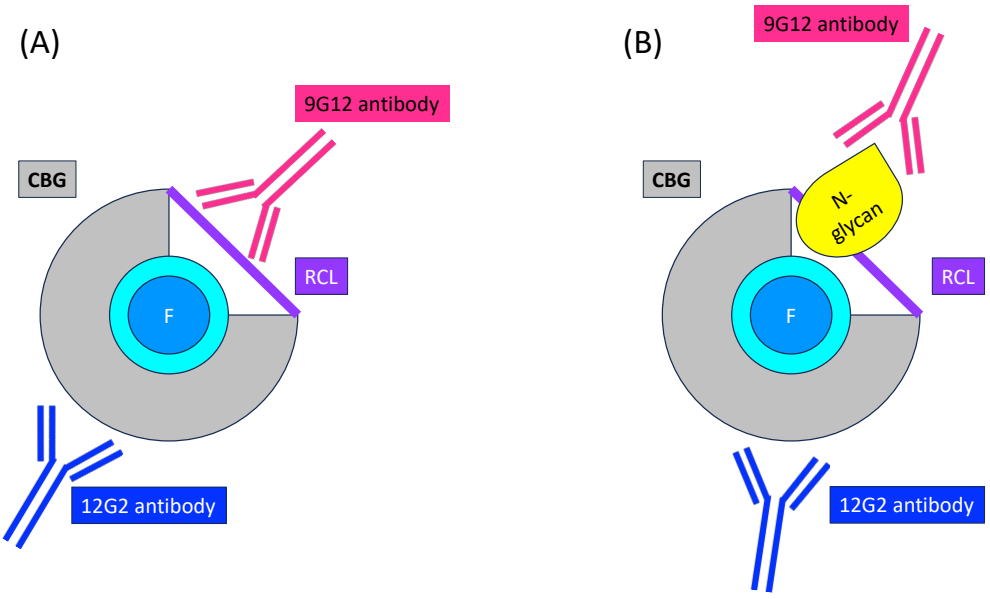

FIGURE 1.5 Monoclonal antibodies used in the measurement of CBG concentration

The CBG protein is shown in grey, with cortisol (blue) bound at the steroid-binding site (turquoise). The 12G2 antibody (shown in dark blue) recognises a surface epitope of CBG, is unperturbed by glycosylation of the RCL and can therefore be used to provide a measure of total CBG concentration in both (A) and (B). The 9G12 antibody (shown in pink) recognises an epitope that spans the NE cleavage site within the RCL of CBG and is proposed to provide a measurement of RCL-intact CBG concentration. In (A) the 9G12 antibody is able to access and detect its target epitope within the RCL, but in (B) it cannot bind this epitope because epitope availability is blocked because of N-glycosylation of CBG.

1.2.8 Transcriptional regulation of the *SERPINA6* gene encoding CBG

Of the 13 clade A family members, 11 including CBG (*SERPINA6*) are found in a syntenic cluster on chromosome 14q32.1. Further division of the human *SERPIN* gene locus reveals that a syntenic multi-gene locus of approximately 90 kb includes the gene encoding AAT (*SERPINA1*) (Namciu et al., 2004). A locus control region (LCR) upstream of *SERPINA1* is responsible for transcriptional activation of this sub-cluster of *SERPIN* genes (Zhao et al., 2007). The *SERPINA6* promoter contains TATA and CAAT-box motifs, as well as other sequence elements which appear to be responsible for its liver specific expression (Underhill and Hammond, 1989). These were originally established in rat studies, which identified five *cis*-acting sequence elements within the *Serpina6* proximal promoter that are also highly conserved in human *SERPINA6* (Underhill and Hammond, 1995). These protein binding sites (P1-P5) resembled recognition sequences for known transcription factors, including hepatic nuclear factor 1-beta (HNF-1β), CCAAT-binding protein CP-2, D-site-binding protein, hepatic nuclear factor 3-alpha (HNF-3α) and CAAT/enhancer binding protein beta (C/EBPβ), respectively.

1.2.8.1 Proximal promoter

Reporter gene plasmids under the control of rat *Serpina6* promoter fragments were introduced into rat hepatoma cells (H4IIEC3) and used to further characterize regulatory elements that participate in *Serpina6* expression (Underhill and Hammond, 1995). The fragment containing *cis*-elements P1-P5, from -300 to +1 (transcription start site), produced maximal transcription activity. A significant decline in transcription was observed when the promoter was extended to -800, suggesting that repressor sequences are located within this region. Further characterization of P1 and P2 demonstrated that although HNF-1β interacts

with P1, this site is not required for the basal activity of the rat *Serpina6* promoter. In contrast, deletion of the CCAAT-binding protein site, P2, abolished basal transcriptional activity, suggesting that this site is a key determinant of rat *Serpina6* expression (Zhao et al., 1997).

Similar work was undertaken subsequently by Li *et al* in humans, to determine whether single nucleotide polymorphisms (SNPs) within the proximal human *SERPINA6* promoter alter transcriptional activity. Of the six *SERPINA6* SNPs investigated, two increased promoter activity in human hepatoblastoma cells (HepG2); three others located close to HNF-1 binding sites differentially altered the transcriptional effect of HNF-1β and HNF-1α (Li et al., 2012).

1.2.8.2 Glucocorticoid regulation

It has been found consistently that glucocorticoids reduce plasma CBG levels, in both humans and rodents. Clinically, low plasma CBG levels are seen in individuals with cortisol excess (e.g. Cushing's syndrome) and in patients receiving either physiological replacement or supraphysiological treatment doses of exogenous glucocorticoids (Schlechte and Hamilton, 1987). In addition, treatment of rats and isolated rat livers with glucocorticoids was shown to inhibit hepatic CBG synthesis and secretion (Feldman et al., 1979). The mechanism for this phenomenon is still not fully understood. The synthetic glucocorticoid, dexamethasone, was shown to decrease plasma CBG levels in rats, even after hypophysectomy (Yamamoto and Ohsawa, 1976), which would suggest that the effect is mediated by alterations in gene expression. This was supported by a study which found that dexamethasone administration decreased hepatic *Serpina6* mRNA levels due to a reduction in gene transcription (Smith and Hammond, 1992). However, glucocorticoid response elements have not been identified within the proximal promoter regions of the genes encoding CBG in rats, mice or humans. It

has therefore been proposed that glucocorticoids mediate their effects on *SERPINA6* expression via GR acting together with other transcription factors, rather than through direct GR-mediated actions (Underhill and Hammond, 1995). This idea has been supported by a subsequent study which indicated that C/EBPβ mediates dexamethasone-induced repression of CBG via the co-recruitment of ligand activated GR, thus suggesting a tethering mechanism (Verhoog et al., 2014).

1.2.8.3 Oestrogen and growth hormone

Plasma CBG levels do not differ between human males and females under normal physiological conditions (Brien, 1981). However in pregnancy, and in women using oral contraceptives, two-fold increases are typically observed (Durber et al., 1976; Gagliardi et al., 2010; Perogamvros et al., 2012). The molecular mechanism for this is yet to be fully elucidated, however an oestrogen receptor alpha (ERα) dependent mechanism is likely since it has been shown that mitotane (an agent used in the treatment of Cushing's syndrome and adrenocortical carcinoma) increases plasma CBG levels via an ERα dependent mechanism (Nader et al., 2006; van Seters and Moolenaar, 1991).

In contrast to the stimulatory effect of oestrogen, human growth hormone (GH) replacement therapy is associated with significant reductions in plasma CBG (Tschöp et al., 2000). Additionally, treatment of human HepG2 cells with insulin-like growth factor 1 (IGF-1), produced by the liver in response to pulsatile secretion of GH, results in decreased CBG mRNA and protein secretion in a dose-dependent manner (Crave et al., 1995).

1.2.8.4 Cytokines

A number of pro-inflammatory cytokines regulate human CBG levels. Of these, IL-6 has been perhaps the most extensively studied; *in vitro* studies using HepG2 cells confirmed an inverse relationship between IL-6 and CBG (Emptoz-Bonneton et al., 1997). IL-6 is proposed to act at both the transcriptional and post-transcriptional levels, given both the presence of an IL-6 regulatory element within the *Serpina6* proximal promoter (Underhill and Hammond, 1995), and evidence of destabilising effects on *SERPINA6* mRNA stability (Bartalena et al., 1993). An inverse relationship between IL-6 and plasma CBG levels has also been observed *in vivo* in studies of burn patients (Bernier et al., 1998) and healthy volunteers (Tsigos et al., 1998).

Tumour necrosis factor-alpha (TNF-α) has been shown to decrease rat serum CBG levels (Fleshner et al., 1997) but this has not been replicated when studied in humans (Nenke et al., 2017b). In contrast, interleukin 1 beta (IL-1β) has been shown to stimulate CBG secretion from HepG2 cells, without affecting *SERPINA6* mRNA levels, suggesting that the effects of IL-1β are confined to acting on the post-translation processing and/or secretion mechanisms of CBG (Emptoz-Bonneton et al., 1997).

1.2.9 Hepatic and extra-hepatic CBG expression in humans

Evidence for the production of CBG by human hepatocytes came in the mid-eighties, when it was demonstrated that CBG could be synthesised from a cell-free translation of human liver mRNA (Sueda et al., 1985), and found that human CBG was secreted by HepG2 cells (Khan et al., 1984). Hepatocytes are responsible for the production of the plasma CBG pool (Hammond, 2016).

Extra-hepatic expression of *SERPINA6* has been detected at comparatively lower levels in the lung, kidney (Hammond et al., 1987) and heart (Caldwell and Jirikowski, 2013; Schäfer et al., 2015). In the heart *SERPINA6* mRNA has been found within cardiomyocytes, co-localising with MR. Since CBG is thought to buffer systemic glucocorticoids, and given that chronic hypercortisolism is associated with a detectable decrease in Troponin T (indicating myocardial injury) (Lazzarino et al., 2013) cardioprotection is thought to be among the functions of CBG expressed in heart (Schäfer et al., 2015). In women, *SERPINA6* expression has been detected within the endometrium, corpus luteum and placenta (Misao et al., 1999a; Misao et al., 1999b). Immunohistochemical studies have detected CBG within lymphocytes (Werthamer et al., 1973) and interestingly in regions of the central nervous system (CNS) including the hypothalamus (Sivukhina et al., 2006) and cerebrospinal fluid (CSF); specifically, CBG has been measured in CSF at concentrations approximately two thirds that of paired plasma CBG (Predine et al., 1984). Within the hypothalamus, CBG is co-localised with AVP, which acts synergistically with CRH to stimulate ACTH release from the anterior pituitary (Lightman, 2008). These findings may be significant as they suggest that CBG could play a role in HPA axis negative feedback (chapter 1.1.2.1).

Generally the functions of human CBG in the aforementioned tissues remain unknown, but since most would be considered target tissues for CBG ligands (glucocorticoids and progesterone), it is likely to play a vital role in regulating local availability of steroid hormones.

1.2.10 Roles of CBG in pregnancy, obesity and metabolic disease

1.2.10.1 Pregnancy

In humans, maternal plasma CBG levels rise between two- and threefold during the second and third trimesters of pregnancy, associated with concomitant increases in the concentrations and total and free cortisol (Jung et al., 2011). Plasma CBG levels are higher during pregnancy because of oestrogen-stimulated increases in hepatic CBG production (Ho et al., 2007) and an extension of the half-life of CBG (Strel'chyonok and Avvakumov, 1990). The pregnancy-induced glycosylation partly responsible for prolonging the half-life of CBG is also proposed to reduce CBG cleavage in pregnancy (Nenke et al., 2017c).

Approaching term, maternal plasma CBG levels then begin to decline, accompanied by higher free cortisol levels (Ho et al., 2007). Even greater increases in maternal progesterone levels occur as pregnancy progresses towards term, as a result of local progesterone production by placental trophoblasts. Such huge increases in progesterone are capable of displacing cortisol from the CBG binding site, to the extent that CBG becomes a major plasma progesterone transport protein during late gestation (Hammond, 2016), altering the local concentration and bioavailability of steroid ligands at the maternal-foetal interface (Benassayag et al., 2001) and increasing foetal free cortisol concentrations (Hodyl et al., 2020). The physiological significance of this is not yet understood; when studied there were no obvious differences in pregnancy outcomes or the health of neonates in CBG-deficient pregnant women as compared with women with normal plasma CBG levels (Lei et al., 2015).

Maternal plasma CBG, total and free cortisol concentrations are reduced in pre-eclampsia and gestational hypertension from week 36 onwards, and markedly reduced in gamete recipient pregnancies from as early as 20 weeks' gestation (Ho et al., 2007).

Postpartum, plasma CBG levels are relatively low in human neonates and remain so for the first month (Scott and Wells, 1995). Reductions in plasma CBG in foetuses and neonates during the peripartum period may play a key role in increasing free cortisol levels required for lung maturation (Hammond, 2016). Human adult CBG levels are attained by 12 months of age (Hadjian et al., 1975).

1.2.10.2 Obesity and metabolic disease

Glucocorticoids are important regulators of appetite, through complex interactions with orexigenic and anorexigenic neuropeptides and hormones. As their name suggests, they also play an important role in the regulation of glucose metabolism, mainly by maintaining glycogen reserves in the liver. They also play an intricate role in fatty acid metabolism and storage. Cortisol excess, found in Cushing's syndrome or glucocorticoid therapy, leads to central obesity associated with hyperphagia, insulin resistance, and development of fatty liver disease (Rose and Herzig, 2013).

In human obesity, both cortisol secretion and metabolism/clearance are increased, such that urinary free cortisol and cortisol metabolites may be raised while total plasma cortisol levels remain within the normal reference range (Andrew et al., 1998; Best and Walker, 1997; Incollingo Rodriguez et al., 2015). Plasma CBG concentration has been found to be a marker of insulin secretion, and has been both negatively and positively correlated with markers of

obesity (BMI and waist-to-hip ratio) depending on the degree of insulin resistance (Fernández-Real et al., 2000; Fernández-Real et al., 2001). Indeed, insulin treatment has been shown to downregulate CBG mRNA levels and protein secretion *in vitro* in a dose-dependent manner (Crave et al., 1995); this has been interpreted as providing an explanation for low CBG levels in obese hyperinsulinaemic individuals and high CBG levels in insulin-resistant diabetes patients (Moisan and Castanon, 2016). Plasma CBG levels are also negatively correlated with various biochemical markers of the metabolic syndrome (fasting glucose, insulin resistance and adiponectin) and inflammation (IL-6 and C-reactive protein (CRP)) (Fernandez-Real et al., 2002; Fernandez-Real et al., 2005; Manco et al., 2007). Interestingly, significant reductions in plasma CBG levels have been seen following extreme weight loss due to calorie restriction, which may be an adaptive response (Manco et al., 2007; Yanovski et al., 1997).

In rodent models of obesity, altered CBG levels have been reported. For example, obese Zucker rats exhibit plasma CBG levels around half those of lean controls (Grasa et al., 1998; Grasa et al., 2001). Availability of the CBG-deficient mice described above in section 1.2.5 (Petersen et al., 2006) then provided the opportunity to clarify the specific role of CBG in obesity. Compared with wild-type (WT) mice over 12 weeks, CBG knockout mice had increased body weight and food intake when fed either a standard or a high fat diet (HFD), and significantly higher visceral (retroperitoneal and epididymal) adipose accumulation (weight) but significantly lower subcutaneous adipose tissue weight on the HFD only. On the HFD epididymal adipocytes of CBG knockout mice grew larger than those of WT mice, but in contrast, adipocytes in the subcutaneous depot developed less in CBG knockout mice compared with WT mice. These data suggest that not only is adipose sensitive to changes in

CBG, but that CBG may have a major role in determining adipose tissue architecture. In addition, these CBG knockout mice had increased free corticosterone (the major glucocorticoid in rodents) alongside markedly reduced total corticosterone levels, in association with reduced subcutaneous adipose tissue expression of one of the enzymes responsible for inactivating glucocorticoids, 11β-hydroxysteroid dehydrogenase type 2 (11β-HSD2). In contrast to what was seen in the obese rats, hepatic CBG levels were increased in this obese model (Gulfo et al., 2016).

1.3 Genetic studies of CBG in humans

1.3.1 Naturally-occurring mutations

The first kindred of CBG mutation was identified as a result of low plasma CBG concentrations which failed to increment in response to oestrogen (Doe et al., 1965). Indeed before DNA sequencing was widely available, CBG variants were suspected based on low plasma CBG binding capacities (Robinson and Hammond, 1985; Roitman et al., 1984) – initially genetic variations in *SERPINA6* were thought to be very rare, but in more recent years a number of non-synonymous SNPs have been described, which can affect CBG production and/or function.

The first non-synonymous substitution identified in the human CBG coding sequence that was associated with abnormal cortisol binding, was CBG Leuven (L93H) (Smith et al., 1992; Van Baelen et al., 1982; Van Baelen et al., 1993). It and the subsequently identified CBG Lyon (D367N) (Emptoz-Bonneton et al., 2000), CBG G237V (Perogamvros et al., 2010) and CBG Athens (W371S) mutations (Hill et al., 2012) cause decreased or undetectable CBG binding

capacity. These rare *SERPINA6* mutations were identified following clinical inquiry into patients presenting with hypocortisolaemia in association with a broad spectrum of clinical sequelae of variable severity, ranging from chronic pain, depression and fatigue, to hypotension and excess body weight (Gagliardi et al., 2010). However, not all individuals with CBG variants manifest clinically, and an environmental impact on phenotype has been proposed (Cizza et al., 2011).

Two rare *SERPINA6* variants result in a reduction in plasma CBG levels (CBG Null/Adelaide (Torpy et al., 2001) and CBG Santiago (Torpy et al., 2012)). In these cases, single nucleotide deletions in codons for residues (Leu5 and Trp11) within the secretion signal polypeptide result in premature termination of CBG synthesis and a complete lack of CBG production. Additional mutations have been identified through population screening; CBG A51V and CBG E102G within a Han Chinese population resulting in reduced plasma CBG levels and reduced cortisol-binding capacity, respectively (Lin et al., 2012). Interestingly, the non-synonymous SNP (rs146744332) that results in the production of a secretion-deficient CBG A51V variant is relatively common (frequency of 1:37 in Han Chinese), and the decreased CBG cortisol-binding capacity found with the E102G variant was attributed to a folding defect (Lin et al., 2012). In contrast, a common CBG variant (A224S) and two other rare CBG variants (R64Q and R64W) do not affect CBG production or function (Lin et al., 2012; Torpy et al., 2004).

As many as 15 human *SERPINA6* polymorphisms which compromise the production or function of CBG have now been characterised (Simard et al., 2015) (Table 1.1). An awareness of these variants is important when measuring free cortisol in human samples (Hammond, 2016), especially as some of these mutations have been shown to have a higher prevalence

in certain ethnic groups (Lin et al., 2012), and/or within particular geographical areas (Cizza et al., 2011).

TABLE 1.1 Non-synonymous* SERPINA6 *polymorphisms associated with abnormalities of CBG production or steroid-binding activity

SNP ID	Amino acid	Effect on production or steroid binding	References
N/A	L(5)CfsX26	Translation stop – no production	(Torpy et al., 2012)
rs777245398	W(11)Stop	Translation stop – no production	(Torpy et al., 2001)
rs148218218	H14R	Produced, but decreased capacity	(Simard et al., 2015)
rs143058829	H14Q	Produced, but decreased affinity	(Simard et al., 2015)
rs370353870	I48N	Low production/secretion	(Simard et al., 2015)
rs146744332	A51V	Low production/secretion	(Lin et al., 2012)
rs187253929	H89Y	Produced, but decreased affinity	(Simard et al., 2015)
rs113418909	L93H	Produced, but decreased affinity	(Smith et al., 1992)
rs202107375	E102G	Produced, but decreased capacity	(Lin et al., 2012)
rs754814260	G237V	Produced, but no binding activity	(Perogamvros et al., 2010)
rs201880274	P246Q	Produced, but not secreted	(Simard et al., 2015)
rs267604111	R260L	Produced, but no binding activity	(Simard et al., 2015)
rs374191911	I279F	Produced, but decreased affinity	(Simard et al., 2015)
rs28929488	D367N	Produced, but decreased affinity	(Emptoz-Bonneton et al., 2000)
rs267607282	W371S	Produced, but no binding activity	(Hill et al., 2012)

1.3.2 Genome Wide Association Studies

Morning plasma total cortisol concentration has a heritability of between an estimated 30-60% (Bartels et al., 2003; Inglis et al., 1999; Mormede et al., 2011). Until recently, attempts at identification of genetic variants which contribute to this variation in morning cortisol values were essentially confined to small candidate gene studies (Mormede et al., 2011). This

prompted the formation of the CORtisol NETwork (CORNET) consortium, which undertook genome wide association meta-analysis (GWAMA) for plasma cortisol in 12,597 Caucasian participants, replicated in a further 2,795 participants (Bolton et al., 2014). Genetic polymorphism was found to account for less than 1% of the variance in cortisol, in a single region of chromosome 14 spanning both *SERPINA6* (CBG) and *SERPINA1* (AAT). Three SNPs reaching GWAS significance ($P<5x10^{-8}$) within this region were associated with variation in total cortisol binding capacity in plasma, some variants influenced total CBG concentrations, while the top hit (rs12589136) influenced the immunoreactivity of the RCL of CBG. Crucially, this large study revealed for the first time that the heritability of plasma cortisol levels is determined by the total concentration and binding capacity of CBG (Bolton et al., 2014).

These data were replicated in a subsequent candidate gene study, where SNPs within the *SERPINA6* gene were also found to be associated with morning plasma cortisol and plasma CBG concentrations in a cohort of 1,077 adolescents (Anderson et al., 2014). Six genome-wide significant SNPs derived from the CORNET GWAMA were then later used to generate a weighted polygenic risk score, which revealed that variation at *SERPINA6/A1* also associates with diurnal and stress-induced salivary cortisol in children (Utge et al., 2018).

However, it remained unclear from the CORNET GWAMA if this effect is mediated directly through *SERPINA6*, or indirectly through the product of *SERPINA1*, AAT, by modulating NE-mediated cleavage of CBG. The CORNET consortium addressed this question in a subsequent extension of its original GWAMA (Bolton et al., 2014), from 12,597 to 25,314 subjects and from around 2.2 million to approximately 7 million SNPs, in 17 population-based cohorts of European ancestries (Crawford et al., 2021). This confirmed that *SERPINA6/A1* is the only

locus where common genetic variation could be shown to affect plasma cortisol, and amongst the aims of the extended GWAMA was establishing whether *SERPINA6/A1* variation influences tissue-specific expression of CBG and AAT. Expression quantitative trait loci (eQTL) analyses undertaken in one cohort of 600 individuals showed that specific genetic variants within the *SERPINA6/A1* locus influence expression of *SERPINA6* rather than *SERPINA1* in the liver. In addition, trans-eQTL analysis demonstrated effects on adipose tissue gene expression, which suggests that variations in CBG levels have an effect on delivery of cortisol to peripheral tissues (Crawford et al., 2021). While these latest results from GWAMA, which came to light when the research for this thesis had been completed, suggest that the associations of the *SERPINA6/A1* locus with plasma cortisol are mediated through CBG expression rather than CBG cleavage, nevertheless the potential interactions between AAT and CBG represent a potentially exciting new mechanism for modulation of glucocorticoid action. Exploring this interaction *in vivo* forms the major focus of this thesis.

1.4 Alpha-1 antitrypsin deficiency

AAT is a 52 kDa glycoprotein, and strongly inhibits NE (Beatty et al., 1980). AAT is synthesised in the liver (also within intestinal and pulmonary alveolar cells, neutrophils, macrophages and the cornea) then secreted into the circulation, where its primary role is the regulation of the proteolytic effects of NE in the lungs (Strnad et al., 2020). AAT is present in plasma at concentrations typically between 150-300 mg/dL; its levels increase during acute phase reactions and it has a relatively long half-life of 4.5-6 days (Sanrattana et al., 2019).

1.4.1 Clinical syndrome

AAT deficiency predisposes to liver and lung disease, but patients with AAT deficiency may also be affected with asthma, granulomatosis with polyangiitis and panniculitis. Liver disease in AAT deficiency is the consequence of accumulation of misfolded AAT in the endoplasmic reticulum (ER) of hepatocytes, leading to ER stress (Strnad et al., 2020). Currently, there is no cure for severe liver disease aside from liver transplantation (Greene et al., 2016). By contrast, lung disease in AAT deficiency occurs as a consequence of low or undetectable circulating AAT; neutrophils are increased and NE activity is unopposed. NE can cleave many structural proteins of the lung as well as innate immune proteins. Tissue damage and susceptibility to infection occur, and airspace enlargement ensues. The clinical manifestations of lung disease associated with AAT deficiency are mainly indistinguishable from those of non-hereditary emphysema, although the pathology differs. This is partly why severe AAT deficiency remains undiagnosed in up to 90% of cases, with an interval of 5 to 7 years from the onset of symptoms to diagnosis (Strnad et al., 2020). Treatment for the pulmonary disease associated with AAT deficiency is essentially the same as treatment for chronic obstructive pulmonary disease (COPD); the only licensed disease-specific therapy for AAT deficiency is intravenous augmentation therapy with plasma-purified AAT (Greene et al., 2016).

1.4.2 Genetic basis of AAT deficiency

AAT is encoded by the *SERPINA1* gene, which is located at chromosomal region 14q32.13. *SERPINA1* is organised into seven exons; the first 3 (IA, IB and IC) are untranslated regions, with the remaining 4 exons (II-V) making up the coding region and terminal untranslated region (Marsden and Fournier, 2005). Of the over 120 *SERPINA1* variants reported so far (Seixas and Marques, 2021), the two most common alleles causing AAT deficiency, S and Z,

have a carrier rate in Western European populations estimated at approximately 1:1000 to 1:1500 respectively (Thun et al., 2012). The Z allele is characterized by a p.Glu342Lys (rs28929474) mutation, which causes AAT to misfold and polymerise within hepatocytes and pneumocytes, reducing secretion of AAT into the bloodstream by up to 85% (Ferrarotti et al., 2014). The S allele is defined by a p.Glu264Val (rs17580) mutation; the loss of a hydrogen bond linking the glutamic acid to a tyrosine residue located in the opposed 38 position affects the stability of the AAT molecule and susceptibility to polymerisation. This leads to retention in hepatocytes, although to a lesser extent than the Z allele, so secretion of AAT is reduced to 50-60% of the normal level (Elliott et al., 1996). Of the published GWAS which aimed to identify genetic determinants of serum AAT levels outside of the *SERPINA1* locus, SNPs found to be significantly associated with AAT concentrations were either not shown to be independent of these S & Z variants (Thun et al., 2013), or not generalisable to our reference population in Scotland since they have only been described in the Japanese population (Setoh et al., 2015).

1.4.3 Imbalance between AAT and NE in human and murine obesity

A possible role for CBG may inferred from studies which have evaluated the metabolic consequences of imbalance between NE and AAT. Mansuy-Aubert et al reported that obese mice have increased NE activity and decreased serum levels of AAT. Both NE knockout mice and transgenic mice overexpressing human AAT were resistant to HFD-induced weight gain, insulin resistance, inflammation and fatty liver. They validated these data in humans with a range of BMI, across two cohorts of differing ethnicity. In 62 healthy South Asian subjects, serum AAT levels negatively correlated with BMI, and were 27% lower in the obese compared with the non-obese group; notably AAT levels in subjects with a BMI >30 kg/m^2 were about

40% lower than in the lean subjects with BMI <23 kg/m^2. These findings were confirmed in a smaller American cohort, using sera from 17 US Caucasian males. In the obese men, serum AAT was lower than in their lean counterparts; NE activity was negatively correlated with AAT, and significantly higher in obese subjects than in lean (Mansuy-Aubert et al., 2013).

To date no studies have determined whether NE mediates these effects on obesity and metabolism through CBG cleavage and subsequent effects of glucocorticoid action.

1.5 Neutrophil elastase inhibition

The exciting findings outlined in section 1.4 suggest that preventing cleavage of CBG, either by increasing AAT activity or by reducing NE activity, could provide a new therapeutic approach to reducing cortisol delivery to tissues. This could be of therapeutic benefit, for example, in obesity. Also, use of NE inhibitors provides an experimental strategy to explore the physiological role of CBG cleavage.

Mansuy-Aubert et al tested whether pharmacological inhibition of NE could reverse obesity in mice; WT mice on a HFD for 19 weeks were given a specific NE inhibitor GW311616A, which covalently binds to NE. This treatment inhibited serum NE activity by 60% within 1 week, which was sustained during a 6-week treatment, and resulted in significant reductions in HFD-induced bodyweight gain (Mansuy-Aubert et al., 2013). Moreover, treatment of HFD fed mice with exogenous AAT improves insulin sensitivity, specifically in adipose tissue (D'Souza et al., 2021). These data provide a rationale for testing whether NE inhibitors can alter tissue delivery of cortisol by preventing CBG cleavage in obesity. Preincubation of CBG with AAT has

been shown to prevent CBG cleavage by elastase derived from activated neutrophils *in vitro* (Hammond et al., 1990a), but the effect of NE inhibition on CBG and glucocorticoids *in vivo* remains untested.

1.5.1 Endogenous inhibitors of NE

Epithelial tissues are protected from excessive proteolysis by NE by protease inhibitors, unlike other organs such as the CNS, arterial wall and myocardium which have less well developed mechanisms for mediating the actions of neutrophils and human NE (Henriksen, 2014). While the liver generates saturating concentrations of AAT in the general circulation, other protease inhibitors are produced locally at sites of inflammation by epithelial cells, neutrophils and macrophages especially in the lungs and skin. Two such examples are elafin and secretory leucocyte protease inhibitor (SLPI) (Williams et al., 2006), which have anti-inflammatory activity by modulation of intracellular signalling pathways (Moreau et al., 2008).

1.5.2 Exogenous NE inhibitors

A number of exogenous NE inhibitors have been developed as therapeutic agents. Perhaps the best known of these is Sivelestat sodium hydrate, a small molecular weight specific NE inhibitor produced as Elaspol by the Ono Pharmaceutical Company (Osaka, Japan). It is available in Japan as a treatment for acute lung injury (ALI) associated with sepsis and systemic inflammatory response. A meta-analysis of randomised trials conducted in Japan indicated a possible reduction in mortality (Iwata et al., 2010). Small clinical trials and retrospective analyses from Japan subsequently suggest marginal benefit from sivelestat treatment, in terms of inflammatory markers (including IL-6) (Tsujii et al., 2012), duration of intensive care admission (Makino et al., 2011) and survival (Miyoshi et al., 2013).

AZD9668 (Alvelestat) is a newer and fully reversible oral NE inhibitor which has been studied in COPD (Kuna et al., 2012; Vogelmeier et al., 2012), bronchiectasis (Stockley et al., 2013) and cystic fibrosis (Elborn et al., 2012) – like sivelestat it is well tolerated with no significant toxicity, but its clinical efficacy in these trials has been similarly rather limited. Hitherto the quality of clinical trials with NE inhibitors has been poor generally, for a variety of reasons (Henriksen, 2014). As a result these agents have not progressed to widespread clinical use for the treatment of respiratory disease, and large multi-centre clinical trials are needed. Recently there has been a renewed interest in exogenous NE inhibitors as potential therapeutic options for the management of ALI and acute respiratory distress syndrome or disseminated intravascular coagulation in the context of COVID-19 infection (Sahebnasagh et al., 2020) and they could yet be re-profiled, for obesity for example, if they are shown to be efficacious in inhibiting NE-mediated CBG cleavage.

1.6 Hypotheses

1. CBG cleavage occurs in human tissues *in vivo*.
2. CBG cleavage influences tissue cortisol delivery.
3. AAT deficiency allows greater CBG cleavage.
4. Greater cleavage of CBG influences tissue GC action both peripherally and in HPA axis negative feedback.

1.7 Aims

1. To discover whether CBG cleavage occurs *in vivo* in liver, brain, skeletal muscle and abdominal adipose in humans.
2. To evaluate whether CBG cleavage within, and cortisol delivery to, adipose tissue and skeletal muscle is increased in carriers of AAT deficiency *in vivo*.
3. To evaluate whether any differences in CBG cleavage and cortisol delivery alter HPA axis negative feedback in AAT deficiency.
4. To assess the impact of the endogenous NE inhibitor elafin on CBG cleavage during post-surgical stress in humans *in vivo.*

Chapter 2: Methods

2.1 Equipment

2.1.1 Laboratory-based

2.1.1.1 Balance

- Mettler HK 60 microbalance (Mettler Instrumente Ag, Zürich, Switzerland).

2.1.1.2 Centrifuge

- General laboratory use: Eppendorf centrifuge 5810R (Cambridge, UK).
- Clinical sample processing (Chapter 4): Sigma laboratory centrifuge 4K15 (Osterode am Harz, Germany).
- Real Time qPCR (Chapters 3 and 4): Eppendorf centrifuge 5415R (Cambridge, UK).

2.1.1.3 Incubator

- Grant-bio PHMP-4 Thermoshaker (Grant Instruments, Cambridge, UK).

2.1.1.4 Liquid chromatography systems

- Waters Acquity Classic ultra high performance liquid chromatography system (UPLC).
- Shimadzu Nexera LC-30AD ultra high performance liquid chromatograph (uHPLC) pump with Nexera SIL-30 AC autosampler (Shimadzu, Kyoto, Japan).

2.1.1.5 Mass spectrometer

QTrap 5500 mass spectrometer configured with electrospray ionisation (ESI) source (AB Sciex, Linear ion trap QTRAP® 6500+ triple quadrupole mass spectrometer configured with an ESI Turbo V source (Ab Sciex, Framingham, MA, USA).

2.1.1.6 Microplate shaker

- GFL Orbital Shaker 3005 (GFL, Burgwedel, Germany).

2.1.1.7 Microplate reader

- Optimax tuneable microplate reader (Molecular Devices, Sunnyvale, Ca).

2.1.1.8 Nitrogen dry-block

- Dri-Block® DB3A sample concentrator (Techne, Staffordshire, UK).
- Argonaut SPE Dry 96 Dual (Biotage, Uppsala, Sweden).

2.1.1.9 Real Time PCR System

- LightCycler® 480 (Roche Diagnostics Ltd, Burgess Hill, UK), operated with LightCycler® 480 software version 1.5.

2.1.1.10 Spectrophotometer

- Nanodrop Spectrophotometer (Thermo Scientific Inc., Waltham, MA, USA).

2.1.1.11 Thermal cycler

- TC-512 Gradient Thermal Cycler (Techne, Staffordshire, UK).

2.1.1.12 Vortex mixer

- Rotamixer (Hook and Tucker Instruments, Longfield, UK).

2.1.1.13 Water purification

- Milli-Q® Advantage A10 Water Purification System (Merck Millipore Corporation, Darmstadt, Germany).

2.1.1.14 96-well vacuum manifold

- IST VacMaster®-96 (Biotage, Uppsala, Sweden).

2.1.2 Clinical-based

2.1.2.1 Bioelectrical impedance

- OMRON BF302, OMRON Healthcare (UK) Ltd, Henfield, UK.

2.1.2.2 Blood pressure and pulse measurement

- OMRON 705IT BP monitor, OMRON Healthcare (UK) Ltd, Henfield, UK.

2.1.2.3 Electronic scales

- SECA 704, SECA Electronic Scales, Hamburg, Germany.

2.1.2.4 Warm air box

- Manufactured in-house, calibrated to 60°C.

2.1.2.5 Plethysmography

- AG101 Cuff Inflator source (Hokanson, WA, USA).
- E20 Rapid Cuff inflator (Hokanson, WA, USA).
- EC4 plethysmograph (Hokanson, WA, USA).
- Data displayed and analysed using Powerlab 4120 and LabChart® Reader (version 8) (AD Instruments, Oxford, UK).

2.1.2.6 Red light probe

- KL2500 LCD (Schott UK Ltd, Stafford, UK).

2.1.2.7 Microdialysis pump

- 107 Microdialysis Pump (M Dialysis AB, Stockholm, Sweden).

2.2 Materials

2.2.1 Solutions and solvents for clinical study

Saline (NaCl):

- Sodium chloride (0.9% weight/volume(w/v)) (Baxter, Newbury, UK), containing 77 mmol/500 mL (154 mM) sodium and 77 mmol/500 mL (154 mM) chloride

Perfusion Fluid T1 for Microdialysis:

- Sterile isotonic solution (M Dialysis AB, Stockholm, Sweden) containing NaCl 147 mmol/L, KCl 4mmol/L, $CaCl_2$ 2.3 mmol/L (total chloride contents 155.6 mmol/L, osmolality 290 mOsm/kg, pH ~6)

0.1% (v/v) Diethylpyrocarbonate (DEPC) water:

- DEPC (1mL) was added to distilled water (1L). This was mixed and allowed to stand (room temperature) for 24 hours before autoclaving. Storage was at room temperature.

2.2.2 Drugs for clinical study

2.2.2.1 Stable isotopically labelled tracer of cortisol

2.2.2.1.1 D4-cortisol

9,9,11,12-$[^2H]_4$-cortisol, 98% purity as determined by thin layer chromatography (Cambridge Isotope Laboratories, Andover, MA, USA). Supplied as 3 mg/3mL ethanolic solution for injection.

2.2.2.2 Other drugs

2.2.2.2.1 Lidocaine

2% Lidocaine hydrochloride 100 mg in 5 mL (Hameln Pharmaceuticals Ltd, Gloucester, UK).

2.2.2.2.2 Spironolactone

Spironolactone (Tayside Pharmaceuticals, Dundee, UK), 200 mg capsules.

2.2.2.2.3 RU468/Mifepristone

RU468/Mifepristone (Tayside Pharmaceuticals, Dundee, UK), 200 mg capsules.

2.2.2.2.4 Placebo

Placebo (Microcrystalline Cellulose) to match Spironolactone 200 mg and RU486 200 mg capsules (Tayside Pharmaceuticals, Dundee, UK).

2.3 Quantitation of total and RCL-intact CBG by ELISA

An estimate of CBG cleavage in human specimens can be made using specific antibody ELISAs (Lewis and Elder, 2011), which it is proposed are capable of detecting total and RCL-intact CBG – calculating the difference between these levels provides an estimate of 'cleaved' CBG. A human monoclonal antibody to the 12G2 epitope located outside the RCL is used to provide a measure of total CBG concentration, and a different human monoclonal antibody targeting the 9G12 epitope within the RCL is used to measure RCL-intact CBG concentration. Once the RCL is cleaved, it is thought that this 9G12 epitope on human CBG is no longer detectable. As discussed in sections 1.2.6 and 1.2.7, CBG is heavily glycosylated and evidence suggests that the attached *N*-glycans may serve a protective role, restricting the access of proteases to cleavage sites within the RCL (Sumer-Bayraktar et al., 2016). This raises concerns regarding the possible impact of *N*-glycosylation on the performance of the ELISA directed at the 9G12 epitope within the RCL, which will be explored in further detail in chapter 3. Of note, deglycosylation of CBG prior to performing the 9G12 ELISA is infeasible since glycosylation of CBG is essential to the structure and function of its steroid-binding site (Avvakumov and Hammond, 1994a).

High binding 96-well ELISA plates (Corning Inc, Maine, USA) were coated (200 µL/well) with rabbit polyclonal CBG antibody (1:300) (used as a capture antibody, donated by our collaborator John G Lewis) in a coating buffer and incubated overnight. This ELISA coating

buffer (made up fresh daily) was made by dissolving 5.3g of Na_2CO_3 in 900 mL of distilled water, then adding 4.2 g of $NaHCO_3$ and 1 g of sodium azide (Thermo Scientific, Waltham, Massachusetts, USA). The pH was adjusted to 9.6, and volume adjusted to 1L by adding additional distilled water. The capture antibody was pipetted out of the wells the next day, and stored in a fridge at 4^oC to be re-used for up to two weeks. Plates were washed three times (with the Labtech LT-3500 plate washer) using 300 µL/well of a wash buffer consisting of 0.05% Tween20 (Sigma Life Science, St Louis, Missouri, USA) in PBS (Oxoid Ltd, Basingstoke, Hampshire, UK) (pH 7.4), then the plate was blocked with 250 µL/well of a blocking buffer consisting of 3.5% protease-free bovine serum albumin (Sigma Life Science, St Louis, Missouri, USA) and 0.1% Tween20 in PBS (pH 7.4). The blocking buffer was then aspirated and samples and standards (150 µL/well) were then added incubated for an hour at room temperature. Plates were washed a further 3 times using the wash buffer as described above, and the primary detection antibody – monoclonal human CBG 12G2 (total) or human CBG 9G12 (RCL) antibody (1:20 in blocking buffer) added, 150 µL/well for 90min at room temperature. Plates were washed a further three times as above, and then the appropriate secondary antibody was added; for total CBG goat antimouse Ig-peroxidase was used, but for intact CBG the goat antimouse Ig-peroxidase was directed at the IgG2 alpha subunit only (1:2000 in blocking buffer), 150 µL/well for 30min at room temperature. Plates were again washed three times using the wash buffer as above, and 150 µL/well of substrate buffer added at room temperature. This substrate buffer was made up by adding 600 mL of distilled water, 8.2g CH_3COONa (anhydrous sodium acetate) and 3.6g $C_6H_8O_7$ (citric acid) (both from Fisher Scientific UK Ltd, Loughborough, Leicestershire, UK) to 400 mL methanol containing 270mg tetramethyl benzidine (TMB) (Alfa Aesar, Massachusetts, USA), and then finally pipetting in 500 µL of 30% H_2O_2 (hydrogen peroxide). Plates were kept covered with tin foil once the

substrate buffer was added, and monitored closely for colour development. Colour development was terminated by addition of 100 µL of stop solution, 1.25M H_2SO_4 (sulphuric acid) (Sigma Life Science, St Louis, Missouri, USA), and absorbance measured at 450 nm.

2.4 Quantification of CBG binding capacity by radioligand-saturation assay

Plasma cortisol-binding capacity of CBG was measured using an established radioligand-saturation assay (Hammond and Lähteenmäki, 1983), in which dextran-coated charcoal (DCC) is used to separate unbound from CBG-bound radioligand [^{3}H]-cortisol. Samples were diluted (1:1000-1:3000) in phosphate buffered saline (PBS) (Sigma Life Science, St Louis, Missouri, USA) and stripped of endogenous steroids by incubation with DCC for 30 minutes at room temperature, followed by centrifugation. To monitor non-specific binding, samples were then incubated with ∼10 nmol l^{-1} [^{3}H]-cortisol (PerkinElmer Life Sciences, Waltham, USA) in the absence or presence of excess cortisol to monitor non-specific binding. After separation of free [^{3}H]-cortisol by adsorption with DCC for 10 minutes and centrifugation at 0°C, CBG-bound [^{3}H]-cortisol in the supernatants was determined in a scintillation spectrophotometer.

2.5 Quantification of mRNA abundance in subcutaneous adipose tissue

2.5.1 Materials and reagents

RNA was extracted from adipose tissue using QIAGEN® RNeasy Mini Kit (QIAGEN®, Hilden, Germany). RLT, RPE and RW1 buffers were provided in the kit. Qiazol was obtained separately from QIAGEN® (Hilden, Germany).

Tris/Borate/EDTA buffer (TBE): Tris base (0.89M), boric acid (0.89M) and EDTA (0.5M, 40 mL) were dissolved in distilled water (800 mL). pH was adjusted to 8.0 with the addition of NaOH (1M), the volume was adjusted to 1L with distilled water. Storage was at room temperature.

2.5.2 Adipose tissue collection

A biopsy of subcutaneous adipose tissue was taken with informed written consent, as per the clinical study protocol (chapter 4.4.5.6). Samples were cleaned with DEPC water and frozen immediately on dry ice and stored at -80°C until analysis.

2.5.3 RNA extraction from subcutaneous adipose

Frozen adipose tissue (100mg) was placed in a RNase-free 2 mL Eppendorf with Qiazol Lysis Reagent (1 mL) (Qiagen) and a 2mm sterile metal bead. Samples were placed in the Qiagen TissueLyser II (90Hz, 90 seconds x2) until samples were homogenised. Samples were transferred to a fresh, RNase-free Eppendorf and chloroform (200 µL) added, vortexed briefly and subjected to centrifugation (at 12,000g for 15 minutes at 4°C). The supernatant (approximately 600 µL) was transferred to a 1.5 mL Eppendorf and an equal volume of ethanol (70%, v/v) was added and mixed. The solution was transferred to an RNeasy Mini Column (Qiagen) and the eluate discarded after centrifugation (12,000g for 30 seconds at room temperature). The column was washed with Buffer RW1 (700 µL) and Buffer RPE (500 µL) sequentially and eluate was discarded after centrifugation (12,000g for 30 seconds at room temperature). A further wash of the membrane with Buffer RPE (500 µL) was subject to centrifugation again (12,000g for 2 minutes at room temperature). The RNeasy spin column was placed in a fresh collection tube and subject to centrifugation until dry (12,000g for 1

minute at room temperature). The RNase spin column was placed in a fresh eppendorf (1.5 mL). RNase-free water (30 µL) was added to the spin column, incubated for 1 minute and eluted by centrifugation (12,000g for 1 minute at room temperature). The eluate was then added back to the RNeasy spin column, incubated for 1 minute and subject to centrifugation again (12,000g for 1 minute at room temperature). RNA was stored at -80°C.

2.5.4 RNA quantification

RNA was quantified using a Nanodrop Spectrophotometer (Thermo Fisher, West Sussex, UK). Concentration was determined by the absorbance at 260 nm wavelength and the purity assessed by the ratio of RNA/DNA (260/280), which was deemed acceptable if between 1.8 and 2.0.

2.5.5 RNA quality

RNA quality was assessed by electrophoresis on a denaturing agarose gel (1.2% w/v in 1 x TBE). Samples (2 µL) were prepared by adding loading dye (Promega, WI, USA; 1 in 5 dilution in RNase free water; 10 µL). Prepared samples were electrophoresed on the gel (100 V, 45 minutes) and RNA integrity was deemed satisfactory if clear 28S and 18S bands were present without smearing, and if the 28S rRNA band was approximately twice the intensity of the 18S rRNA band.

2.5.6 Reverse transcription polymerase chain reaction

RNA was reverse transcribed using the Quantitect Reverse Transcription kit (Qiagen, UK). 500ng of RNA was used and made up to 12 µL with RNase free water. RNA was added to genomic DNA (gDNA) wipeout buffer (2 µL) and incubated (at 42°C for 2 minutes) to eliminate

any contaminating gDNA. Quantiscript Reverse Transcriptase (1 µL), Quantiscript RT buffer (4 µL) and RT primer mix (1 µL) were added to each sample. A negative control was prepared as above except replacing reverse transcriptase with water (denoted "–RT control"). Samples were incubated (at 42°C for 15 minutes, then 95°C for 3 minutes) in PCR thermal cycler, before being cooled to 4°C. Resultant cDNA was stored at -20°C.

2.5.7 Real-time polymerase chain reaction (RT-PCR)

2.5.7.1 Materials and reagents

Primers were obtained from Invitrogen Life Technologies (Thermo Fisher Scientific Co, Waltham, MA, USA). Universal Probe Library (UPL®) Probes, Probe Mastermix and Lightcycler RNase free water were obtained from Roche Diagnostics Ltd (Burgess Hill, UK). Intron-spanning primer-probe sets were designed using online software (Universal Probe Library Assay Design Centre).

2.5.7.2 RT-PCR of adipose tissue

For each gene, a standard curve was made up from pooling all samples and prepared by serial dilution in RNase free water at concentrations of: 1:8; 1:16; 1:32; 1:64; 1:128; 1:256; 1:512. cDNA samples were diluted (1:10) with RNase free water. A Mastermix of UPL Fastmix (5 µL), RNase free water (2.7 µL), forward primer (0.1 µL), reverse primer (0.1 µL) and probe (0.1 µL) was prepared for each sample. One gene was analysed with SYBR green master mix (Table 2.3) where mastermix (5 µL), RNase free water (2 µL), forward primer (0.5 µL) and reverse primer (0.5 µL) were prepared for each sample. A –RT control was analysed with each gene.

Diluted cDNA (2 µL) was added to each well along with 8 µL of master mix. All samples and standards were assessed in triplicate.

Samples were run on a Lightcycler 480 (Roche) under the following conditions; denatured by heating (95°C, 5 minutes), then amplified for 50 cycles of consisting of denaturation (10 seconds, 95°C), annealing (30 seconds, 60°C) and elongation (1 second, 72°C) and cooling (30 seconds, 40°C).

All samples were analysed in triplicate and interpolated from the standard curve. Amplification curves were plotted for each sample (y = fluorescence, x = cycle number). Triplicates were deemed acceptable if the standard deviation of the crossing point was <0.5 cycles. The standard curve generated for each gene (y = crossing point, x = log concentration) was deemed acceptable if the reaction efficiency was between 1.7 and 2.1.

2.5.7.3 Data analysis

The abundance of each gene was expressed relative to the mean of two housekeeping genes (Cyclophillin A and 18S) (e.g. abundance of gene of interest in sample X/mean abundance of housekeeping genes in sample X) and expressed as arbitrary units. Tables 2.1 and 2.2 give details of the primers and UPL probes used.

TABLE 2.1 Housekeeping genes

Target	Gene Name	UPL Probe	Forward primer sequence	Reverse primer sequence
Peptidylprolyl isomerase A (cyclophilin A)	*PPIA*	48	ATGCTGGACCCAACACAAAT	TCTTTCACTTTGCCAAACACC
18S Ribosomal	*18S*	46	CTTCCACAGGAGGCCTACAC	CGCAAAATATGCTGGAACTTT

TABLE 2.2 Primer sequence for qPCR and corresponding probe number for genes of interest from Roche Universal Probe Library (UPL®)

Target	Gene Name	UPL Probe	Forward primer sequence	Reverse primer sequence
Adiponectin	*ADIPOQ*	85	GGTGAGAAGGGTGAGAAAGGA	TTCACCGATGTCTCCCTTAG
Adipose Triglyceride Lipase	*PNPLA2*	89	CTCCACCAACATCCACGAG	CCCTGCTTGCACATCTCTC
Lipoprotein Lipase	*LPL*	25	ATGTGGCCCGGTTTATCA	CTGTATCCCAAGAGATGGACATT
Period Circadian Clock 1	*PER1*	87	CTCTTCCACAGCTCCCTCA	CTTTGGATCGGCAGTGGT
Phosphoenolpyruvate carboxykinase	*PEPCK*	20	CGAAAGCTCCCCAAGTACAA	GCTCTCTACTCGTGCCACATC

TABLE 2.3 Primer sequence for qPCR using SYBR® Green master mix

Target	Gene Name	Forward primer sequence	Reverse primer sequence
Hormone Sensitive Lipase	*LIPE*	GGAAGTGCTATCGTCTCTGG	GGCAGTCAGTGGCATCTC

2.6 Routine laboratory tests

Routine laboratory blood tests for screening in the clinical studies were sent for processing by the NHS Lothian clinical biochemistry and haematology laboratories at the Western General Hospital and Royal Infirmary of Edinburgh (Edinburgh, UK). The laboratories participate in the UK National External Quality Assessment Service to ensure quality control. Sample collection is described in Chapters 4 and 5.

Full blood count was measured by a XE-5000 automated flow cytometer (Sysmex UK, Milton Keynes, UK). Thyroid function was measured using Architect i2000 immunoassay (Abbott Diagnostics Ltd, Maidenhead, UK). All other analytes including renal and liver function, fasting glucose and insulin were measured on an Architect c16000 analyser (Abbott Diagnostics Ltd, Maidenhead, UK) using manufacturer's kit materials according to laboratory protocols.

2.7 Quantification of serum alpha-1 antitrypsin by ELISA

Serum AAT was measured using an ELISA kit (Immunology Consultants Laboratory Inc, Portland, Oregon, USA). All reagents were stored at 4-8°C and allowed to come to room temperature before each assay. The 5X diluent concentrate and 20X wash solution concentrate were diluted 1:5 and 1:20 respectively with deionised water immediately before use. Samples were diluted 1:50,000 in 1X sample diluent and mixed thoroughly. Samples were prepared by serial dilution to 500, 250, 125, 62.5, 31.25, 15.63 and 7.81 ng/mL concentrations and used within 60 minutes of preparation. Samples and standards (100 µL) were added in duplicate to a 96-well plate, and incubated at room temperature for 60 minutes. Following

incubation, the contents of the wells were aspirated and washed 4 times with 1X wash solution. After the final wash, 100 µL of enzyme-antibody conjugate (diluted 1:100 in 1X sample diluent) was added to each well and incubated in the dark at room temperature for 30 minutes. Contents of the wells were again aspirated and washed 4 times with wash buffer. 100 µL of 3,3',5,5'-Tetramethylbenzidine (TMB) substrate solution was added to each well, and incubated in the dark at room temperature for precisely 10 minutes. 100 µL of stop solution was added to each well and the absorbance was read at 450 nm in a spectrophotometric microtiter plate reader. A standard curve was generated by plotting absorbance against AAT concentration for each standard by fitting to a 4-parameter logistics curve (GraphPad Prism, San Diego, California, USA).

2.8 Quantitation of endogenous and deuterium labelled tracer glucocorticoids in plasma and adipose using liquid chromatography mass spectrometry

Over the course of the PhD, newer and more reliable equipment for sample extraction, chromatography and mass spectrometry became available and these technological improvements were exploited throughout. Two discrete LC-MS/MS methods were developed, validated and applied to measure steroids and isotopically labelled tracer steroids in plasma and adipose and these and the different reagents, consumables, equipment and instrumentation are detailed as discrete and complete methods, in the sub-sections below.

2.8.1 Materials and reagents

2.8.1.1 Reagents

High performance liquid chromatography (HPLC) grade water, LC-MS grade methanol and ammonium hydroxide (35%) were from Fisher Scientific (Loughborough, UK). HPLC grade methanol, dichloromethane, 2-propanol and LC-MS grade water, formic acid and acetonitrile were obtained from VWR (Lutterworth, Leicestershire, UK).

2.8.1.2 Analytical Standards

Cortisol (F) was supplied by Sigma Aldrich (Dorset, UK) while epi-cortisol (epi-F) and cortisone (E) were supplied by Steraloids (Newport, RI, USA). (9,11,12,12)-$[^2H]_4$-cortisol, (D4-cortisol) and (9,12,12)-$[^2H]_3$-cortisol, (D3-cortisol) was supplied by QMX (Thaxted, Essex, UK). Solutions of each of these steroids were prepared by weighing and dissolving in methanol to a final concentration of 1 mg/mL, and storing at -20°C, prior to dilution.

2.8.2 Measurement of d4F, d3F, F, E and d3E in human plasma by LC-MS/MS

Due to a mass difference of only 1 a.m.u which leads to signal contributions of d3F to d4F it is necessary to prepare two calibration curves to account for this and quantify d3F and d4F; one for d4F, F and E measurement and a separate one for d3F. Epi-F is used as the internal standard for all steroids. D3F contributes to the d4F signal and so calibration curve for d3F must be prepared separately. Its contribution to d4F signal is calculated in the 0 std and the peak area subtracted from the final data when assessing d4F tracer kinetics.

2.8.2.1 Preparation of calibration standards of d4F, F and E

Stock solutions of d4F, F and E (1 mg/mL) were used to prepare a mixed stock at 5 µg/mL, which was further diluted in methanol to give 500 ng/mL, 50 ng/mL and 5 ng/mL stock

solutions. A calibration curve was prepared into individual glass tubes with the following points – 0.025 ng, 0.05 ng, 0.1 ng, 0.25 ng, 0.5 ng, 1 ng, 2.5 ng, 5 ng, 10 ng, 25 ng, 50 ng and 100 ng. The internal standard used for each steroid was Epi-F and a stock solution of 1 mg/mL was diluted to 100 ng/mL and 20 µL of this stock was added to each standard and sample, to give 10 ng total Epi-F. were added. Each standard was made up to 400 µL with water prior to extraction.

2.8.2.2 Preparation of calibration standard of d3F

A stock solution of d3F, was used to prepare a stock at 5 µg/mL, which was further diluted in methanol to give 500 ng/mL, 50 ng/mL and 5 ng/mL stock solutions. A calibration curve of d3F was prepared into individual glass tubes with the following points – 0.025 ng, 0.05 ng, 0.1 ng, 0.25 ng, 0.5 ng, 1 ng, 2.5 ng, 5 ng, 10 ng, 25 ng, 50 ng and 100 ng. The internal standard used was Epi-F where 20 µL of 100 ng/mL d3F was added to each standard and sample, to give 10 ng total Epi-F. Each standard was made up to 400 µL with water prior to extraction.

2.8.3 Extraction of d4F, d3F, d3E, E and F from plasma

Plasma samples were defrosted at room temperature. Samples (200 µL) enriched with Epi-F (10 ng) were extracted alongside calibration curves (prepared as detailed in 2.8.2.1 and 2.8.2.2) by supported liquid extraction (SLE). Samples and calibration standards were transferred to an SLE 400+ 96-well plate (Biotage, Uppsala, Sweden) using a glass Pasteur pipette. The plate was placed in a 96-well vacuum manifold and a vacuum was applied for 5 minutes. Samples were eluted with 0.8 mL of dichloromethane and isopropanol (98:2; v/v) twice into a 96-well collection plate (Waters, Hertfordshire, UK). Each sample was allowed to elute under gravity for 5 minutes followed by application of a vacuum for 2 minutes. Samples

and standards were dried down under nitrogen at 60°C using a 96 well nitrogen dry block (Biotage, Uppsala, Sweden) and stored at -20°C until analysis. Prior to LC-MS/MS analysis, samples were re-suspended in HPLC grade water and acetonitrile (70 µL; 70:30, v/v), sealed with a plate seal and mixed on a plate shaker.

2.8.4 Manual homogenisation and extraction of tracer glucocorticoids from adipose

Calibration standards were prepared in glass tubes as described in 2.8.2.1 (F, E, d4F) and 2.8.2.2 (d3F) and extracted with ethyl acetate (1 mL) and reduced to dryness. Frozen adipose tissue biopsies were cut using a scalpel to a weight of 250 mg and kept on dry ice. 1 mL of ethyl acetate was added to all samples, then samples homogenised for 5 minutes. Samples were enriched with internal standard (epi-cortisol), vortexed and placed on wet ice. Using a glass Pasteur pipette, each sample was slowly dripped onto 10 mL of chilled ethanol:acetic acid:water (95:3:2, v/v) in 20 mL glass tubes kept on dry ice. Samples were then stored at -80°C overnight. Next day, samples were removed from the freezer, left on wet ice for 30 minutes then sonicated in 8x 15 second bursts, separated by 1 minute intervals. Samples were then split into two disposable 10 mL glass tubes with a glass Pasteur pipette, spun at 3000g for 30 minutes at 4°C. Sample supernatant was transferred to 20 mL glass tubes again using glass Pasteur pipettes, and dried down under oxygen free nitrogen at 60°C. When dried, samples and calibration standards as above, were stored as a dried residue at -20°C, followed by resuspension in (70:30, water/methanol; 70 µL) ready for steroid analysis by LC-MS/MS as detailed in section 2.8.5.

2.8.5 Liquid chromatography tandem mass spectrometry (LC-MS/MS) of F, E, d3F, d4F, d3E from plasma and adipose extracts

2.8.5.1 Instrumentation

A Waters Acquity Classic UPLC (Wilmslow, UK) coupled to a QTRAP® 5500 (AB Sciex, Warrington, UK) was used.

2.8.5.2 Chromatography conditions

Steroids were separated on a ACE Excel C18-AR column (150 x 2.1 mm; 2 µm) at 25°C using a mobile phase system of water with 0.1% formic acid (FA) and acetonitrile with 0.1% FA at a flow rate of 0.5 mL/min. The gradient was used, with a total run time of 7 minutes, as shown in Table 2.4.

TABLE 2.4 Chromatographic gradient

Chromatographic gradient for separation on C18-AR (150 x 2.1 mm; 2 µm) using a system of water and acetonitrile

Time (mins)	Flow rate (mL/min)	Water with 0.1% formic acid (FA)	Acetonitrile with 0.1% FA
0	0.5	70	30
4	0.5	70	30
5	0.5	40	30
5.5	0.5	10	90
6	0.5	10	90
6.1	0.5	70	30
7	0.5	70	30

2.8.5.3 Mass spectrometry conditions

Ionisation was performed in positive electrospray mode with curtain gas 40 psi, collision gas medium, spray voltage 5500 V, source temperature 700°C, entrance potential 10 V, ion source gas 1 and 2 at 40 and 60 units. Mass transitions, retention times, declustering potential, collision energy and collision exit potential of the analytes are given in Table 2.5. Typical chromatography is shown in Figure 2.1. Data was collected in Analyst 1.6.2 software.

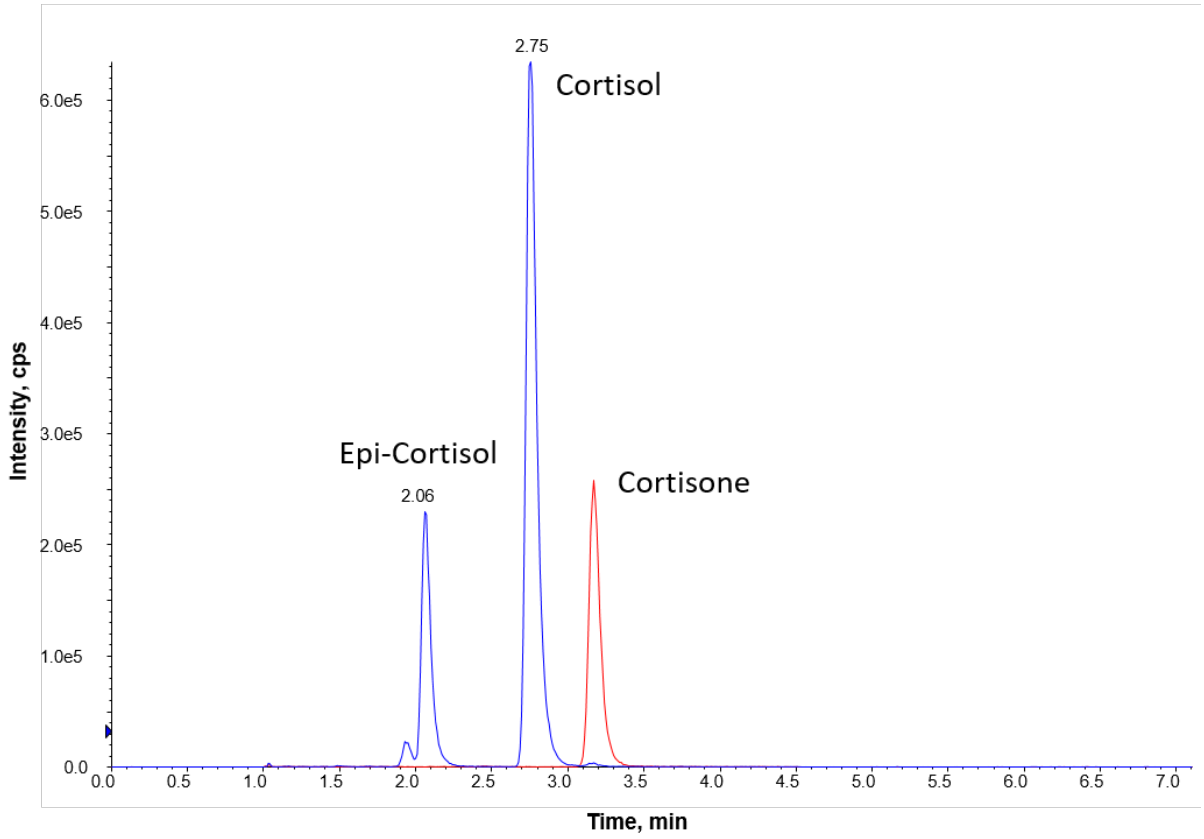

FIGURE 2.1 Typical chromatography for deuterium labelled tracer glucocorticoids in plasma and adipose method

Separation of Cortisol (2.75 mins) and Cortisone (3.16 mins) from Epi-cortisol (2.06 mins) on C18-AR (150 x 2.1 mm; 2 um) on a Nexera X2 uHPLC using a water and acetonitrile mobile phase system. Flow rate 0.5 mL/min, 25°C and a gradient elution over 9 minutes. Note that d4F, d3F elute at the same time as 2.75 mins.

TABLE 2.5 Mass spectrometric conditions for steroid analysis on a 5500 QTrap mass spectrometer

Analyte	Parent ion (m/z)*)*	Product ion (m/z)	Retention Time (mins)	De- clustering potential (V)	Collision Energy (V)	Collision Cell Exit Potential (V)
Cortisone	361.1	163.1	3.16	81	107	10
Cortisone	361.1	77.0	3.16	81	31	26
D3-cortisone	364.2	77.0	3.14	100	31	26
Cortisol 1	363.1	121.2	2.75	76	83	10
Cortisol 2	363.1	91.0	2.75	76	83	10
D3-cortisol	366.2	107.1	2.72	121	25	20
D4-cortisol	367.2	121.0	2.70	80	29	16
Epi-cortisol	363.1	121.2	2.06	131	29	14

2.8.6 Analysis of LC-MS/MS data of F, E, d3F, d3E and d4F

MultiQuant® 3.0.3 software (AB Sciex, Framingham, USA), was used to integrate the area under the peak for each steroid, according to the retention time defined by the method, and the internal standard, Epi-F. The ratio of the peak area ratio of the steroid to the internal standard was used to plot a standard curve – a line of best fit (y = mx + c) using the concentration of each calibration curve point (x axis) against the peak area (y axis) with an equal or weighting of 1/x. A regression coefficient (r^2) of >0.999 was accepted for each standard curve plotted with a minimum of 6 points of the 12 points of the calibration curve. The amount of F, E, d3F and d4F in the samples was calculated using the corresponding standard curve equation in the MultiQuant software. Due to the lack of commercial availability of d3-cortisone (d3E) then, the amount of d3E was calculated using the peak area ratio of d3E/epi-F and the standard curve equation of E, using Microsoft Excel, where it is assumed that E and d3E have the same ionisability.

2.9 Quantitation of endogenous steroids in plasma using liquid chromatography mass spectrometry

2.9.1 Materials and reagents

2.9.1.1 Reagents

HPLC grade water, LC-MS grade methanol were from Fisher Scientific (Loughborough, UK) and ammonium fluoride was from Sigma-Aldrich (Dorset, UK). HPLC grade methanol, dichloromethane, 2-propanol and LC-MS grade water, formic acid and acetonitrile were obtained from VWR (Lutterworth, Leicestershire, UK).

2.9.1.2 Analytical Standards

Cortisol (F) was supplied by Sigma Aldrich (Dorset, UK) while epi-cortisol (epi-F) and cortisone (E) were supplied by Steraloids (Newport, RI, USA). (9,11,12,12)-$[^2H]_4$-cortisol, (D4-cortisol) was supplied as a certified reference material at 100 µg/mL and (2,2,4,6,6,9,12,12)-$[^2H]_8$-cortisone, (D8-cortisone) was supplied as a powder by Sigma-Aldrich (Dorset, UK). A stock solution of d8E was prepared by weighing and dissolving in methanol to a final concentration of 1 mg/mL, and storing at -20°C, prior to dilution.

2.9.2 Preparation of calibration standards of F and E

A stock solution of F and E (1 mg/mL) was used to prepare a mixed stock at 5 µg/mL, which was further diluted in methanol to give 500 ng/mL, 50 ng/mL and 5 ng/mL stock solutions. A calibration curve was prepared into individual glass tubes with the following points – 0.025

ng, 0.05 ng, 0.1 ng, 0.25 ng, 0.5 ng, 1 ng, 2.5 ng, 5 ng, 10 ng, 25 ng, 50 ng and 100 ng. The internal standards used were d4F and d8E for F and E, respectively and a stock solution of 1 mg/mL of d8E was prepared and combined with the certified reference material d4F (100 µg/mL and together diluted to 100 ng/mL and 20 µL of this stock was added to each standard and sample, to give 10 ng total d4F and d8E were added. Each standard was made up to 400 µL with water prior to extraction.

2.9.3 Automated extraction by liquid handling robot of F and E from plasma

Plasma samples were defrosted at room temperature. Samples (200 µL) were transferred to a 96-well deep well plate, enriched with d4F and d8E (10 ng) alongside calibration standards (prepared as detailed in section 2.9.2). An Extrahera liquid handling robot (Biotage, Uppsala, Sweden) was used to extract samples and calibration standards through an SLE 400+ 96-well plate (Biotage, Uppsala, Sweden), by dilution with 0.1% formic acid in water (200 µL, v/v). The diluted samples and standards were allowed to absorb to the extraction material for 5 minutes. Samples were pulled through the material under positive pressure and solvents were added, causing elution with 0.6 mL of dichloromethane and isopropanol (98:2; v/v) three times into a 2 mL 96-well collection plate (Waters, Hertfordshire, UK) placed below. Positive pressure was applied for 2 minutes. The 96-well plate containing the eluted samples and standards were transferred to a 96-well nitrogen dual dry system (Biotage, Uppsala, Sweden), reduced to dryness and stored at -20°C until analysis. Prior to LC-MS/MS analysis, samples were re-suspended in HPLC grade water and methanol (100 µL; 70:30, v/v), sealed with a plate seal and mixed on a plate shaker (10 mins at 400 rpm).

2.9.4 Liquid chromatography tandem mass spectrometry (LC-MS/MS) of endogenous glucocorticoids in plasma

2.9.4.1 Instrumentation for plasma glucocorticoid measurement

A Shimadzu Nexera UPLC coupled to a QTRAP® 6500+ (AB Sciex, Warrington, UK) was used.

2.9.4.2 Chromatography conditions

Steroids were separated on a Kinetex C18 column (150 x 3.0 mm; 2.6 µm) at 40°C using a mobile phase system of water with 0.05 mM ammonium fluoride in water and methanol at a flow rate of 0.5 mL/min. The gradient was used, with a total run time of 16 minutes, as shown in Table 2.6.

TABLE 2.6 Chromatographic gradient *for separation on C18 Kinetex (150 x 3.0 mm; 2.6 µm) using a system of water and methanol with 50 uM ammonium fluoride*

Time (mins)	Flow rate (mL/min)	Water with 50 uM ammonium fluoride	Methanol with 50 uM ammonium fluoride
0	0.5	45	55
4	0.5	45	55
10	0.5	0	100
12	0.5	0	100
12.1	0.5	45	55
16	0.5	45	55

2.9.4.3 Mass spectrometry conditions

Ionisation was performed in positive electrospray mode with curtain gas 40 psi, collision gas medium, spray voltage 5500 V, source temperature 600°C, entrance potential 10 V, ion source

gas 1 and 2 at 40 and 60 units. Mass transitions, retention times, declustering potential, collision energy and collision exit potential of the analytes are given in Table 2.7. Typical chromatography is shown in Figure 2.2. Data was collected in Analyst 1.7.1 software.

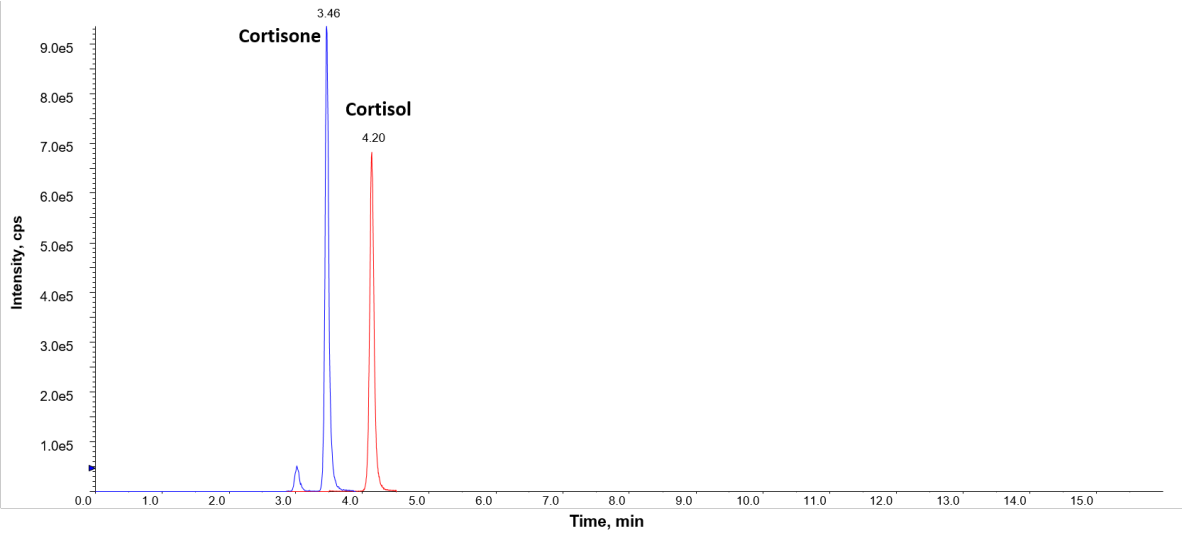

FIGURE 2.2 Typical chromatography for endogenous steroids in plasma method

Separation of Cortisone (3.46 mins) and Cortisol (4.20 mins) on Kinetex C18 (150 x 3.0 mm; 2.6 um) on a Nexera X2 uHPLC, using a water and methanol mobile phase system. Flow rate 0.5 mL/min, 40°C and a gradient elution over 16 minutes. Note that the internal standards d4F and d8E co-elute with F and E respectively.

TABLE 2.7 Mass spectrometric conditions for steroid analysis on a 6500 QTrap mass spectrometer

Analyte	Parent ion (m/z)	Product ion (m/z)	Retention Time (mins)	De- clustering potential (V)	Collision Energy (V)	Collision Cell Exit Potential (V)
Cortisone	361.1	163.1	3.46	81	107	10
Cortisone	361.1	77.0	3.46	81	31	26
D8-cortisone	369.2	169.0	3.40	81	31	26
Cortisol 1	363.1	121.2	4.20	76	31	8
Cortisol 2	363.1	91.0	4.20	76	83	10
D4-cortisol	367.2	121.0	4.10	80	29	16

2.9.4.4 Data analysis of LC-MS/MS data of endogenous steroids in plasma

MultiQuant® 3.0.3 software (AB Sciex, Framingham, USA), was used to integrate the area under the peak for each analyte and internal standard, according to the retention time defined by the method. The ratio of the peak area ratio of cortisol/d4F and cortisone/d8E was used to plot standard curves – a line of best fit (y = mx + c) using the concentration of each calibration curve point (x axis) against the peak area (y axis) with an equal or weighting of 1/x. A regression coefficient (r^2) of >0.999 was accepted for each standard curve plotted with a minimum of 6 points of the 12 points of the calibration curve. The amount of F, E in the samples was calculated using the corresponding standard curve equation in the MultiQuant software.

2.10 Total isotope dilution ultrafiltration for measurement of free cortisol levels in human plasma

A total isotope dilution ultrafiltration assay was used for measurement of free cortisol levels in plasma. The ^{3}H-cortisol was prepared to a concentration of 1 mCi/mL, and reconstituted in PBS containing 0.1% gelatin. This working stock ^{3}H-cortisol was diluted 1:40 to yield a concentration of 25 uCi/mL, by drying down under nitrogen before reconstituting in the PBS/Gelatin. 100 µL of human plasma was added to 10 µL of the diluted ^{3}H-cortisol, and incubated at 37°C for 1 hour. 10 µL of the 'retentate' was then removed and placed in a scintillation vial containing 2 mL of scintillation fluid (Ultima Gold, PerkinElmer Inc), the remainder loaded onto an ultrafiltration column (Millipore Centrifree Ultrafiltration Devices; Cat No. 4104), then spun at 2000 x g for 30 minutes at 25°C. 10 µL of the 'filtrate' was pipetted

into a scintillation vial containing 2 mL scintillation fluid. All (retentate and filtrate) samples were read on a Hidex 300 SL beta-counter. This method does not provide a direct measurement of free cortisol concentration; this was calculated by dividing the number of counts per minute (CPM) in the sample 'filtrate' by the CPM of the sample retentate, and multiplying this ratio by the concentration of the total cortisol, as measured by LC-MS/MS.

2.11 Quantification of ethanol in human microdialysis samples

Ethanol in microdialysis samples was measured using the ab65343 Ethanol Assay Kit (Abcam, Cambridge, UK). Alcohol oxidase oxidizes ethanol to generate H_2O_2 which reacts with a probe to generate colour which can be read with a microplate reader at 570 nm. All kit components were stored in the dark at -20°C until the components were reconstituted on the day samples were assayed. The ethanol assay buffer was equilibrated to room temperature before use, the ethanol probe warmed for 5 minutes at 37°C in a water bath, and the enzyme mix reconstituted with 220 µL of ethanol assay buffer. Fresh standards were made up at room temperature using the kit ethanol standard supplied, and used within 4 hours. Standards were made up by serial dilution in the kit ethanol assay buffer, to provide end amounts of 0, 2, 4, 6, 8 and 10 nmol of ethanol for the standard curve. 5 µL of each sample was diluted (1:400) by adding to 1995 µL of kit ethanol assay buffer and 25 µL added to each well. Finally, 25 µL of reaction mix was made up for each well by adding 23 µL of ethanol assay buffer to 1 µL of the ethanol probe and 1 µL of the ethanol enzyme mix. When samples/standards and reaction mix were pipetted into wells together, the final volume in each well was 50 µL. Plates were incubated at 37°C for 30 minutes while protected from light, then put on a microplate reader

and colour measured at OD 570 nm. The ethanol concentration in samples was read off the standard curve using linear regression.

2.12 Quantitation of plasma ACTH by ELISA

Plasma ACTH was measured using a two-site ELISA (Enzo Life Sciences Inc, Farmingdale, New York, USA). All kit components except the wash buffer concentrate (which was stored at room temperature until dilution, to avoid precipitation) were stored at 2-8°C and allowed to come to room temperature before each assay. Assay calibrators and controls were reconstituted with deionised water (2 mL) and mixed gently. Reconstituted calibrators and controls were stored (-20°C) for 6 weeks with up to 3 freeze thaw cycles. Wash buffer concentrate (30 mL) was diluted 1:20 in deionised water. The diluted wash buffer was stable for up to 90 days at room temperature.

Samples from each subject were assayed together. Assay standards (0-476 pg/mL), controls and samples (200 µL) were added in duplicate to a 96-well microtitre plate coated with streptavidin. Biotinylated ACTH antibody (25 µL) was added to each well followed by horseradish peroxidase (HRP) enzyme labelled ACTH antibody (25 µL). The plate was covered in aluminium foil to avoid light exposure and placed on a plate shaker for incubation (at room temperature for 4 hours). Unbound antibodies and buffer matrix were then removed by washing 5 times with wash solution (350 µL). For the detection of the immunocomplex, tetramethylbenzidine (TMB) substrate solution (150 µL) was added to each well and incubated for a further 30 minutes on a plate shaker (covered with aluminium foil). The HRP/TMB reaction was terminated with acidic stopping solution (100 µL) and mixed gently. The absorbance was read within 10 minutes in a spectrophotometric microtitre plate reader

at both 405 and 450 nm. A standard curve was generated by plotting absorbance against plasma ACTH concentration for each calibrator by fitting to a 4-parameter curve (GraphPad Prism, San Diego, California, USA).

2.13 Quantitation of plasma cortisol by ELISA

Due to limited sample volumes and sensitivity of the LC-MS/MS (requirement for 200 µL of plasma) precluding the use of LC-MS/MS, in chapter 5 plasma cortisol was measured using ELISA (Enzo Life Sciences, Farmingdale, New York, USA). All reagents were stored at 2-8°C and allowed to come to room temperature for at least 30 minutes before each assay. Assay and wash buffers were prepared with deionised water at 1:10 and 1:20 dilutions respectively. Standards were prepared by serial dilution to 10,000, 5,000, 2,500, 1,250, 625, 312.5 and 156.25 pg/mL concentrations and used within 60 minutes of preparation. 10 µL of each sample was added to 10 µL of 1:100 Steroid Displacement Reagent (SDR) solution (made up using deionised water), vortexed and left to stand for 5 minutes. 380 µL of ELISA assay buffer was then added, giving a final sample dilution of 1:40. Samples and standards (100 µL) were added to a 96-well plate coated with goat antibody specific to mouse IgG. Alkaline phosphatase conjugated with cortisol (50 µL) was added to each well along with 50 µL of a mouse monoclonal antibody to cortisol. The plate was incubated at room temperature on a plate shaker for 2 hours. The contents of the wells were emptied and washed 3 times with wash buffer (400 µL). After the final wash, 200 µL of substrate p-nitrophenyl phosphate buffer solution was added to each well and left for 1 hour at room temperature without shaking. The enzyme reaction was stopped with 50 µL of stop solution and the absorbance was read (405 nm; correction between 570 and 590 nm) in a spectrophotometric microtiter plate

reader. A standard curve was generated by plotting absorbance against cortisol concentration for each standard by fitting to a 4-parameter curve, and samples were interpolated from this standard curve (GraphPad Prism, San Diego, California, USA).

Chapter 3: Tissue-specific cleavage of CBG *in vivo* in humans

3.1 Introduction

CBG binds >85% of plasma cortisol and undergoes proteolytic cleavage by NE. *In vitro*, this results in a permanent transition to cleaved CBG which has a 9-10 fold lower affinity for cortisol, from which it has been inferred that CBG cleavage potentially releases cortisol to inflamed tissues (Hammond et al., 1990a). However, this has never been shown *in vivo* and central questions remain, firstly whether CBG cleavage occurs at all, and secondly (if it does occur *in vivo*) whether this happens principally at sites of inflammation, or whether different target tissues have a specific role in cleavage of CBG. NE levels are expected to be high at the location of an acute inflammatory insult, but outside of this context NE levels in different tissues, for instance adipose, are likely to vary widely depending on the abundance and specific populations of neutrophils present (Michailidou et al., 2022). Neutrophils are produced in the bone marrow and enter the circulation, where they remain for just a few hours (estimated half-life of 6-12 hours) before they migrate into tissues (Summers et al., 2010). In normal homeostasis neutrophils are found in many tissues, but there is very little knowledge on how neutrophils are directed to different organs. A large number of neutrophils preferentially accumulate in the lungs, while evidence suggests other subpopulations of neutrophils aggregate in lymph nodes and the spleen (Rosales, 2018). Metabolic health and disease are key determinants of NE levels; neutrophils have been shown to accumulate in the adipose tissue of mice within the first few days of starting a HFD (Elgazar-Carmon et al., 2008; Talukdar et al., 2012).

Much of what is known about cleavage of CBG in humans has been by study of CBG in the context of acute inflammation, as discussed in chapter 1.2.5. There is a relative paucity of

data on the role of CBG in chronic inflammation, such as chronic inflammatory diseases (e.g. rheumatoid arthritis) or metabolic disorders, including obesity. A very limited number of studies suggest that CBG cleavage may differ in acute and chronic inflammation. Taking the example of rheumatoid arthritis, in a recent prospective, cross-sectional observational study comparing 53 outpatients with rheumatoid arthritis with 73 healthy controls, it was concluded that patients with rheumatoid arthritis have paradoxically reduced CBG cleavage compared to healthy controls, and that cleavage is reduced further with higher disease activity. Moreover, the authors suggested that impaired CBG-mediated delivery of cortisol may perpetuate chronic inflammation in rheumatoid arthritis (Nenke et al., 2016b). These findings go against the hypothesis, and are surprising given the role that neutrophils have been shown to play in the pathogenesis of rheumatoid arthritis; recent evidence has demonstrated that neutrophil activity correlates with levels of antibodies to citrullinated antigens (ACPAs) which are thought to be pathogenic in rheumatoid arthritis (Khandpur et al., 2013).

It is known that insulin downregulates CBG mRNA levels and protein secretion *in vitro* (Crave et al., 1995). Plasma CBG has been found to be marker of insulin secretion (concentrations), and has been both negatively and positively correlated with markers of obesity (BMI and waist-to-hip ratio) depending on the degree of insulin resistance (Fernández-Real et al., 2000; Fernández-Real et al., 2001). Plasma CBG levels also negatively correlate with various biochemical markers of the metabolic syndrome (fasting glucose, insulin resistance and adiponectin) (Fernandez-Real et al., 2002; Fernandez-Real et al., 2005; Manco et al., 2007), but little is known about the role of CBG cleavage in human obesity beyond this. Because elevated levels of elastase have been associated with obesity and insulin resistance (Mansuy-

Aubert et al., 2013), a recent study examined the respective levels of high- and low-affinity CBG, in a cohort of 100 volunteers. CBG cleavage was found to be reduced in subjects with central obesity and the metabolic syndrome, which was interpreted as the sign of altered CBG protein in obesity that would no longer be sensitive to elastase cleavage (Nenke et al., 2016c).

Human CBG cleavage has been inferred from two ELISAs using antibodies that bind specific epitopes on intact CBG (Lewis and Elder, 2011), but this has yet to be corroborated by other groups. Considerable uncertainty exists about whether the accuracy of the RCL-intact CBG ELISA measurements are affected by CBG *N*-glycosylation (as discussed in sections 1.2.6 and 1.2.7, and illustrated in Figure 1.5). It is important to note that in both studies outlined above (Nenke et al., 2016b; Nenke et al., 2016c), only these antibodies were used in the estimation of CBG cleavage. In this chapter, all calculations of CBG cleavage made using these antibodies will therefore be compared with contemporaneous measurement of CBG binding capacity.

3.2 Hypotheses

We hypothesise that:

1. CBG concentration and binding capacity is higher in lean subjects than in obese, due to enhanced cleavage of CBG by NE in obesity
2. CBG concentration and binding capacity increase across the liver due to CBG production
3. CBG concentration and binding capacity decrease across brain, skeletal muscle and adipose tissue due to CBG cleavage by NE *in vivo*

4. Exogenous insulin administration reduces CBG concentration and binding capacity, due to downregulation of CBG production and enhanced cleavage of CBG *in vivo*

3.3 Aims

We aimed to:

1. Quantify whole body and tissue-specific CBG levels (concentration and binding capacity) in lean and obese individuals *in vivo*
2. Discover whether CBG production and/or cleavage occurs *in vivo* in liver, brain, skeletal muscle and abdominal adipose
3. Investigate whether exogenous insulin affects CBG concentration, CBG binding capacity or CBG cleavage *in vivo*

3.4 Methods

3.4.1 Study design

In four published studies of tissue-specific cortisol metabolism we collected arterialised blood (from dorsal hand veins heated in a 'hot box' at 60^{o}C for 5 minutes) and plasma samples from veins draining the liver (hepatic vein) (study 1) (Stimson et al., 2011), brain (internal jugular vein) (study 2) (Kilgour et al., 2015), forearm skeletal muscle (median cubital vein) and abdominal subcutaneous adipose (branch of the superficial epigastric vein) (studies 3 & 4) (Anderson et al., 2020; Hughes et al., 2012). For context, details of the aims and the specifics

about participants and clinical protocols for each of these 4 studies are described in further detail below.

3.4.1.1 Liver (Study 1)

The aim of this study was to quantify *in vivo* whole-body, splanchnic, and hepatic 11β-HSD1 activity in obese type 2 diabetic and normal weight control subjects.

Participants were male, aged 20–70 years, with normal full blood count and normal renal, liver, and thyroid function. Subjects had no history of glucocorticoid therapy in the past year and an alcohol intake of <21 units per week. Two groups were recruited: 7 healthy control subjects (BMI 20–26 kg/m^2) with no significant medical history or current use of any medication and 10 men with diet- or tablet-treated type 2 diabetes (T2DM) (BMI 30–40 kg/m^2).

Subjects were given 1 mg oral dexamethasone at 11pm and fasted until they attended the Clinical Research Facility at 7.30am the following morning. Blood pressure and anthropometric measurements were taken. Cannulae (21G) were sited in the antecubital fossa of the right arm for infusion and in a dorsal left hand vein that was placed in a box heated to 60°C to achieve arterialisation for repeated blood sampling. An infusion was commenced 60 min later (t = 0), which contained 60% unlabelled cortisol (Calbiochem, Nottingham, U.K.) and 40% 9,11,12,12-[^{2}H]$_4$-cortisol (D4-cortisol; Cambridge Isotopes, Andover, MA) (at a rate of 1.74 mg/h for 6.5 h after an initial bolus of 3.5 mg) and dexamethasone (at 240 mg/h) to maintain adrenal suppression. At t = +30 min, the right femoral vein was cannulated under local anaesthesia (5 mL 2% lidocaine), and a 7F Swan-

Ganz catheter (Edward Lifesciences, Berkshire, UK) was inserted into one of the hepatic veins under fluoroscopic guidance for sampling. From *t* = +120 min, indocyanine green (Pulsion Medical, Middlesex, UK) was infused into the right antecubital vein at 30 mg/h to measure liver blood flow. After steady state was achieved (*t* = +180–210 min) (Stimson et al., 2011). The analysis in this chapter is based on samples collected at *t* = +195 min.

3.4.1.2 Brain (Study 2)

The aim of this study was to quantify cortisol regeneration by 11β-HSD1 in the brain, both to assess its contribution to systemic cortisol/cortisone turnover and to develop a tool for measuring 11β-HSD1 in dementia and following administration of 11β-HSD1 inhibitors.

Participants were 8 healthy male volunteers between 18 and 70 years old. Exclusion criteria were glucocorticoid medication (by any route of administration) within the past 3 months; diabetes mellitus, cerebrovascular disease or other significant chronic illness; history of recent heavy alcohol or illegal drug use; current use of any immunosuppressive medication; abnormal screening liver, thyroid, renal or coagulation function (ie, INR > 1.5 or platelets < 50 x 10^9/L) or abnormal full blood count or random blood glucose; research participant in the previous 3 months; any contraindication to magnetic resonance imaging (MRI).

Screening tests were performed within the 2 weeks prior to the procedure. On the day of the study, subjects attended the Clinical Research Facility at 8.30am. A cannula was inserted into the left antecubital fossa and blood was taken to measure baseline endogenous steroids and their background isotopomers. At t = -5 min a 0.7 mg loading bolus of D4-cortisol was given intravenously (IV), followed by an infusion at 0.35 mg/h (15.94 nmol/min) at t = 0 min. A

cannula was inserted into a vein in the dorsum of the right hand in a retrograde direction and when required the hand was placed in a hot box at 60°C to arterialise the blood. Arterialisation of the blood was accepted if the oxygen saturation was >98%. A jugular bulb cannula was inserted in the dominant internal jugular vein under ultrasound guidance. The oxygen saturation of the blood was checked to ensure it was <85%. At t = 145 min a 76.0 ug bolus of D2-cortisone was administered IV, followed by an infusion at 105.3 ug/h (4.88 nmol/min). From t = 180 min four sets of simultaneous blood samples were taken from the arterialised and jugular bulb cannulae at 10 min intervals (t = 180, 190, 200, and 210 min) into lithium heparin and plasma separated and stored at -80°C until analysis (Kilgour et al., 2015). In the analysis in this chapter, arterialised samples used are from t = 210 min, and we used jugular venous samples collected at t = 120 min.

3.4.1.3 Skeletal muscle and abdominal adipose in normal weight (Study 3)

The aim of this study was to use stable isotope tracers to test the hypothesis that both 11β-HSD1 reductase and dehydrogenase activities occur in human metabolic tissues *in vivo*.

Participants had normal blood indices (haemoglobin, renal function and glucose) and had not received glucocorticoid treatment by any route for 3 months prior to the studies. Six healthy lean men attended after an overnight fast. A cannula (18G) was placed anterogradely into a right antecubital fossa vein for infusions. Retrograde 20G cannulae were placed as follows: 1) in a superficial vein on the anterior abdominal wall, under ultrasound guidance, to sample from subcutaneous adipose (Frayn et al., 1989); 2) in a deep branch of the median cubital vein in the left antecubital fossa to sample from forearm skeletal muscle (Butler and Home, 1987); and 3) in a dorsal vein of the right hand, with the hand warmed to 60°C to sample arterialised blood (Roddie et al., 1956). For confirmation of correct placement of cannulae,

O_2 saturation (GEM OPL; Instrumentation Laboratory, Bedford, MA) was confirmed to be >85, <40, and >98% in the adipose, skeletal muscle, and arterialised samples, respectively.

D2-cortisone and D4-cortisol (40% in cortisol) were administered in 0.9% saline, wt/vol, as intravenous boluses of 76.0 ug and 3.5 mg followed by continuous intravenous infusions of 105.3 ug/h and 1.74 mg/h, respectively. Arterialised samples were obtained pre-infusion and at hourly intervals for 3 h. From 3 h, four sets of blood samples were obtained simultaneously from all sites at 10 min intervals. Prior to taking of samples from the deep forearm vein, a wrist cuff was inflated to 200 mmHg for 2 min to remove blood flow from the hand. Forearm blood flow was measured by venous occlusion plethysmography (Benjamin et al., 1995) (Hokanson, Bellevue, WA) immediately after sampling using the mean of three readings during intermittent occlusion of the upper arm with a cuff inflated to 40 mmHg. Adipose tissue blood flow was measured continuously during the study using a Mediscint gamma-counter probe after a subcutaneous injection of 1–2 MBq ^{133}Xe lateral to the umbilicus (Larsen et al., 1966). The data included in the analysis in this chapter are based on an average of the results from samples obtained at t = 0, 190, 340 and 360 mins (Hughes et al., 2012).

3.4.1.4 Effect of obesity and insulin on adipose and muscle tissue cortisol balance (Study 4)

This study aimed to determine whether 11β-HSD1 equilibrium in metabolic tissues is regulated by insulin and obesity. Participants were screened to exclude significant systemic illness or a history of diabetes mellitus or glucocorticoid use in the preceding 3 months. They were included if their alcohol intake was less than 21 units per week, their screening blood tests (full blood count, random blood glucose, kidney, liver, and thyroid function) were normal, and they were not receiving regular anticoagulation.

10 lean (body mass index 20-25 kg/m^2) and 10 obese (body mass index > 30 kg/m^2) healthy male volunteers were recruited to a randomised, 2-phase, crossover, single-blinded study, attending 2 weeks apart. All participants were between age 20 and 70 years. Participants attended at 8am after an overnight fast at the Clinical Research Facility and measurements were taken of clothed weight and height. Body fat was assessed by bioelectrical impedance (Omron BF-302). The study visit commenced at 8am and was completed 5 hours from the start of the tracer infusion. Participants continued to fast and remained supine throughout each study visit. Each participant attended 2 identical study visits except for a hyperinsulinemic infusion at one and placebo saline infusion at the other in random order.

A cannula (20G) was inserted into the antecubital fossa for infusion of D4-cortisol and D2-cortisone. Three further retrograde cannulas were inserted to measure 11β-reductase and dehydrogenase activities across whole-body, forearm skeletal muscle, and abdominal subcutaneous adipose tissue: one cannula (20G) was inserted into a vein on the dorsum of the hand that was placed in a heated box (controlled at 60 °C) for 5 minutes before sampling to arterialise the blood (oxygen saturation confirmed as > 98%); a second cannula (20G) was placed in a branch of the cubital vein near the antecubital fossa on the opposite side (oxygen saturation confirmed < 40%), and an inflatable cuff was placed at the wrist and inflated (200 mm Hg, 2 minutes before sampling) to minimise contamination of venous blood from the hand; and a third cannula (18G) was placed in a branch of the superficial epigastric vein in subcutaneous adipose tissue of the abdominal wall, inserted under the guidance of filtered red light (Schott UK Ltd) and the tip kept above the inguinal ligament to prevent contamination from venous drainage from the leg.

^{133}Xenon (2 MBq) was injected into subcutaneous abdominal adipose tissue to measure adipose tissue blood flow (Frayn et al., 1989). D4-cortisol and D2-cortisone were administered diluted in 0.9% saline as an intravenous bolus of 1.4 mg and 76.0 µg followed by a continuous infusion of 0.7 mg/ hour and 105.3 µg/hour, respectively. Arterialised and venous blood were sampled before commencing the infusion, then at 60 minutes and again once steady state plasma concentrations were achieved after 2 hours. Blood was collected in lithium heparin tubes and plasma stored at –80 °C until analysis. At the time of sampling, blood flow through the skeletal forearm muscle and subcutaneous abdominal wall adipose tissue were measured using occlusion venous plethysmography (Benjamin et al., 1995) and washout of ^{133}Xenon, respectively. The "intervention" phase started at 3 hours. At the 2 visits, each participant received either a hyperinsulinemic euglycemic clamp or a placebo saline infusion in random order. For the clamp, insulin was infused at 35 mU/m^2/minute based on body surface area. Capillary glucose concentrations were checked at 5-minute intervals (Accu-Chek, Roche) and dextrose (10%) infused at variable rates to maintain euglycemia (capillary glucose between 4.5 and 5.5 mmol/L). During the placebo phase, saline (0.9%) was administered in place of dextrose and capillary glucose measurements were taken every 5 minutes to provide blinding of participants. Arterialised and venous blood were sampled as stated earlier every 15 minutes for a further 120 minutes.

3.4.2 Sample analysis

Total and RCL-intact CBG concentrations (using the 12G2 and 9G12 ELISAs, respectively, as described in chapter 2.3) and CBG binding capacity (using the radiolabelled ligand saturation assay, see chapter 2.4) were measured in 2016 by Lesley Hill at the University of British Columbia (UBC) in Vancouver, Canada, several months prior to the start of this PhD.

I calculated arterio-venous (A-V) differences in four CBG measures across the tissues (all except (c) are quoted as nmol/L):

(a) 'Total' CBG concentration

(b) CBG binding capacity

(c) CBG binding capacity normalised by CBG concentration (expressed as a ratio), which shows CBG binding capacity after adjustment for concentration of CBG. This enables detection of subtle changes in CBG binding capacity which would be likely to signal proteolytic cleavage, rather than changes in hepatic CBG expression and production

(d) 'RCL-intact' CBG concentration. Apparent 'cleaved' CBG can be calculated by subtracting RCL-intact CBG from 'total' CBG (Equation 3.1)

Equation 3.1: **Apparent 'cleaved' CBG**

$$Cleaved\ CBG\ (nmol/L) = Total\ CBG - RCL\ intact\ CBG\ (nmol/L)$$

3.4.3 Measurement of tissue blood flow

Blood flow across tissues was measured using indocyanine green infusion (liver) (study 1), ECG-gated phase-contrast magnetic resonance imaging (brain) (study 2), venous occlusion plethysmography (muscle) or ^{133}Xenon washout (adipose) (studies 3 and 4), respectively. Blood flow rate was expressed L/min (per 100g of tissue for adipose and skeletal muscle). Measures of CBG for each tissue (quoted as nmol/L) were then multiplied by the relevant tissue blood flow rate to provide a standardised measure of CBG concentration or cleavage, expressed as nmol/min (Equation 3.2).

Equation 3.2: **Net balance of CBG across tissue**

$$Net\ balance\ (nmol/min) = [Arterial\ CBG - Venous\ CBG\ (nmol/L)]\ x\ Tissue\ Blood\ Flow\ (L/min)$$

3.4.4 Statistical analysis

Data were analysed using GraphPad Prism® (version 9.5.1). Study group means were compared with 0 using one sample t tests, or a non-parametric method (Wilcoxon Signed Rank Test). Comparisons between groups were made using unpaired sample t tests (or Mann-Whitney U test if data were not normally distributed) or by one-way ANOVA. The effects of placebo and insulin were compared using two-way repeated measures ANOVA. Data are expressed as mean ± SEM, and p values below 0.05 were considered statistically significant.

3.5 Results

3.5.1 Subject characteristics

Characteristics of the 48 participants used in this analysis are summarised in Table 3.1 below.

Table 3.1 Baseline characteristics by study group

Data are number of patients or mean +/- SEM. All participants were male.

Study group	**Number**	**Age (yrs)**	**BMI (kg/m^2)**
Study 1 (liver) lean	7	47.5 ± 6.0	23.5 ± 1.1
Study 1 (liver) obese T2DM	9	52.3 ± 2.9	35.0 ± 1.0
Study 2 (brain)	8	38.1 ± 5.8	24.9 ± 1.3
Study 3 (muscle & adipose) lean	6	42.0 ± 4.0	24.6 ± 0.9
Study 4 (muscle & adipose) lean	8	50.5 ± 3.3	23.7 ± 0.4
Study 4 (muscle & adipose) obese	10	50.0 ± 3.3	32.9 ± 0.9

3.5.2 Whole body CBG

No differences in total CBG concentration, CBG binding capacity, normalised binding capacity or 'cleaved' CBG in arterialised blood were seen between groups in study 1 (Figure 3.1), study 2 (Figure 3.2), study 3 (Figure 3.3) or study 4 (Figure 3.4). In study 3, insulin tended to reduce total CBG concentration, by approximately 25 nmol/L (p=0.08 vs study 3 placebo), and CBG binding capacity, by 20 nmol/L (p=0.06 vs placebo). There was also a trend towards higher apparent 'cleaved' CBG in the obese group in study 4 (p=0.06 vs lean).

(a) Total CBG concentration

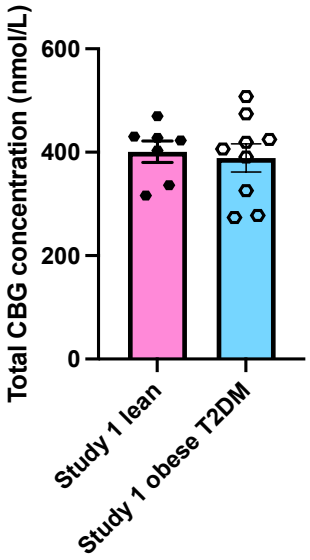

(b) CBG binding capacity

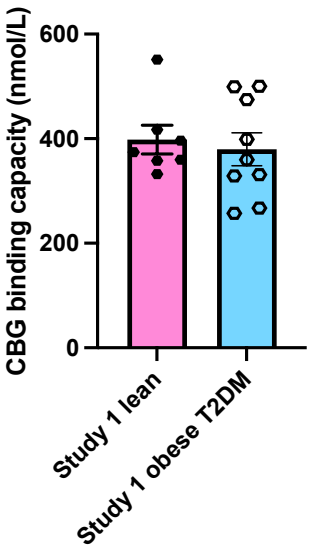

(c) Normalised CBG binding capacity

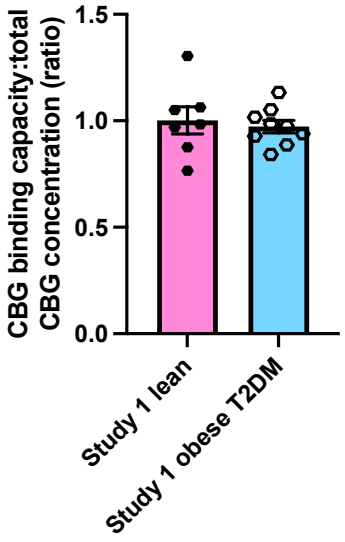

(d) Cleaved CBG

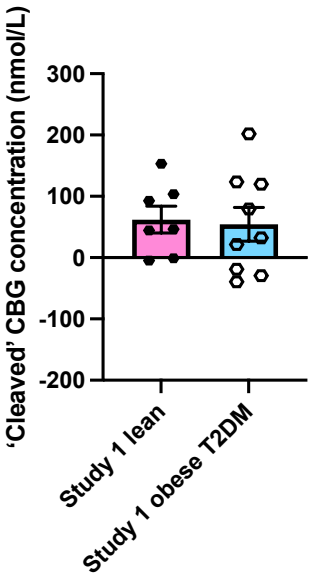

FIGURE 3.1 Whole body (arterialised) measures of plasma CBG in study 1

Data are mean ± SEM for plasma (a) CBG concentration, (b) CBG binding capacity, (c) CBG binding capacity normalised to CBG concentration and (d) apparent 'cleaved' CBG in; study 1 lean (filled hexagons, pink bar), study 1 obese T2DM (empty hexagons, blue bar). Comparisons between groups were made by unpaired t tests.

(a) Total CBG concentration

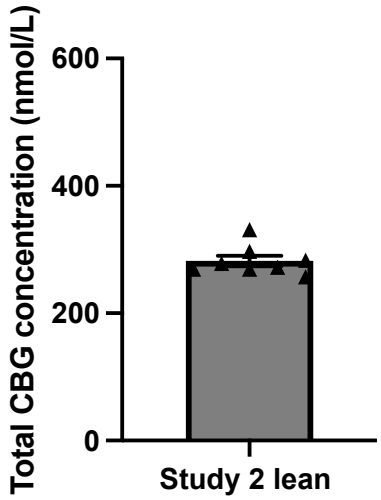

(b) CBG binding capacity

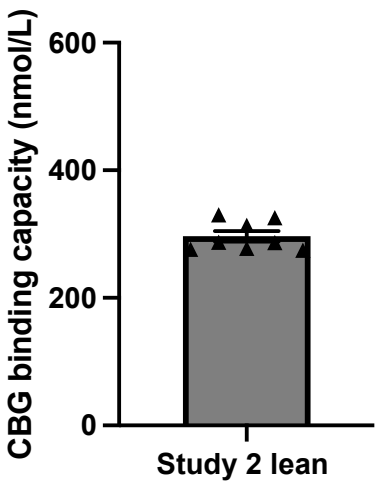

(c) Normalised CBG binding capacity

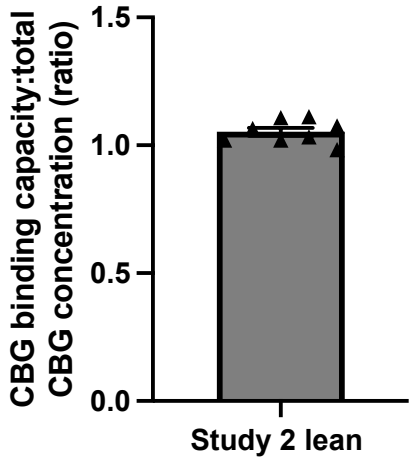

(d) Cleaved CBG

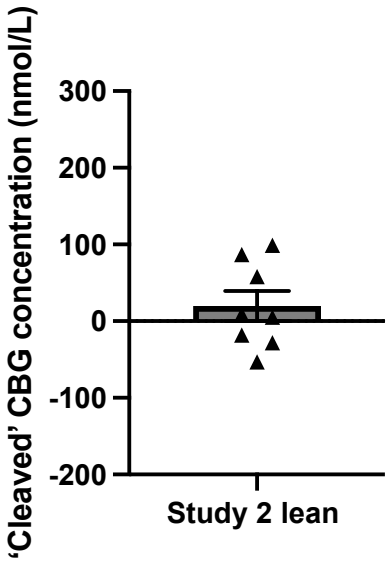

FIGURE 3.2 Whole body (arterialised) measures of plasma CBG in study 2

Data are mean ± SEM for plasma (a) CBG concentration, (b) CBG binding capacity, (c) CBG binding capacity normalised to CBG concentration and (d) apparent 'cleaved' CBG in study 2 subjects.

(a) Total CBG concentration

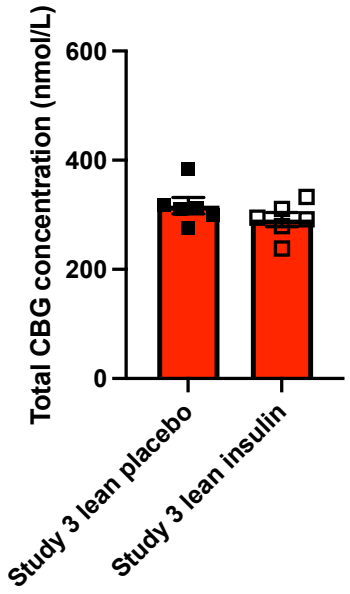

(b) CBG binding capacity

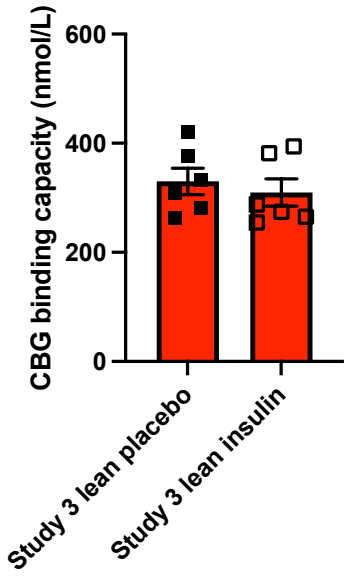

(c) Normalised CBG binding capacity

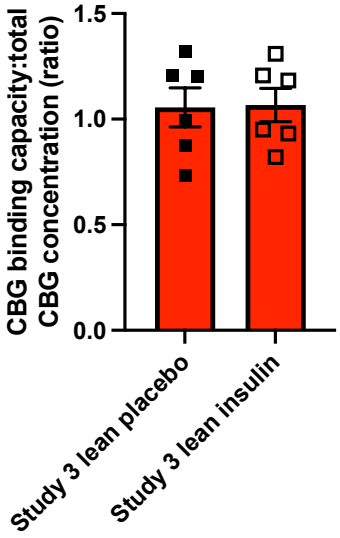

(d) Cleaved CBG

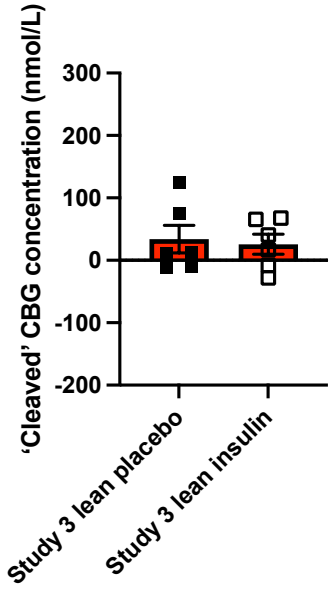

FIGURE 3.3 Whole body (arterialised) measures of plasma CBG in study 3

Data are mean ± SEM for plasma (a) CBG concentration, (b) CBG binding capacity, (c) CBG binding capacity normalised to CBG concentration and (d) apparent 'cleaved' CBG in study 3 lean placebo (filled squares, red bar) and study 3 lean insulin (empty squares, red bar). Comparisons between study 3 groups were made with paired t tests.

(a) Total CBG concentration

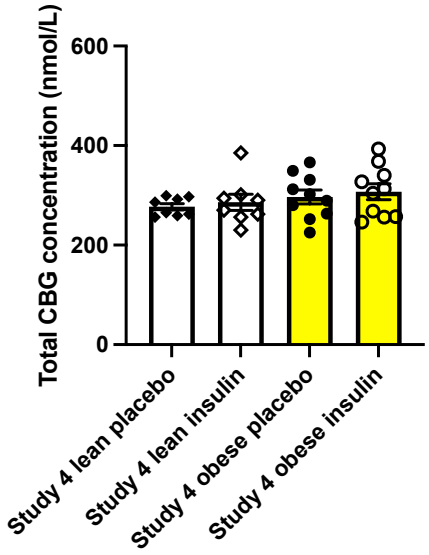

(b) CBG binding capacity

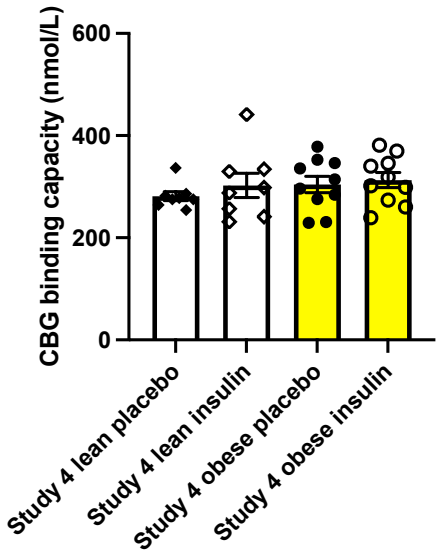

(c) Normalised CBG binding capacity

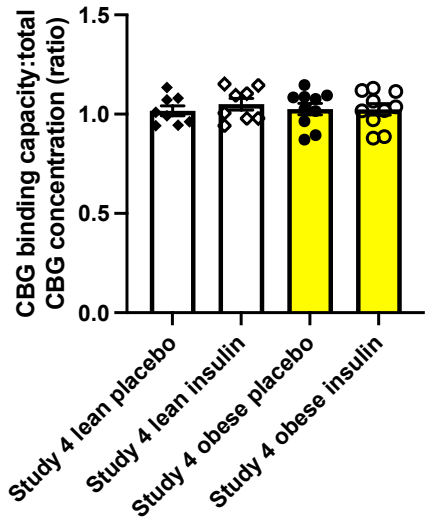

(d) Cleaved CBG

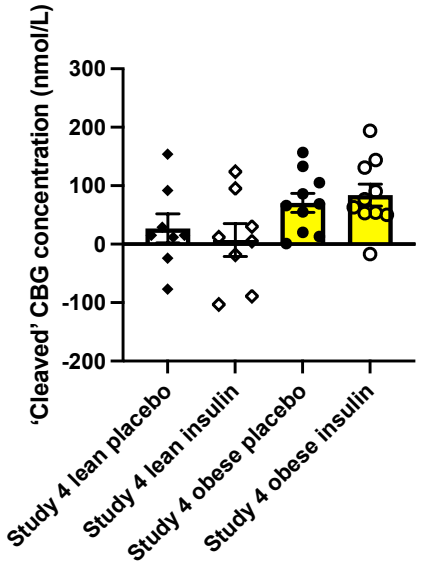

FIGURE 3.4 Whole body (arterialised) measures of plasma CBG in study 4

Data are mean ± SEM for plasma (a) CBG concentration, (b) CBG binding capacity, (c) CBG binding capacity normalised to CBG concentration and (d) apparent 'cleaved' CBG in study 4 lean placebo (filled diamonds, white bar), study 4 lean insulin (empty diamonds, white bar), study 4 obese placebo (filled circles, yellow bar) and study 4 obese insulin (empty circles, yellow bar). Comparisons between groups in study 4 were compared using two-way repeated measures ANOVA.

3.5.3 Liver (Study 1)

CBG binding capacity (Figure 3.5b) was higher in the hepatic vein than in the artery, but only in the obese T2DM group (p=0.008 vs lean), consistent with net release of CBG in this study group. This finding is supported by a tendency towards net release of CBG in the obese T2DM group (p=0.09 vs lean) (Figure 3.5a). Differences in CBG binding capacity disappeared when CBG binding capacity was normalised to CBG concentration (Figure 3.5c), which suggests that changes in CBG binding capacity are as a result of changes in CBG levels (concentration) rather than binding affinity (cleavage). There was no evidence of CBG cleavage across the liver based on ELISA measurements (Figure 3.5d).

(a) Total CBG concentration

(b) CBG binding capacity

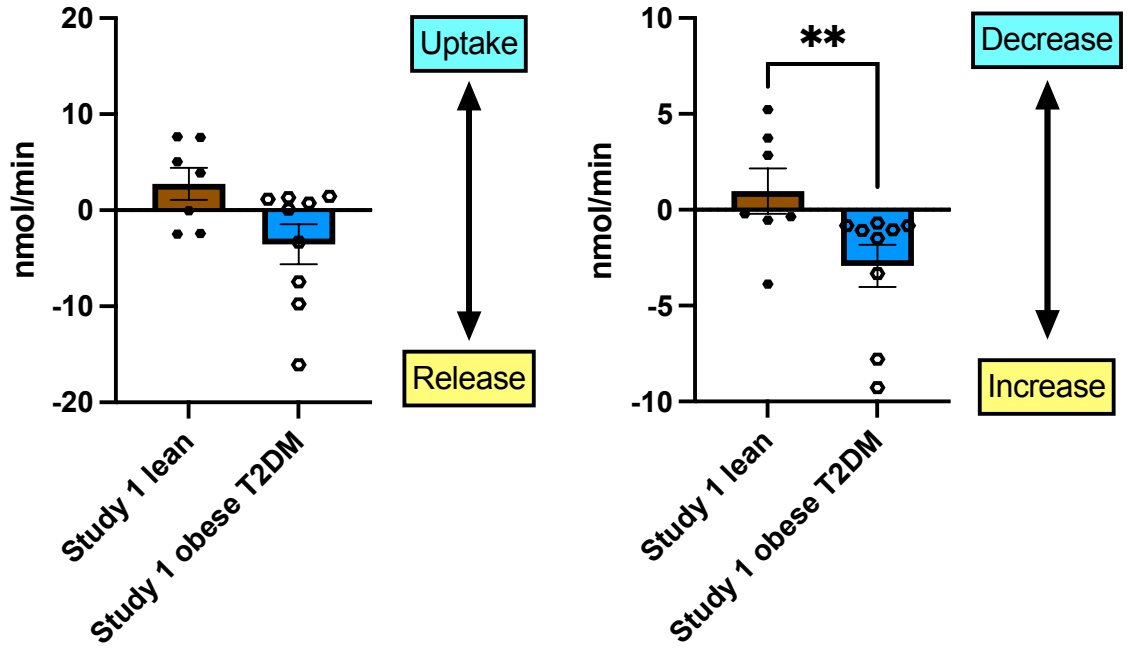

(c) Normalised CBG binding capacity

(d) Cleaved CBG

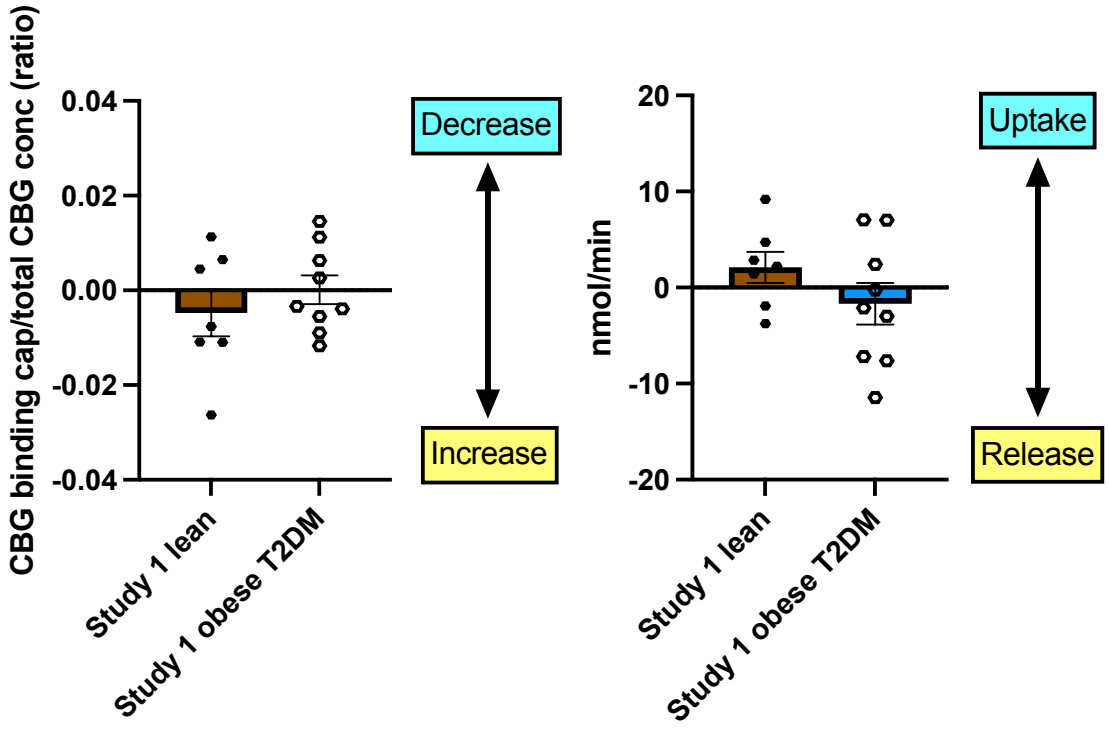

FIGURE 3.5 Arterio-venous differences in plasma CBG across the liver* in vivo *in humans

Data are mean ± SEM for plasma (a) total CBG concentration, (b) CBG binding capacity, (c) CBG binding capacity normalised to CBG concentration and (d) apparent 'cleaved' CBG across liver in study 1 lean

(filled hexagons, brown bars) and study 1 obese T2DM (clear hexagons, blue bars) groups (n=7 for lean and n=9 for obese T2DM). Comparisons with 0 were made using one sample t tests, or the Wilcoxon signed rank test if data were not normally distributed. Comparisons between groups were made either with unpaired t tests or the Mann-Whitney U test, depending on whether the data were normally distributed. There was a trend towards net release of CBG (a) in the obese T2DM group (p=0.09 vs lean). There was a net increase in CBG binding capacity across the liver in the obese T2DM group (b) (p=0.004 vs 0 and p=0.008 vs lean), in keeping with net production/release of CBG. There were no differences in CBG binding capacity normalised to CBG concentration (c), or in apparent 'cleaved' CBG (d).

3.5.4 Brain (Study 2)

There were no net differences in total CBG concentration, CBG binding capacity, CBG binding capacity normalised to CBG concentration or apparent 'cleaved' CBG across brain in study 2 (Figure 3.6a-d).

(a) Total CBG concentration

(b) CBG binding capacity

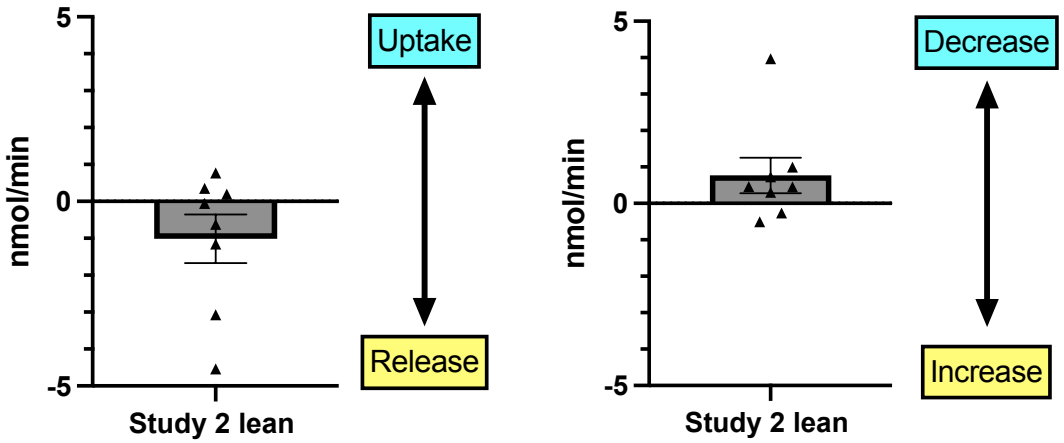

(c) Normalised CBG binding capacity

(d) Cleaved CBG

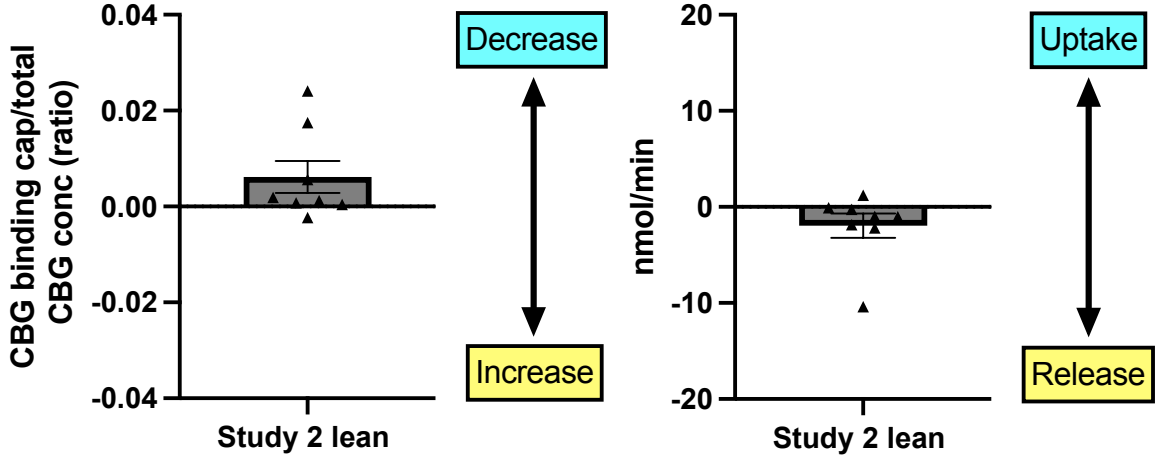

FIGURE 3.6 Arterio-venous differences in plasma CBG across the brain* in vivo *in humans

Data are mean ± SEM for plasma (a) total CBG concentration, (b) CBG binding capacity, (c) CBG binding capacity normalised to CBG concentration and (d) apparent 'cleaved' CBG across brain in study 2 lean subjects (black triangles, grey bars) (n=8). Comparisons with 0 were made using one sample t tests, or the Wilcoxon signed rank test if data were not normally distributed. No net differences were observed.

3.5.5 Skeletal muscle (Studies 3 and 4)

No net differences in total CBG concentration were observed across skeletal muscle (Figure 3.7a). In two of the three study groups, study 3 lean and study 4 obese, there was a net increase in CBG binding capacity across skeletal muscle (in keeping with release of CBG), but only during the placebo phase – there was no effect of insulin on net CBG binding capacity (Figure 3.7b). As with liver, net differences did not persist when CBG binding capacity was normalised to total CBG concentration (Figure 3.7c). No net differences in apparent 'cleaved' CBG were observed across muscle, except in the study 4 lean group (Figure 3.7d) following insulin treatment, suggestive of net release of cleaved CBG.

(a) Total CBG concentration (b) CBG binding capacity

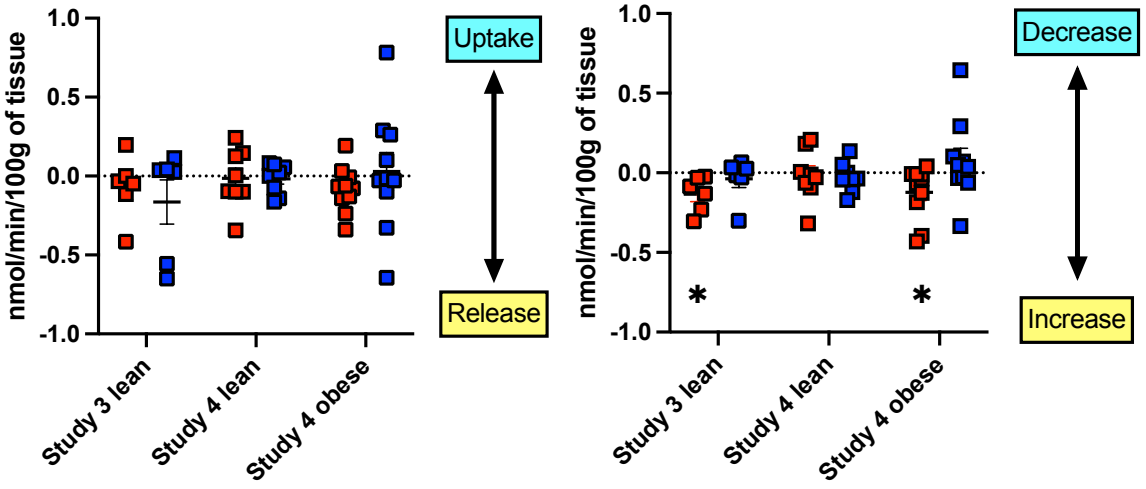

(c) Normalised CBG binding capacity (d) Cleaved CBG

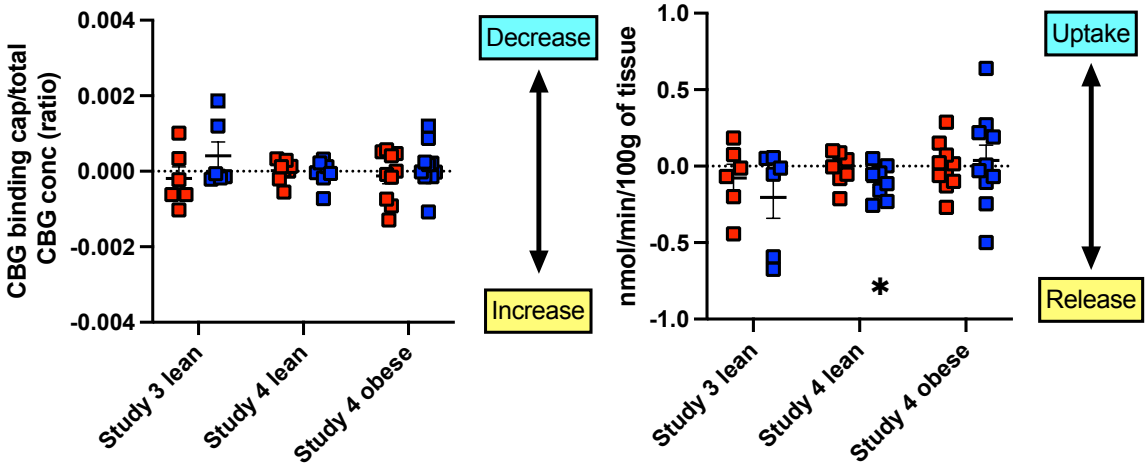

FIGURE 3.7 Arterio-venous differences in plasma CBG across skeletal muscle* in vivo *in humans

Data are mean ± SEM for plasma (a) CBG concentration, (b) CBG binding capacity, (c) CBG binding capacity normalised to CBG concentration and (d) apparent 'cleaved' CBG in study 3 lean (n=6), study 4 lean (n=8) and study 4 obese (n=10) groups following treatment with placebo (red squares) and insulin (blue squares). Comparisons with 0 were made using one sample t tests, or the Wilcoxon signed rank test if data were not normally distributed. Study 3 groups were compared by Wilcoxon matched-pairs signed rank tests, and study 4 groups by two-way repeated measures ANOVA. There was a net increase in CBG binding capacity across muscle in the study 3 lean (p=0.03) and study 4 obese (p=0.05) groups with placebo, suggesting net release of CBG (b). Net release of apparent 'cleaved' CBG across

muscle was seen in study 4 lean with insulin treatment (p=0.04) (d). No other net A-V differences were observed.

3.5.6 Adipose tissue (Studies 3 and 4)

No net differences in total CBG concentration or apparent 'cleaved' CBG were found across abdominal adipose tissue in any study 3 or 4 group (Figures 3.8a and 3.8d). CBG binding capacity decreased across adipose in both the lean and obese study 4 groups, suggesting uptake of CBG, but only following insulin treatment (Figure 3.8b). These small net changes in CBG binding capacity did not persist when adjusted for CBG concentration (Figure 3.8c).

(a) Total CBG concentration

(b) CBG binding capacity

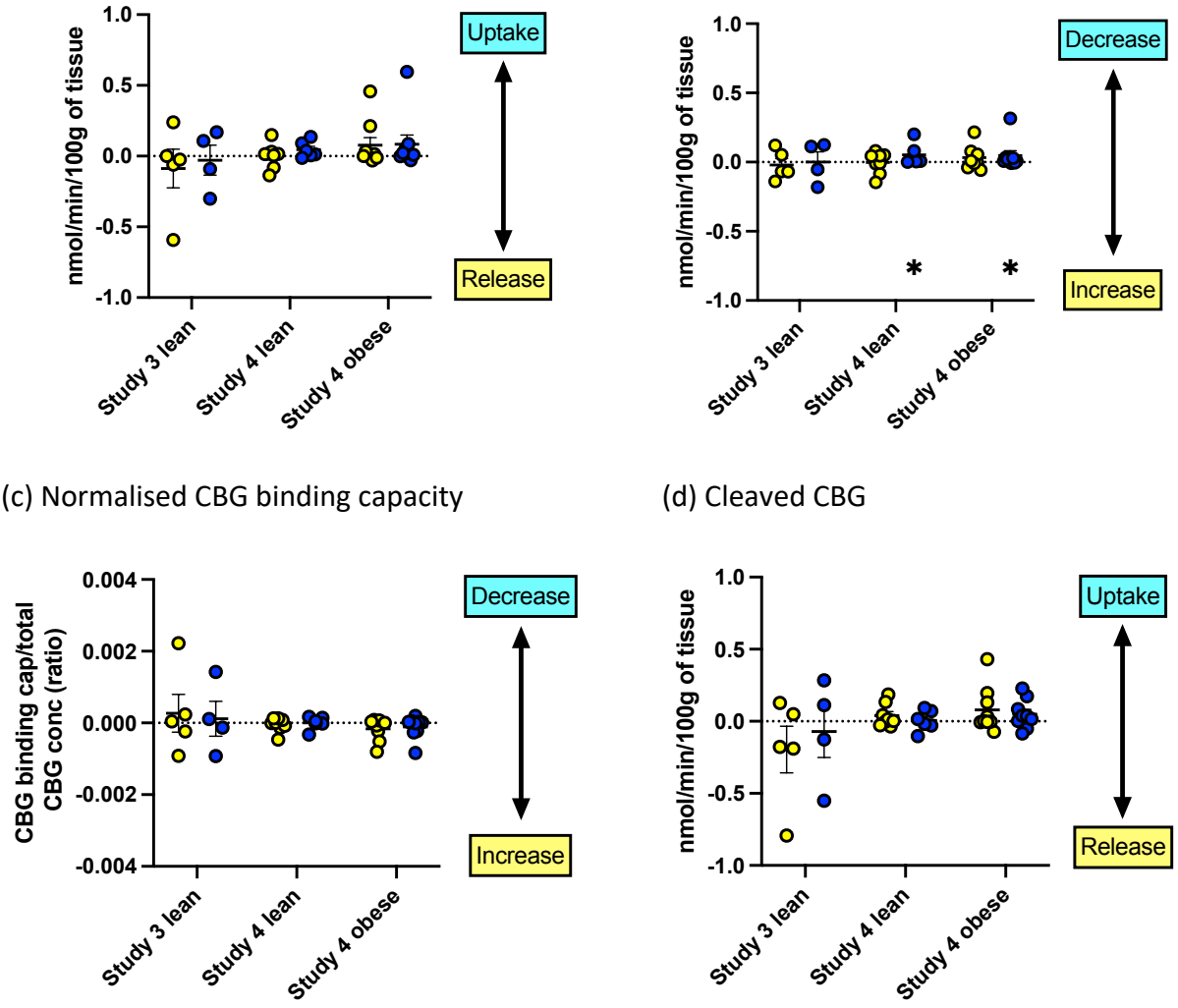

(c) Normalised CBG binding capacity

(d) Cleaved CBG

FIGURE 3.8 Arterio-venous differences in plasma CBG across adipose tissue* in vivo *in humans

Data are mean ± SEM for plasma (a) CBG concentration, (b) CBG binding capacity, (c) CBG binding capacity normalised to CBG concentration and (d) apparent 'cleaved' CBG in study 3 lean (n=6), study 4 lean (n=8) and study 4 obese (n=10) groups following treatment with placebo (yellow circles) and insulin (blue circles). Comparisons with 0 were made using one sample t tests. Study 3 group differences were compared by paired t tests, and differences between study 4 groups by two-way repeated measures ANOVA. There were no net A-V differences in total CBG concentration (a) or apparent 'cleaved' CBG across adipose tissue (d). In study group 4, there were net decreases in CBG binding capacity across adipose associated with insulin treatment in both lean (p=0.03) and obese (p=0.04) groups (b). This effect disappeared upon adjustment for CBG concentration (c).

3.6 Discussion

In this chapter we hypothesised that total CBG concentration and binding capacity is higher in lean than in obese subjects, due to enhanced NE-mediated CBG cleavage in obesity. We also hypothesised that total CBG concentration and binding capacity increase across liver as the principal site of CBG production, and decrease across target tissues due to NE-mediated CBG cleavage *in vivo*. We further hypothesised that insulin reduces total CBG concentration and binding capacity, due to downregulation of hepatic CBG production and enhanced CBG cleavage *in vivo*. Taken together our findings in this chapter refute the first hypothesis; we have shown that whole body total CBG concentration, CBG binding capacity and apparent 'cleaved' CBG do not differ by BMI. Total CBG concentration and binding capacity increased measurably across liver only in the obese group with T2DM, not in lean and otherwise healthy subjects. Contrary to our hypothesis, we could not detect any compelling evidence of *in vivo* cleavage of CBG across tissues including brain, skeletal muscle and abdominal adipose. Although insulin tended to reduce whole body total CBG concentration and CBG binding capacity in one study group (study group 3), there was only limited evidence that it decreased CBG binding capacity (indicative of CBG cleavage) in both the study 4 groups.

Our arterio-venous data from study of the total CBG concentrations and CBG binding capacity across the liver are perhaps the most interesting of these data. As the liver is the principal site of CBG production, we would expect to see a net release of CBG (as assessed by both CBG concentration and binding capacity) from the liver in lean, healthy individuals. What we actually see here is the reverse, with net uptake of CBG across the liver of lean subjects and

net release of CBG from the liver of obese subjects with T2DM. However, our results may not be as surprising when insulin resistance is taken into account; earlier data revealed that plasma total CBG concentrations were significantly increased in obese subjects with glucose intolerance (Fernández-Real et al., 1999). Endogenous and exogenous insulin do not affect circulating CBG concentrations in insulin resistant obese subjects, but in contrast insulin does decrease circulating CBG concentration in lean subjects (Fernández-Real et al., 2001). Our obese subjects with T2DM are likely to have a higher degree of insulin resistance than lean subjects, and since insulin downregulates CBG expression and secretion *in vitro* (Crave et al., 1995), it seems likely that differences in insulin resistance may, in part, explain the net release of CBG across liver in our obese group with T2DM treated with dietary modification or tablets (Moisan and Castanon, 2016).

It is perhaps less of a surprise that we could not detect any alterations in CBG concentration, binding capacity and apparent cleavage across the brain. Neutrophils in cerebrospinal fluid are commonly considered a pathological feature, often associated with e.g. sepsis or recent seizure (Dietzel et al., 2008). Outside of the setting of central nervous system (CNS) infection, it is unlikely that neutrophils would be present in the CNS in sufficient number and producing enough NE to bring out measurable alterations in cleavage of CBG here, but this is not known.

Relatively little is known about NE activity in skeletal muscle, the few studies which have been done have focused on acute inflammation caused by exercise and ischaemia-reperfusion injury (Rose et al., 1998; Wang et al., 2023). However, NE levels are higher in adipose tissue in both obese humans and animals compared with lean (Mansuy-Aubert et al., 2013) due to the presence of activated neutrophils (Talukdar et al., 2012). In this chapter we found no

convincing evidence of net arterio-venous differences in CBG concentration, CBG binding capacity or apparent 'cleaved' CBG across either skeletal muscle or subcutaneous adipose.

Our data have generated interesting observations about two CBG measures in particular – normalised CBG binding capacity, and apparent 'cleaved' CBG. On review of both whole body and tissue-specific CBG binding capacity, where arterio-venous net differences were seen (i.e. across the liver and to a lesser extent across muscle and adipose), they were not observed when appropriate adjustment was made for the actual total concentration of CBG present. Obesity is characterised by chronic inflammation therefore a like-for-like comparison with acute inflammation cannot be made, but this observation may challenge the interpretation that the fall in CBG binding capacity during acute inflammation occurs early due to proteolytic cleavage (Hammond et al., 1990a; Hill et al., 2016), with downregulation of hepatic CBG production occurring at a later stage due to subsequent high free glucocorticoid and cytokine (IL-6) levels (Emptoz-Bonneton et al., 1997; Hammond, 2016). What our data demonstrates here is that the major determinant of plasma CBG binding capacity is plasma total CBG concentration, and that changes in CBG binding capacity are a result of, and dependent on, changes in CBG concentration as opposed to proteolytic cleavage.

The results presented throughout this chapter enable an important observation to be made about the performance of the 9G12 ELISA used to produce a measure of RCL-intact CBG, from which apparent 'cleaved' was calculated (as described in full in section 1.2.7). 'Cleaved' CBG has been reported in bronchoalveolar lavage fluid of patients with inflammatory lung disease, yet CBG cleavage products were absent in serum from the same patients (Williams et al., 2009). It is still unclear whether CBG cleavage occurs in the circulation. If we assume it does,

the means by which RCL-cleaved CBG is metabolised also remains unknown. Despite this, there are numerous reports in the literature of the existence of RCL-cleaved CBG in the circulation (Nenke et al., 2016a; Nenke et al., 2016b; Nenke et al., 2017a; Nenke et al., 2016c; Nenke et al., 2015; Nenke et al., 2017c) which accounts for up to 30% of total CBG in plasma (Lewis and Elder, 2011). However, reduced levels of RCL-cleaved CBG in patients with abdominal obesity (Nenke et al., 2016c), AAT deficiency (Nenke et al., 2016a) and active rheumatoid arthritis (Nenke et al., 2016b) are paradoxical and difficult to explain since activated neutrophils in these conditions would be expected to increase CBG cleavage. Evidence for RCL-cleaved CBG within the circulation in these studies has been based solely on differences between CBG measurements in the two ELISAs described in section 1.2.7 (Lewis and Elder, 2011; Lewis et al., 2003). The data presented in this chapter demonstrate that discrepancies in these two ELISAs cannot be used to calculate or infer the presence of cleaved CBG. We observed a strong correlation between plasma total CBG concentration measured by the 12G2 ELISA and CBG binding capacity, but significant discordance between the 9G12 ELISA and CBG binding capacity values across all tissues studied. Further detailed study of the samples used in this chapter, and others, has shown that *N*-glycosylation may be responsible for the discordance between 9G12 ELISA values and the gold standard CBG binding capacity measurements. This is because *N*-glycosylation may mask the 9G12 antibody binding site within the RCL (Hill et al., 2019b). *N*-glycosylation has a significant influence on epitope availability and is particularly relevant here because the synthetic polypeptide used to develop the 9G12 monoclonal antibody was not glycosylated, and recognition of this epitope is likely influenced by the presence or absence of different *N*-glycans attached to the RCL sequence. Indeed, it has now been shown that an *N*-glycan at N347 within the CBG RCL limits the 9G12 antibody from recognising its epitope, whereas the 12G2 antibody reactivity is

unaffected (Hill et al., 2019a). The samples described in this chapter, together with those from other cohorts (including a group of critically ill patients), have been used to confirm that 'cleaved' CBG is absent in human plasma, a finding corroborated using both a heat-dependent polymerization assay and by mass spectrometry (Hill et al., 2019b).

The strengths of the analyses set out in this chapter are that we were able to study several measures of CBG concentration, binding capacity and cleavage both in whole body and across a range of target tissues, and evaluate the impact of BMI and insulin in multiple study groups. An obvious weakness is that we cannot provide evidence of inflammation or NE activity in the tissues studied, however (in adipose tissue) activated neutrophils are expected to be present (Dam et al., 2016) and cleaving the RCL. In addition, we studied only a single adipose tissue depot, when evidence suggests that adipose tissue depot heterogeneity may be important when considering the complexities of CBG cleavage and tissue GC delivery (Gulfo et al., 2016). An additional weakness is that small numbers of participants were included in each study group and so these studies have limited statistical power. A prior power calculation was not undertaken in the absence of any prior data on which to base estimates of variance of the outcome measurements, and because the samples had already been obtained in previous studies.

Another limitation is the use of historical samples, which has informed how these data have been presented, particularly in Figures 3.1-3.4. The samples from the 4 different studies, from which CBG measurements were made, were collected at different times over a 7-year period (between 2008 and 2015) and then assayed together by a collaborator in 2016. While all samples used were carefully stored at -80°C and kept frozen during transport to UBC where

the assays were performed, we cannot exclude the possibility of a decline in the quality of older samples (particularly those from studies 1 and 3) and this must be taken into account when comparing different study groups.

Our findings in this chapter do not support CBG cleavage as a physiological mechanism controlling cortisol delivery to tissues in the subjects tested. In view of our findings, the 9G12 ELISA will not be used in subsequent chapters of this thesis. It remains to be determined if CBG cleavage occurs in acute pathological inflammation or with perturbation of the NE/AAT system. The latter is the focus on the following two chapters which study the influence of AAT and NE in turn.

Chapter 4: The effect of alpha-1 antitrypsin deficiency on circulating and tissue glucocorticoids *in vivo* in humans

4.1 Introduction

CBG binds >85% of plasma cortisol and controls the circulating free cortisol pool. Proteolytic cleavage by NE is proposed to reduce CBG binding affinity and increase free cortisol availability to inflamed tissues (Hammond et al., 1990a). The CORtisol NETwork (CORNET) consortium found that genetic variation at a locus spanning *SERPINA1* (encoding AAT, the endogenous inhibitor of NE) and *SERPINA6* (CBG) contributes to morning total plasma cortisol variation (Bolton et al., 2014). In an extension of this GWAMA, trans-eQTL analysis by CORNET demonstrated effects on adipose tissue gene expression, which suggests that variations in CBG levels have an effect on delivery of cortisol to peripheral tissues (Crawford et al., 2021).

AAT deficiency predisposes patients to early-onset emphysema due to increased proteolytic destruction of lung parenchymal elastin from the inherent proteinase-antiproteinase imbalance (Greene et al., 2016). The term 'AAT deficiency' is used to cover a broad spectrum of subjects and a range of AAT reductions. As it is an autosomal recessive condition, homozygotes (Proteinase inhibitor ZZ genotype (PiZZ)) develop the disease and can become very unwell with plasma AAT levels that may be over 70% below the normal reference range, while compound heterozygotes (PiSZ/PiSS) may also exhibit clinical manifestations with plasma AAT levels 30-50% below the normal range (Ferrarotti et al., 2012). Heterozygotes for a deficiency allele and the wildtype M allele are usually asymptomatic despite having plasma AAT levels approximately 10-30% below normal (Ferrarotti et al., 2012); those heterozygous for mutations in AAT could therefore have altered CBG cleavage *in vivo* without confounding effects of systemic pathology.

In 2016, Nenke et al hypothesised that AAT deficiency may result in increased CBG cleavage *in vivo* due to uninhibited NE activity. They tested this in a small case-control study at a single tertiary centre in Adelaide, South Australia involving 10 patients diagnosed with AAT deficiency, and 28 healthy age-, gender- and BMI-matched controls (Nenke et al., 2016a). No differences in total CBG concentrations were found between the two groups, however the AAT patients with the most severe PiZZ phenotype had higher 'high affinity' CBG (p=0.0004), lower 'low affinity' CBG (p=0.01) and a higher proportion of 'high affinity' CBG as a percentage of total CBG (p <0.0001) than controls. There was a trend towards lower total, free and percentage of free cortisol in these two patients compared to controls. The authors concluded that their findings demonstrated for the first time that, despite low circulating levels of AAT and thus presumed excessive NE activity, proteolytic cleavage of CBG is paradoxically decreased in patients with AAT deficiency compared with healthy controls. The authors concluded that this suggests that NE may not be the primary mechanism for systemic CBG cleavage under "low inflammatory" conditions. However, these comparisons were confounded by the extent of systemic pathology and the use of exogenous GC therapy in the AAT-deficient patients.

An alternative approach to investigate the influence of AAT on CBG cleavage would be to study healthy carriers of *SERPINA1* mutations. These carriers exhibit mild 'subclinical' AAT deficiency, but crucially do not develop confounding comorbidities such as lung or liver disease (Ferrarotti et al., 2012). This paradigm provides an opportunity to assess the effect of a 10-20% reduction in AAT levels on CBG and GC measurements. Accordingly, we addressed these questions using a large clinical research study described in this chapter.

4.2 Hypothesis

We hypothesise that tissue cortisol delivery in subjects who are heterozygous for inactivating mutations in *SERPINA1* is amplified by increased CBG cleavage by NE in the circulation and within target tissues. We further hypothesise that increased CBG cleavage in peripheral tissues leads to increased negative feedback to HPA axis activity via changes in systemic free cortisol.

4.3 Aims

Specifically, we aimed to evaluate:

1. Whether CBG cleavage within, and cortisol delivery to, adipose tissue and muscle is increased in carriers of AAT deficiency
2. Whether increased CBG cleavage alters adipose tissue cortisol concentrations and expression of GC-regulated genes
3. Whether any differences in CBG cleavage and cortisol delivery alter HPA axis negative feedback

4.4 Methods

4.4.1 Ethical and research governance approvals

This study was approved by the Academic and Clinical Central Office for Research and Development (ACCORD) Medical Research Ethics Committee (AMREC) (reference 17-HV-032)

and by NHS Lothian Research and Development (2017/0193). Research support approvals were secured with the Wellcome Trust Clinical Research Facility (WTCRF), NHS Lothian laboratories and the pharmacy at the Western General Hospital (WGH). Informed consent was obtained from each participant.

4.4.2 Study design

16 asymptomatic carriers (cases) of AAT deficiency alleles (genotypes PiMS, PiMZ & PiSS in a 'first come' approach) and 16 non-carriers (controls, genotype PiMM) were recruited to this age, sex- and BMI-matched case-control healthy volunteer study examining the role of AAT in CBG cleavage and cortisol action. Participants attended for one screening visit, followed by 3 study visits (Figure 4.1). Visit 1 was at least 48 hours after screening, and visit 2 followed a minimum of 3 weeks after visit 1. Visits 2 and 3 were separated by at least one week to allow washout between visits.

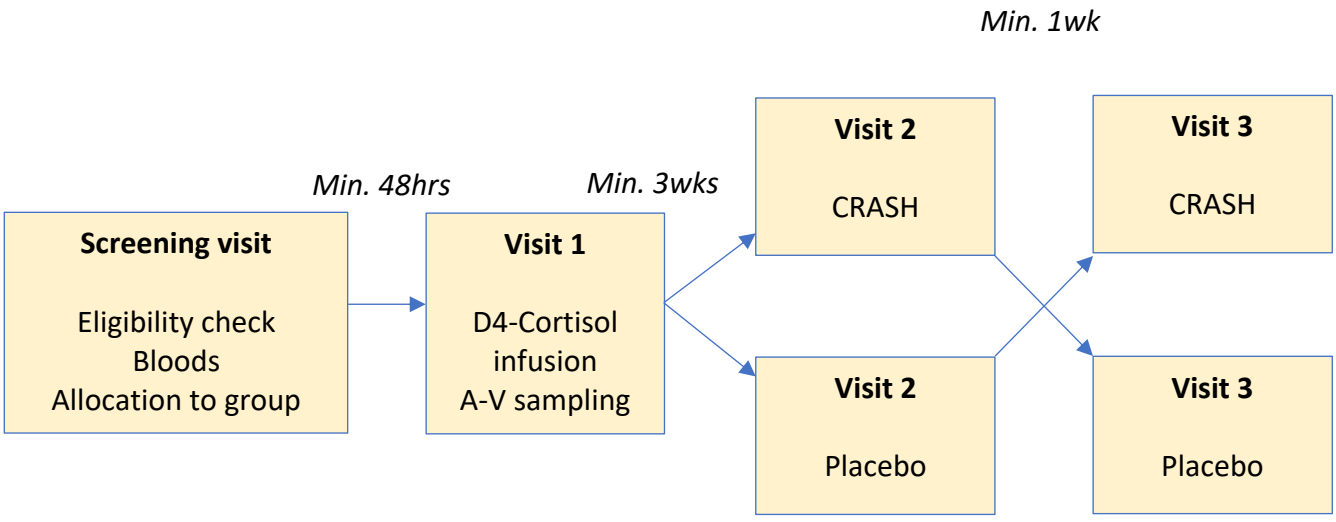

FIGURE 4.1 Study design

On study visit 1, to test the hypothesis that AAT deficiency leads to increased tissue GC exposure as a result of enhanced NE-mediated CBG cleavage, we obtained arterio-venous plasma samples across subcutaneous adipose and skeletal muscle at regular intervals during steady-state 9,11,12,12-$[^2H]_4$-cortisol (D4-cortisol) tracer infusion (Andrew et al., 2002). The tracer was infused in order to quantify *in vivo* whole body glucocorticoid appearance and clearance rates, and to estimate cortisol uptake by the tissues under study. We measured total CBG concentration (specific antibody ELISA (Lewis and Elder, 2011), see chapter 2.3) and binding capacity (radioligand-saturation assay (Hammond and Lähteenmäki, 1983), see chapter 2.4) and uptake/release of cortisol (total and free cortisol (total isotope dilution ultrafiltration), see chapter 2.10), adjusted for blood flow in adipose tissue (measured by ethanol microdialysis, (Felländer et al., 1996)) and in skeletal muscle (by venous occlusion plethysmography) (Hughes et al., 2012).

On study visits 2 and 3, the HPA axis was assessed with Combined Receptor Antagonist Stimulation of the HPA axis (CRASH) testing using spironolactone and RU486 (Mattsson et al., 2009) or placebo in a double-blind randomised crossover design. CRASH is a dynamic test used to evaluate endogenous negative feedback of the HPA axis using combined blockade of MR (with spironolactone) and GR (with RU486) (see section 1.1.4.1); a greater incremental effect of receptor antagonism to elevate plasma cortisol is consistent with higher tonic endogenous negative feedback. Randomisation was undertaken by Tayside Pharmaceuticals.

Adipose tissue biopsies taken at the end of all three visits were used to measure mRNA levels of glucocorticoid-responsive genes by quantitative real time PCR, and tissue glucocorticoid concentrations by liquid chromatography tandem mass spectrometry (Nixon et al., 2016).

4.4.3 Participant recruitment

Participants (n=32) from across Scotland were originally identified from the Generation Scotland (GS) biobank, using a recall-by-genotype recruitment strategy. They were then sent an invitation letter by GS with a copy of the participant information sheet (PIS) enclosed. Interested subjects who responded had a brief 'pre-screening' discussion on the phone, and if willing to proceed, a 1-hour screening visit at the WGH in Edinburgh was arranged at a mutually convenient time. At the screening visit, the study was discussed in detail with subjects and written informed consent was obtained. Eligibility was assessed through acquisition of relevant medical history, clinical examination and baseline blood tests. After screening, participants attended the WTCRF at the WGH (arriving fasted) for study visits on 3 occasions.

4.4.3.1 Inclusion criteria

- Aged 18-70 years
- Male or female
- Asymptomatic carriers and non-carriers of AAT deficiency (age-, sex- and body mass index-matched controls)
- Women of a childbearing potential who are willing to use a barrier method of contraception

4.4.3.2 Exclusion criteria

- Abnormal screening bloods (full blood count and renal, liver and thyroid function) of clinical significance
- Pregnancy, seeking to become pregnant, lactating females

- Active acute or chronic medical conditions requiring a therapy (including hormonal contraceptive use) which alters CBG or cortisol metabolism
- Oral, topical or inhalational corticosteroid use in the preceding six months
- Allergy to local anaesthetic

4.4.4 Sample size calculation

In our previously published work on tracer measurement in adipose (Hughes et al., 2012), the mean arteriovenous difference in D4-cortisol concentration across adipose tissue was 3.39 nmol/L, with a standard deviation of 0.95. An n of 16 per group provides 80% power to detect a 20% difference in subcutaneous adipose vein D4-cortisol concentration.

4.4.5 Clinical protocol

4.4.5.1 Visit 1

On visit 1 participants received a D4-cortisol tracer infusion (material from Cambridge Isotopes and prepared by Tayside Pharmaceuticals through filter sterilisation). Participants attended the WTCRF for their visit 1 at 8am, having fasted from 11pm the night before. On arrival, height, weight (clothed) and BMI were measured as per standard operating procedure. A self-standing height measurement was used to measure height to the vertex of the head with their shoes off and back of heels and head against the measuring board (to one decimal place).

An anterograde 22G cannula was positioned using an aseptic technique in the right antecubital fossa. This allowed blood withdrawal for measures including AAT and fasting

insulin, lipids and glucose. Subsequently, this cannula allowed for intravenous infusion of D4-cortisol. Participants were then provided a standard light breakfast, comprising cereal and toast (250 kcal) – caffeine was prohibited. After breakfast, the participant was cannulated using aseptic technique at three sites for blood sampling (Figure 4.2). A retrograde 20G intravenous cannula (Braun, Sheffield, UK) was inserted in the deep branch of the medial cubital vein in the antecubital fossa of the left arm for forearm skeletal muscle sampling. An inflatable cuff was placed at the wrist and inflated to 200 mmHg for 2 minutes prior to sampling to minimise contamination of blood from the hand. A further retrograde cannula was inserted in the dorsum of the left hand. The left hand was placed in a hot box (manufactured in house) heated to 60°C for 5 minutes prior to sampling in order to obtain arterialised samples. This technique has been shown to mimic arterial blood and has been used in previous clinical studies to avoid the need for invasive arterial cannulation (Hughes et al., 2012; Roddie et al., 1956; Stimson et al., 2009).

A branch of the superficial epigastric vein on the anterior abdominal wall was cannulated for adipose tissue sampling (Karpe et al., 2002). A 24G paediatric cannula (Braun, Sheffield, UK) was inserted using the Seldinger technique with the aid of a filtered red light (Frayn et al., 1989; Hughes et al., 2012). Sampling cannulae were kept patent with a slow infusion of 0.9% saline. Infusions were stopped and the 0.5 mL dead space was discarded before blood samples were obtained.

A microdialysis catheter (63 Microdialysis catheter, M Dialysis AB, Stockholm, Sweden) was inserted (using an aseptic technique and under local anaesthetic) lateral to the umbilicus, on

the side of the abdomen contralateral to the superficial abdominal wall cannula (see chapter 4.4.5.5.1).

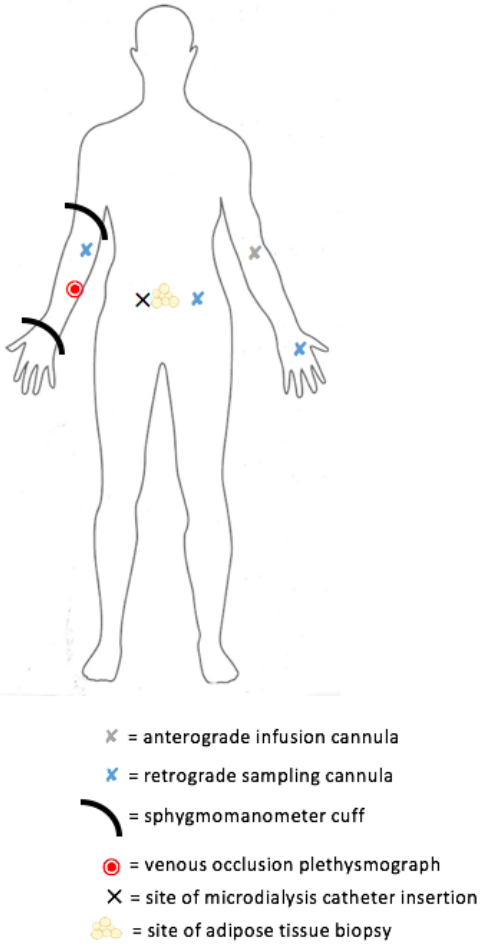

FIGURE 4.2 Participant set up for visit 1

At t-5 minutes, an intravenous bolus of 0.92 µmol D4-cortisol diluted in sodium chloride 0.9% was given over 4 minutes followed by an infusion (starting at t=0 minutes) at 17.2 nmol/min for 295 minutes (Figure 4.3) to achieve a steady state concentration of deuterated steroids of ~200nM by 2.5 hours. At t+275 minutes a subcutaneous abdominal adipose tissue biopsy was performed (see chapter 4.4.5.6) to enable measurement of tissue GC concentrations and GC-dependent transcript levels. At t+295 minutes following the adipose tissue biopsy, the D4-

cortisol infusion was stopped and all cannulae removed. At t+300 minutes participants were given lunch and allowed home. They were given their capsules for visit 2, and females with childbearing potential were also provided with a urine pregnancy test kit for the morning of visit 2, in case they had been randomised to receive RU486 on their second study visit.

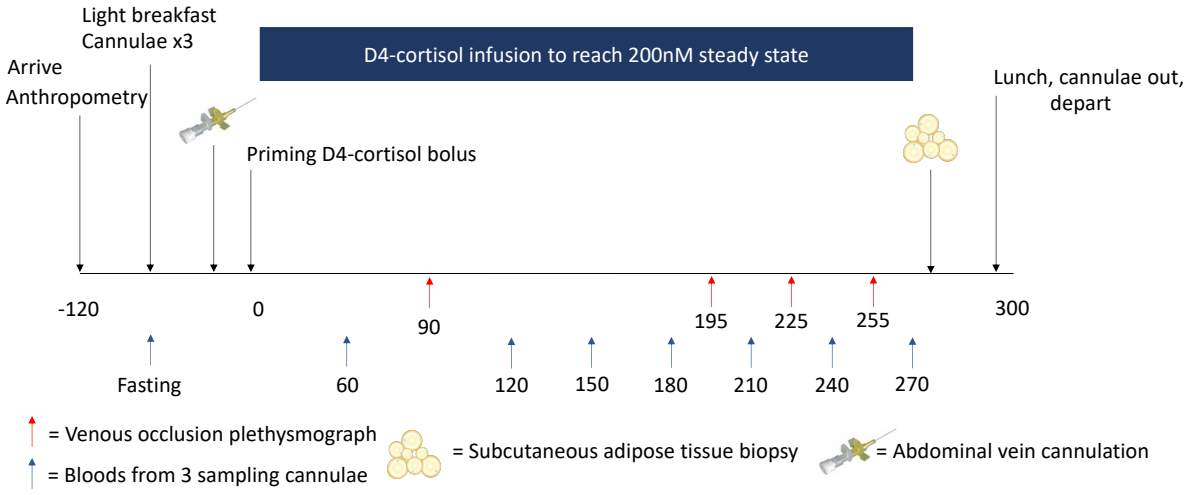

FIGURE 4.3 Study diagram for visit 1

4.4.5.2 Visits 2 and 3

On visits 2 and 3, participants took either placebo or spironolactone 200mg/RU486 400mg, administered twice on study visit days. These capsules were also manufactured by Tayside Pharmaceuticals. Participants were given placebo and spironolactone/RU486 in random order. Randomisation was undertaken by Tayside Pharmaceuticals and kept securely in a sealed envelope until all measurements were complete; the investigator was blinded to the investigational product but not to the genotype of participants. For visits 2 and 3, participants were asked to abstain from alcohol the night before, and to avoid caffeine after breakfast. Participants were provided written instructions; after taking their capsules at 11am, they were advised to have a brunch between 11am and 12pm (spironolactone and RU486 ideally

taken with food) and then to fast from noon. Participants presented to the WTCRF at 3.30pm, and following a blood pressure check, one anterograde 22G intravenous cannula was inserted in either arm for blood sampling. As during visit 1, this sampling cannula was kept patent with a slow infusion of 0.9% saline. The infusion was stopped and a dead space discarded before blood samples were obtained. A second dose of the capsules the participant had at 11am was dispensed by the WGH pharmacy, collected by the WTCRF research nurses and ingested by the participant at precisely 4pm. At t+215 minutes an abdominal adipose tissue biopsy was performed (see chapter 4.4.5.5). At t+230 minutes the sampling cannula was removed, a light supper was provided and then the participant was discharged (Figure 4.4).

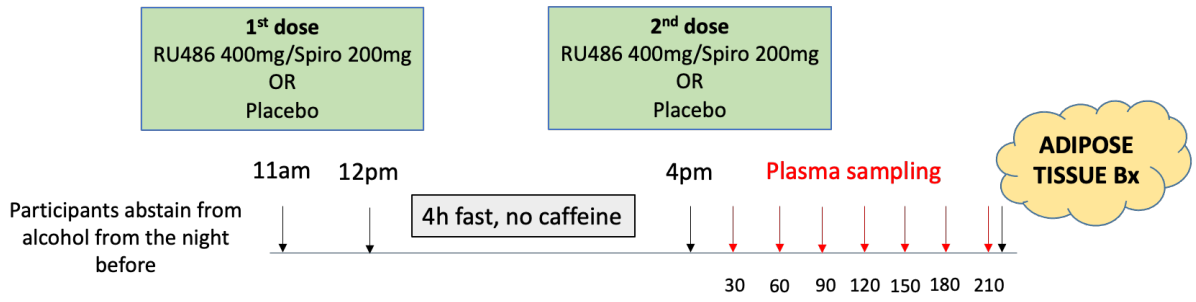

FIGURE 4.4 Study diagram for visits 2 and 3

4.4.5.3 Blood sampling protocol

During visit 1, plasma EDTA samples were taken from 3 sites: arterialised (4.9 mL), skeletal muscle (4.9 mL) and adipose tissue (2.7 mL). Samples were collected at t+60, t+120, t+150, t+180, t+210, t+240 and t+270 minutes (Figure 4.3). During visits 2 and 3, plasma EDTA samples were taken from the sampling cannula every 30 minutes between t+30 and t+210 minutes (Figure 4.4).

4.4.5.4 Sample collection and processing

Samples were obtained in plasma EDTA (2.7 and 4.9 mL) tubes (both Monovette®, Starstedt, Numbrecht, Germany). Samples were gently mixed by inverting several times. Plasma EDTA samples were subject to centrifugation at 2000 x g for 10 minutes at 4°C immediately after sampling. All samples were separated and stored at -80°C until analysis.

4.4.5.5 Blood flow measurements

Blood flow was measured during visit 1 in adipose tissue and skeletal muscle to allow tissue specific *in vivo* kinetic calculations.

4.4.5.5.1 Adipose tissue blood flow

Ethanol microdialysis was used to measure blood flow in abdominal subcutaneous adipose tissue (Felländer et al., 1996). 50 mmol/L ethanol in T1 perfusate (M Dialysis AB, Stockholm, Sweden) solution was made up for the microdialysis syringe pump. Ethanol absolute (17.196 mmol/L) was diluted (1:344) in T1 perfusate to a concentration of 50 mmol/L. 3 mL of the 50 mmol/L ethanol was drawn up and kept on wet ice until the pump infusion was commenced at t-10 minutes. The dual lumen microdialysis catheter was then inserted percutaneously using an aseptic technique, and under local anaesthetic into the subcutaneous abdominal adipose tissue as described in chapter 4.4.5.1 above. The probe at the end of this catheter sits in the tissue with a semipermeable membrane. At t-10 minutes the microdialysis pump was started, infusing 50 mmol/L ethanol in T1 perfusate at a rate of 1 µL/min. This rate was chosen to achieve an outflow:inflow ratio of 0.5, which was tested in preliminary method development work. Dialysate was collected in microdialysis vials which were changed every

30 minutes from t+0 to t+300 minutes, and snap frozen on dry ice before storage at -80^{o}C until analysis. The measured ethanol (see chapter 2.11) outflow (dialysate)/inflow (perfusate) concentration ratio is inversely proportional to adipose tissue blood flow, and has been shown to be a valid indicator of small changes within the physiological range (Felländer et al., 1996).

4.4.5.5.2 Skeletal muscle blood flow

Skeletal muscle forearm blood flow was measured using venous occlusion plethysmography (Hokanson et al., 1975; Rojek et al., 2007; Wilkinson and Webb, 2001). Venous occlusion plethysmography works on the principle that when venous drainage of the arm is interrupted, arterial inflow is unaltered and there is an increase in the circumference of the forearm directly proportional to blood flow (Wilkinson and Webb, 2001). For all blood flow measurements, the arm was supported on foam blocks at the elbow and wrist. A mercury-in-silastic strain gauge was applied across the mid forearm and blood flow was obstructed at the wrist using a cuff inflated to 200 mmHg. A further cuff was placed around the upper arm and rapidly inflated to 50 mmHg which is sufficient to occlude venous blood flow, but below arterial pressure. Intermittent inflation every 10 seconds, followed by deflation for 10 seconds and release of venous outflow above the forearm, resulted in dilation of the forearm which was detected by the strain gauge. This corresponds to arterial blood flow rate.

Calibration of the strain gauge was performed prior to each study visit so that 1% change in length of the gauge was equal to 1% change in limb volume. Forearm blood flow (mL/min/100g of tissue) was calculated from the slope of the voltage-time curve from the strain gauge using LabChart Reader (Version 8) software (AD Instruments, Oxford, UK). Four

measurements were taken during visit 1 (t+90, t+195, t+225 and t+255 minutes) and the mean flow rate calculated.

4.4.5.6 Biopsy of subcutaneous abdominal fat

Three biopsies of subcutaneous abdominal adipose tissue were obtained in total (at t+275 minutes during visit 1, and at t+215 minutes during visits 2 and 3) using an aseptic technique from a site lateral to the umbilicus. Local anaesthetic was injected (5mL of 2% lignocaine, Hameln Pharmaceuticals, Gloucester, UK) and a 14G 2.1x80mm needle (Braun, Sheffield, UK) with a 30mL syringe attached was inserted subcutaneously, directed towards the umbilicus. The plunger was withdrawn to create a vacuum and held in place with a 13 x 100 mm glass test tube. The sample of adipose tissue was collected in the syringe and placed on autoclaved aluminium mesh before washing with 0.1% DEPC treated water (chapter 2.2.1). The sample was then divided using autoclaved forceps and placed into three 2 mL microcentrifuge tubes (3 aliquots per biopsy) on dry ice before storage and stored at -80°C. Up to 2 attempts were made on each occasion.

4.4.6 Sample analysis

Full blood count as well as renal, liver and thyroid function, fasting glucose and insulin were assayed by Clinical Chemistry in the NHS Lothian laboratory, as described in chapter 2.6. In July 2019, Caroline Underhill (from UBC) measured CBG binding capacity by radioligand-saturation assay, as described in section 2.4. Plasma and tissue glucocorticoids and tracer levels were assessed by two LC-MS/MS methods (sections 2.8 and 2.9); the majority of this work was carried out by Natalie Homer, Scott Denham and colleagues in the University of Edinburgh Mass Spectrometry Core Facility. Subsequent data analysis and tracer kinetic

calculations were undertaken by Marisa Magennis, Ruth Andrew and Roland Stimson. Adipose tissue mRNA transcripts were measured using real-time PCR by Allende Miguelez-Crespo and Mark Nixon, as described in section 2.5.

I performed the remainder of the sample analysis. Serum AAT was measured by ELISA, as described in section 2.7. CBG concentration was measured by ELISA, as described in section 2.3. Free cortisol in plasma was quantified by isotopic dilution and ultrafiltration (section 2.10), and ethanol in microdialysis samples as set out in section 2.11. ACTH was measured using the ELISA described in section 2.12.

4.4.7 Data analysis

4.4.7.1 Tracer kinetics

The tracer D4-cortisol was used to quantify the rate of appearance and clearance of endogenous cortisol (the 'tracee'). The tracer:tracee ratio (TTR) (Equation 4.1) was used to determine the rate of appearance of cortisol and D3-cortisol once D4-cortisol concentrations were in steady state. The clearance of both tracer and tracee should be similar in order to calculate whole body rate of appearance. This was calculated for D4-cortisol using Equation 4.2 and compared to previously published clearance data for cortisol (Andrew et al., 2002).

Equation 4.1: **Tracer:tracee ratio**

$$TTR\ Cortisol = \frac{D4\ cortisol}{Cortisol}$$

Equation 4.2: **Clearance of D4-cortisol**

$$Clearance\ (L/min)\ = \frac{D4\ cortisol\ infusion\ rate\ (nmol/min)}{D4\ cortisol\ concentration\ (nmol/L)}$$

Rate of appearance (Ra) of cortisol and D3-cortisol were calculated from arterialised [A] measurements (using the mean of blood samples collected from T180-240) by dividing the rate of infusion of tracer by the corresponding TTR (Stimson et al., 2009; Wolfe and Chinkes, 2005). Concentrations are denoted by square brackets in the equations which follow below.

Ra of D3-cortisol provides a measurement of total cortisol regeneration by 11β-HSD1 (chapter 1.1.6.1), independent of adrenal production (illustrated in Figure 1.3); Ra of cortisol differs because this measure includes the adrenal contribution, in addition to 11β-HSD1 activity.

Equation 4.3: **Whole body Ra of Cortisol**

$$\text{Ra Cortisol} = \left(\frac{Rate\ of\ D4\ cortisol\ infusion}{\frac{D4F}{F} TTR[A]ss} \right)$$

Equation 4.4: **Whole body Ra of D3-cortisol**

$$\text{Ra D3 cortisol} = \left(\frac{Rate\ of\ D4\ cortisol\ infusion}{\frac{D4F}{D3F} TTR[A]ss} \right)$$

The rate of appearance of cortisol across tissues (skeletal muscle [M] and adipose tissue [F]) was calculated using arteriovenous differences in TTR whilst factoring in blood flow rate through the tissue (Equation 4.5).

Equation 4.5: **Ra Cortisol across tissue**

$$Ra\ Cortisol\ across\ tissue\ (pmol/100g\ tissue/min)$$

$$= \left(Tissue\ blood\ Flow\ (TBF) x \left[Cortisol_{Artery}\right] x \frac{\frac{D4F}{F} TTR_{Artery}}{\frac{D4F}{F} TTR_{Tissue}} \right)$$

$$- BF x \left[Cortisol_{Artery}\right]$$

Net balance of cortisol across skeletal muscle and was calculated to demonstrate either net release or uptake within the tissue. This was demonstrated by calculating the difference in arterial and tissue glucocorticoid concentration and multiplying by blood flow (Equation 4.6). Due to the semi-quantitative nature of the adipose tissue blood flow measurements, measurements across adipose tissue are presented merely as change in concentration.

Equation 4.6: **Net balance of cortisol across tissue**

$$Net\ balance\ (pmol/100ml\ tissue/min)$$

$$= \left[\left[Cortisol_{Artery}\right] - \left[Cortisol_{Tissue}\right] \right] x\ Tissue\ Blood\ Flow\ (TBF)$$

4.4.7.2 Statistical analysis

All data are mean ± SEM unless otherwise stated. Data were analysed using GraphPad Prism® (version 9.5.1) and checked for normality of distribution using the Kolmogorov-Smirnov test.

Differences in categorical variables between groups were tested using Fisher's exact test. Differences between groups in continuous variables were tested using unpaired t tests, or Mann-Whitney U tests if not normally distributed. Differences with 0 were tested using either one sample t tests, or Wilcoxon signed-rank tests if not normally distributed. Differences

between groups and over time were tested using two-way repeated measures ANOVA, and differences between groups and placebo/CRASH interventions over time by three-way repeated measures ANOVA. Due to occasional difficulties with sampling from the multiple sampling sites, there were a number of individuals with missing data points. Where these were minimal, specific time points were excluded in the analyses. When multiple data points were missing, data were combined by calculated average values for each subject during steady state. $P<0.05$ was considered significant.

mRNA transcript levels in adipose tissue were expressed in relation to the abundance of two housekeeping genes (see chapter 2.5). These data were compared using a two-way ANOVA.

4.5 Results

4.5.1 Characteristics of study participants

Characteristics of all participants are summarised in Table 4.1 below.

Abdominal adipose vein cannulation was technically challenging and ultimately unsuccessful on the majority of study visits. In total, 10 participants had adipose plasma samples available from visit 1 (for 7 $AAT^{+/-}$ participants and for 3 in the control group). Arterialised and skeletal muscle data are presented for all 32 participants, while adipose arterio-venous data are presented from those 10 participants with venous samples collected from the abdominal wall. However, adipose tissue biopsies were obtained from every participant on all 3 study visits.

TABLE 4.1 Participant demographic data

Data are number of participants (%) or mean ± SEM for baseline characteristics of subjects in control and AAT$^{+/-}$ groups. The sex composition of each group was compared using Fisher's exact test, fasting glucose was compared with an unpaired t test and comparisons for age, BMI, fasting insulin and Homeostatic Model Assessment for Insulin Resistance (HOMA-IR) by Mann-Whitney U tests. The two study groups were similar and there were no differences between them in respect of; sex (p=0.65), age (p=0.32), BMI (p=0.21), fasting glucose (p=0.88), fasting insulin (p=0.33) or HOMA-IR (p=0.40).

Baseline characteristics	**Control group**	**AAT$^{+/-}$ group**
Sex (females / males)	14 (87.5) / 2 (12.5)	12 (75.0) / 4 (25.0)
Age (years)	56.3 (2.7)	59.3 (2.4)
BMI (kg/m^2)	26.3 (0.9)	30.4 (2.2)
Fasting glucose (mmol/L)	5.0 (0.1)	5.0 (0.1)
Fasting insulin (pmol/L)	51.1 (5.4)	74.3 (17.4)
HOMA-IR	1.7 (0.2)	2.5 (0.7)

In the control group, participants were prescribed; stable doses of Levothyroxine (4), ramipril (2), ibuprofen (2), naproxen (1), co-codamol (2), fluoxetine (1), terbinafine (1) and colecalciferol (1). In the AAT$^{+/-}$ group, participants were prescribed; Levothyroxine (1), proton pump inhibitors (4), co-codamol (1), amitriptyline (1), fexofenadine (1), terbinafine (1), tolterodine (1) and statin therapy (1).

4.5.2 Serum AAT concentration

Mean serum AAT concentrations were almost 30% lower in the AAT$^{+/-}$ group than in controls, as shown in Figure 4.5. All participants had a normal set of liver function tests at screening.

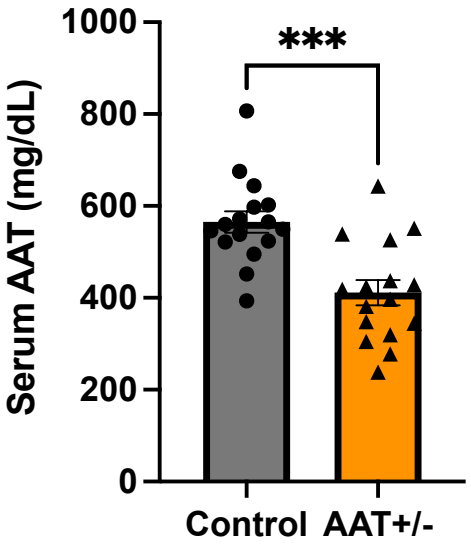

FIGURE 4.5 Serum AAT concentration by study group

Data are mean ± SEM for serum AAT concentration in the control (circles, grey bar) and AAT$^{+/-}$ (triangles, orange bar) groups (n=16 per group). Groups were compared using an unpaired t test. Mean serum AAT concentration was confirmed significantly lower in the AAT$^{+/-}$ group (p=0.0002 vs control).

4.5.3 Whole body CBG concentration and CBG binding capacity

Whole body (arterialised) CBG concentration and CBG binding capacity during steady state are shown in Figure 4.6. There were no differences between groups in either measure of CBG.

(a) CBG concentration

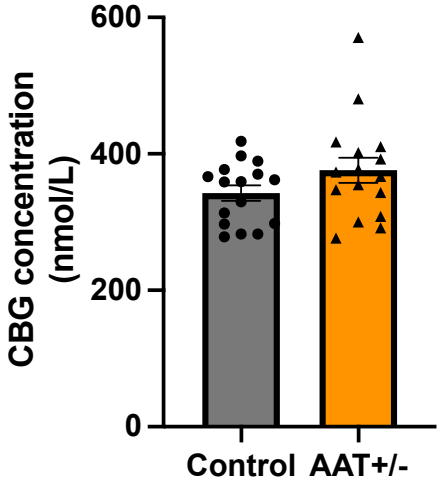

(b) CBG binding capacity

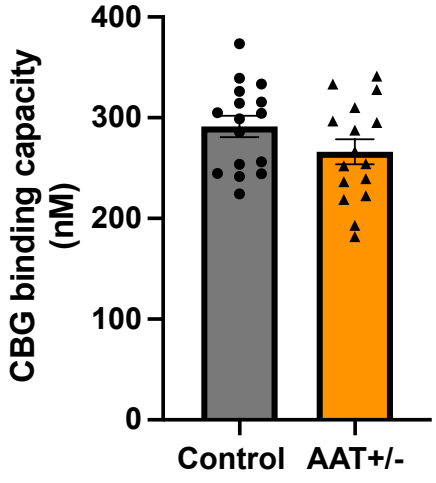

FIGURE 4.6 Whole body CBG concentration and binding capacity

Data are mean ± SEM for arterialised/whole body (a) CBG concentration and (b) CBG binding capacity in control (circles, grey bars) and AAT$^{+/-}$ (triangles, orange bars) groups (n=16 per group). Data presented for CBG concentration in (a) are from samples collected at two time points (180 and 240 minutes), for CBG binding capacity in (b) measurements at the 180 minute time point only. Comparisons between study groups were made using the Mann-Whitney U test for CBG concentration and using an unpaired t test for CBG binding capacity. There were no differences between the groups in respect of either CBG concentration (p=0.22) or binding capacity (p=0.13).

4.5.4 Whole body glucocorticoid measurements

4.5.4.1 Arterialised total cortisol measurements

Arterialised total plasma cortisol concentrations are presented in Figure 4.7. Arterialised plasma total cortisol declined over the time course visit 1 in both groups (p<0.0001), though tended to be higher (by a mean of approximately 20 nmol/L) in the AAT$^{+/-}$ group (p=0.08).

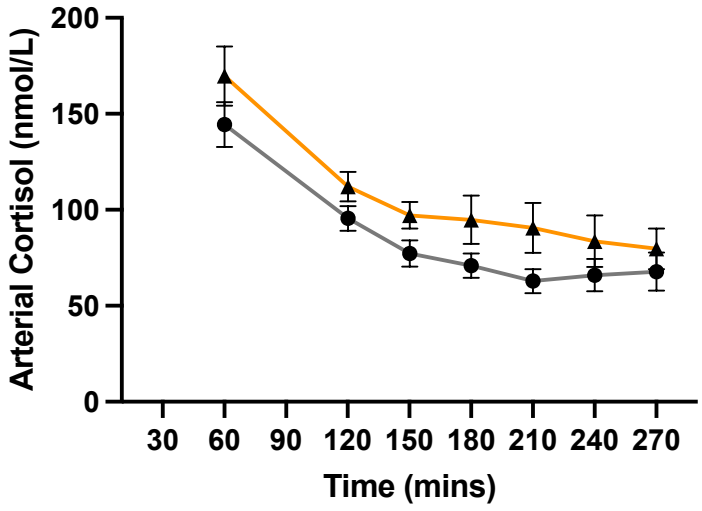

FIGURE 4.7 Arterialised total plasma cortisol concentrations

Data are mean ± SEM for plasma cortisol concentrations in arterialised samples at time points 60-270 minutes in control (circles, grey lines) and AAT$^{+/-}$ (triangles, orange lines) groups (n=16 per group). Comparisons between groups were tested using a two-way repeated measures ANOVA. Plasma cortisol decreased over time in both groups (p<0.0001 vs time) and there was a trend towards higher plasma cortisol in the AAT$^{+/-}$ group (p=0.08).

4.5.4.2 Arterialised free cortisol measurements

Arterialised free plasma cortisol percentages and concentrations during steady state are presented in Figure 4.8. Calculated arterialised plasma free cortisol fraction was higher in the AAT$^{+/-}$ group (p<0.0001), as was arterialised free cortisol concentration (p=0.01).

(a) Percentage free cortisol

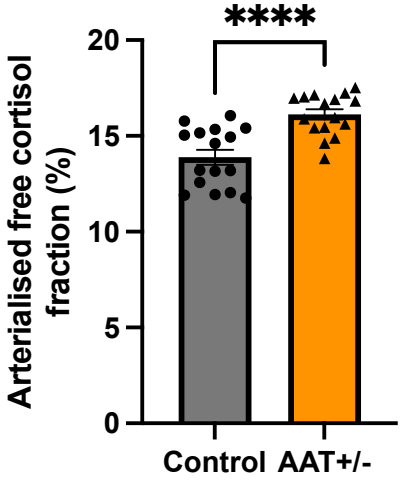

(b) Free cortisol concentration

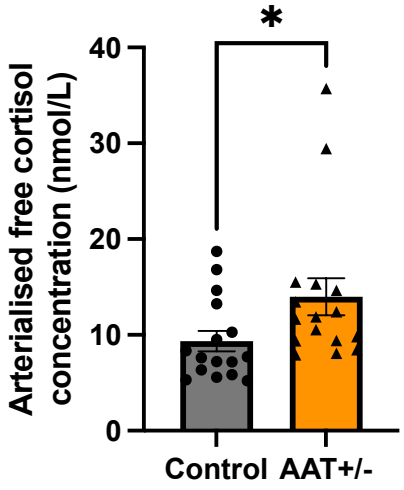

FIGURE 4.8 Whole body plasma free cortisol

Data are mean ± SEM for arterialised free cortisol (a) percentage and (b) concentration in control (circles, grey bars) and AAT$^{+/-}$ (triangles, orange bars) groups (n=16 per group). Data presented are the mean of measurements from samples collected at two steady state time points (180 and 240 minutes). Comparisons between study groups were made using an unpaired t test for percentage free cortisol,

and using the Mann-Whitney U test for free cortisol concentration. Arterialised plasma free cortisol percentage and concentration were higher in the AAT$^{+/-}$ group (p<0.0001 and p=0.01 respectively).

4.5.4.3 Arterialised tracer measurements

Arterialised D4-cortisol concentrations and enrichment with D3-cortisol were in steady state by 180 minutes, with the coefficient of variation for both the D4-cortisol:cortisol ratio and D4-cortisol:D3-cortisol ratio confirmed as less than 5% in both study groups by this time point (Figure 4.9). The ratio of D4-cortisol:Cortisol did not differ between groups, but the D4-cortisol:D3-cortisol ratio was higher in the AAT$^{+/-}$ group than in controls (p=0.049).

(a) D4-cortisol:Cortisol

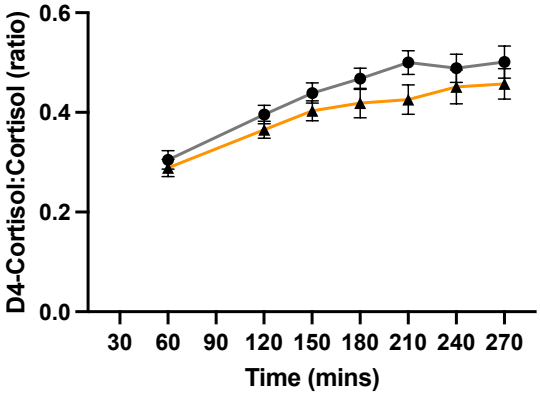

(b) D4-cortisol:D3-cortisol

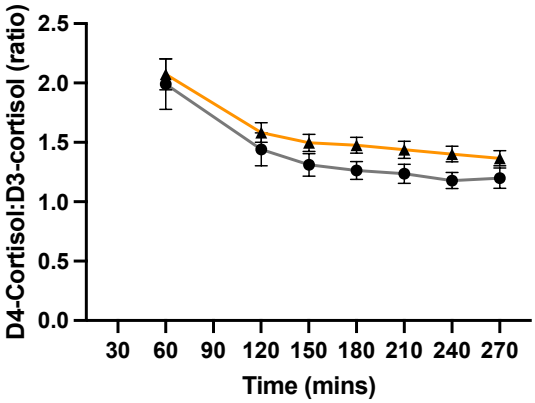

FIGURE 4.9 Arterialised tracer to tracee ratios

Data are mean ± SEM for the ratios of (a) D4-cortisol:Cortisol and (b) D4-cortisol:D3-cortisol in arterialised samples at time points 60-270 minutes in control (circles, grey lines) and AAT$^{+/-}$ (triangles, orange lines) groups (n=16 per group). D4-cortisol:Cortisol reached steady state by 180 minutes in both groups (coefficient of variation 3.19% for control, 4.29% for AAT$^{+/-}$) and steady state D4-Cortisol:D3-Cortisol was reached by 150 minutes in both groups (coefficient of variation 4.24% for control, 3.69% for AAT$^{+/-}$). Comparisons between groups were made using the mean of steady state values (180-270 minutes) and tested using unpaired t tests. There was no difference in the ratio of D4-cortisol:Cortisol

between groups (p=0.21), however the ratio of D4-cortisol:D3-cortisol was higher in the AAT$^{+/-}$ group (p=0.049 vs control).

4.5.4.4 Whole body rate of appearance of glucocorticoids

Plasma D4-cortisol concentrations and calculated clearance (using Equation 4.2) are shown in Figure 4.10. Clearance was unchanged over time once steady state was achieved and there was no difference between groups at any point (p=0.60).

(a) Plasma D4-cortisol concentration (b) D4-cortisol clearance

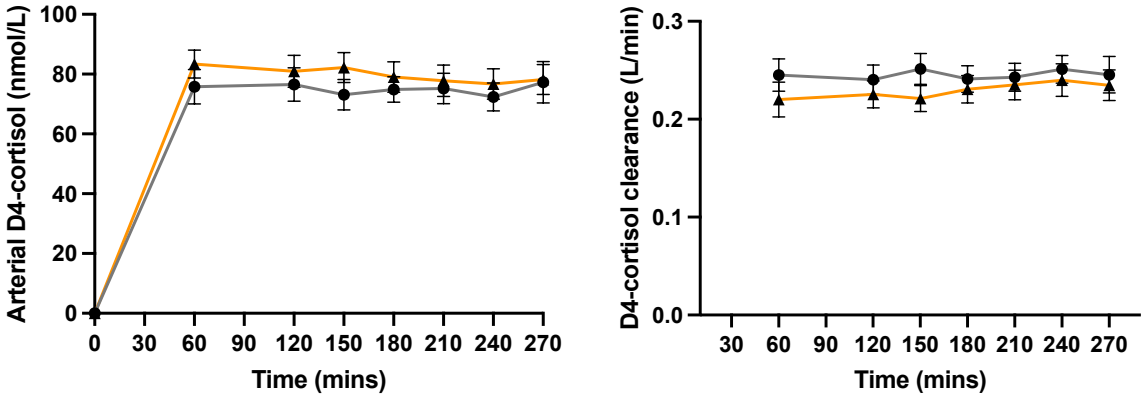

FIGURE 4.10 Arterialised D4-cortisol plasma concentration and clearance

Data are mean ± SEM for (a) plasma D4-cortisol concentration and (b) clearance of D4-cortisol in control (circles, grey lines) and AAT$^{+/-}$ (triangles, orange lines) groups (n=16 per group). Comparisons were tested by two-way repeated measures ANOVA during steady state (180-270 minutes). Steady state plasma concentration was achieved from 180 minutes with no significant difference thereafter against time (p=0.59 vs time) and no difference between groups (p=0.64). Clearance was unchanged with time or between study groups at steady state (p=0.54 vs time, p=0.60 comparing groups).

Whole body rate of appearance of glucocorticoids during steady state were calculated using Equations 4.3 and Equation 4.4, and the data is presented in Figure 4.11. Rate of appearance

of cortisol did not differ between the two groups (p=0.30), but rate of appearance of D3-cortisol (a specific measure of cortisol regeneration by 11β-HSD1) was significantly lower in the $AAT^{+/-}$ group (p=0.03 vs control).

(a) Whole body Ra of cortisol

(b) Whole body Ra of D3-cortisol

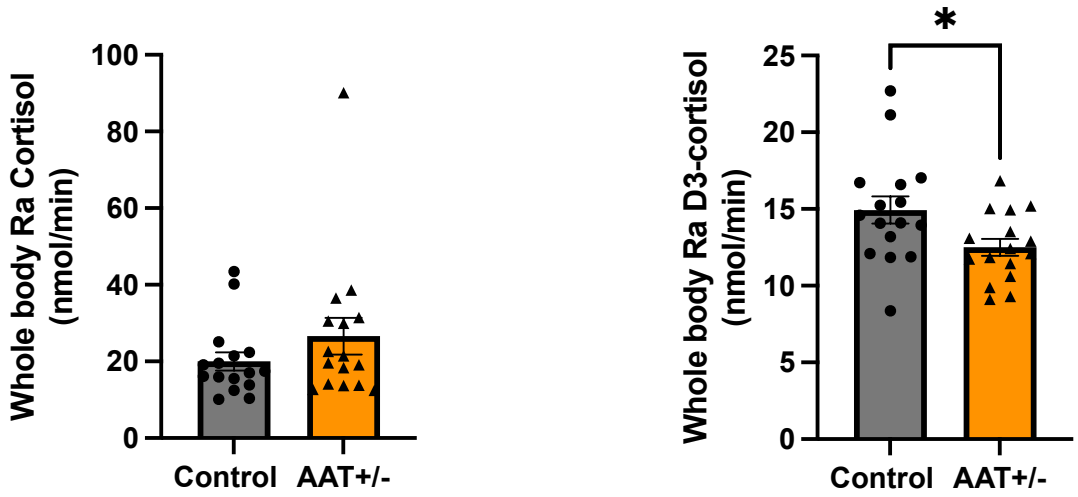

FIGURE 4.11 Whole body rate of appearance of cortisol and D3-cortisol

Data are mean ± SEM for whole body rate of appearance of (a) cortisol and (b) D3-cortisol in control (circles, grey lines) and $AAT^{+/-}$ (triangles, orange lines) groups (n=16 per group) during steady state (180-270 minutes). Comparison for Ra cortisol was tested by Mann-Whitney U test, and for Ra D3-cortisol by an unpaired t test. Whole body Ra cortisol did not differ between the groups (p=0.30), however Ra D3-cortisol was significantly lower in the $AAT^{+/-}$ group (p=0.03 vs control).

4.5.5 Skeletal muscle

4.5.5.1 Skeletal muscle blood flow

Skeletal muscle blood flow was measured on four occasions over the study period and is presented in Figure 4.12. Skeletal muscle blood flow did not change over time (p=0.81) and there were no differences between the groups.

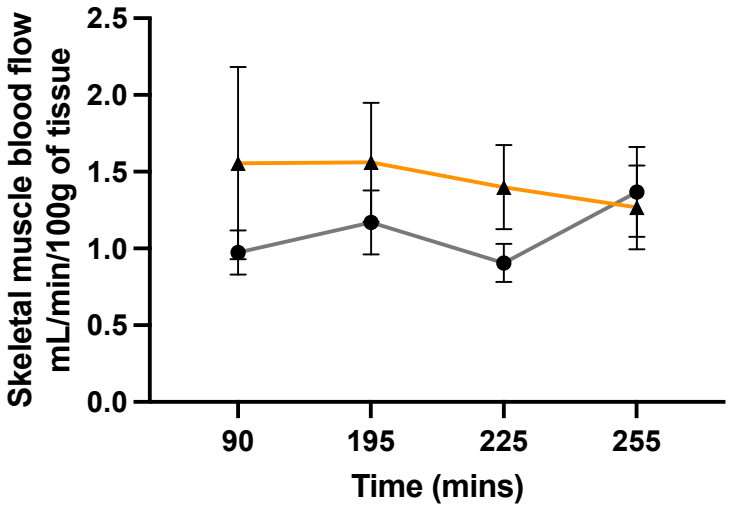

FIGURE 4.12 Skeletal muscle blood flow

Data are mean ± SEM for skeletal muscle blood flow at individual time points in control (circles, grey lines) and AAT$^{+/-}$ (triangles, orange lines) groups (n=15 per group). Comparison was made using two-way repeated measures ANOVA. There were no differences between the two study groups (p=0.24) and no change with time (p=0.81 vs time).

4.5.5.2 Net balance of CBG across skeletal muscle

Net balance of mean CBG concentration and mean CBG binding capacity in skeletal muscle during steady state are shown in Figure 4.13. CBG concentration in the skeletal muscle vein tended to be lower than in the artery, consistent with uptake of CBG across the tissue in both

groups (p=0.07 for AAT$^{+/-}$ and p=0.08 for control), but there were no differences between the two groups in net balance of CBG as assessed by either concentration and binding capacity.

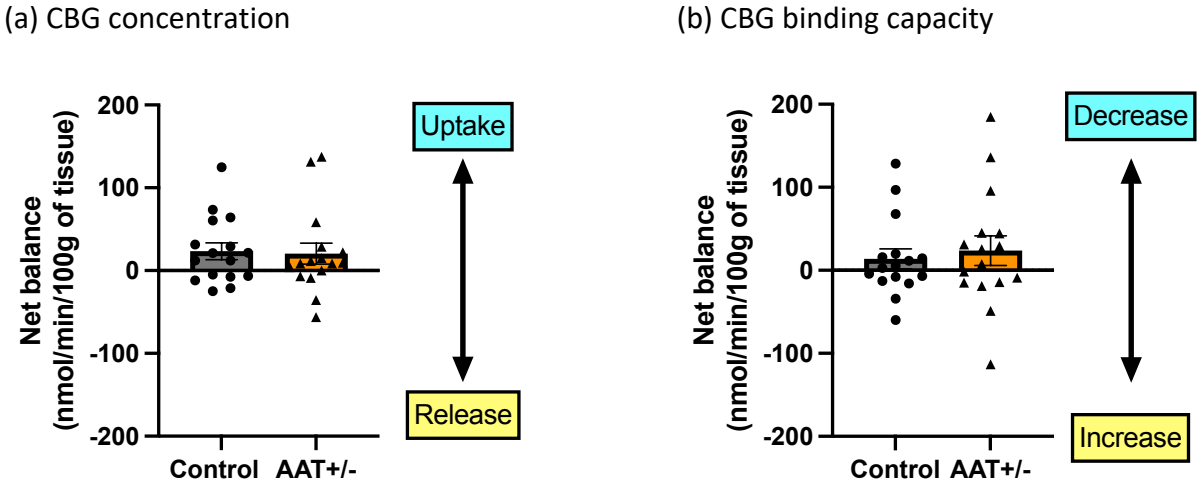

FIGURE 4.13 Net balance of CBG concentration and CBG binding capacity across skeletal muscle

Data are mean ± SEM for (a) net balance of CBG concentration and (b) net change in CBG binding capacity across skeletal muscle during steady state (data illustrated was calculated from the mean of two plasma samples collected at the 180 and 240 minute time points for net CBG concentration, but only from a single time point at 180 minutes for net CBG binding capacity) in control (circles, grey bars) and AAT$^{+/-}$ (triangles, orange bars) groups (n=16 per group). Comparisons with 0 were made using either one sample t or Wilcoxon signed-rank tests, and comparison between groups were made using multiple Mann-Whitney tests. There was a trend towards net uptake of CBG across skeletal muscle in both groups (p=0.07 vs 0 for AAT+/- and p=0.08 vs 0 for control). There were no differences between the groups in either net balance of CBG concentration (p=0.64) or change in binding capacity (p=0.69).

4.5.5.3 Net balance of glucocorticoids across skeletal muscle

Net balance of glucocorticoids in skeletal muscle are shown in Figure 4.14. During steady state there was net uptake of cortisol (p=0.03 vs 0), D4-cortisol (p=0.03 vs 0) and D3-cortisone (p=0.02 vs 0) in skeletal muscle in the control group only. Cortisol release across muscle was

higher in the AAT$^{+/-}$ group (p=0.01 vs control) and there was a similar trend for D4-cortisol (p=0.06). Net balance of cortisone and D3-cortisone were similar between groups.

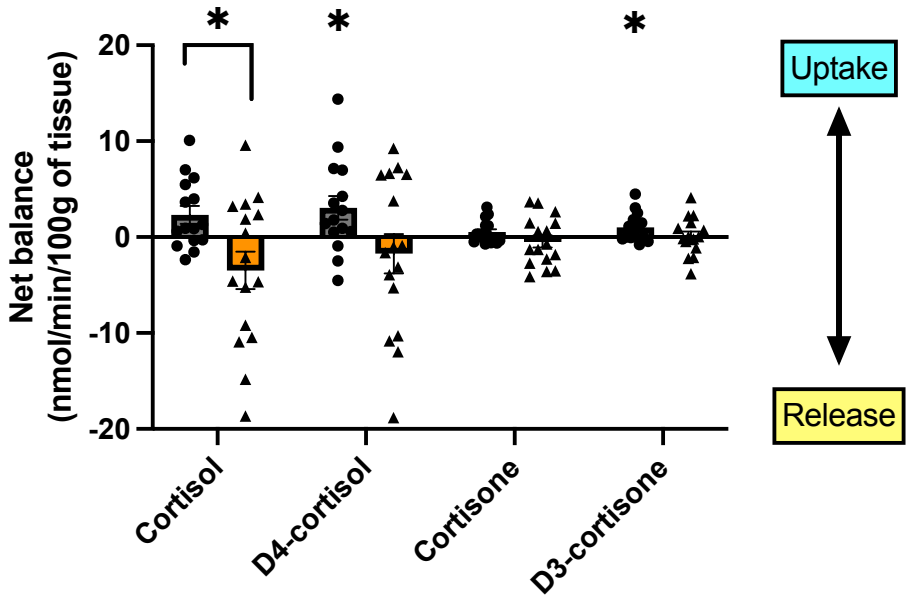

FIGURE 4.14 Net balance of glucocorticoids across skeletal muscle during steady state

Data are mean ± SEM for net balance of cortisol, D4-cortisol, cortisone and D3-cortisone across skeletal muscle during steady state (180-270 minutes) in control (circles, grey bars) and AAT$^{+/-}$ (triangles, orange bars) groups (n=15 for control and n=16 for AAT$^{+/-}$). Comparisons with 0 were made using one sample t tests for cortisol, D4-cortisol and D3-cortisone, and using the Wilcoxon signed-rank test for cortisone. Between group comparisons were made by multiple unpaired t tests for cortisol, D4-cortisol and D3-cortisone, and by the Mann-Whitney U test for cortisone. There was a net uptake of cortisol in the control group (p=0.03 vs 0) and a tendency towards net uptake of total cortisol in the AAT$^{+/-}$ group (p=0.09 vs 0). There was a net uptake of D4-cortisol in the control group (p=0.03 vs 0) but no difference in net balance of D4-cortisol the AAT$^{+/-}$ group (p=0.41 vs 0). No differences were observed in net balance of cortisone in either control (p=0.42 vs 0) or AAT$^{+/-}$ groups (p=0.50 vs 0). There was net uptake of D3-cortisone in controls (p=0.02 vs 0), but no difference in net balance of D3-cortisone in AAT$^{+/-}$ subjects (p=0.84 vs 0). The two study groups differed in net balance of cortisol (p=0.01), and there was

a trend towards a difference in net balance of D4-cortisol (p=0.06). There were no between group differences in net balance of cortisone (p=0.22) or D3-cortisone (p=0.15).

4.4.5.4 Rate of appearance of glucocorticoids across skeletal muscle

Rate of appearance of cortisol and D3-cortisol across skeletal muscle are shown in Figure 4.15. There was an increased rate of appearance of D3-cortisol in the $AAT^{+/-}$ group (p=0.04), consistent with increased cortisol regeneration by 11β-HSD1.

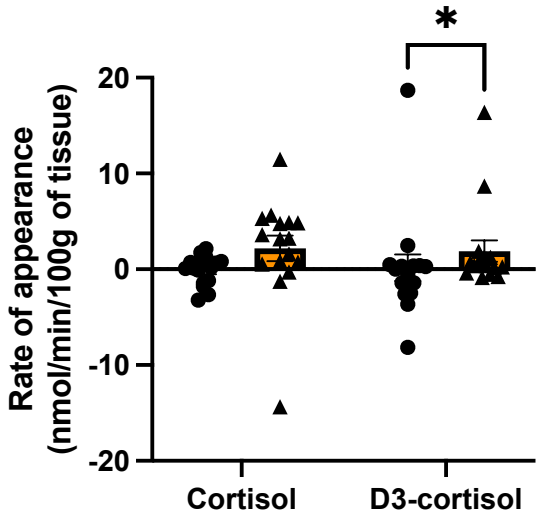

FIGURE 4.15 Rate of appearance of cortisol and D3-cortisol across skeletal muscle

Data are mean ± SEM for rate of appearance of cortisol and D3-cortisol in skeletal muscle during steady state (180-270 minutes) in control (circles, grey bars) and $AAT^{+/-}$ (triangles, orange bars) groups (n=16 per group). Comparisons with 0 were made using one sample t tests for cortisol, and Wilcoxon signed-rank tests for D3-cortisol. Comparisons between groups were made using an unpaired t test for cortisol, and the Mann-Whitney U test for D3-cortisol. There were no differences in rate of appearance of cortisol, either compared to 0 or between groups. There was an increased rate of appearance of D3-cortisol in skeletal muscle in the $AAT^{+/-}$ group (p=0.04 vs 0) and a significant difference between study groups in rate of appearance of D3-cortisol (p=0.04 vs control).

4.5.5.5 Net balance of free cortisol across skeletal muscle

Net balance of free cortisol in skeletal muscle is shown in Figure 4.16. Free cortisol tended to be higher in the skeletal muscle vein than the artery, consistent with release of free cortisol in the $AAT^{+/-}$ group (p=0.06), and there was a difference between the two groups (p=0.048).

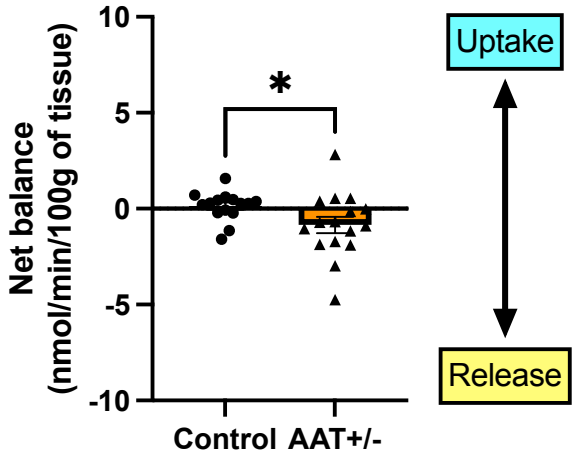

FIGURE 4.16 Net balance of free cortisol across skeletal muscle during steady state

Data are mean ± SEM for net balance of free cortisol across skeletal muscle during steady state (180-270 minutes) in control (circles, grey bars) and $AAT^{+/-}$ (triangles, orange bars) groups (n=15 for control and n=16 for $AAT^{+/-}$). Comparisons with 0 were made using one sample t tests, and between groups with an unpaired t test. There was no change in net balance of free cortisol in the control group (p=0.50 vs 0), while there was a trend towards net release of free cortisol in the $AAT^{+/-}$ group (p=0.06 vs 0). There was a significant difference between the two study groups in net balance of free cortisol (p=0.048).

4.5.6 Adipose tissue

4.5.6.1 Adipose tissue blood flow

Due to difficulties with adipose vein cannulation, data are presented for n=7 subjects in the $AAT^{+/-}$ group and n=3 subjects in the control group. These small numbers precluded statistical testing and between group comparisons of net balance of CBG and glucocorticoids in adipose tissue. The nature of the blood flow technique itself also prevents this from being fully quantitative. However, the results of the ethanol microdialysis (described in chapter 4.4.5.5.1) shown in Figure 4.17 suggest no difference in adipose tissue blood flow between the two study groups.

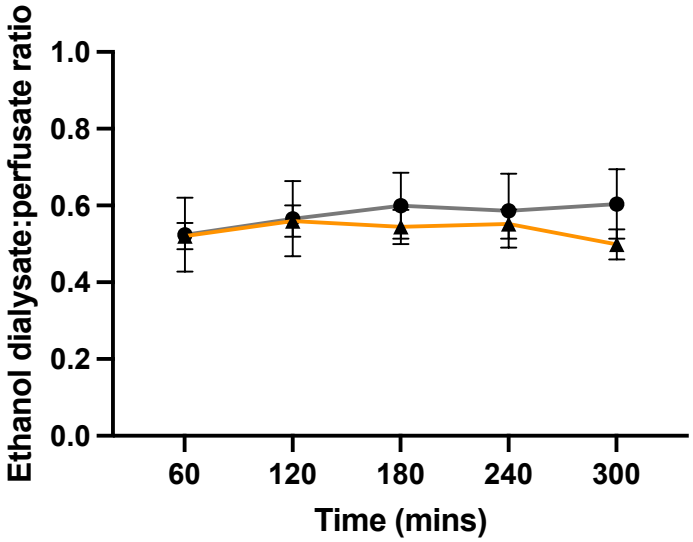

FIGURE 4.17 Adipose tissue ethanol washout

Data are mean ± SEM for ethanol dialysate:perfusate ratio (inversely proportional to adipose tissue blood flow) from ethanol microdialysis in adipose tissue at individual time points in control (circles, grey lines) and $AAT^{+/-}$ (triangles, orange lines) groups (n=3 for control and n=7 for $AAT^{+/-}$).

4.5.6.2 Change in CBG concentration and binding capacity across adipose tissue

Arterio-venous differences in mean CBG concentration and mean CBG binding capacity in adipose tissue (without taking blood flow into account) during steady state are shown in Figure 4.18.

(a) CBG concentration

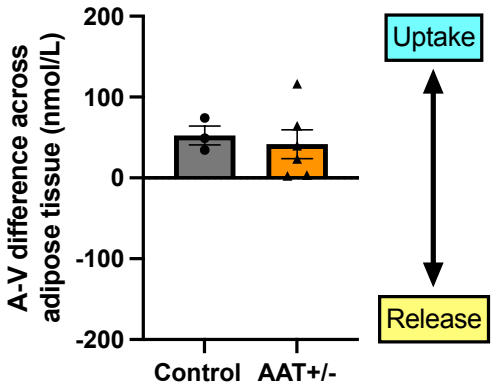

(b) CBG binding capacity

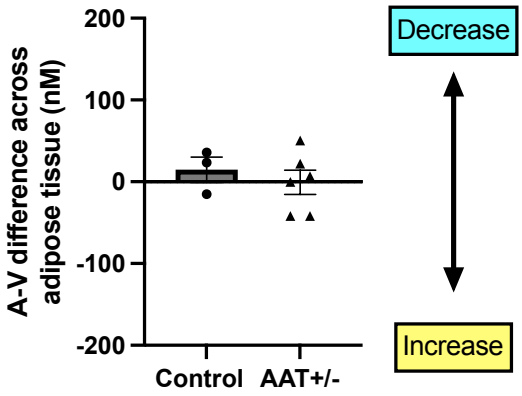

FIGURE 4.18 A-V differences CBG concentration and CBG binding capacity across adipose tissue

Data are mean ± SEM for arterio-venous differences in (a) CBG concentration and (b) CBG binding capacity across adipose tissue during steady state in control (circles, grey bars) and AAT$^{+/-}$ (triangles, orange bars) groups (n=3 for control and n=6 for AAT$^{+/-}$). No statistical comparisons (either vs 0 or between groups) were made due to underpowering.

4.5.6.3 Change in glucocorticoid concentrations across adipose tissue

Changes in the concentrations (arterio-venous differences without blood flow measurements) of glucocorticoids across adipose tissue during steady state are shown in Figure 4.19.

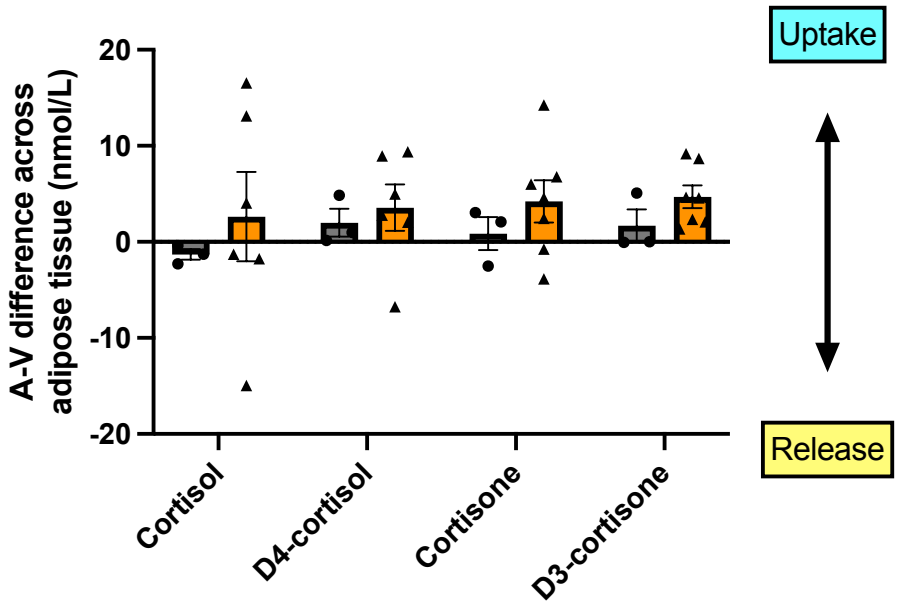

FIGURE 4.19 A-V differences in glucocorticoids across adipose tissue

Data are mean ± SEM for arterio-venous differences in cortisol, D4-cortisol, cortisone and D3-cortisone across adipose tissue during steady state in control (circles, grey bars) and AAT$^{+/-}$ (triangles, orange bars) groups (n=3 for control and n=6 for AAT$^{+/-}$). No statistical comparisons (either vs 0 or between groups) were made due to underpowering.

4.5.6.4 Change in free glucocorticoids in adipose tissue

Net balance of free cortisol is shown in Figure 4.20, expressed as both arterio-venous difference in percentage free cortisol, and arteriovenous difference in free cortisol concentration (again without inclusion of the corresponding blood flow measurements).

(a) Percentage free cortisol

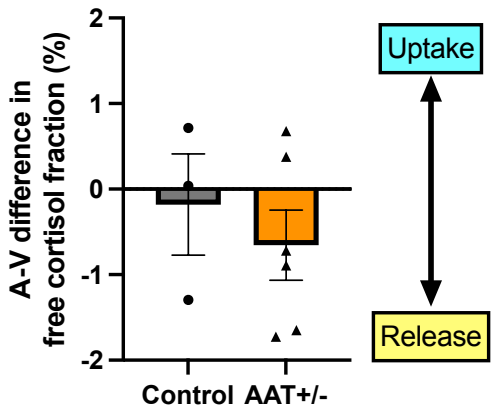

(b) Free cortisol concentration

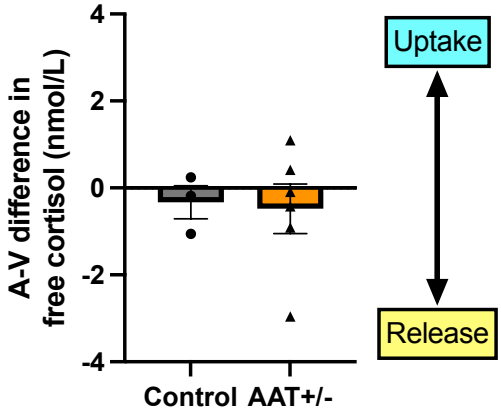

FIGURE 4.20 A-V differences free cortisol across adipose tissue

Data are mean ± SEM for arterio-venous differences in (a) percentage free cortisol and (b) free cortisol concentration across adipose during steady state in control (circles, grey bars) and AAT$^{+/-}$ (triangles, orange bars) groups (n=3 for control and n=6 for AAT$^{+/-}$). No statistical comparisons were made.

4.5.7 Concentrations of glucocorticoids in subcutaneous adipose tissue

Concentrations of glucocorticoids in subcutaneous adipose tissue are shown in Figure 4.21. Comparison is made between study groups using the adipose biopsy sample at the conclusion of visit 1 (t +275 minutes). Data are expressed as glucocorticoid concentration (ng) per mg of adipose tissue. While there were no between-group differences in adipose tissue concentrations of cortisone, cortisol or D4-cortisol, the concentrations of both D3-cortisol and D3-cortisone were lower in subcutaneous adipose tissue in the AAT$^{+/-}$ group than controls (p=0.04 and p=0.02 respectively).

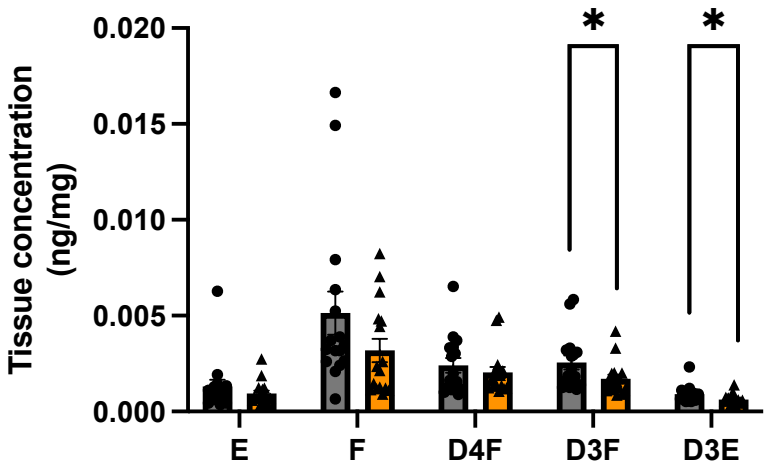

FIGURE 4.21 Concentrations of glucocorticoids in subcutaneous adipose tissue

Data are mean ± SEM for subcutaneous adipose tissue concentrations of cortisone, cortisol, D4-cortisol, D3-cortisol and D3-cortisone. Comparisons between the control (circles, grey bars) and AAT$^{+/-}$ (triangles, orange bars) groups were made with multiple Mann-Whitney U tests (n=16 per group). There were no differences between study groups in adipose tissue concentrations of cortisone (p=0.25), cortisol (p=0.12) or D4-cortisol (p=0.81), but D3-cortisol and D3-cortisone concentrations were both higher in adipose tissue in the control group than in the AAT$^{+/-}$ group (p=0.04 and p=0.02 respectively).

4.5.8 Glucocorticoid-responsive gene expression in subcutaneous adipose tissue

Expression of glucocorticoid responsive genes in subcutaneous adipose tissue are shown in Figure 4.22. Comparison is made between study groups using the adipose biopsy sample at the conclusion of visit 1 (t +275 minutes). Data were normalised to housekeeping controls. Gene transcripts were higher in the AAT$^{+/-}$ for PER1 (p=0.01), ATGL and HSL (p=0.04 for both).

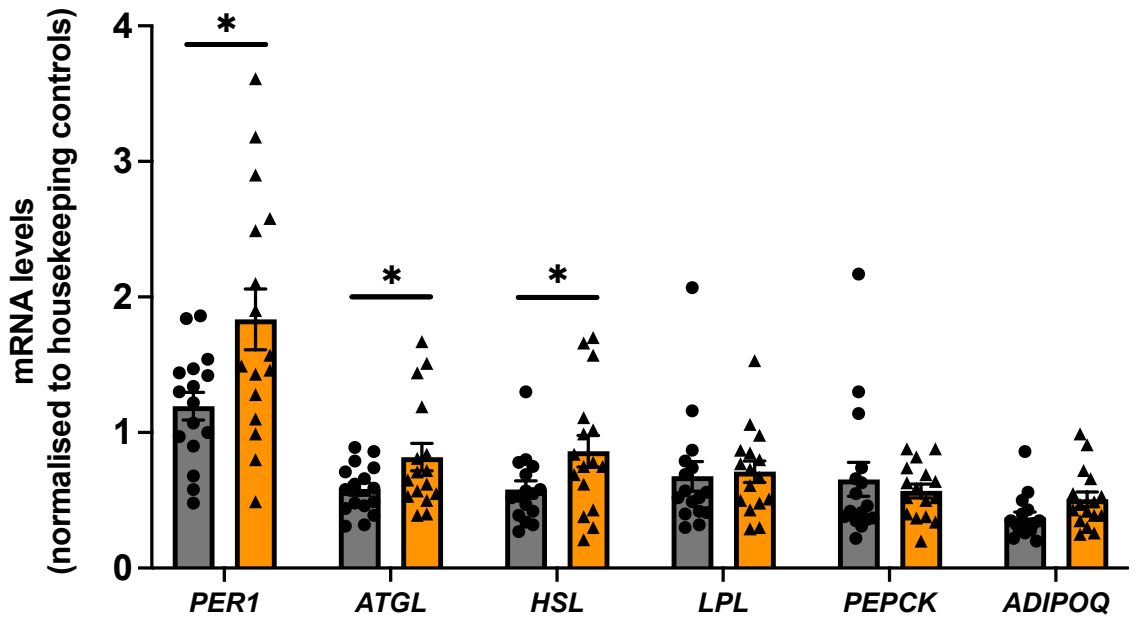

FIGURE 4.22 mRNA transcript levels of glucocorticoid responsive genes in subcutaneous adipose tissue

Data are mean ± SEM for mRNA transcript levels of glucocorticoid responsive genes Period Circadian Regulator 1 (PER1), Adipose Triglyceride Lipase (ATGL), Hormone-sensitive Lipase (HSL), Lipoprotein Lipase (LPL), Phosphoenolpyruvate carboxykinase (PEPCK) and Adiponectin (ADIPOQ). Data are expressed as a ratio to the mean of two housekeeping genes. Comparisons between control (circles, grey bars) and AAT$^{+/-}$ (triangles, orange bars) groups were made by multiple unpaired t tests (n=16 per group). Transcript levels of PER1, ATGL and HSL were higher in AAT$^{+/-}$ than in controls (p=0.01, 0.04 and 0.04 respectively). There were no significant between-group differences in the transcript levels of LPL, PEPCK or ADIPOQ.

4.5.9 CBG concentration during placebo and CRASH testing

During study visits 2 and 3, there was a trend towards higher CBG concentration in the AAT$^{+/-}$ group (p=0.06 vs control) during both visits, but there were no differences in CBG concentration by intervention (placebo or CRASH), nor over time using three-way ANOVA (Figure 4.23).

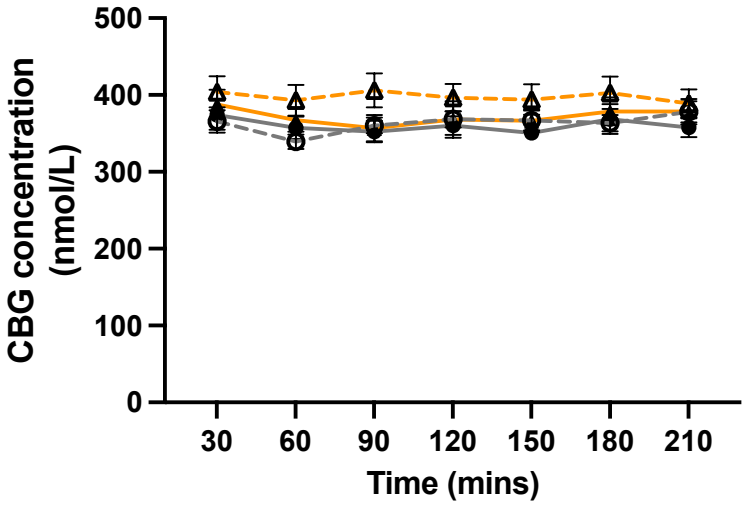

FIGURE 4.23 Plasma CBG concentration during placebo and CRASH testing

Data are mean ± SEM for CBG concentration during study visits 2 and 3 for; control during placebo (unbroken grey line, solid circles), AAT$^{+/-}$ during placebo (unbroken orange line, filled triangles), control during CRASH (dashed grey line, hollow circles) and AAT$^{+/-}$during CRASH (dashed orange line, hollow triangles) at time points 30-210 minutes (n=16 per group). Comparisons were made by three-way ANOVA. There was a trend towards higher CBG concentration in the AAT$^{+/-}$ group (p=0.06 vs control), but CBG concentration was not altered by intervention (p=0.22 placebo vs CRASH) or by time (p=0.15).

4.5.10 Total cortisol during placebo and CRASH testing

Plasma total cortisol gradually decreased over the course of study visits 2 and 3 with placebo ($p<0.0001$ vs time) as shown in Figure 4.24, and was increased significantly by CRASH testing ($p<0.0001$ vs placebo). Plasma total cortisol did not differ significantly between study groups during placebo or CRASH testing ($p=0.34$ for interaction of study group and placebo/CRASH test intervention).

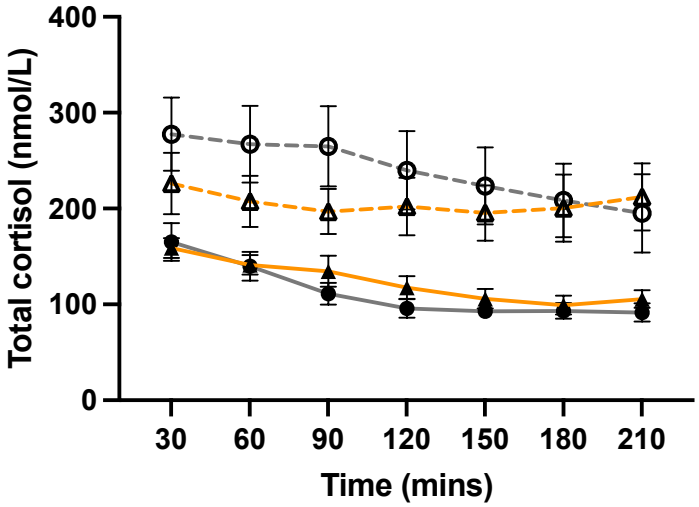

FIGURE 4.24 Plasma total cortisol during placebo and CRASH testing

Data are mean ± SEM for total cortisol during study visits 2 and 3 for; control during placebo (unbroken grey line, solid circles), AAT$^{+/-}$ during placebo (unbroken orange line, filled triangles), control during CRASH (dashed grey line, hollow circles) and AAT$^{+/-}$ during CRASH (dashed orange line, hollow triangles) at time points 30-210 minutes (n=16 per group). Comparisons were by three-way ANOVA. Plasma total cortisol was significantly altered by both time and CRASH testing (p<0.0001 for both). Control and AAT$^{+/-}$ groups did not differ significantly (p=0.67, however p=0.005 for interaction of group and time).

4.5.11 Free cortisol fraction during placebo and CRASH testing

Plasma free cortisol, expressed here as a percentage and shown in Figure 4.25, decreased over time (p=0.01). Plasma free cortisol fraction was higher in the AAT$^{+/-}$ group vs control (p<0.0001), and was significantly increased by CRASH vs placebo (p<0.0001). There was no interaction between CRASH and group (p=0.39), in keeping with an effect in both study groups.

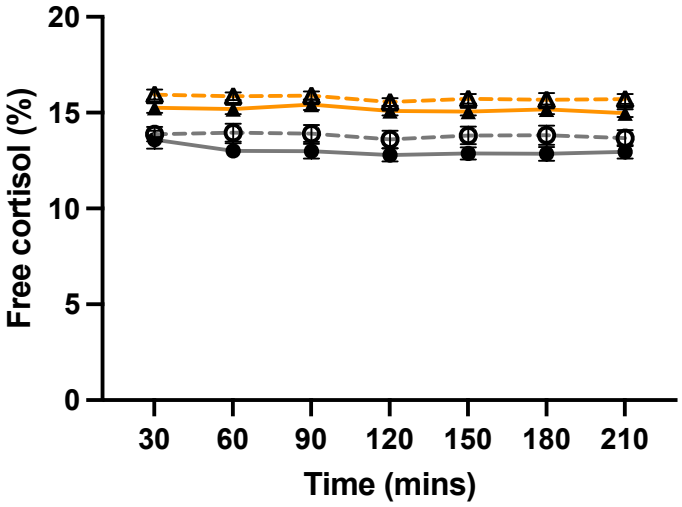

FIGURE 4.25 Plasma free cortisol fraction during placebo and CRASH testing

Data are mean ± SEM for free cortisol fraction during study visits 2 and 3 for; control during placebo (unbroken grey line, solid circles), AAT$^{+/-}$ during placebo (unbroken orange line, filled triangles), control during CRASH (dashed grey line, hollow circles) and AAT$^{+/-}$during CRASH (dashed orange line, hollow triangles) at time points 30-210 minutes (n=16 per group). Comparisons were made using three-way repeated measures ANOVA. Plasma free cortisol fraction was altered by time (p=0.01 vs time, p=0.80 for interaction of time and study group, p=0.68 for interaction of time and placebo/CRASH intervention). Plasma free cortisol fraction was higher in the AAT$^{+/-}$ group than in the control group (p<0.0001), and increased by CRASH testing as compared to placebo in both study groups (p<0.0001).

4.5.12 Free cortisol concentration during placebo and CRASH testing

Plasma free cortisol concentration during placebo and CRASH testing is shown in Figure 4.26. Free cortisol concentration was altered across time (p<0.0001) and was higher during CRASH testing in both study groups (p=0.0001 vs placebo). The AAT$^{+/-}$ group had higher free cortisol concentration (mean difference of 3.9 nmol/L), but only on the placebo arm (p=0.05 vs control).

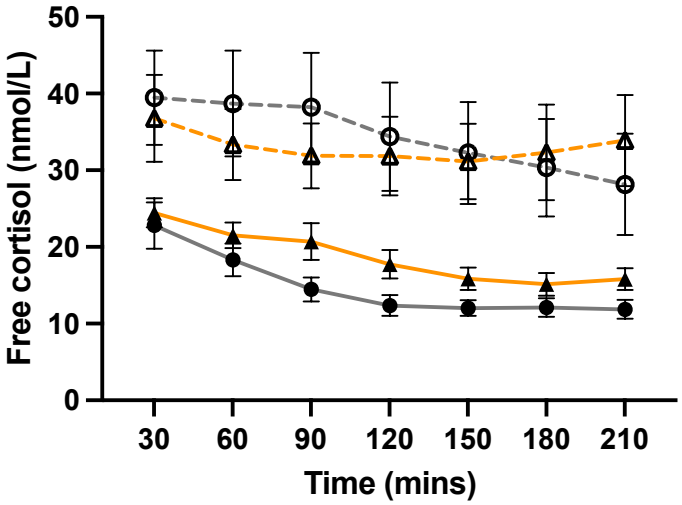

FIGURE 4.26 Plasma free cortisol concentration during placebo and CRASH testing

Data are mean ± SEM for free cortisol concentration during study visits 2 and 3 for; control during placebo (unbroken grey line, solid circles), AAT$^{+/-}$ during placebo (unbroken orange line, filled triangles), control during CRASH (dashed grey line, hollow circles) and AAT$^{+/-}$during CRASH (dashed orange line, hollow triangles) at time points 30-210 minutes (n=16 per group). Comparisons were made using three-way repeated measures ANOVA. Plasma free cortisol concentration declined over time (p<0.0001 vs time). Plasma free cortisol concentration did not differ significantly between the groups (p=0.79 for control vs AAT$^{+/-}$, p=0.06 for interaction of time and study group, p=0.48 for interaction of placebo/CRASH intervention and study group). Free cortisol was higher with CRASH testing in both groups (p=0.0001 vs placebo).

4.5.13 ACTH concentration during placebo and CRASH testing

Plasma ACTH during both placebo and CRASH testing is shown in Figure 4.27. ACTH was altered by time (p<0.0001) but there were no differences between control and AAT+/- groups, or between placebo and CRASH testing.

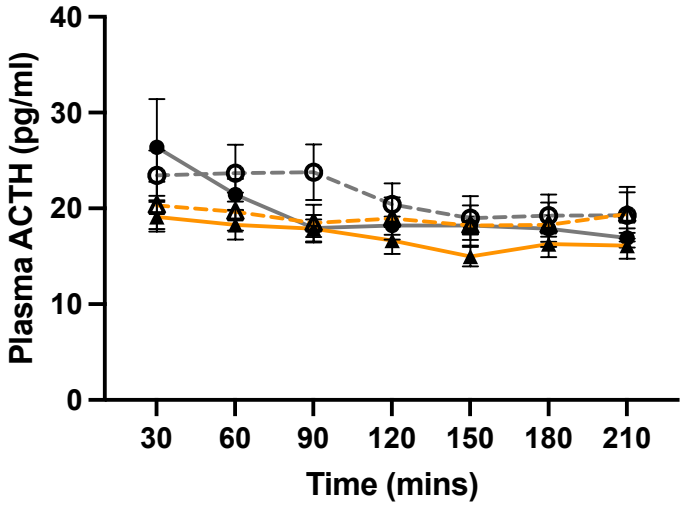

FIGURE 4.27 ACTH concentration during placebo and CRASH testing

Data are mean ± SEM for plasma ACTH concentration during study visits 2 and 3 for; control during placebo (unbroken grey line, solid circles), AAT$^{+/-}$ during placebo (unbroken orange line, filled triangles), control during CRASH (dashed grey line, hollow circles) and AAT$^{+/-}$ during CRASH (dashed orange line, hollow triangles) at time points 30-210 minutes (n=16 per group). Comparisons were made by three-way ANOVA. ACTH concentration decreased over time (p<0.0001 vs time, p=0.30 interaction of time and placebo/CRASH, p=0.17 interaction of time and study group), but ACTH was not altered by intervention (p=0.15 placebo vs CRASH) nor was there a difference between the study groups (p=0.30).

4.6 Discussion

In this chapter we hypothesised that delivery of cortisol to target tissues in AAT$^{+/-}$ subjects is amplified by increased NE-mediated CBG cleavage, and that increased CBG cleavage would lead to inhibition of HPA axis activity via changes in systemic free cortisol and increased negative feedback. We have some data in support this hypothesis; in visit 1 we observed greater whole body free cortisol, net release of free endogenous cortisol across skeletal muscle alongside higher expression of GC-responsive genes in adipose in the AAT$^{+/-}$ group,

which is consistent with greater tissue GC delivery and activity. In visits 2 and 3, again we found that $AAT^{+/-}$ participants had a significantly higher free cortisol fraction and free cortisol concentration than controls, although we found no alteration in HPA axis negative feedback as assessed by CRASH testing. However, we did not find measurable differences in CBG cleavage, either in the circulation or within target tissues; moreover, the tendency was actually towards higher total CBG concentrations in the plasma of $AAT^{+/-}$ individuals, contrary to our hypothesis. Interestingly, whole body rate of appearance of D3-cortisol was reduced in the $AAT^{+/-}$ group, consistent with decreased cortisol regeneration by 11β-HSD1. The reverse was found across muscle, where rate of appearance of D3-cortisol was increased, in keeping with increased cortisol regeneration by 11β-HSD1.

It is intriguing that no changes in CBG concentration or CBG binding capacity were observed in association with the increased free cortisol seen in the $AAT^{+/-}$ group, either in the circulation or across skeletal muscle. It has long been thought that NE-mediated CBG cleavage does not occur in the systemic circulation due to the presence of saturating levels of AAT (Hammond et al., 1990a); AAT is produced by the liver in an order of magnitude estimated at up to twice that of CBG production, therefore rapidly neutralises low circulating levels of NE (Henriksen, 2014). In our study, although the mean serum AAT concentration was almost 30% lower in the $AAT^{+/-}$ subjects compared with controls, it is therefore possible (or even probable) that the lower levels of AAT in these healthy volunteers are still sufficient to inhibit the low circulating levels of NE in plasma. However, the same cannot be said of muscle because there is scant evidence of NE activity in skeletal muscle in the literature, even in the settings of ischaemia-reperfusion injury (Rose et al., 1998; Wang et al., 2023), dystrophic muscle (Arecco et al., 2016) and intense exercise (Paulsen et al., 2013), none of which apply to our study. It is

plausible that cleavage of CBG does occur across skeletal muscle, but either we were unable to detect this using our existing techniques, or it occurs outside the vasculature in the interstitium. It is unclear why the higher free cortisol fraction observed in $AAT^{+/-}$ was associated with a trend towards higher plasma total CBG concentration in $AAT^{+/-}$ participants. One possibility is that CBG may not bind cortisol as effectively in $AAT^{+/-}$ subjects, another is that CBG cleavage does occur in tissues but we were simply unable to detect it in this study.

11β-HSD1 activity could be another reason why we found greater cortisol release across skeletal muscle in the $AAT^{+/-}$ group, but this seems unlikely as D4-cortisol follows a similar pattern of release, which is independent of 11β-HSD1. However, there is some evidence to suggest that greater GC concentrations can have a 'feed-forward' effect on 11β-HSD1 activity (Cooper et al., 2002; Morgan et al., 2014). This would be consistent with the increased rate of appearance of D3-cortisol we saw across muscle in the $AAT^{+/-}$ group, but does not explain the decreased whole body (i.e. predominantly liver) 11β-HSD1 activity, since a higher free cortisol fraction might be expected to also increase hepatic 11β-HSD1 activity in humans (Dube et al., 2015).

We can make even fewer inferences about CBG cleavage across adipose tissue in this study because these measurements were underpowered due to technical difficulties with the cannulations. However, interestingly we found increased expression of GC-dependent transcripts in adipose tissue biopsies in the $AAT^{+/-}$ group, which would be in keeping with increased GC action. This could potentially be as a result of altered NE-mediated CBG cleavage in $AAT^{+/-}$ across adipose, or due to greater free cortisol in the circulation, although this is despite no measurable difference between the groups in adipose tissue cortisol

concentration. Of the two techniques, tissue transcript levels are likely to provide a more reliable and robust estimate of GC action, and indeed the *PER1* mRNA levels we found are comparable to those our group has published previously (Anderson et al., 2020). In addition, our choice of housekeeping control genes used in RT-PCR, *PPIA* and *RNA18S5*, was informed by our previous study of glucocorticoid sensitive transcripts in adipose and brain (Kyle et al., 2022).

To our knowledge this is only the second *in vivo* study of CBG cleavage in the context of human AAT deficiency. Nenke et al reported in 2016 that CBG cleavage is paradoxically reduced in a small number of patients with a diagnosis of AAT deficiency (Nenke et al., 2016a). In their study serum free cortisol concentrations were found to be lower in AAT deficiency, with a trend towards a lower serum free cortisol fraction (Nenke et al., 2016a). In our study we have shown the reverse, with a higher free plasma cortisol fraction in AAT deficiency, which is in support of our hypothesis. However, the study by Nenke et al had a number of limitations which makes the interpretation of these data difficult and limits the generalisability of their findings. Calculations of supposed cleaved CBG in the case-control study by Nenke et al were based on measurements made using the ELISA targeting an epitope within the RCL of CBG (described in section 1.2.7), the limitations of which were discussed in detail in chapter 3.6. We have since confirmed that NE-cleaved CBG is absent in human plasma and discredited this ELISA (Hill et al., 2019b). Secondly, 8 of the 10 subjects in the AAT deficiency group were taking inhaled corticosteroids for COPD, and of the 2 remaining subjects in that group, one was on long term prednisolone (5mg/day); none of the 28 subjects in the control group were on exogenous corticosteroids – this is a critical confounder since we know glucocorticoids downregulate CBG production (Smith and Hammond, 1992). 'Active infection' formed part of

the exclusion criteria, but this would have been difficult to ascertain at enrolment especially since 3 participants in the study had used a high dose of oral corticosteroids during the month prior, ostensibly for (infective) exacerbations of COPD. Thirdly, serum AAT was measured in the patient group but not in controls, so it is uncertain whether AAT levels actually differed between the groups. The patients had a median AAT level of 28 mg/dL, compared with a normal reference range of 90-200 mg/dL. Additionally, morning cortisol samples were collected from AAT deficient subjects on average around an hour later than they were taken from controls, which could go some way to explaining why there was a trend towards higher total and free cortisol in the control group. Finally, while individuals with a previous liver transplant were excluded from participating in their study, no further information on liver function (an obvious potential confounder since it is the source of plasma CBG) was provided (Nenke et al., 2016a).

We have shown for the first time that in AAT deficiency, whole body 11β-HSD1 activity is reduced, but increased in skeletal muscle. It is unclear why 11β-HSD1 activity is altered in AAT deficiency, and further investigation is needed. It is possible that $AAT^{+/-}$ subjects have reduced liver function and 11β-HSD1 activity accordingly (albeit not detectable by liver function testing or without changes in cortisol clearance). We know that cytokines including TNF-alpha and IL-1 can upregulate 11β-HSD1 activity (Friedberg et al., 2003), while growth hormone (and/or IGF-1) inhibit 11β-HSD1 (Stewart et al., 2001). While we did not measure these compounds in this study, we measured fasting insulin, which is one of the most important known regulators of 11β-HSD1. An acute increase in circulating insulin with a hyperinsulinaemic euglycaemic clamp increased whole body and adipose tissue 11β-HSD1 activity *in vivo* (Wake et al., 2006). Generally the effects of insulin on 11β-HSD1 activity appear

to vary between individuals and tissues. The liver accounts for 11β-HSD1 activity almost entirely in non-obese humans (Basu et al., 2009; Stimson et al., 2009). *In vivo* obese euglycaemic individuals display downregulated hepatic 11β-HSD1 activity (Rask et al., 2001; Rask et al., 2002; Stewart et al., 1999); which is upregulated by the addition of relative insulin deficiency, as occurs in T2DM (Stimson et al., 2011). 11β-HSD1 activity in adipose tissue is positively correlated with obesity in both men (Rask et al., 2001) and women (Rask et al., 2002), and thought to potentiate adverse metabolic consequences to a greater degree in subcutaneous adipose than in visceral adipose tissue (Alberti et al., 2007). In our study of AAT deficiency in this chapter, matching was effective insofar as there were no statistically significant differences between groups. However, BMI, fasting insulin and HOMA-IR were numerically higher in the $AAT^{+/-}$ group, which may (at least partly) explain the reduced whole body 11β-HSD1 activity in AAT deficient subjects. It is unclear whether adipose tissue 11β-HSD1 activity is reduced in the $AAT^{+/-}$ group, because an insufficient number of blood flow measurements precludes statistical comparisons. In addition, the lower adipose tissue concentrations of D3-cortisol and D3-cortisone observed in $AAT^{+/-}$ may simply reflect lower delivery of these metabolites to adipose as a consequence of reduced whole body 11β-HSD1 activity. However, given that cortisone is not CBG-bound, it could be argued that the finding of reduced delivery of both D3-cortisol and D3-cortisone to adipose in $AAT^{+/-}$ again suggests that it is more likely to be 11β-HSD1 activity (as opposed to NE-mediated CBG cleavage) which is the greater determinant of adipose tissue GC exposure.

The opposite was seen in skeletal muscle in AAT deficiency, with 11β-HSD1 activity increased. Skeletal muscle is the major site of glucose disposal, and glucocorticoids are known to impair the insulin induced glucose uptake (Morgan et al., 2009). However, the activity of 11β-HSD1

in skeletal muscle in humans *in vivo* has been seldom studied hitherto. Myocyte 11β-HSD1 is negatively correlated with glucose disposal rate and positively correlated with BMI and systolic BP, which suggests a possible role in the development of the metabolic syndrome (Whorwood et al., 2002). Earlier studies are conflicting; while myotubes from obese patients with T2DM were shown to have a twofold increase in 11β-HSD1 mRNA compared with controls (Abdallah et al., 2005), ex vivo muscle biopsies from individuals with T2DM demonstrated downregulated 11β-HSD1 reductase activity, again attributed due to relative insulin deficiency (Jang et al., 2007). In the recently published work by our group, 11β-HSD1 dehydrogenase activity was reduced by insulin, but in lean men only (Anderson et al., 2020).

This study has a number of limitations. Our adipose arteriovenous data was limited to n=7 $AAT^{+/-}$ subjects and only n=3 controls due to technical difficulties with cannulation, and was therefore underpowered which precludes any statistical comparisons. Furthermore, the nature of the measurements of adipose tissue blood flow made using the ethanol microdialysis technique do not enable absolute quantitation of net GC uptake/release per time. However, informative data on adipose tissue glucocorticoid concentrations and transcript levels were available for the full n=16 in each group. We failed to reach the target steady state of plasma D4-cortisol concentration of 200 nmol/L, using a protocol similar to that our group used previously when administering D4-cortisol to patients with Addison's disease (Nixon et al., 2016). However, the approximately 135 mmol/L steady state concentration we reached (by adding D3-cortisol and D4-cortisol concentrations together) is very similar to that which was achieved in an earlier study by our group (described in chapter 3.4.1.3), when D4-cortisol was infused in healthy volunteers (Hughes et al., 2012). Another weakness of this study is that we have no measurement of neutrophils or NE activity, either

in the circulation or across tissues, an important aspect which will be explored further in chapter 5. Our measurement of CBG binding capacity in this study was limited to visit 1, primarily due to sample availability as well as logistics issues, as this assay was provided by a collaborator. However, we know from the data presented in chapter 3 that the ELISA we used to measure the concentration of total CBG provides an accurate estimation of CBG binding capacity, and the two measures are closely correlated (Hill et al., 2019b). We must also acknowledge the uncertainties of the CRASH test; firstly, it is not be possible to determine whether any alterations in negative feedback detected by this test are due to impaired GR function, or due to reduced MR expression in the CNS. Other possibilities, which may affect the endogenous feedback signal, include impaired cortisol transport into the CNS (Mattsson et al., 2009), altered CNS 11β-HSD1 activity (Sandeep et al., 2004) or heterodimerization of GR and MR in the CNS (Trapp et al., 1994). While only GR and MR are involved in HPA axis negative feedback, a further limitation of the CRASH test is that neither RU486 nor spironolactone are completely selective, since RU486 is a progesterone receptor antagonist and spironolactone an androgen receptor antagonist (Mattsson et al., 2009).

However, the strengths of our study are that we did demonstrate a significant difference in mean serum AAT concentration between the groups, without the risk of confounding by co-morbidities or exogenous glucocorticoid use. All participants in our study had normal liver function, supported by the finding of no difference in D4-cortisol clearance between groups. The two study groups were also well matched otherwise, not only in respect of age, BMI and sex; there were no differences between the groups in glucose, insulin or HOMA-IR, which could all have altered our measurements of CBG and 11β-HSD1 reductase activity in this study.

Our data represents the first evidence that AAT deficiency is associated with a higher plasma free cortisol fraction *in vivo* in humans. However, we were unable to demonstrate enhanced CBG cleavage in AAT deficiency, and our data raise the possibility that 11β-HSD1 reductase activity may be an important determinant of tissue cortisol exposure in human AAT deficiency. Having addressed the role of AAT, the next chapter will focus on the role of NE in the context of acute inflammation.

Chapter 5: The effect of pharmacological inhibition of neutrophil elastase on CBG cleavage *in vivo* in humans

5.1 Introduction

CBG is an important biomarker of inflammation onset and severity; plasma CBG levels fall in response to an acute inflammatory insult, and thus it has been described as a 'negative' acute phase reactant (Hill et al., 2016). CBG is proposed to act as a reservoir for glucocorticoids, which could be released if its RCL is cleaved between the valine[344] and threonine[345] residues by NE at sites of inflammation (Hammond et al., 1990a). During inflammation, reductions in plasma CBG concentration and binding capacity can be attributed primarily to downregulation of hepatic CBG production, but perhaps also to proteolytic cleavage by NE, which is the focus of this chapter.

As described in the results section of chapter 3, we observed a net 'release' of CBG across liver in people with obesity/T2DM, and there was limited evidence of 'release' of CBG across muscle based on CBG binding capacity measurements, but we could not detect *in vivo* cleavage of CBG even in inflamed tissues such as obese adipose. While our findings do not support CBG cleavage as a physiological mechanism controlling cortisol delivery to tissues in the subjects tested, the context is vital. Obese adipose is characterised by chronic, low-grade inflammation; it remains to be determined if CBG cleavage occurs in acute, pathological inflammation. While neutrophils are one of several leucocytes playing a role in local inflammation within obese adipose (Blaszczak et al., 2021), activated neutrophils predominate in the context of acute, systemic inflammation (Rosales, 2018).

In chapter 4, we demonstrated that plasma free cortisol fraction is higher in subjects heterozygous for (inactivating) mutations in *SERPINA1*. This was associated with increased

mRNA levels of glucocorticoid-dependent transcripts in subcutaneous abdominal adipose, in keeping with enhanced cleavage of CBG and greater tissue glucocorticoid exposure. These findings could be relevant in obesity, where reducing tissue delivery of cortisol by inhibiting NE-mediated CBG cleavage may be advantageous – but might be even more significant in acute neutrophilic inflammation. The results of chapter 4 are also consistent with chronic activation of CBG cleavage increasing tissue glucocorticoid action, which provides a rationale for testing the acute regulation of CBG cleavage in an appropriate model of acute inflammation.

There has been some discussion in the literature about the prospect of manipulating the RCL of CBG as a vehicle for drug delivery (Chan et al., 2014). Moreover, it has been shown *in vitro* that pre-incubation of human CBG with monoclonal antibodies targeting the RCL of CBG can protect against (delay) cleavage of CBG by three proteases – NE, elastase from Pseudomonas Aeruginosa (LasB), and bovine chymotrypsin (Lewis and Elder, 2017). Preincubation of CBG with AAT has been shown to prevent CBG cleavage by elastase derived from activated neutrophils *in vitro* (Hammond et al., 1990a), so the natural corollary of this is the question of whether inhibition of NE can prevent CBG cleavage *in vivo*. However, to the best of our knowledge, no prior studies have examined the effects of inhibition of NE on CBG cleavage *in vivo* in humans.

A growing number of synthetic NE inhibitors now exist. While pre-clinical studies have been encouraging in terms of reduced NE-mediated injury and inflammation, clinical translation has been frustrated by lack of efficacy and concerns around toxicity (Alam et al., 2012). Sivelestat (Ono Pharmaceutical) remains arguably the best known of these synthetic agents,

and is a low molecular weight reversible competitive NE inhibitor. In observational studies, its administration was associated with reduced mortality in critically ill patients and attenuated pulmonary dysfunction in patients with acute respiratory distress syndrome (Hoshi et al., 2005; Okayama et al., 2006). In prospective double-blinded controlled trials, it has been reported to reduce IL-8 production and acute lung injury after cardiopulmonary bypass, and reduce duration of ventilation in intensive care (Ryugo et al., 2006; Tamakuma et al., 2004). However, the only multi-centre double-blind placebo-controlled trial of sivelestat failed to show a decrease in mortality or reduced ventilator requirement in critically ill patients (Zeiher et al., 2004).

AAT by contrast is the primary endogenous NE inhibitor produced by the liver, present at saturating levels within the general circulation and providing systemic inhibitory activity against NE. Like AAT, elafin is a natural endogenous inhibitor of NE, but unlike AAT is instead produced locally at sites of inflammation by epithelial tissues primarily in organs which are regularly exposed to inflammatory insults, for example the skin and the lung (Alam et al., 2012). Elafin was first isolated from human psoriatic skin (Wiedow et al., 1990) and sputum (Sallenave and Ryle, 1991). Cloning of elafin cDNA revealed that transcription produces a protein consisting of 117 amino acid residues, which undergoes intracellular cleavage of an N-terminal hydrophobic signal sequence to produce pro-elafin (Molhuizen et al., 1993; Sallenave and Silva, 1993). The pro-elafin protein is composed of 2 domains, a C-terminus consisting of 57 amino acids and an N-terminus consisting of 60 amino acids, also known as the ‘cementoin’ domain (Francart et al., 1997; Nara et al., 1994; Schalkwijk et al., 1999). The N-terminus contains sequences that provide the substrate for transglutaminase; transglutaminisation allows elafin to be cross-linked to the extracellular matrix so that it can

persist as a tissue-bound inhibitor of NE (Nara et al., 1994). The C-terminus has a four-disulphide core and is responsible for NE inhibition. Elafin has an equilibrium dissociation constant for NE of 0.8 x 10^{-10} M (Zani et al., 2004). The aim of this study was to determine if elafin has an effect on NE-mediated cleavage of CBG during inflammation *in vivo* in humans, using Coronary Artery Bypass Grafting (CABG) surgery as a model of acute inflammation.

CABG is a major open surgery done under general anaesthetic, usually over 3-6 hours. It is an effective treatment for coronary artery disease, in which blood vessels from the leg (saphenous vein), chest (internal mammary artery) or arm (radial artery) are used to bypass occlusions in the coronaries caused by e.g. atherosclerosis, thus restoring blood supply to the myocardium. CABG is a good model not only because it induces neutrophil-mediated acute inflammation, but we also know that open-heart surgery decreases plasma CBG levels (Tinnikov et al., 1996). In addition, *SERPINA6* expression has been noted (albeit at low levels) in the human heart, and NE (which cleaves the RCL of CBG) has also been found near and within the plasma membrane of cardiomyocytes (Caldwell and Jirikowski, 2013; Schäfer et al., 2015) Given the failure to demonstrate CBG cleavage *in vivo* in other circumstances, this context suggests that CABG may be an optimal circumstance in which to detect CBG cleavage and any effect of elafin *in vivo*.

5.2 Hypotheses

We hypothesise that:

1. Plasma CBG concentration and CBG binding capacity decrease during CABG surgery, with a simultaneous rise in plasma free cortisol, in keeping with increased cleavage of CBG
2. Inhibition of NE by elafin attenuates the expected drop in both plasma total CBG and CBG binding capacity, and attenuates the rise in plasma free cortisol during CABG surgery

5.3 Aims

We aimed to:

1. Confirm that elafin effectively inhibits plasma NE activity *in vivo*
2. Quantify expression of cytokines known to regulate hepatic CBG production during CABG surgery
3. Quantify changes in CBG concentration, CBG binding capacity, total cortisol and free cortisol during CABG surgery
4. Assess the effect of elafin on CBG cleavage *in vivo*

5.4 Methods

These hypotheses were tested using samples collected from a subset of participants in the previously published EMPIRE (Elafin Myocardial Protection from Ischaemia Reperfusion) randomised-controlled clinical trial (Alam et al., 2015). The primary objective of this trial was to determine whether a single-dose elafin treatment could inhibit myocardial ischaemia-

reperfusion injury during CABG surgery; myocardial injury was measured as cardiac troponin I release over 48 hours (area under the curve (AUC)) and myocardial infarction identified with MRI.

5.4.1 Study design

In a randomised double-blind placebo-controlled parallel group clinical trial, 87 patients undergoing CABG surgery were randomised 1:1 to receive intravenous elafin 200mg or saline placebo after induction of anaesthesia and prior to sternotomy.

5.4.2 Subjects

Between June 2011 and September 2013, consecutive patients referred to elective CABG surgery were recruited from two clinics at the Edinburgh Heart Centre.

5.4.2.1 Inclusion criteria

- 18 years or older
- Referred for isolated CABG surgery requiring two or more grafts

5.4.2.2 Exclusion criteria

- Patients with recent myocardial infarction (within 1 month of surgery)
- Emergency or concomitant valve surgery
- Significant renal impairment (estimated glomerular filtration rate < 40mL/min)
- Severe respiratory disease (maintenance corticosteroid therapy or forced expiratory volume in 1 second < 50% of predicted)
- Severe left ventricular impairment (ejection fraction < 40%)

- Contraindication to magnetic resonance scanning
- Treatment for chronic inflammatory disease
- Women of childbearing potential
- Inability to provide consent

5.4.3 Clinical protocol

Intravenous recombinant human elafin (Proteo Biotech AG, Germany) 200mg or saline placebo was prepared and infused as aqueous solution of 250mL 0.9% saline. Patients were randomised (1:1) to receive elafin or matched placebo by the Edinburgh Clinical Trials Unit to ensure allocation concealment. Randomisation incorporated minimisation for age, presence of diabetes mellitus, extent of coronary artery disease, renal function and surgeon A or B. To ensure blinding, study drugs were prepared by staff independent of the study investigators or clinical team responsible for the patient's care.

Intravenous elafin 200mg causes complete inhibition of plasma NE activity for 2 hours and >50% inhibition for 6 hours (Alam et al., 2015; Shaw and Wiedow, 2011). This dosage regimen was selected to cover the increased NE release following CABG surgery that peaks at the time of weaning from cardiopulmonary bypass, and has returned to baseline by 6–7 hours (Alam et al., 2015). The study drug was administered to the patient through a central venous cannula over a period of 30 minutes. The intravenous infusion was started at first skin incision and completed at least 20 minutes before cardiopulmonary bypass was commenced.

General anaesthesia was maintained with isoflurane and propofol infusion during bypass. The surgical approach was via a median sternotomy and cardiopulmonary bypass was started

after heparin administration with a non-pulsatile flow and a membrane oxygenator. Cardioprotection was provided by cold blood cardioplegia (1:4), which was administered antegradely, after cross-clamping the aorta, into the coronary arteries or by cross-clamp fibrillation.

Blood samples were taken at baseline (time 0, skin incision) and at 2, 6, 24 and 48 hours postoperatively.

5.4.4 Measurements

Plasma NE activity and serum elafin concentrations were measured previously by Oliver Wiedow and his team based in the Department of Dermatology at The University of Kiel, Germany, by fluorometric assay and LC-MS, respectively. Plasma concentrations of IL-6, TNF-alpha, NE and myeloperoxidase (MPO) were quantified using ELISAs (R&D Systems, UK; Elastase ELISA, Cambridge Biosciences, UK) in Edinburgh by the EMPIRE investigators. All of these assays were performed prior to publication of the trial in 2015 (Alam et al., 2015).

Due to limited sample availability, for the present analysis we used plasma samples from 19 subjects from the elafin group and 16 subjects from the placebo group, at four time points – baseline, 2, 6 and 24 hours. In these 130 samples we measured total CBG (by ELISA as described in section 2.3), CBG binding capacity (radioligand-saturation assay, section 2.4), total cortisol (ELISA, section 2.12) and free cortisol (isotopic dilution and ultrafiltration, section 2.10). I performed both CBG assays using these 130 samples when visiting Geoffrey Hammond's laboratory at UBC in January 2017; the total cortisol ELISA and free cortisol assay I later performed in our laboratory in Edinburgh, in 2019.

5.4.5 Statistical analysis

Data were analysed using GraphPad Prism version 9. Differences between groups and across time points were determined using mixed-effects models (rather than two-way ANOVA due to 10 missing data points). All data are reported as mean +/- SEM unless otherwise stated. Plasma elafin concentration and NE activity were analysed as area under the curve (AUC) at 24 hours.

5.5 Results

5.5.1 Subject characteristics

Characteristics of the 35 EMPIRE trial participants used in this analysis are summarised in Table 5.1 below, presented alongside characteristics of all 87 EMPIRE trial participants for comparison. There were no differences between either the two elafin or two placebo groups in any of the baseline characteristics.

TABLE 5.1 Baseline characteristics by treatment group

Data are number of patients (%) or mean +/- SEM for n=19 for elafin and n=16 for placebo. Study groups are representative of the larger groups used in the EMPIRE trial (n=44 for elafin and n=43 for placebo).

Baseline characteristics	***Elafin***	***EMPIRE Elafin***	***Placebo***	***EMPIRE Placebo***
Age	65.2 ± 1.6	63.9 ± 1.2	61.6 ± 2.2	63.6 ± 1.3
Male gender	16 (84.2)	38 (86.4)	14 (87.5)	36 (83.7)

BMI	30.9 ± 1.3	30.8 ± 0.67	28.2 ± 0.8	28.7 ± 0.58
Diabetes mellitus	4 (21.1)	11 (25.0)	2 (12.5)	9 (20.9)
Surgeon A	8 (42.1)	18 (40.9)	4 (25.0)	16 (37.2)
Surgeon B	11 (57.9)	26 (59.1)	12 (75.0)	27 (62.8)

5.5.2 Elafin and NE activity

Elafin infusion resulted in >1000-fold higher plasma concentrations than those of endogenous elafin in the placebo group (mean AUC at 24 h; 30.9 ± 7.7 vs 0.03 ± 0.11 µg/mL for placebo), associated with a marked reduction in plasma NE activity (mean AUC at 24 h; 3.83 ± 1.99 vs 8.04 ± 2.97 units/mL) as shown in Figure 5.1 below.

(a) Plasma elafin concentration (b) Plasma NE activity

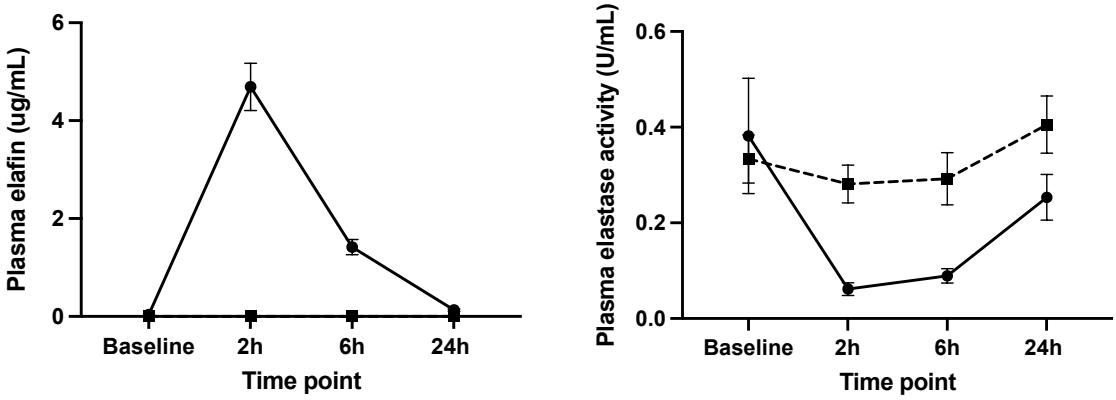

FIGURE 5.1 Plasma elafin concentration and corresponding NE activity during CABG surgery

Data are mean ± SEM for (a) plasma elafin concentration and (b) plasma NE activity during CABG surgery in elafin (circles, solid line) (n=19) and placebo (squares, dashed line) (n=16) treated groups.

5.5.3 Plasma NE and myeloperoxidase (MPO) concentrations

NE rose rapidly in both groups during the first 2 hours of CABG surgery, then began to fall. MPO, which provides a readout of neutrophil activity, exhibited the same profile (Figure 5.2).

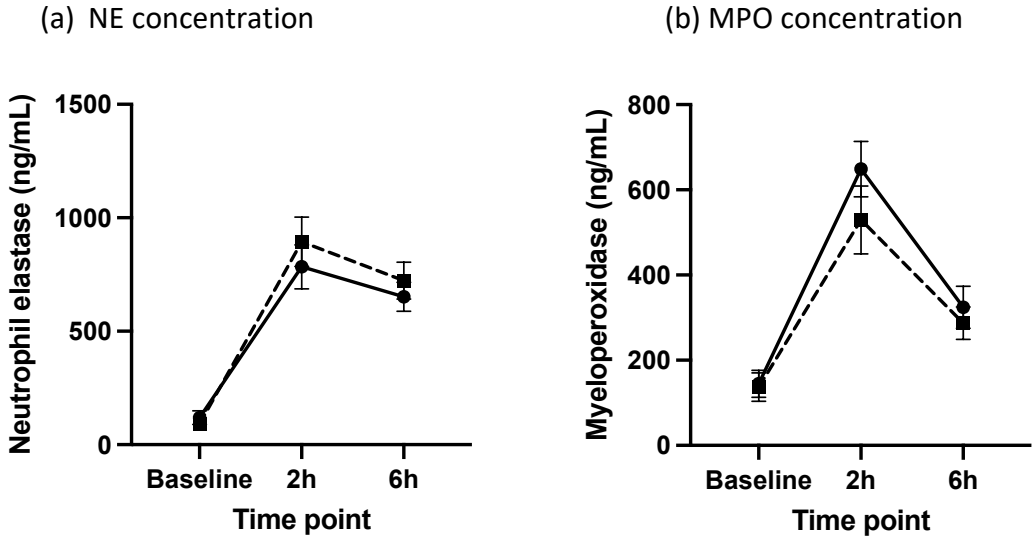

FIGURE 5.2 Plasma NE and MPO concentrations during CABG surgery

Data are mean ± SEM for (a) plasma NE concentration and (b) plasma MPO concentration during CABG surgery in elafin (circles, solid line) (n=19) and placebo (squares, dashed line) (n=16) treated groups. Comparisons between groups and across time were made by two-way repeated measures ANOVA. There were no significant differences between groups in either NE (mean difference 55.8 ng/mL, 95% CI -216.8 to 105.1, p=0.49) or MPO (mean difference 52.4 ng/mL, 95% CI -67.5 to 172.3, p=0.38) concentrations.

5.5.4 Plasma cytokines

Plasma cytokines increased from baseline in both groups (p=0.0003 vs time for IL-6 and p=0.002 vs time for TNF-alpha). There was a trend towards a greater rise in plasma IL-6 concentration across the first 2 hours of CABG surgery in the placebo group, but this did not

reach statistical significance. There was also a trend towards higher TNF-alpha concentration in the elafin group, but again there was no difference between groups (Figure 5.3).

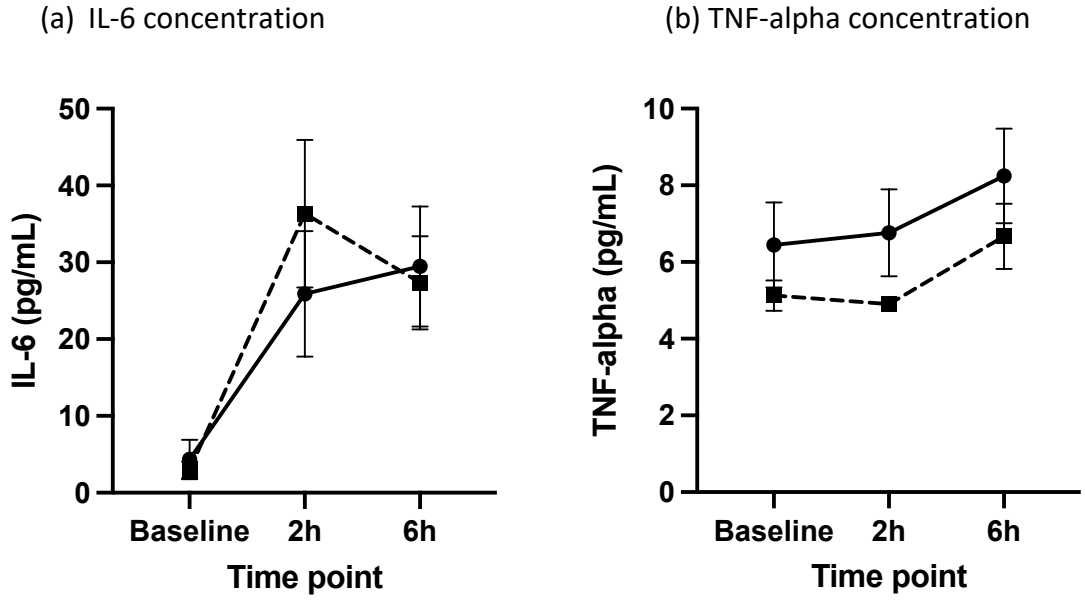

FIGURE 5.3 Plasma IL-6 and TNF-alpha concentrations during CABG surgery

Data are mean ± SEM for plasma concentrations of (a) IL-6 and (b) TNF-alpha during CABG surgery in elafin (circles, solid line) (n=19) and placebo (squares, dashed line) (n=16) treated groups. Comparisons between groups over time were made by two-way repeated measures ANOVA. There were no significant differences between groups in respect of either IL-6 (mean difference 2.29 pg/mL, 95% CI -13.8 to 9.2, p=0.69) or TNF-alpha (mean difference 1.53 pg/mL, 95% CI -0.94 to 4.01, p=0.22) concentrations.

5.5.5 Plasma CBG and CBG binding capacity

In both groups, plasma CBG and CBG binding capacity fell acutely between the start of CABG surgery and the 2h time point ($p<0.0001$), then plateaued. There was no difference between the elafin and placebo treated groups in respect of either, at any of the time points (Figure 5.4).

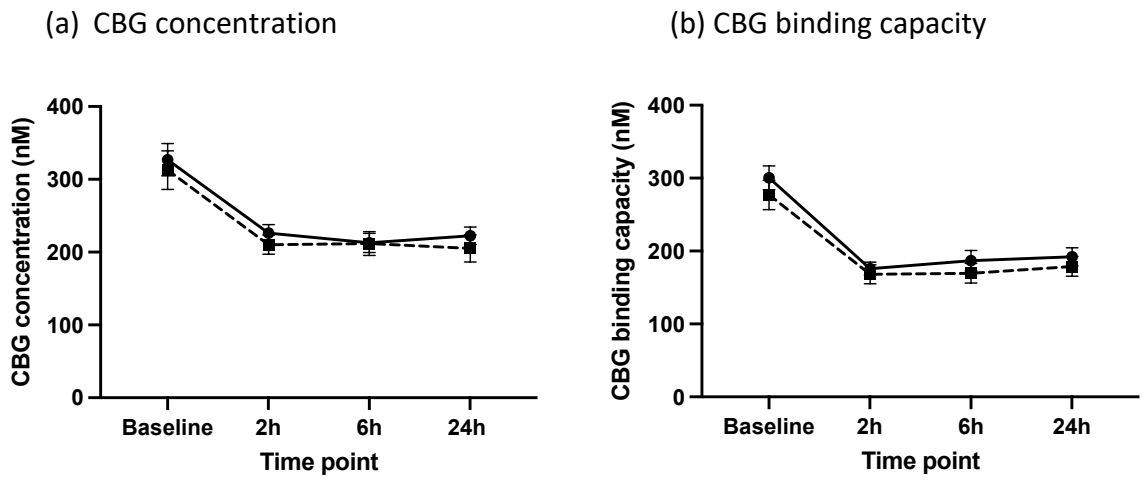

FIGURE 5.4 Plasma CBG concentration and CBG binding capacity during CABG surgery

Data are mean ± SEM for plasma (a) CBG concentration and (b) CBG binding capacity during CABG surgery in elafin (circles, solid line) (n=19) and placebo (squares, dashed line) (n=16) treated groups. Comparisons between groups and across time were made by two-way repeated measures ANOVA. There were no significant differences between groups in respect of either CBG concentration (mean difference 9.44 nM, 95% CI -25.89 to 44.77, p=0.59) or CBG binding capacity (mean difference 12.6 nM, 95% CI -20.03 to 45.22, p=0.44).

5.5.6 Plasma total cortisol

Plasma total cortisol rose sharply during CABG surgery. Between the 2h and 6h time points, mean total cortisol rose from 98.3nM ± 32.0 to 434.6nM ± 41.4 in the elafin group, and from 61.7nM ± 19.6 to 405.4nM ± 53.8 in the placebo group (Figure 5.5).

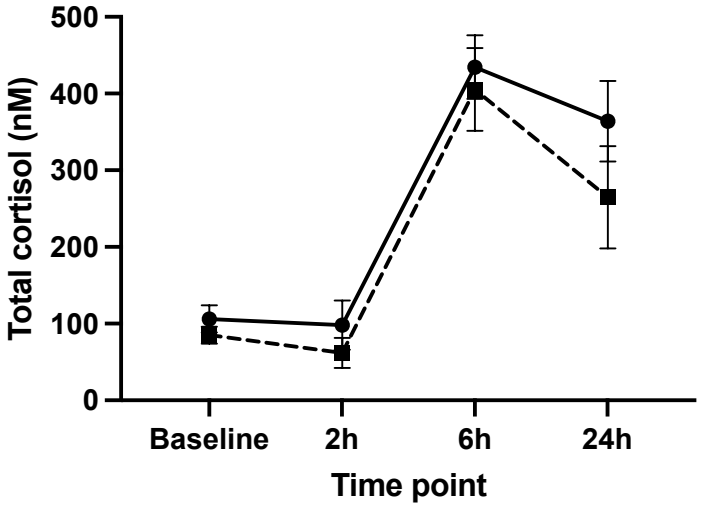

FIGURE 5.5 Plasma total cortisol during CABG surgery

Data are mean ± SEM for plasma total cortisol during CABG surgery in elafin (circles, solid line) (n=19) and placebo (squares, dashed line) (n=16) treated groups. Comparisons between groups and across time were made by two-way repeated measures ANOVA. Total cortisol concentration rose as expected during CABG surgery in both groups (p<0.0001), however there was no significant difference between groups at any time point (p=0.16).

5.5.7 Plasma free cortisol

Plasma free cortisol rose during CABG surgery. Between baseline and 6h, plasma free cortisol fraction increased from 16.1% ± 0.3 to 31.6% ± 1.4 in the elafin group, and from 16.4% ± 0.4 to 30.7% ± 1.6 in the placebo group (Figure 5.6a). Plasma free cortisol concentration increased between these time points, and while there was no statistically significant difference between the groups (p = 0.062), if anything the trend was actually towards higher plasma free cortisol in the elafin treated group (Figure 5.6b).

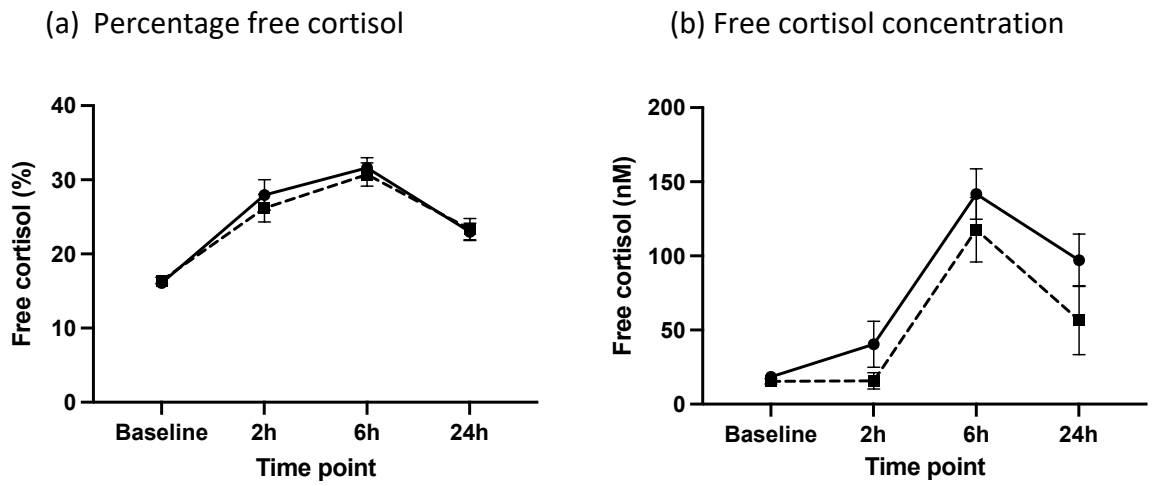

FIGURE 5.6 Plasma free cortisol during CABG surgery

Data are mean ± SEM for plasma total cortisol during CABG surgery in elafin (circles, solid line) (n=19) and placebo (squares, dashed line) (n=16) treated groups. Comparisons between groups and across time were made by two-way repeated measures ANOVA. Plasma free cortisol rose during CABG surgery, expressed here as both (a) a percentage and (b) concentration ($p<0.0001$ for both). There were no significant differences between groups in respect of either free cortisol fraction ($p=0.74$) or concentration ($p=0.062$).

5.6 Discussion

In this chapter we hypothesised that plasma CBG concentration and CBG binding capacity decrease during CABG surgery, with a simultaneous rise in plasma free cortisol, in keeping with increased cleavage of CBG. We further hypothesised that inhibition of NE by elafin attenuates the expected drop in both plasma total CBG and CBG binding capacity, and attenuates the rise in plasma free cortisol during CABG surgery. In this study we have shown that during CABG surgery, plasma CBG concentration and CBG binding capacity both fall acutely, associated with a commensurate rise in plasma free cortisol, which is in keeping with

our first hypothesis. We have also shown that expression of cytokines which downregulate hepatic CBG production rose during CABG surgery in both study groups. However, these results refute our second hypothesis because there was no effect of elafin on the decrease in both plasma total CBG and CBG binding capacity during CABG surgery. Elafin had no effect on plasma free cortisol expressed as either percentage or concentration; intriguingly however the trend was toward higher free cortisol concentration in the elafin treated group – contrary to our hypothesis.

This study supports what we know already about the effect of acute inflammation on CBG. During acute inflammation, the plasma concentration and binding capacity of CBG decrease rapidly, caused principally by both down-regulation of hepatic CBG production (Emptoz-Bonneton et al., 1997) and proteolytic cleavage of CBG (Hammond et al., 1990a). In our study plasma CBG concentration and binding capacity fell rapidly (over a period of two hours). It could be argued that this finding supports the observation that proteolysis of the RCL of CBG by NE happens early during acute inflammation (Hill et al., 2016); it is proposed that this is in order to release CBG-bound cortisol at sites of inflammation (Hammond, 1990; Perogamvros et al., 2012), but this has never been proven *in vivo*. This decrease in CBG binding capacity caused by RCL cleavage causes a rapid plasma redistribution of cortisol, with an increase in the unbound 'free' fraction (Hammond, 2016). As a result, in our study the free cortisol concentration increased by approximately fourfold, in keeping with other reports in the literature (Chan et al., 2013). These higher cortisol concentrations downregulate CBG production (Smith and Hammond, 1992), together with circulating cytokines e.g. IL-6 which repress CBG synthesis (Bartalena et al., 1993); of note both IL-6 and TNF-alpha both rose in this study across the time points. A key discussion point here is whether it is downregulation

of hepatic production, or proteolytic cleavage by NE, or by other pathways of proteolysis, which is primarily responsible for the decline in CBG concentration and binding capacity observed. Since we have found no effect of elafin, it is more likely that hepatic production is the major determinant of plasma CBG concentration and binding capacity; as we've seen in this study, CBG binding capacity closely mirrors CBG concentration. An alternative possibility is that proteolysis/clearance of CBG may occur by a non-NE dependent mechanism, which is also supported by the lack of effect of elafin.

Ultimately while no published studies have evaluated CBG cleavage during CABG surgery, our findings are in keeping with other studies in humans which have shown similar reductions in CBG concentrations and binding capacity in response to major inflammatory insults. Significant decreases in plasma CBG levels have been described most commonly in patients with sepsis (Ho et al., 2010) and septic shock (Bendel et al., 2008; Ho et al., 2006; Meyer et al., 2018; Nenke et al., 2015; Pugeat et al., 1989; Savu et al., 1981), but have also been observed in patients suffering from a variety of other conditions which are also characterised by acute inflammation, including burns (Bernier et al., 1998; Garrel, 1996), multi-trauma (Beishuizen et al., 2001), necrotising pancreatitis (Muller et al., 2007), myocardial infarction (Zouaghi et al., 1985) and those undergoing mitral valve repair surgery (Tinnikov et al., 1996).

In this study total plasma cortisol rose dramatically during CABG surgery, most likely because of activation of the HPA axis induced by the stress associated with CABG surgery (Sapolsky et al., 2000), which would further amplify tissue cortisol exposure. In response to systemic inflammation, any increases in ACTH-driven cortisol production would be expected to overwhelm a reduced CBG binding capacity, further increasing plasma free cortisol

(Hammond, 2016). As an alternative explanation to ACTH drive however, is that it has been shown that in critical illness, cortisol clearance is reduced (Boonen et al., 2013), associated with suppressed pulsatile ACTH secretion (Boonen et al., 2014). Admittedly the total cortisol data in our study does need to be interpreted with some caution, particularly at baseline where the results appear relatively low, for two reasons; firstly the time of day the baseline sample was collected varied between subjects. These samples were not necessarily collected in the early morning because the timing of CABG surgery would have varied between patients, by the very nature of a clinical service. Secondly, these cortisol measurements were assayed by ELISA which is nonideal, but insufficient sample volumes were available from the original trial to enable the gold standard LC-MS/MS measurement. Nevertheless, this was a robust ELISA used to measure cortisol in human plasma in earlier published studies (Ray et al., 2009; Skornyakov et al., 2019; Watt et al., 2016); all samples were assayed in duplicate and the intra- and inter-assay coefficients of variation were 4.6% and 5.2%, respectively.

This study has also shown that inhibition of NE by elafin does not appear to reduce CBG cleavage, when compared with saline placebo, and there may be several reasons for this. The first and perhaps most obvious question is whether the dose of elafin used was actually sufficient to inhibit NE activity as intended, and thereby reduce CBG cleavage. We know that the 200mg elafin dose reduced plasma NE 'activity' by > 50% over the 24 hour period, but it was not suppressed to an undetectable level – which could partly explain why we found no differences between the groups in respect of CBG and free cortisol. Plasma elafin concentration was at its peak with NE activity at its nadir at 2h, but we did not observe any significant differences between the groups at this particular time point. Systemic administration of recombinant endogenous or synthetic NE inhibitors is an approach which

has been used in both pre-clinical and clinical studies, but it has been acknowledged that this approach may fail to achieve effective delivery and constant therapeutic concentrations at sites of tissue injury such as the airway, luminal bowel surface and skin (Henriksen, 2014). There is therefore a possibility that the elafin 200mg administered did not inhibit CBG cleavage within tissues, and it is of note that the EMPIRE trial did not meet its primary endpoint (Alam et al., 2015).

The second caveat relates to our chosen model of acute inflammation – it may be that the degree of inflammation during CABG surgery and the sheer turnover of CBG make any assessment of subtle alterations in CBG cleavage impossible. Since CBG as a substrate is changing at such a high rate, we may not be able to detect whether NE inhibition by elafin has any effect on cleavage of CBG. Furthermore, one of the other limitations of our model is that the measurements of CBG and cortisol we have made provide a readout of what is happening (or not) in the systemic circulation, and do not necessarily reflect the dynamics of CBG cleavage at a local level, within target tissues themselves.

Thirdly, we may be underpowered to detect subtle differences between the two treatment groups. These data are based on 19 subjects in the elafin treated group, and 16 subjects from the placebo treated group – a sample size of 16 per group provides 80% power to detect a 15.5% difference in plasma CBG concentration and a 20% difference in CBG binding capacity.

Finally, it has been known for some time that factors other than NE-mediated cleavage can alter the binding affinity of CBG for cortisol, resulting in changes in free cortisol concentration in a physiologically relevant range, albeit to a much lesser extent than NE. These variables

include glycosylation of CBG and temperature (Chan et al., 2013). More recent (limited) data suggests that pyrexia and acidosis act independently of NE-mediated cleavage to effect cortisol release from CBG – a 2^{o}C increase in temperature was shown *in vitro* to lower CBG binding affinity 3.5-fold (Meyer et al., 2020). We have no evidence to suggest that temperature and pH varied significantly between subjects or indeed groups in this study during CABG surgery, and all plasma samples we used were assayed at the same temperature.

In summary, in this study we found that plasma CBG concentration and binding capacity fell during CABG surgery, associated with an increase in plasma free cortisol, in keeping with CBG cleavage secondary to acute inflammation. Inhibition of NE using elafin was not shown to reduce our estimates of CBG cleavage in the subjects tested. Further studies using different models of (less severe) acute inflammation, involving different NE inhibitors and focusing on individual target tissues would be informative.

Chapter 6: Conclusions

In 1956, a human plasma protein capable of binding glucocorticoids was first discovered (Daughaday, 1956). This protein, referred to as 'transcortin' in the early literature, is now known as CBG. CBG binds over 85% of plasma cortisol and modulates free cortisol levels. It was not until 1990 that a role for CBG in delivery of cortisol to activated neutrophils was first proposed by Hammond et al (Hammond et al., 1990a), upon observing *in vitro* that CBG undergoes proteolytic cleavage by NE at its RCL, a mechanism proposed to reduce CBG binding capacity by approximately ten-fold and increase the availability of free cortisol to tissues at sites of inflammation (Hammond et al., 1990b). However, detection of cleaved CBG *in vivo* in human plasma is controversial, and any influence of NE on CBG cleavage has not been demonstrated *in vivo*. The CORtisol NETwork (CORNET) consortium found that genetic variation at a locus spanning *SERPINA1* (encoding AAT, the endogenous inhibitor of NE) and *SERPINA6* (CBG) contributes to morning total plasma cortisol variation, providing further circumstantial evidence for an influence of CBG cleavage on plasma cortisol. This thesis aimed to test the hypotheses that: (i) CBG cleavage occurs in tissues *in vivo*; (ii) CBG cleavage controls tissue cortisol delivery; (iii) AAT deficiency increases CBG cleavage and hence free plasma cortisol; (iv) greater cleavage of CBG results in increased tissue cortisol delivery in adipose and in hypothalamic-pituitary-adrenal (HPA) axis negative feedback; and (v) NE inhibition reduces CBG cleavage and thus plasma free cortisol *in vivo*.

The studies presented in this thesis were designed to perturb the AAT/NE system proposed to control CBG cleavage in a number of ways; using BMI variation, insulin administration, AAT deficiency and NE inhibition. However despite this, we did not demonstrate that proteolytic cleavage of CBG by NE is responsible for any alterations in total or free cortisol, even in chapter 4 where we demonstrate higher plasma free cortisol fraction, net total and free

cortisol release across skeletal muscle and greater expression of GC-dependent transcripts in AAT deficiency – all of which are in keeping with NE-mediated cleavage of CBG. We cannot conclude that CBG cleavage is responsible for these observations, particularly as we are currently limited by the techniques available for measurement of CBG cleavage, which include total CBG concentration and CBG binding capacity. Given the growing number of variants identified with abnormal steroid-binding activity (section 1.3.1), there is a need to develop robust clinical chemical assays to measure both the levels and steroid-binding activity of CBG (particularly *in vivo*), in conjunction with direct measurements of plasma free cortisol levels. The development of new assays is now particularly urgent given that our results presented in chapter 3 were used to prove that the performance of the 9G12 ELISA designed to detect RCL-intact CBG is poor (Hill et al., 2019b). This is likely due to differential *N*-glycosylation of Asn347 in the RCL, which alters 9G12 antibody recognition and is responsible for discrepancies between our CBG binding capacity and apparent 'cleaved' CBG ELISA values (Hill et al., 2019a).

Assuming NE-mediated CBG cleavage does occur *in vivo*, it remains unclear whether it happens in the circulation or within inflamed tissues. CBG cleavage is thought less likely to occur in the general circulation due to the presence of saturating levels of AAT (Hammond et al., 1990a). An alternative is that 'cleaved' CBG could be rapidly cleared from the circulation (Mast et al., 1991), but this seems unlikely in light of more recent evidence which has shown a complete absence of NE-cleaved CBG in human plasma (Hill et al., 2019b). In this thesis no measurable *in vivo* cleavage of CBG was observed across the tissues we studied. We chose to focus primarily on skeletal muscle and adipose tissue because these are two key metabolic tissues which are amenable to arterio-venous sampling, and the Edinburgh group has extensive experience in using these techniques to quantify cortisol balance across both. In

addition, neutrophils are expected to be present and secreting elastase in adipose tissue (Talukdar et al., 2012). However, it may be possible to detect NE-mediated cleavage in tissues with higher neutrophil content, such as the lymphatics or spleen (Rosales, 2018). Future studies could also consider different sampling approaches, especially because arteriovenous sampling from adipose poses technical challenges, and in this thesis these have unfortunately restricted our interpretation of any net changes in CBG and GC across subcutaneous adipose. Arteriovenous measurements of CBG readouts may not be sensitive enough to detect changes in GC concentrations resulting from cleavage. While arteriovenous sampling provides the best readout we have currently for net changes across tissue beds, instead future studies could consider employing microdialysis approaches which are technically less difficult in subcutaneous adipose (Wake et al., 2007). Microdialysis could enable measurement of free GCs and potentially CBG binding capacity in the interstitium of tissues, and thus an assessment to be made of whether CBG cleavage is occurring outside the vasculature, in the interstitial fluid of inflamed tissues.

In chapter 4 we present the first data that 11β-HSD1 activity is increased in muscle in AAT deficiency, alongside decreased whole body (liver) 11β-HSD1 activity in these same subjects. The higher free cortisol fraction in AAT deficient subjects could explain the higher 11β-HSD1 activity in muscle in a 'feed-forward' mechanism (Morgan et al., 2014), but this would not explain their reduced hepatic 11β-HSD1 activity (Dube et al., 2015). Therefore, a key question for future study would be why hepatic 11β-HSD1 activity is decreased in AAT deficiency; perhaps this reflects a compensatory response to the higher whole body free cortisol fraction. It would also be useful to measure adipose 11β-HSD1 transcript levels in AAT deficiency in future work.

This thesis has focused exclusively on the role of NE in CBG cleavage, however at least two other proteases are capable of cleaving CBG, chymotrypsin (Lewis and Elder, 2014) and LasB, an elastase produced by the bacteria Pseudomonas aeruginosa (Simard et al., 2014). Of these three proteases the most extensive literature exists for NE, primarily because its role was first proposed over 30 years ago. Despite focusing solely on the role of NE in CBG cleavage, we have not provided any measures of NE in chapters 3 and 4 of this thesis – we have presumed that adipose tissue has greater NE activity in obesity than in normal weight (Elgazar-Carmon et al., 2008), but this may not necessarily be the case. Similarly in chapter 4, given that serum AAT concentrations were confirmed approximately 30% lower in the AAT deficient group, we assume that NE activity was increased but this may not be the case. In future such studies, measurements of whole body and/or tissue-specific NE activity would be informative.

In chapter 5, we did measure both NE activity and concentrations in plasma; significant increases in plasma levels of inflammatory cytokines were associated with both evidence of dramatically reduced CBG concentrations and binding capacity, and associated increases in total and free cortisol concentrations. These observations were in keeping with CBG cleavage and in support of our hypotheses, however elafin did not attenuate the decreases in CBG. It may be that the turnover of CBG during CABG is so great that any impact of elafin was missed, so future studies should consider alternative models of acute inflammation in which to test the effects of NE inhibitors on CBG cleavage *in vivo*.

In summary, the hypothesis put forward by Hammond et al over 3 decades ago (Hammond et al., 1990a) has not been supported by this thesis; NE-mediated cleavage of CBG is unlikely

to account for the observations made by the CORNET consortium (Bolton et al., 2014), and we now know that the associations of the *SERPINA6/A1* locus with plasma cortisol are more attributable to hepatic CBG production rather than CBG cleavage (Crawford et al., 2021). Further work could explore non-NE mediated mechanisms.

Chapter 7: References

Abdallah, B.M., Beck-Nielsen, H., and Gaster, M. (2005). Increased expression of 11beta-hydroxysteroid dehydrogenase type 1 in type 2 diabetic myotubes. Eur J Clin Invest *35*, 627-634.

Alam, S.R., Lewis, S.C., Zamvar, V., Pessotto, R., Dweck, M.R., Krishan, A., Goodman, K., Oatey, K., Harkess, R., Milne, L., et al. (2015). Perioperative elafin for ischaemia-reperfusion injury during coronary artery bypass graft surgery: a randomised-controlled trial. Heart *101*, 1639-1645.

Alam, S.R., Newby, D.E., and Henriksen, P.A. (2012). Role of the endogenous elastase inhibitor, elafin, in cardiovascular injury: from epithelium to endothelium. Biochem Pharmacol *83*, 695-704.

Alberti, L., Girola, A., Gilardini, L., Conti, A., Cattaldo, S., Micheletto, G., and Invitti, C. (2007). Type 2 diabetes and metabolic syndrome are associated with increased expression of 11beta-hydroxysteroid dehydrogenase 1 in obese subjects. Int J Obes (Lond) *31*, 1826-1831.

Anderson, A.J., Andrew, R., Homer, N.Z.M., Hughes, K.A., Boyle, L.D., Nixon, M., Karpe, F., Stimson, R.H., and Walker, B.R. (2020). Effects of Obesity and Insulin on Tissue-Specific Recycling Between Cortisol and Cortisone in Men. The Journal of Clinical Endocrinology & Metabolism *106*, e1206-e1220.

Anderson, L.N., Briollais, L., Atkinson, H.C., Marsh, J.A., Xu, J., Connor, K.L., Matthews, S.G., Pennell, C.E., and Lye, S.J. (2014). Investigation of genetic variants, birthweight and hypothalamic-pituitary-adrenal axis function suggests a genetic variant in the SERPINA6

gene is associated with corticosteroid binding globulin in the western Australia pregnancy cohort (Raine) study. PLoS One *9*, e92957.

Andrew, R., Phillips, D.I., and Walker, B.R. (1998). Obesity and gender influence cortisol secretion and metabolism in man. J Clin Endocrinol Metab *83*, 1806-1809.

Andrew, R., Smith, K., Jones, G.C., and Walker, B.R. (2002). Distinguishing the activities of 11beta-hydroxysteroid dehydrogenases in vivo using isotopically labeled cortisol. J Clin Endocrinol Metab *87*, 277-285.

Antoni, F.A. (1986). Hypothalamic control of adrenocorticotropin secretion: advances since the discovery of 41-residue corticotropin-releasing factor. Endocr Rev *7*, 351-378.

Antoni, F.A., Holmes, M.C., Makara, G.B., Kárteszi, M., and László, F.A. (1984). Evidence that the effects of arginine-8-vasopressin (AVP) on pituitary corticotropin (ACTH) release are mediated by a novel type of receptor. Peptides *5*, 519-522.

Arakane, F., King, S.R., Du, Y., Kallen, C.B., Walsh, L.P., Watari, H., Stocco, D.M., and Strauss, J.F., 3rd (1997). Phosphorylation of steroidogenic acute regulatory protein (StAR) modulates its steroidogenic activity. J Biol Chem *272*, 32656-32662.

Arecco, N., Clarke, C.J., Jones, F.K., Simpson, D.M., Mason, D., Beynon, R.J., and Pisconti, A. (2016). Elastase levels and activity are increased in dystrophic muscle and impair myoblast cell survival, proliferation and differentiation. Sci Rep *6*, 24708.

Arriza, J.L., Simerly, R.B., Swanson, L.W., and Evans, R.M. (1988). The neuronal mineralocorticoid receptor as a mediator of glucocorticoid response. Neuron *1*, 887-900.

Arriza, J.L., Weinberger, C., Cerelli, G., Glaser, T.M., Handelin, B.L., Housman, D.E., and Evans, R.M. (1987). Cloning of human mineralocorticoid receptor complementary DNA: structural and functional kinship with the glucocorticoid receptor. Science *237*, 268-275.

Avvakumov, G.V., and Hammond, G.L. (1994a). Glycosylation of human corticosteroid-binding globulin. Differential processing and significance of carbohydrate chains at individual sites. Biochemistry *33*, 5759-5765.

Avvakumov, G.V., and Hammond, G.L. (1994b). Substitutions of tryptophan residues in human corticosteroid-binding globulin: impact on steroid binding and glycosylation. J Steroid Biochem Mol Biol *49*, 191-194.

Avvakumov, G.V., Warmels-Rodenhiser, S., and Hammond, G.L. (1993). Glycosylation of human corticosteroid-binding globulin at aspargine 238 is necessary for steroid binding. J Biol Chem *268*, 862-866.

Bartalena, L., Hammond, G.L., Farsetti, A., Flink, I.L., and Robbins, J. (1993). Interleukin-6 inhibits corticosteroid-binding globulin synthesis by human hepatoblastoma-derived (Hep G2) cells. Endocrinology *133*, 291-296.

Bartels, M., de Geus, E.J., Kirschbaum, C., Sluyter, F., and Boomsma, D.I. (2003). Heritability of daytime cortisol levels in children. Behav Genet *33*, 421-433.

Basu, R., Basu, A., Grudzien, M., Jung, P., Jacobson, P., Johnson, M., Singh, R., Sarr, M., and Rizza, R.A. (2009). Liver is the site of splanchnic cortisol production in obese nondiabetic humans. Diabetes *58*, 39-45.

Basu, R., Singh, R.J., Basu, A., Chittilapilly, E.G., Johnson, C.M., Toffolo, G., Cobelli, C., and Rizza, R.A. (2004). Splanchnic cortisol production occurs in humans: evidence for conversion of cortisone to cortisol via the 11-beta hydroxysteroid dehydrogenase (11beta-hsd) type 1 pathway. Diabetes *53*, 2051-2059.

Basu, R., Singh, R.J., Basu, A., Chittilapilly, E.G., Johnson, M.C., Toffolo, G., Cobelli, C., and Rizza, R.A. (2005). Obesity and type 2 diabetes do not alter splanchnic cortisol production in humans. J Clin Endocrinol Metab *90*, 3919-3926.

Beatty, K., Bieth, J., and Travis, J. (1980). Kinetics of association of serine proteinases with native and oxidized alpha-1-proteinase inhibitor and alpha-1-antichymotrypsin. J Biol Chem *255*, 3931-3934.

Beishuizen, A., Thijs, L.G., and Vermes, I. (2001). Patterns of corticosteroid-binding globulin and the free cortisol index during septic shock and multitrauma. Intensive Care Med *27*, 1584-1591.

Benassayag, C., Souski, I., Mignot, T.M., Robert, B., Hassid, J., Duc-Goiran, P., Mondon, F., Rebourcet, R., Dehennin, L., Nunez, E.A., et al. (2001). Corticosteroid-binding globulin status at the fetomaternal interface during human term pregnancy. Biol Reprod *64*, 812-821.

Bendel, S., Karlsson, S., Pettilä, V., Loisa, P., Varpula, M., and Ruokonen, E. (2008). Free cortisol in sepsis and septic shock. Anesth Analg *106*, 1813-1819.

Benjamin, N., Calver, A., Collier, J., Robinson, B., Vallance, P., and Webb, D. (1995). Measuring forearm blood flow and interpreting the responses to drugs and mediators. Hypertension *25*, 918-923.

Bergthorsdottir, R., Leonsson-Zachrisson, M., Oden, A., and Johannsson, G. (2006). Premature mortality in patients with Addison's disease: a population-based study. J Clin Endocrinol Metab *91*, 4849-4853.

Bernier, J., Jobin, N., Emptoz-Bonneton, A., Pugeat, M.M., and Garrel, D.R. (1998). Decreased corticosteroid-binding globulin in burn patients: Relationship with interleukin-6 and fat in nutritional support. Critical Care Medicine *26*, 452-460.

Bertagna, X., Bertagna, C., Luton, J.P., Husson, J.M., and Girard, F. (1984). The new steroid analog RU 486 inhibits glucocorticoid action in man. J Clin Endocrinol Metab *59*, 25-28.

Best, R., and Walker, B.R. (1997). Additional value of measurement of urinary cortisone and unconjugated cortisol metabolites in assessing the activity of 11 beta-hydroxysteroid dehydrogenase in vivo. Clin Endocrinol (Oxf) *47*, 231-236.

Blaszczak, A.M., Jalilvand, A., and Hsueh, W.A. (2021). Adipocytes, Innate Immunity and Obesity: A Mini-Review. Front Immunol *12*, 650768.

Bodnar, T.S., Hill, L.A., Taves, M.D., Yu, W., Soma, K.K., Hammond, G.L., and Weinberg, J. (2015). Colony-Specific Differences in Endocrine and Immune Responses to an Inflammatory Challenge in Female Sprague Dawley Rats. Endocrinology *156*, 4604-4617.

Bolton, J.L., Hayward, C., Direk, N., Lewis, J.G., Hammond, G.L., Hill, L.A., Anderson, A., Huffman, J., Wilson, J.F., Campbell, H., et al. (2014). Genome wide association identifies common variants at the SERPINA6/SERPINA1 locus influencing plasma cortisol and corticosteroid binding globulin. PLoS Genet *10*, e1004474.

Boonen, E., Meersseman, P., Vervenne, H., Meyfroidt, G., Guïza, F., Wouters, P.J., Veldhuis, J.D., and Van den Berghe, G. (2014). Reduced nocturnal ACTH-driven cortisol secretion during critical illness. Am J Physiol Endocrinol Metab *306*, E883-892.

Boonen, E., Vervenne, H., Meersseman, P., Andrew, R., Mortier, L., Declercq, P.E., Vanwijngaerden, Y.M., Spriet, I., Wouters, P.J., Vander Perre, S., et al. (2013). Reduced cortisol metabolism during critical illness. N Engl J Med *368*, 1477-1488.

Bradbury, M.J., Akana, S.F., and Dallman, M.F. (1994). Roles of type I and II corticosteroid receptors in regulation of basal activity in the hypothalamo-pituitary-adrenal axis during the diurnal trough and the peak: evidence for a nonadditive effect of combined receptor occupation. Endocrinology *134*, 1286-1296.

Brattsand, R., and Linden, M. (1996). Cytokine modulation by glucocorticoids: mechanisms and actions in cellular studies. Aliment Pharmacol Ther *10 Suppl 2*, 81-90; discussion 91-82.

Brien, T.G. (1981). Human corticosteroid binding globulin. Clin Endocrinol (Oxf) *14*, 193-212.

Butler, P.C., and Home, P.D. (1987). The measurement of metabolite exchange across muscle beds. Baillieres Clin Endocrinol Metab *1*, 863-878.

Caldwell, J.D., and Jirikowski, G.F. (2013). An active role for steroid-binding globulins: an update. Horm Metab Res *45*, 477-484.

Cameron, A., Henley, D., Carrell, R., Zhou, A., Clarke, A., and Lightman, S. (2010). Temperature-responsive release of cortisol from its binding globulin: a protein thermocouple. J Clin Endocrinol Metab *95*, 4689-4695.

Carroll, J.A., Gaines, A.M., Spencer, J.D., Allee, G.L., Kattesh, H.G., Roberts, M.P., and Zannelli, M.E. (2003). Effect of menhaden fish oil supplementation and lipopolysaccharide exposure on nursery pigs. I. Effects on the immune axis when fed diets containing spray-dried plasma. Domest Anim Endocrinol *24*, 341-351.

Chalmers, D.T., Lovenberg, T.W., and De Souza, E.B. (1995). Localization of novel corticotropin-releasing factor receptor (CRF2) mRNA expression to specific subcortical nuclei in rat brain: comparison with CRF1 receptor mRNA expression. J Neurosci *15*, 6340-6350.

Chan, W.L., Carrell, R.W., Zhou, A., and Read, R.J. (2013). How changes in affinity of corticosteroid-binding globulin modulate free cortisol concentration. J Clin Endocrinol Metab *98*, 3315-3322.

Chan, W.L., Zhou, A., and Read, R.J. (2014). Towards engineering hormone-binding globulins as drug delivery agents. PLoS One *9*, e113402.

Cizza, G., Bernardi, L., Smirne, N., Maletta, R., Tomaino, C., Costanzo, A., Gallo, M., Lewis, J.G., Geracitano, S., Grasso, M.B., et al. (2011). Clinical manifestations of highly prevalent corticosteroid-binding globulin mutations in a village in southern Italy. J Clin Endocrinol Metab *96*, E1684-1693.

Conway-Campbell, B.L., McKenna, M.A., Wiles, C.C., Atkinson, H.C., de Kloet, E.R., and Lightman, S.L. (2007). Proteasome-dependent down-regulation of activated nuclear hippocampal glucocorticoid receptors determines dynamic responses to corticosterone. Endocrinology *148*, 5470-5477.

Cooper, M.S., Rabbitt, E.H., Goddard, P.E., Bartlett, W.A., Hewison, M., and Stewart, P.M. (2002). Osteoblastic 11beta-hydroxysteroid dehydrogenase type 1 activity increases with age and glucocorticoid exposure. J Bone Miner Res *17*, 979-986.

Crave, J.C., Lejeune, H., Brébant, C., Baret, C., and Pugeat, M. (1995). Differential effects of insulin and insulin-like growth factor I on the production of plasma steroid-binding globulins by human hepatoblastoma-derived (Hep G2) cells. J Clin Endocrinol Metab *80*, 1283-1289.

Crawford, A.A., Bankier, S., Altmaier, E., Barnes, C.L.K., Clark, D.W., Ermel, R., Friedrich, N., van der Harst, P., Joshi, P.K., Karhunen, V., et al. (2021). Variation in the SERPINA6/SERPINA1 locus alters morning plasma cortisol, hepatic corticosteroid binding

globulin expression, gene expression in peripheral tissues, and risk of cardiovascular disease. J Hum Genet *66*, 625-636.

D'Elia, M., Patenaude, J., Hamelin, C., Garrel, D.R., and Bernier, J. (2005). Corticosterone binding globulin regulation and thymus changes after thermal injury in mice. Am J Physiol Endocrinol Metab *288*, E852-860.

D'Souza, R.F., Masson, S.W.C., Woodhead, J.S.T., James, S.L., MacRae, C., Hedges, C.P., and Merry, T.L. (2021). α1-Antitrypsin A treatment attenuates neutrophil elastase accumulation and enhances insulin sensitivity in adipose tissue of mice fed a high-fat diet. Am J Physiol Endocrinol Metab *321*, E560-e570.

Dallman, M.F., Akana, S.F., Cascio, C.S., Darlington, D.N., Jacobson, L., and Levin, N. (1987a). Regulation of ACTH secretion: variations on a theme of B. Recent Prog Horm Res *43*, 113-173.

Dallman, M.F., Akana, S.F., Jacobson, L., Levin, N., Cascio, C.S., and Shinsako, J. (1987b). Characterization of corticosterone feedback regulation of ACTH secretion. Ann N Y Acad Sci *512*, 402-414.

Dallman, M.F., and Jones, M.T. (1973). Corticosteroid feedback control of ACTH secretion: effect of stress-induced corticosterone ssecretion on subsequent stress responses in the rat. Endocrinology *92*, 1367-1375.

Dam, V., Sikder, T., and Santosa, S. (2016). From neutrophils to macrophages: differences in regional adipose tissue depots. Obes Rev *17*, 1-17.

Daughaday, W.H. (1956). Binding of corticosteroids by plasma proteins. I. Dialysis equilibrium and renal clearance studies. J Clin Invest *35*, 1428-1433.

de Medeiros, G.F., Minni, A.M., Helbling, J.C., and Moisan, M.P. (2016). Chronic stress does not further exacerbate the abnormal psychoneuroendocrine phenotype of Cbg-deficient male mice. Psychoneuroendocrinology *70*, 33-37.

Deuschle, M., Weber, B., Colla, M., Müller, M., Kniest, A., and Heuser, I. (1998). Mineralocorticoid receptor also modulates basal activity of hypothalamus-pituitary-adrenocortical system in humans. Neuroendocrinology *68*, 355-360.

Dhabhar, F.S., McEwen, B.S., and Spencer, R.L. (1993). Stress response, adrenal steroid receptor levels and corticosteroid-binding globulin levels--a comparison between Sprague-Dawley, Fischer 344 and Lewis rats. Brain Res *616*, 89-98.

Dietzel, J., Krebs, A., Lüdemann, J., Roser, M., and Dressel, A. (2008). Neutrophils in cerebrospinal fluid without pleocytosis. Eur J Neurol *15*, 634-636.

Doe, R.P., Lohrenz, F.N., and Seal, U.S. (1965). FAMILIAL DECREASE IN CORTICOSTEROID-BINDING GLOBULIN. Metabolism *14*, 940-943.

Dube, S., Slama, M.Q., Basu, A., Rizza, R.A., and Basu, R. (2015). Glucocorticoid Excess Increases Hepatic 11β-HSD-1 Activity in Humans: Implications in Steroid-Induced Diabetes. J Clin Endocrinol Metab *100*, 4155-4162.

Dunn, J.F., Nisula, B.C., and Rodbard, D. (1981). Transport of steroid hormones: binding of 21 endogenous steroids to both testosterone-binding globulin and corticosteroid-binding globulin in human plasma. J Clin Endocrinol Metab *53*, 58-68.

Durber, S.M., Lawson, J., and Daly, J.R. (1976). The effect of oral contraceptives on plasma cortisol and cortisol binding capacity throughout the menstrual cycle in normal women. Br J Obstet Gynaecol *83*, 814-818.

Edwards, C.R., Stewart, P.M., Burt, D., Brett, L., McIntyre, M.A., Sutanto, W.S., de Kloet, E.R., and Monder, C. (1988). Localisation of 11 beta-hydroxysteroid dehydrogenase--tissue specific protector of the mineralocorticoid receptor. Lancet *2*, 986-989.

Elborn, J.S., Perrett, J., Forsman-Semb, K., Marks-Konczalik, J., Gunawardena, K., and Entwistle, N. (2012). Efficacy, safety and effect on biomarkers of AZD9668 in cystic fibrosis. Eur Respir J *40*, 969-976.

Elgazar-Carmon, V., Rudich, A., Hadad, N., and Levy, R. (2008). Neutrophils transiently infiltrate intra-abdominal fat early in the course of high-fat feeding. J Lipid Res *49*, 1894-1903.

Elliott, P.R., Stein, P.E., Bilton, D., Carrell, R.W., and Lomas, D.A. (1996). Structural explanation for the deficiency of S alpha 1-antitrypsin. Nat Struct Biol *3*, 910-911.

Emptoz-Bonneton, A., Cousin, P., Seguchi, K., Avvakumov, G.V., Bully, C., Hammond, G.L., and Pugeat, M. (2000). Novel human corticosteroid-binding globulin variant with low cortisol-binding affinity. J Clin Endocrinol Metab *85*, 361-367.

Emptoz-Bonneton, A., Crave, J.C., Lejeune, H., Brébant, C., and Pugeat, M. (1997). Corticosteroid-Binding Globulin Synthesis Regulation by Cytokines and Glucocorticoids in Human Hepatoblastoma-Derived (HepG2) Cells1. The Journal of Clinical Endocrinology & Metabolism *82*, 3758-3762.

Evanson, N.K., Tasker, J.G., Hill, M.N., Hillard, C.J., and Herman, J.P. (2010). Fast feedback inhibition of the HPA axis by glucocorticoids is mediated by endocannabinoid signaling. Endocrinology *151*, 4811-4819.

Feldman, D., Mondon, C.E., Horner, J.A., and Weiser, J.N. (1979). Glucocorticoid and estrogen regulation of corticosteroid-binding globulin production by rat liver. Am J Physiol *237*, E493-499.

Felländer, G., Linde, B., and Bolinder, J. (1996). Evaluation of the microdialysis ethanol technique for monitoring of subcutaneous adipose tissue blood flow in humans. Int J Obes Relat Metab Disord *20*, 220-226.

Fernández-Real, J.M., Grasa, M., Casamitjana, R., Pugeat, M., Barret, C., and Ricart, W. (1999). Plasma total and glycosylated corticosteroid-binding globulin levels are associated with insulin secretion. J Clin Endocrinol Metab *84*, 3192-3196.

Fernández-Real, J.M., Grasa, M., Casamitjana, R., and Ricart, W. (2000). The insulin resistance syndrome and the binding capacity of cortisol binding globulin (CBG) in men and women. Clin Endocrinol (Oxf) *52*, 93-99.

Fernández-Real, J.M., Pugeat, M., Emptoz-Bonneton, A., and Ricart, W. (2001). Study of the effect of changing glucose, insulin, and insulin-like growth factor-I levels on serum corticosteroid binding globulin in lean, obese, and obese subjects with glucose intolerance. Metabolism *50*, 1248-1252.

Fernandez-Real, J.M., Pugeat, M., Grasa, M., Broch, M., Vendrell, J., Brun, J., and Ricart, W. (2002). Serum corticosteroid-binding globulin concentration and insulin resistance syndrome: a population study. J Clin Endocrinol Metab *87*, 4686-4690.

Fernandez-Real, J.M., Pugeat, M., López-Bermejo, A., Bornet, H., and Ricart, W. (2005). Corticosteroid-binding globulin affects the relationship between circulating adiponectin and cortisol in men and women. Metabolism *54*, 584-589.

Ferrarotti, I., Carroll, T.P., Ottaviani, S., Fra, A.M., O'Brien, G., Molloy, K., Corda, L., Medicina, D., Curran, D.R., McElvaney, N.G., et al. (2014). Identification and characterisation of eight novel SERPINA1 Null mutations. Orphanet J Rare Dis *9*, 172.

Ferrarotti, I., Thun, G.A., Zorzetto, M., Ottaviani, S., Imboden, M., Schindler, C., von Eckardstein, A., Rohrer, L., Rochat, T., Russi, E.W., et al. (2012). Serum levels and genotype distribution of α1-antitrypsin in the general population. Thorax *67*, 669-674.

Fleshner, M., Silbert, L., Deak, T., Goehler, L.E., Martin, D., Watkins, L.R., and Maier, S.F. (1997). TNF-alpha-induced corticosterone elevation but not serum protein or corticosteroid binding globulin reduction is vagally mediated. Brain Res Bull *44*, 701-706.

Francart, C., Dauchez, M., Alix, A.J., and Lippens, G. (1997). Solution structure of R-elafin, a specific inhibitor of elastase. J Mol Biol *268*, 666-677.

Frayn, K.N., Coppack, S.W., Humphreys, S.M., and Whyte, P.L. (1989). Metabolic characteristics of human adipose tissue in vivo. Clin Sci (Lond) *76*, 509-516.

Friedberg, M., Zoumakis, E., Hiroi, N., Bader, T., Chrousos, G.P., and Hochberg, Z. (2003). Modulation of 11 beta-hydroxysteroid dehydrogenase type 1 in mature human subcutaneous adipocytes by hypothalamic messengers. J Clin Endocrinol Metab *88*, 385-393.

Funder, J.W. (2005). Mineralocorticoid receptors: distribution and activation. Heart Fail Rev *10*, 15-22.

Funder, J.W., Pearce, P.T., Smith, R., and Smith, A.I. (1988). Mineralocorticoid action: target tissue specificity is enzyme, not receptor, mediated. Science *242*, 583-585.

Gagliardi, L., Ho, J.T., and Torpy, D.J. (2010). Corticosteroid-binding globulin: the clinical significance of altered levels and heritable mutations. Mol Cell Endocrinol *316*, 24-34.

Gardill, B.R., Vogl, M.R., Lin, H.Y., Hammond, G.L., and Muller, Y.A. (2012). Corticosteroid-binding globulin: structure-function implications from species differences. PLoS One *7*, e52759.

Garrel, D.R. (1996). Corticosteroid-binding globulin during inflammation and burn injury: nutritional modulation and clinical implications. Horm Res *45*, 245-251.

Garrel, D.R., Zhang, L., Zhao, X.F., and Hammond, G.L. (1993). Effect of burn injury on corticosteroid-binding globulin levels in plasma and wound fluid. Wound Repair Regen *1*, 10-14.

Gillies, G.E., Linton, E.A., and Lowry, P.J. (1982). Corticotropin releasing activity of the new CRF is potentiated several times by vasopressin. Nature *299*, 355-357.

Grasa, M.M., Cabot, C., Balada, F., Virgili, J., Sanchis, D., Monserrat, C., Fernández-López, J.A., Remesar, X., and Alemany, M. (1998). Corticosterone binding to tissues of adrenalectomized lean and obese Zucker rats. Horm Metab Res *30*, 699-704.

Grasa, M.M., Cabot, C., Fernández-López, J.A., Remesar, X., and Alemany, M. (2001). Modulation of corticosterone availability to white adipose tissue of lean and obese Zucker rats by corticosteroid-binding globulin. Horm Metab Res *33*, 407-411.

Greene, C.M., Marciniak, S.J., Teckman, J., Ferrarotti, I., Brantly, M.L., Lomas, D.A., Stoller, J.K., and McElvaney, N.G. (2016). α1-Antitrypsin deficiency. Nat Rev Dis Primers *2*, 16051.

Groeneweg, F.L., Karst, H., de Kloet, E.R., and Joëls, M. (2011). Rapid non-genomic effects of corticosteroids and their role in the central stress response. J Endocrinol *209*, 153-167.

Gulfo, J., Ledda, A., Serra, E., Cabot, C., Esteve, M., and Grasa, M. (2016). Altered lipid partitioning and glucocorticoid availability in CBG-deficient male mice with diet-induced obesity. Obesity (Silver Spring) *24*, 1677-1686.

Hadjian, A.J., Chedin, M., Cochet, C., and Chambaz, E.M. (1975). Cortisol Binding to Proteins in Plasma in the Human Neonate and Infant. Pediatric Research *9*, 40-45.

Hammond, G.L. (1990). Molecular properties of corticosteroid binding globulin and the sex-steroid binding proteins. Endocr Rev *11*, 65-79.

Hammond, G.L. (2016). Plasma steroid-binding proteins: primary gatekeepers of steroid hormone action. J Endocrinol *230*, R13-25.

Hammond, G.L., and Lähteenmäki, P.L. (1983). A versatile method for the determination of serum cortisol binding globulin and sex hormone binding globulin binding capacities. Clin Chim Acta *132*, 101-110.

Hammond, G.L., Smith, C.L., Goping, I.S., Underhill, D.A., Harley, M.J., Reventos, J., Musto, N.A., Gunsalus, G.L., and Bardin, C.W. (1987). Primary structure of human corticosteroid

binding globulin, deduced from hepatic and pulmonary cDNAs, exhibits homology with serine protease inhibitors. Proc Natl Acad Sci U S A *84*, 5153-5157.

Hammond, G.L., Smith, C.L., Paterson, N.A., and Sibbald, W.J. (1990a). A role for corticosteroid-binding globulin in delivery of cortisol to activated neutrophils. J Clin Endocrinol Metab *71*, 34-39.

Hammond, G.L., Smith, C.L., Underhill, C.M., and Nguyen, V.T. (1990b). Interaction between corticosteroid binding globulin and activated leukocytes in vitro. Biochem Biophys Res Commun *172*, 172-177.

Hammond, G.L., Smith, C.L., and Underhill, D.A. (1991). Molecular studies of corticosteroid binding globulin structure, biosynthesis and function. J Steroid Biochem Mol Biol *40*, 755-762.

Han, T.S., Walker, B.R., Arlt, W., and Ross, R.J. (2014). Treatment and health outcomes in adults with congenital adrenal hyperplasia. Nat Rev Endocrinol *10*, 115-124.

Henley, D.E., and Lightman, S.L. (2011). New insights into corticosteroid-binding globulin and glucocorticoid delivery. Neuroscience *180*, 1-8.

Henley, D.E., and Lightman, S.L. (2014). Cardio-metabolic consequences of glucocorticoid replacement: relevance of ultradian signalling. Clin Endocrinol (Oxf) *80*, 621-628.

Henriksen, P.A. (2014). The potential of neutrophil elastase inhibitors as anti-inflammatory therapies. Curr Opin Hematol *21*, 23-28.

Heuser, I., Deuschle, M., Weber, B., Stalla, G.K., and Holsboer, F. (2000). Increased activity of the hypothalamus-pituitary-adrenal system after treatment with the mineralocorticoid receptor antagonist spironolactone. Psychoneuroendocrinology *25*, 513-518.

Hill, L.A., Bodnar, T.S., Weinberg, J., and Hammond, G.L. (2016). Corticosteroid-binding globulin is a biomarker of inflammation onset and severity in female rats. J Endocrinol *230*, 215-225.

Hill, L.A., Sumer-Bayraktar, Z., Lewis, J.G., Morava, E., Thaysen-Andersen, M., and Hammond, G.L. (2019a). N-Glycosylation influences human corticosteroid-binding globulin measurements. Endocr Connect *8*, 1136-1148.

Hill, L.A., Vassiliadi, D.A., Dimopoulou, I., Anderson, A.J., Boyle, L.D., Kilgour, A.H.M., Stimson, R.H., Machado, Y., Overall, C.M., Walker, B.R., et al. (2019b). Neutrophil elastase-cleaved corticosteroid-binding globulin is absent in human plasma. J Endocrinol *240*, 27-39.

Hill, L.A., Vassiliadi, D.A., Simard, M., Pavlaki, A., Perogamvros, I., Hadjidakis, D., and Hammond, G.L. (2012). Two different corticosteroid-binding globulin variants that lack cortisol-binding activity in a greek woman. J Clin Endocrinol Metab *97*, 4260-4267.

Ho, J.T., Al-Musalhi, H., Chapman, M.J., Quach, T., Thomas, P.D., Bagley, C.J., Lewis, J.G., and Torpy, D.J. (2006). Septic shock and sepsis: a comparison of total and free plasma cortisol levels. J Clin Endocrinol Metab *91*, 105-114.

Ho, J.T., Chapman, M.J., O'Connor, S., Lam, S., Edwards, J., Ludbrook, G., Lewis, J.G., and Torpy, D.J. (2010). Characteristics of plasma NOx levels in severe sepsis: high interindividual variability and correlation with illness severity, but lack of correlation with cortisol levels. Clin Endocrinol (Oxf) *73*, 413-420.

Ho, J.T., Lewis, J.G., O'Loughlin, P., Bagley, C.J., Romero, R., Dekker, G.A., and Torpy, D.J. (2007). Reduced maternal corticosteroid-binding globulin and cortisol levels in pre-eclampsia and gamete recipient pregnancies. Clin Endocrinol (Oxf) *66*, 869-877.

Hodyl, N.A., Stark, M.J., Meyer, E.J., Lewis, J.G., Torpy, D.J., and Nenke, M.A. (2020). High binding site occupancy of corticosteroid-binding globulin by progesterone increases fetal free cortisol concentrations. Eur J Obstet Gynecol Reprod Biol *251*, 129-135.

Hokanson, D.E., Sumner, D.S., and Strandness, D.E., Jr. (1975). An electrically calibrated plethysmograph for direct measurement of limb blood flow. IEEE Trans Biomed Eng *22*, 25-29.

Hoshi, K., Kurosawa, S., Kato, M., Andoh, K., Satoh, D., and Kaise, A. (2005). Sivelestat, a neutrophil elastase inhibitor, reduces mortality rate of critically ill patients. Tohoku J Exp Med *207*, 143-148.

Htun, H., Barsony, J., Renyi, I., Gould, D.L., and Hager, G.L. (1996). Visualization of glucocorticoid receptor translocation and intranuclear organization in living cells with a green fluorescent protein chimera. Proc Natl Acad Sci U S A *93*, 4845-4850.

Hughes, K.A., Manolopoulos, K.N., Iqbal, J., Cruden, N.L., Stimson, R.H., Reynolds, R.M., Newby, D.E., Andrew, R., Karpe, F., and Walker, B.R. (2012). Recycling between cortisol and cortisone in human splanchnic, subcutaneous adipose, and skeletal muscle tissues in vivo. Diabetes *61*, 1357-1364.

Hum, D.W., and Miller, W.L. (1993). Transcriptional regulation of human genes for steroidogenic enzymes. Clin Chem *39*, 333-340.

Incollingo Rodriguez, A.C., Epel, E.S., White, M.L., Standen, E.C., Seckl, J.R., and Tomiyama, A.J. (2015). Hypothalamic-pituitary-adrenal axis dysregulation and cortisol activity in obesity: A systematic review. Psychoneuroendocrinology *62*, 301-318.

Inglis, G.C., Ingram, M.C., Holloway, C.D., Swan, L., Birnie, D., Hillis, W.S., Davies, E., Fraser, R., and Connell, J.M. (1999). Familial pattern of corticosteroids and their metabolism in adult human subjects--the Scottish Adult Twin Study. J Clin Endocrinol Metab *84*, 4132-4137.

Iwata, K., Doi, A., Ohji, G., Oka, H., Oba, Y., Takimoto, K., Igarashi, W., Gremillion, D.H., and Shimada, T. (2010). Effect of neutrophil elastase inhibitor (sivelestat sodium) in the treatment of acute lung injury (ALI) and acute respiratory distress syndrome (ARDS): a systematic review and meta-analysis. Intern Med *49*, 2423-2432.

Jamieson, A., Wallace, A.M., Andrew, R., Nunez, B.S., Walker, B.R., Fraser, R., White, P.C., and Connell, J.M. (1999). Apparent cortisone reductase deficiency: a functional defect in 11beta-hydroxysteroid dehydrogenase type 1. J Clin Endocrinol Metab *84*, 3570-3574.

Jang, C., Obeyesekere, V.R., Dilley, R.J., Krozowski, Z., Inder, W.J., and Alford, F.P. (2007). Altered activity of 11beta-hydroxysteroid dehydrogenase types 1 and 2 in skeletal muscle confers metabolic protection in subjects with type 2 diabetes. J Clin Endocrinol Metab *92*, 3314-3320.

Jones, B.C., Sarrieau, A., Reed, C.L., Azar, M.R., and Mormède, P. (1998). Contribution of sex and genetics to neuroendocrine adaptation to stress in mice. Psychoneuroendocrinology *23*, 505-517.

Jones, M.T., Hillhouse, E.W., and Burden, J.L. (1977). Dynamics and mechanics of corticosteroid feedback at the hypothalamus and anterior pituitary gland. J Endocrinol *73*, 405-417.

Jung, C., Ho, J.T., Torpy, D.J., Rogers, A., Doogue, M., Lewis, J.G., Czajko, R.J., and Inder, W.J. (2011). A longitudinal study of plasma and urinary cortisol in pregnancy and postpartum. J Clin Endocrinol Metab *96*, 1533-1540.

Kadmiel, M., and Cidlowski, J.A. (2013). Glucocorticoid receptor signaling in health and disease. Trends Pharmacol Sci *34*, 518-530.

Karpe, F., Fielding, B.A., Ardilouze, J.L., Ilic, V., Macdonald, I.A., and Frayn, K.N. (2002). Effects of insulin on adipose tissue blood flow in man. J Physiol *540*, 1087-1093.

Kavutharapu, S., Nagalla, B., Abbagani, V., Porika, S.K., Akka, J., Nallari, P., and Ananthapur, V. (2012). Role of proteases and antiprotease in the etiology of chronic pancreatitis. Saudi J Gastroenterol *18*, 364-368.

Keller-Wood, M.E., and Dallman, M.F. (1984). Corticosteroid inhibition of ACTH secretion. Endocr Rev *5*, 1-24.

Khan, M.S., Aden, D., and Rosner, W. (1984). Human corticosteroid binding globulin is secreted by a hepatoma-derived cell line. J Steroid Biochem *20*, 677-678.

Khandpur, R., Carmona-Rivera, C., Vivekanandan-Giri, A., Gizinski, A., Yalavarthi, S., Knight, J.S., Friday, S., Li, S., Patel, R.M., Subramanian, V., et al. (2013). NETs are a source of citrullinated autoantigens and stimulate inflammatory responses in rheumatoid arthritis. Sci Transl Med *5*, 178ra140.

Kilgour, A.H., Semple, S., Marshall, I., Andrews, P., Andrew, R., and Walker, B.R. (2015). 11β-Hydroxysteroid dehydrogenase activity in the brain does not contribute to systemic interconversion of cortisol and cortisone in healthy men. J Clin Endocrinol Metab *100*, 483-489.

Kitchener, P., Di Blasi, F., Borrelli, E., and Piazza, P.V. (2004). Differences between brain structures in nuclear translocation and DNA binding of the glucocorticoid receptor during stress and the circadian cycle. Eur J Neurosci *19*, 1837-1846.

Kling, M.A., Demitrack, M.A., Whitfield, H.J., Jr., Kalogeras, K.T., Listwak, S.J., DeBellis, M.D., Chrousos, G.P., Gold, P.W., and Brandt, H.A. (1993). Effects of the glucocorticoid antagonist RU 486 on pituitary-adrenal function in patients with anorexia nervosa and healthy volunteers: enhancement of plasma ACTH and cortisol secretion in underweight patients. Neuroendocrinology *57*, 1082-1091.

Kuna, P., Jenkins, M., O'Brien, C.D., and Fahy, W.A. (2012). AZD9668, a neutrophil elastase inhibitor, plus ongoing budesonide/formoterol in patients with COPD. Respir Med *106*, 531-539.

Kyle, C.J., Nixon, M., Homer, N.Z.M., Morgan, R.A., Andrew, R., Stimson, R.H., and Walker, B.R. (2022). ABCC1 modulates negative feedback control of the hypothalamic-pituitary-adrenal axis in vivo in humans. Metabolism *128*, 155118.

Larsen, O.A., Lassen, N.A., and Quaade, F. (1966). Blood flow through human adipose tissue determined with radioactive xenon. Acta Physiol Scand *66*, 337-345.

Lazzarino, A.I., Hamer, M., Gaze, D., Collinson, P., and Steptoe, A. (2013). The association between cortisol response to mental stress and high-sensitivity cardiac troponin T plasma concentration in healthy adults. J Am Coll Cardiol *62*, 1694-1701.

Lei, J.H., Yang, X., Peng, S., Li, Y., Underhill, C., Zhu, C., Lin, H.Y., Wang, H., and Hammond, G.L. (2015). Impact of corticosteroid-binding globulin deficiency on pregnancy and neonatal sex. J Clin Endocrinol Metab *100*, 1819-1827.

Lewis, J.G., Bagley, C.J., Elder, P.A., Bachmann, A.W., and Torpy, D.J. (2005). Plasma free cortisol fraction reflects levels of functioning corticosteroid-binding globulin. Clin Chim Acta *359*, 189-194.

Lewis, J.G., and Elder, P.A. (2011). Corticosteroid-binding globulin reactive centre loop antibodies recognise only the intact natured protein: elastase cleaved and uncleaved CBG may coexist in circulation. J Steroid Biochem Mol Biol *127*, 289-294.

Lewis, J.G., and Elder, P.A. (2013). Intact or "active" corticosteroid-binding globulin (CBG) and total CBG in plasma: determination by parallel ELISAs using monoclonal antibodies. Clin Chim Acta *416*, 26-30.

Lewis, J.G., and Elder, P.A. (2014). The reactive centre loop of corticosteroid-binding globulin (CBG) is a protease target for cortisol release. Mol Cell Endocrinol *384*, 96-101.

Lewis, J.G., and Elder, P.A. (2017). Monoclonal antibodies to the reactive centre loop (RCL) of human corticosteroid-binding globulin (CBG) can protect against proteolytic cleavage. J Steroid Biochem Mol Biol *171*, 247-253.

Lewis, J.G., Lewis, M.G., and Elder, P.A. (2003). An enzyme-linked immunosorbent assay for corticosteroid-binding globulin using monoclonal and polyclonal antibodies: decline in CBG following synthetic ACTH. Clin Chim Acta *328*, 121-128.

Lewis, J.G., Saunders, K., Dyer, A., and Elder, P.A. (2015). The half-lives of intact and elastase cleaved human corticosteroid-binding globulin (CBG) are identical in the rabbit. J Steroid Biochem Mol Biol *149*, 53-57.

Li, Y., Wu, L., Lei, J., Zhu, C., Wang, H., Yu, X., and Lin, H. (2012). Single nucleotide polymorphisms in the human corticosteroid-binding globulin promoter alter transcriptional activity. Sci China Life Sci *55*, 699-708.

Libert, C., Wielockx, B., Hammond, G.L., Brouckaert, P., Fiers, W., and Elliott, R.W. (1999). Identification of a locus on distal mouse chromosome 12 that controls resistance to tumor necrosis factor-induced lethal shock. Genomics *55*, 284-289.

Lightman, S.L. (2008). The neuroendocrinology of stress: a never ending story. J Neuroendocrinol *20*, 880-884.

Lin, D., Sugawara, T., Strauss, J.F., 3rd, Clark, B.J., Stocco, D.M., Saenger, P., Rogol, A., and Miller, W.L. (1995). Role of steroidogenic acute regulatory protein in adrenal and gonadal steroidogenesis. Science *267*, 1828-1831.

Lin, H.Y., Muller, Y.A., and Hammond, G.L. (2010). Molecular and structural basis of steroid hormone binding and release from corticosteroid-binding globulin. Mol Cell Endocrinol *316*, 3-12.

Lin, H.Y., Underhill, C., Gardill, B.R., Muller, Y.A., and Hammond, G.L. (2009). Residues in the human corticosteroid-binding globulin reactive center loop that influence steroid binding before and after elastase cleavage. J Biol Chem *284*, 884-896.

Lin, H.Y., Underhill, C., Lei, J.H., Helander-Claesson, A., Lee, H.Y., Gardill, B.R., Muller, Y.A., Wang, H., and Hammond, G.L. (2012). High frequency of SERPINA6 polymorphisms that reduce plasma corticosteroid-binding globulin activity in Chinese subjects. J Clin Endocrinol Metab *97*, E678-686.

Makino, H., Kunisaki, C., Kosaka, T., Akiyama, H., Morita, S., and Endo, I. (2011). Perioperative use of a neutrophil elastase inhibitor in video-assisted thoracoscopic oesophagectomy for cancer. Br J Surg *98*, 975-982.

Manco, M., Fernández-Real, J.M., Valera-Mora, M.E., Déchaud, H., Nanni, G., Tondolo, V., Calvani, M., Castagneto, M., Pugeat, M., and Mingrone, G. (2007). Massive weight loss decreases corticosteroid-binding globulin levels and increases free cortisol in healthy obese patients: an adaptive phenomenon? Diabetes Care *30*, 1494-1500.

Mangelsdorf, D.J., Thummel, C., Beato, M., Herrlich, P., Schütz, G., Umesono, K., Blumberg, B., Kastner, P., Mark, M., Chambon, P., et al. (1995). The nuclear receptor superfamily: the second decade. Cell *83*, 835-839.

Mansuy-Aubert, V., Zhou, Q.L., Xie, X., Gong, Z., Huang, J.Y., Khan, A.R., Aubert, G., Candelaria, K., Thomas, S., Shin, D.J., et al. (2013). Imbalance between neutrophil elastase and its inhibitor α1-antitrypsin in obesity alters insulin sensitivity, inflammation, and energy expenditure. Cell Metab *17*, 534-548.

Marsden, M.D., and Fournier, R.E. (2005). Organization and expression of the human serpin gene cluster at 14q32.1. Front Biosci *10*, 1768-1778.

Mast, A.E., Enghild, J.J., Pizzo, S.V., and Salvesen, G. (1991). Analysis of the plasma elimination kinetics and conformational stabilities of native, proteinase-complexed, and reactive site cleaved serpins: comparison of alpha 1-proteinase inhibitor, alpha 1-antichymotrypsin, antithrombin III, alpha 2-antiplasmin, angiotensinogen, and ovalbumin. Biochemistry *30*, 1723-1730.

Mattsson, C., Reynolds, R.M., Simonyte, K., Olsson, T., and Walker, B.R. (2009). Combined receptor antagonist stimulation of the hypothalamic-pituitary-adrenal axis test identifies impaired negative feedback sensitivity to cortisol in obese men. J Clin Endocrinol Metab *94*, 1347-1352.

Mendel, C.M. (1989). The free hormone hypothesis: a physiologically based mathematical model. Endocr Rev *10*, 232-274.

Meyer, E.J., Nenke, M.A., Rankin, W., Lewis, J.G., Konings, E., Slager, M., Jansen, T.C., Bakker, J., Hofland, J., Feelders, R.A., et al. (2018). Total and high-affinity corticosteroid-

binding globulin depletion in septic shock is associated with mortality. Clin Endocrinol (Oxf) *90*, 232-240.

Meyer, E.J., Torpy, D.J., Chernykh, A., Thaysen-Andersen, M., Nenke, M.A., Lewis, J.G., Rajapaksha, H., Rankin, W., and Polyak, S.W. (2020). Pyrexia and acidosis act independently of neutrophil elastase reactive center loop cleavage to effect cortisol release from corticosteroid-binding globulin. Protein Sci.

Michailidou, Z., Gomez-Salazar, M., and Alexaki, V.I. (2022). Innate Immune Cells in the Adipose Tissue in Health and Metabolic Disease. J Innate Immun *14*, 4-30.

Mickelson, K.E., Forsthoefel, J., and Westphal, U. (1981). Steroid-protein interactions. Human corticosteroid binding globulin: some physicochemical properties and binding specificity. Biochemistry *20*, 6211-6218.

Mihrshahi, R., Lewis, J.G., and Ali, S.O. (2006). Hormonal effects on the secretion and glycoform profile of corticosteroid-binding globulin. J Steroid Biochem Mol Biol *101*, 275-285.

Minni, A.M., Dorey, R., Piérard, C., Dominguez, G., Helbling, J.C., Foury, A., Béracochéa, D., and Moisan, M.P. (2012). Critical role of plasma corticosteroid-binding-globulin during stress to promote glucocorticoid delivery to the brain: impact on memory retrieval. Endocrinology *153*, 4766-4774.

Misao, R., Iwagaki, S., Sun, W.S., Fujimoto, J., Saio, M., Takami, T., and Tamaya, T. (1999a). Evidence for the synthesis of corticosteroid-binding globulin in human placenta. Horm Res *51*, 162-167.

Misao, R., Nakanishi, Y., Fujimoto, J., Iwagaki, S., and Tamaya, T. (1999b). Levels of sex hormone-binding globulin and corticosteroid-binding globulin mRNAs in corpus luteum of human subjects: correlation with serum steroid hormone levels. Gynecol Endocrinol *13*, 82-88.

Mitchell, E., Torpy, D.J., and Bagley, C.J. (2004). Pregnancy-associated corticosteroid-binding globulin: high resolution separation of glycan isoforms. Horm Metab Res *36*, 357-359.

Miyoshi, S., Hamada, H., Ito, R., Katayama, H., Irifune, K., Suwaki, T., Nakanishi, N., Kanematsu, T., Dote, K., Aibiki, M., et al. (2013). Usefulness of a selective neutrophil elastase inhibitor, sivelestat, in acute lung injury patients with sepsis. Drug Des Devel Ther *7*, 305-316.

Moisan, M.P. (2013). CBG: a cortisol reservoir rather than a transporter. Nat Rev Endocrinol *9*, 78.

Moisan, M.P., and Castanon, N. (2016). Emerging Role of Corticosteroid-Binding Globulin in Glucocorticoid-Driven Metabolic Disorders. Front Endocrinol (Lausanne) *7*, 160.

Molhuizen, H.O., Alkemade, H.A., Zeeuwen, P.L., de Jongh, G.J., Wieringa, B., and Schalkwijk, J. (1993). SKALP/elafin: an elastase inhibitor from cultured human keratinocytes.

Purification, cDNA sequence, and evidence for transglutaminase cross-linking. J Biol Chem *268*, 12028-12032.

Moreau, T., Baranger, K., Dadé, S., Dallet-Choisy, S., Guyot, N., and Zani, M.L. (2008). Multifaceted roles of human elafin and secretory leukocyte proteinase inhibitor (SLPI), two serine protease inhibitors of the chelonianin family. Biochimie *90*, 284-295.

Morgan, S.A., McCabe, E.L., Gathercole, L.L., Hassan-Smith, Z.K., Larner, D.P., Bujalska, I.J., Stewart, P.M., Tomlinson, J.W., and Lavery, G.G. (2014). 11β-HSD1 is the major regulator of the tissue-specific effects of circulating glucocorticoid excess. Proc Natl Acad Sci U S A *111*, E2482-2491.

Morgan, S.A., Sherlock, M., Gathercole, L.L., Lavery, G.G., Lenaghan, C., Bujalska, I.J., Laber, D., Yu, A., Convey, G., Mayers, R., et al. (2009). 11beta-hydroxysteroid dehydrogenase type 1 regulates glucocorticoid-induced insulin resistance in skeletal muscle. Diabetes *58*, 2506-2515.

Mormede, P., Foury, A., Barat, P., Corcuff, J.B., Terenina, E., Marissal-Arvy, N., and Moisan, M.P. (2011). Molecular genetics of hypothalamic-pituitary-adrenal axis activity and function. Ann N Y Acad Sci *1220*, 127-136.

Mountjoy, K.G., Mortrud, M.T., Low, M.J., Simerly, R.B., and Cone, R.D. (1994). Localization of the melanocortin-4 receptor (MC4-R) in neuroendocrine and autonomic control circuits in the brain. Mol Endocrinol *8*, 1298-1308.

Muller, C.A., Belyaev, O., Vogeser, M., Weyhe, D., Gloor, B., Strobel, O., Werner, J., Borgstrom, A., Buchler, M.W., and Uhl, W. (2007). Corticosteroid-binding globulin: A possible early predictor of infection in acute necrotizing pancreatitis. Scandinavian Journal of Gastroenterology *42*, 1354-1361.

Nader, N., Raverot, G., Emptoz-Bonneton, A., Déchaud, H., Bonnay, M., Baudin, E., and Pugeat, M. (2006). Mitotane has an estrogenic effect on sex hormone-binding globulin and corticosteroid-binding globulin in humans. J Clin Endocrinol Metab *91*, 2165-2170.

Namciu, S.J., Friedman, R.D., Marsden, M.D., Sarausad, L.M., Jasoni, C.L., and Fournier, R.E. (2004). Sequence organization and matrix attachment regions of the human serine protease inhibitor gene cluster at 14q32.1. Mamm Genome *15*, 162-178.

Nara, K., Ito, S., Ito, T., Suzuki, Y., Ghoneim, M.A., Tachibana, S., and Hirose, S. (1994). Elastase inhibitor elafin is a new type of proteinase inhibitor which has a transglutaminase-mediated anchoring sequence termed "cementoin". J Biochem *115*, 441-448.

Nenke, M.A., Holmes, M., Rankin, W., Lewis, J.G., and Torpy, D.J. (2016a). Corticosteroid-binding globulin cleavage is paradoxically reduced in alpha-1 antitrypsin deficiency: Implications for cortisol homeostasis. Clin Chim Acta *452*, 27-31.

Nenke, M.A., Lewis, J.G., Rankin, W., McWilliams, L., Metcalf, R.G., Proudman, S.M., and Torpy, D.J. (2016b). Reduced corticosteroid-binding globulin cleavage in active rheumatoid arthritis. Clin Endocrinol (Oxf) *85*, 369-377.

Nenke, M.A., Lewis, J.G., Rankin, W., Shaw, D., and Torpy, D.J. (2017a). Corticosteroid-binding globulin cleavage may be pathogen-dependent in bloodstream infection. Clin Chim Acta *464*, 176-181.

Nenke, M.A., Lewis, J.G., Rankin, W., and Torpy, D.J. (2016c). Evidence of Reduced CBG Cleavage in Abdominal Obesity: A Potential Factor in Development of the Metabolic Syndrome. Horm Metab Res *48*, 523-528.

Nenke, M.A., Nielsen, S.T., Lehrskov, L.L., Lewis, J.G., Rankin, W., Møller, K., and Torpy, D.J. (2017b). Pyrexia's effect on the CBG-cortisol thermocouple, rather than CBG cleavage, elevates the acute free cortisol response to TNF-α in humans. Stress *20*, 183-188.

Nenke, M.A., Rankin, W., Chapman, M.J., Stevens, N.E., Diener, K.R., Hayball, J.D., Lewis, J.G., and Torpy, D.J. (2015). Depletion of high-affinity corticosteroid-binding globulin corresponds to illness severity in sepsis and septic shock; clinical implications. Clin Endocrinol (Oxf) *82*, 801-807.

Nenke, M.A., Zeng, A., Meyer, E.J., Lewis, J.G., Rankin, W., Johnston, J., Kireta, S., Jesudason, S., and Torpy, D.J. (2017c). Differential Effects of Estrogen on Corticosteroid-Binding Globulin Forms Suggests Reduced Cleavage in Pregnancy. J Endocr Soc *1*, 202-210.

Nishi, M., and Kawata, M. (2006). Brain corticosteroid receptor dynamics and trafficking: Implications from live cell imaging. Neuroscientist *12*, 119-133.

Nixon, M., Mackenzie, S.D., Taylor, A.I., Homer, N.Z., Livingstone, D.E., Mouras, R., Morgan, R.A., Mole, D.J., Stimson, R.H., Reynolds, R.M., et al. (2016). ABCC1 confers tissue-specific sensitivity to cortisol versus corticosterone: A rationale for safer glucocorticoid replacement therapy. Sci Transl Med *8*, 352ra109.

Nixon, M., Upreti, R., and Andrew, R. (2012). 5α-Reduced glucocorticoids: a story of natural selection. J Endocrinol *212*, 111-127.

Okayama, N., Kakihana, Y., Setoguchi, D., Imabayashi, T., Omae, T., Matsunaga, A., and Kanmura, Y. (2006). Clinical effects of a neutrophil elastase inhibitor, sivelestat, in patients with acute respiratory distress syndrome. J Anesth *20*, 6-10.

Orchinik, M., Murray, T.F., and Moore, F.L. (1991). A corticosteroid receptor in neuronal membranes. Science *252*, 1848-1851.

Paulsen, G., Egner, I., Raastad, T., Reinholt, F., Owe, S., Lauritzen, F., Brorson, S.H., and Koskinen, S. (2013). Inflammatory markers CD11b, CD16, CD66b, CD68, myeloperoxidase and neutrophil elastase in eccentric exercised human skeletal muscles. Histochem Cell Biol *139*, 691-715.

Pemberton, P.A., Stein, P.E., Pepys, M.B., Potter, J.M., and Carrell, R.W. (1988). Hormone binding globulins undergo serpin conformational change in inflammation. Nature *336*, 257-258.

Perogamvros, I., Ray, D.W., and Trainer, P.J. (2012). Regulation of cortisol bioavailability--effects on hormone measurement and action. Nat Rev Endocrinol *8*, 717-727.

Perogamvros, I., Underhill, C., Henley, D.E., Hadfield, K.D., Newman, W.G., Ray, D.W., Lightman, S.L., Hammond, G.L., and Trainer, P.J. (2010). Novel corticosteroid-binding globulin variant that lacks steroid binding activity. J Clin Endocrinol Metab *95*, E142-150.

Petersen, H.H., Andreassen, T.K., Breiderhoff, T., Bräsen, J.H., Schulz, H., Gross, V., Gröne, H.J., Nykjaer, A., and Willnow, T.E. (2006). Hyporesponsiveness to glucocorticoids in mice genetically deficient for the corticosteroid binding globulin. Mol Cell Biol *26*, 7236-7245.

Phillipov, G., Palermo, M., and Shackleton, C.H. (1996). Apparent cortisone reductase deficiency: a unique form of hypercortisolism. J Clin Endocrinol Metab *81*, 3855-3860.

Pratt, W.B., Galigniana, M.D., Harrell, J.M., and DeFranco, D.B. (2004). Role of hsp90 and the hsp90-binding immunophilins in signalling protein movement. Cell Signal *16*, 857-872.

Predine, J., Brailly, S., Delaporte, P., and Milgrom, E. (1984). Protein binding of cortisol in human cerebrospinal fluid. J Clin Endocrinol Metab *58*, 6-11.

Pugeat, M., Bonneton, A., Perrot, D., Rocle-Nicolas, B., Lejeune, H., Grenot, C., Déchaud, H., Brébant, C., Motin, J., and Cuilleron, C.Y. (1989). Decreased immunoreactivity and binding activity of corticosteroid-binding globulin in serum in septic shock. Clin Chem *35*, 1675-1679.

Rask, E., Olsson, T., Söderberg, S., Andrew, R., Livingstone, D.E., Johnson, O., and Walker, B.R. (2001). Tissue-specific dysregulation of cortisol metabolism in human obesity. J Clin Endocrinol Metab *86*, 1418-1421.

Rask, E., Walker, B.R., Söderberg, S., Livingstone, D.E., Eliasson, M., Johnson, O., Andrew, R., and Olsson, T. (2002). Tissue-specific changes in peripheral cortisol metabolism in obese women: increased adipose 11beta-hydroxysteroid dehydrogenase type 1 activity. J Clin Endocrinol Metab *87*, 3330-3336.

Ray, L.A., Mackillop, J., Leggio, L., Morgan, M., and Hutchison, K.E. (2009). Effects of naltrexone on cortisol levels in heavy drinkers. Pharmacol Biochem Behav *91*, 489-494.

Reul, J.M., de Kloet, E.R., van Sluijs, F.J., Rijnberk, A., and Rothuizen, J. (1990). Binding characteristics of mineralocorticoid and glucocorticoid receptors in dog brain and pituitary. Endocrinology *127*, 907-915.

Rhen, T., and Cidlowski, J.A. (2005). Antiinflammatory action of glucocorticoids--new mechanisms for old drugs. N Engl J Med *353*, 1711-1723.

Richard, E.M., Helbling, J.C., Tridon, C., Desmedt, A., Minni, A.M., Cador, M., Pourtau, L., Konsman, J.P., Mormède, P., and Moisan, M.P. (2010). Plasma transcortin influences endocrine and behavioral stress responses in mice. Endocrinology *151*, 649-659.

Rivier, C., and Vale, W. (1983). Interaction of corticotropin-releasing factor and arginine vasopressin on adrenocorticotropin secretion in vivo. Endocrinology *113*, 939-942.

Robinson, P.A., and Hammond, G.L. (1985). Identification and characterization of a human corticosteroid binding globulin variant with a reduced affinity for cortisol. J Endocrinol *104*, 269-277.

Roddie, I.C., Shepherd, J.T., and Whelan, R.F. (1956). Evidence from venous oxygen saturation measurements that the increase in forearm blood flow during body heating is confined to the skin. J Physiol *134*, 444-450.

Roitman, A., Bruchis, S., Bauman, B., Kaufman, H., and Laron, Z. (1984). Total deficiency of corticosteroid-binding globulin. Clin Endocrinol (Oxf) *21*, 541-548.

Rojek, A.M., Wood, R.E., and Stewart, I.B. (2007). The effect of changing limb position on the validity of venous occlusion plethysmography. Physiol Meas *28*, 861-867.

Rosales, C. (2018). Neutrophil: A Cell with Many Roles in Inflammation or Several Cell Types? Front Physiol *9*, 113.

Rose, A.J., and Herzig, S. (2013). Metabolic control through glucocorticoid hormones: an update. Mol Cell Endocrinol *380*, 65-78.

Rose, S., Fiebrich, M., Weber, P., Dike, J., and Bühren, V. (1998). Neutrophil activation after skeletal muscle ischemia in humans. Shock *9*, 21-26.

Ryugo, M., Sawa, Y., Takano, H., Matsumiya, G., Iwai, S., Ono, M., Hata, H., Yamauchi, T., Nishimura, M., Fujino, Y., et al. (2006). Effect of a polymorphonuclear elastase inhibitor

(sivelestat sodium) on acute lung injury after cardiopulmonary bypass: findings of a double-blind randomized study. Surg Today *36*, 321-326.

Sahebnasagh, A., Saghafi, F., Safdari, M., Khataminia, M., Sadremomtaz, A., Talaei, Z., Rezai Ghaleno, H., Bagheri, M., Habtemariam, S., and Avan, R. (2020). Neutrophil elastase inhibitor (sivelestat) may be a promising therapeutic option for management of acute lung injury/acute respiratory distress syndrome or disseminated intravascular coagulation in COVID-19. J Clin Pharm Ther *45*, 1515-1519.

Sallenave, J.M., and Ryle, A.P. (1991). Purification and characterization of elastase-specific inhibitor. Sequence homology with mucus proteinase inhibitor. Biol Chem Hoppe Seyler *372*, 13-21.

Sallenave, J.M., and Silva, A. (1993). Characterization and gene sequence of the precursor of elafin, an elastase-specific inhibitor in bronchial secretions. Am J Respir Cell Mol Biol *8*, 439-445.

Sandeep, T.C., Yau, J.L., MacLullich, A.M., Noble, J., Deary, I.J., Walker, B.R., and Seckl, J.R. (2004). 11Beta-hydroxysteroid dehydrogenase inhibition improves cognitive function in healthy elderly men and type 2 diabetics. Proc Natl Acad Sci U S A *101*, 6734-6739.

Sanrattana, W., Maas, C., and de Maat, S. (2019). SERPINs-From Trap to Treatment. Front Med (Lausanne) *6*, 25.

Sapolsky, R.M., Romero, L.M., and Munck, A.U. (2000). How do glucocorticoids influence stress responses? Integrating permissive, suppressive, stimulatory, and preparative actions. Endocr Rev *21*, 55-89.

Savu, L., Zouaghi, H., Carli, A., and Nunez, E.A. (1981). Serum depletion of corticosteroid binding activities, an early marker of human septic shock. Biochem Biophys Res Commun *102*, 411-419.

Sawchenko, P.E., Swanson, L.W., and Vale, W.W. (1984). Co-expression of corticotropin-releasing factor and vasopressin immunoreactivity in parvocellular neurosecretory neurons of the adrenalectomized rat. Proc Natl Acad Sci U S A *81*, 1883-1887.

Schäfer, H.H., Gebhart, V.M., Hertel, K., and Jirikowski, G.F. (2015). Expression of corticosteroid-binding globulin CBG in the human heart. Horm Metab Res *47*, 596-599.

Schalkwijk, J., Wiedow, O., and Hirose, S. (1999). The trappin gene family: proteins defined by an N-terminal transglutaminase substrate domain and a C-terminal four-disulphide core. Biochem J *340 (Pt 3)*, 569-577.

Schlechte, J.A., and Hamilton, D. (1987). The effect of glucocorticoids on corticosteroid binding globulin. Clin Endocrinol (Oxf) *27*, 197-203.

Scott, S.M., and Wells, L. (1995). Corticosteroid-binding globulin in preterm infants in an intensive care unit. Horm Res *44*, 218-221.

Seckl, J.R., and Walker, B.R. (2001). Minireview: 11beta-hydroxysteroid dehydrogenase type 1- a tissue-specific amplifier of glucocorticoid action. Endocrinology *142*, 1371-1376.

Seixas, S., and Marques, P.I. (2021). Known Mutations at the Cause of Alpha-1 Antitrypsin Deficiency an Updated Overview of SERPINA1 Variation Spectrum. Appl Clin Genet *14*, 173-194.

Setoh, K., Terao, C., Muro, S., Kawaguchi, T., Tabara, Y., Takahashi, M., Nakayama, T., Kosugi, S., Sekine, A., Yamada, R., et al. (2015). Three missense variants of metabolic syndrome-related genes are associated with alpha-1 antitrypsin levels. Nat Commun *6*, 7754.

Shaw, L., and Wiedow, O. (2011). Therapeutic potential of human elafin. Biochem Soc Trans *39*, 1450-1454.

Siiteri, P.K., Murai, J.T., Hammond, G.L., Nisker, J.A., Raymoure, W.J., and Kuhn, R.W. (1982). The serum transport of steroid hormones. Recent Prog Horm Res *38*, 457-510.

Simard, M., Hill, L.A., Lewis, J.G., and Hammond, G.L. (2015). Naturally occurring mutations of human corticosteroid-binding globulin. J Clin Endocrinol Metab *100*, E129-139.

Simard, M., Hill, L.A., Underhill, C.M., Keller, B.O., Villanueva, I., Hancock, R.E., and Hammond, G.L. (2014). Pseudomonas aeruginosa elastase disrupts the cortisol-binding activity of corticosteroid-binding globulin. Endocrinology *155*, 2900-2908.

Simard, M., Underhill, C., and Hammond, G.L. (2018). Functional implications of corticosteroid-binding globulin N-glycosylation. J Mol Endocrinol *60*, 71-84.

Simon, H.U. (2003). Neutrophil apoptosis pathways and their modifications in inflammation. Immunol Rev *193*, 101-110.

Sivukhina, E.V., Jirikowski, G.F., Bernstein, H.G., Lewis, J.G., and Herbert, Z. (2006). Expression of corticosteroid-binding protein in the human hypothalamus, co-localization with oxytocin and vasopressin. Horm Metab Res *38*, 253-259.

Skornyakov, E., Gaddameedhi, S., Paech, G.M., Sparrow, A.R., Satterfield, B.C., Shattuck, N.L., Layton, M.E., Karatsoreos, I., and HPA, V.A.N.D. (2019). Cardiac autonomic activity during simulated shift work. Ind Health *57*, 118-132.

Smith, C.L., and Hammond, G.L. (1992). Hormonal regulation of corticosteroid-binding globulin biosynthesis in the male rat. Endocrinology *130*, 2245-2251.

Smith, C.L., Power, S.G., and Hammond, G.L. (1992). A Leu----His substitution at residue 93 in human corticosteroid binding globulin results in reduced affinity for cortisol. J Steroid Biochem Mol Biol *42*, 671-676.

Spencer, R.L., Kim, P.J., Kalman, B.A., and Cole, M.A. (1998). Evidence for mineralocorticoid receptor facilitation of glucocorticoid receptor-dependent regulation of hypothalamic-pituitary-adrenal axis activity. Endocrinology *139*, 2718-2726.

Spencer, R.L., Miller, A.H., Moday, H., Stein, M., and McEwen, B.S. (1993). Diurnal differences in basal and acute stress levels of type I and type II adrenal steroid receptor activation in neural and immune tissues. Endocrinology *133*, 1941-1950.

Spiga, F., Waite, E.J., Liu, Y., Kershaw, Y.M., Aguilera, G., and Lightman, S.L. (2011). ACTH-dependent ultradian rhythm of corticosterone secretion. Endocrinology *152*, 1448-1457.

Spiga, F., Walker, J.J., Terry, J.R., and Lightman, S.L. (2014). HPA axis-rhythms. Compr Physiol *4*, 1273-1298.

Stewart, P.M., Boulton, A., Kumar, S., Clark, P.M., and Shackleton, C.H. (1999). Cortisol metabolism in human obesity: impaired cortisone-->cortisol conversion in subjects with central adiposity. J Clin Endocrinol Metab *84*, 1022-1027.

Stewart, P.M., Corrie, J.E., Shackleton, C.H., and Edwards, C.R. (1988). Syndrome of apparent mineralocorticoid excess. A defect in the cortisol-cortisone shuttle. J Clin Invest *82*, 340-349.

Stewart, P.M., Toogood, A.A., and Tomlinson, J.W. (2001). Growth hormone, insulin-like growth factor-I and the cortisol-cortisone shuttle. Horm Res *56 Suppl 1*, 1-6.

Stewart, P.M., Wallace, A.M., Valentino, R., Burt, D., Shackleton, C.H., and Edwards, C.R. (1987). Mineralocorticoid activity of liquorice: 11-beta-hydroxysteroid dehydrogenase deficiency comes of age. Lancet *2*, 821-824.

Stimson, R.H., Andersson, J., Andrew, R., Redhead, D.N., Karpe, F., Hayes, P.C., Olsson, T., and Walker, B.R. (2009). Cortisol release from adipose tissue by 11beta-hydroxysteroid dehydrogenase type 1 in humans. Diabetes *58*, 46-53.

Stimson, R.H., Andrew, R., McAvoy, N.C., Tripathi, D., Hayes, P.C., and Walker, B.R. (2011). Increased whole-body and sustained liver cortisol regeneration by 11beta-hydroxysteroid dehydrogenase type 1 in obese men with type 2 diabetes provides a target for enzyme inhibition. Diabetes *60*, 720-725.

Stocco, D.M., and Clark, B.J. (1996). Regulation of the acute production of steroids in steroidogenic cells. Endocr Rev *17*, 221-244.

Stockley, R., De Soyza, A., Gunawardena, K., Perrett, J., Forsman-Semb, K., Entwistle, N., and Snell, N. (2013). Phase II study of a neutrophil elastase inhibitor (AZD9668) in patients with bronchiectasis. Respir Med *107*, 524-533.

Strel'chyonok, O.A., and Avvakumov, G.V. (1990). Specific steroid-binding glycoproteins of human blood plasma: novel data on their structure and function. J Steroid Biochem *35*, 519-534.

Strnad, P., McElvaney, N.G., and Lomas, D.A. (2020). Alpha(1)-Antitrypsin Deficiency. N Engl J Med *382*, 1443-1455.

Sueda, K., Seo, H., and Matsui, N. (1985). Human transcortin synthesis by a cell-free translation of hepatic mRNA. Endocrinol Jpn *32*, 295-303.

Sumer-Bayraktar, Z., Grant, O.C., Venkatakrishnan, V., Woods, R.J., Packer, N.H., and Thaysen-Andersen, M. (2016). Asn347 Glycosylation of Corticosteroid-binding Globulin Fine-tunes the Host Immune Response by Modulating Proteolysis by Pseudomonas aeruginosa and Neutrophil Elastase. J Biol Chem *291*, 17727-17742.

Sumer-Bayraktar, Z., Kolarich, D., Campbell, M.P., Ali, S., Packer, N.H., and Thaysen-Andersen, M. (2011). N-glycans modulate the function of human corticosteroid-binding globulin. Mol Cell Proteomics *10*, M111.009100.

Summers, C., Rankin, S.M., Condliffe, A.M., Singh, N., Peters, A.M., and Chilvers, E.R. (2010). Neutrophil kinetics in health and disease. Trends Immunol *31*, 318-324.

Talukdar, S., Oh, D.Y., Bandyopadhyay, G., Li, D., Xu, J., McNelis, J., Lu, M., Li, P., Yan, Q., Zhu, Y., et al. (2012). Neutrophils mediate insulin resistance in mice fed a high-fat diet through secreted elastase. Nat Med *18*, 1407-1412.

Tamakuma, S., Ogawa, M., Aikawa, N., Kubota, T., Hirasawa, H., Ishizaka, A., Taenaka, N., Hamada, C., Matsuoka, S., and Abiru, T. (2004). Relationship between neutrophil elastase and acute lung injury in humans. Pulm Pharmacol Ther *17*, 271-279.

Thun, G.A., Ferrarotti, I., Imboden, M., Rochat, T., Gerbase, M., Kronenberg, F., Bridevaux, P.O., Zemp, E., Zorzetto, M., Ottaviani, S., et al. (2012). SERPINA1 PiZ and PiS heterozygotes and lung function decline in the SAPALDIA cohort. PLoS One *7*, e42728.

Thun, G.A., Imboden, M., Ferrarotti, I., Kumar, A., Obeidat, M., Zorzetto, M., Haun, M., Curjuric, I., Couto Alves, A., Jackson, V.E., et al. (2013). Causal and synthetic associations of variants in the SERPINA gene cluster with alpha1-antitrypsin serum levels. PLoS Genet *9*, e1003585.

Tinnikov, A.A., Legan, M.V., Sheveluk, N.A., Cvetovskaya, G.A., Naumenko, S.E., and Sidelnikov, S.G. (1996). Corticosteroid and immune responses to cardiac surgery. Steroids *61*, 411-415.

Tomlinson, J.W., Walker, E.A., Bujalska, I.J., Draper, N., Lavery, G.G., Cooper, M.S., Hewison, M., and Stewart, P.M. (2004). 11beta-hydroxysteroid dehydrogenase type 1: a tissue-specific regulator of glucocorticoid response. Endocr Rev *25*, 831-866.

Torpy, D.J., Bachmann, A.W., Gartside, M., Grice, J.E., Harris, J.M., Clifton, P., Easteal, S., Jackson, R.V., and Whitworth, J.A. (2004). Association between chronic fatigue syndrome and the corticosteroid-binding globulin gene ALA SER224 polymorphism. Endocr Res *30*, 417-429.

Torpy, D.J., Bachmann, A.W., Grice, J.E., Fitzgerald, S.P., Phillips, P.J., Whitworth, J.A., and Jackson, R.V. (2001). Familial corticosteroid-binding globulin deficiency due to a novel null mutation: association with fatigue and relative hypotension. J Clin Endocrinol Metab *86*, 3692-3700.

Torpy, D.J., Lundgren, B.A., Ho, J.T., Lewis, J.G., Scott, H.S., and Mericq, V. (2012). CBG Santiago: a novel CBG mutation. J Clin Endocrinol Metab *97*, E151-155.

Trapp, T., Rupprecht, R., Castrén, M., Reul, J.M., and Holsboer, F. (1994). Heterodimerization between mineralocorticoid and glucocorticoid receptor: a new principle of glucocorticoid action in the CNS. Neuron *13*, 1457-1462.

Tschöp, M., Lahner, H., Feldmeier, H., Grasberger, H., Morrison, K.M., Janssen, O.E., Attanasio, A.F., and Strasburger, C.J. (2000). Effects of growth hormone replacement therapy on levels of cortisol and cortisol-binding globulin in hypopituitary adults. Eur J Endocrinol *143*, 769-773.

Tsigos, C., Kyrou, I., Chrousos, G.P., and Papanicolaou, D.A. (1998). Prolonged suppression of corticosteroid-binding globulin by recombinant human interleukin-6 in man. J Clin Endocrinol Metab *83*, 3379.

Tsujii, S., Okabayashi, T., Shiga, M., Takezaki, Y., Sugimoto, T., Kobayashi, M., and Hanazaki, K. (2012). The effect of the neutrophil elastase inhibitor sivelestat on early injury after liver resection. World J Surg *36*, 1122-1127.

Ulrich-Lai, Y.M., and Herman, J.P. (2009). Neural regulation of endocrine and autonomic stress responses. Nat Rev Neurosci *10*, 397-409.

Underhill, D.A., and Hammond, G.L. (1989). Organization of the human corticosteroid binding globulin gene and analysis of its 5'-flanking region. Mol Endocrinol *3*, 1448-1454.

Underhill, D.A., and Hammond, G.L. (1995). cis-regulatory elements within the proximal promoter of the rat gene encoding corticosteroid-binding globulin. Gene *162*, 205-211.

Utge, S., Räikkönen, K., Kajantie, E., Lipsanen, J., Andersson, S., Strandberg, T., Reynolds, R.M., Eriksson, J.G., and Lahti, J. (2018). Polygenic risk score of SERPINA6/SERPINA1 associates with diurnal and stress-induced HPA axis activity in children. Psychoneuroendocrinology *93*, 1-7.

Vale, W., Spiess, J., Rivier, C., and Rivier, J. (1981). Characterization of a 41-residue ovine hypothalamic peptide that stimulates secretion of corticotropin and beta-endorphin. Science *213*, 1394-1397.

Van Baelen, H., Brepoels, R., and De Moor, P. (1982). Transcortin Leuven: a variant of human corticosteroid-binding globulin with decreased cortisol-binding affinity. J Biol Chem *257*, 3397-3400.

Van Baelen, H., Power, S.G., and Hammond, G.L. (1993). Decreased cortisol-binding affinity of transcortin Leuven is associated with an amino acid substitution at residue-93. Steroids *58*, 275-277.

Van Eekelen, J.A., and De Kloet, E.R. (1992). Co-localization of brain corticosteroid receptors in the rat hippocampus. Prog Histochem Cytochem *26*, 250-258.

van Seters, A.P., and Moolenaar, A.J. (1991). Mitotane increases the blood levels of hormone-binding proteins. Acta Endocrinol (Copenh) *124*, 526-533.

Vegiopoulos, A., and Herzig, S. (2007). Glucocorticoids, metabolism and metabolic diseases. Mol Cell Endocrinol *275*, 43-61.

Verhoog, N., Allie-Reid, F., Vanden Berghe, W., Smith, C., Haegeman, G., Hapgood, J., and Louw, A. (2014). Inhibition of corticosteroid-binding globulin gene expression by glucocorticoids involves C/EBPβ. PLoS One *9*, e110702.

Vogelmeier, C., Aquino, T.O., O'Brien, C.D., Perrett, J., and Gunawardena, K.A. (2012). A randomised, placebo-controlled, dose-finding study of AZD9668, an oral inhibitor of neutrophil elastase, in patients with chronic obstructive pulmonary disease treated with tiotropium. Copd *9*, 111-120.

Wake, D.J., Homer, N.Z., Andrew, R., and Walker, B.R. (2006). Acute in vivo regulation of 11beta-hydroxysteroid dehydrogenase type 1 activity by insulin and intralipid infusions in humans. J Clin Endocrinol Metab *91*, 4682-4688.

Wake, D.J., Stimson, R.H., Tan, G.D., Homer, N.Z., Andrew, R., Karpe, F., and Walker, B.R. (2007). Effects of peroxisome proliferator-activated receptor-alpha and -gamma agonists on 11beta-hydroxysteroid dehydrogenase type 1 in subcutaneous adipose tissue in men. J Clin Endocrinol Metab *92*, 1848-1856.

Walker, B.R. (2007). Glucocorticoids and cardiovascular disease. Eur J Endocrinol *157*, 545-559.

Wang, C.L., Wang, Y., Jiang, Q.L., Zeng, Y., Yao, Q.P., Liu, X., Li, T., and Jiang, J. (2023). DNase I and Sivelestat Ameliorate Experimental Hindlimb Ischemia-Reperfusion Injury by Eliminating Neutrophil Extracellular Traps. J Inflamm Res *16*, 707-721.

Watt, P.W., Willmott, A.G., Maxwell, N.S., Smeeton, N.J., Watt, E., and Richardson, A.J. (2016). Physiological and psychological responses in Fire Instructors to heat exposures. J Therm Biol *58*, 106-114.

Werthamer, S., Samuels, A.J., and Amaral, L. (1973). Identification and partial purification of "transcortin"-like protein within human lymphocytes. J Biol Chem *248*, 6398-6407.

Whorwood, C.B., Donovan, S.J., Flanagan, D., Phillips, D.I., and Byrne, C.D. (2002). Increased glucocorticoid receptor expression in human skeletal muscle cells may contribute to the pathogenesis of the metabolic syndrome. Diabetes *51*, 1066-1075.

Wiedow, O., Schröder, J.M., Gregory, H., Young, J.A., and Christophers, E. (1990). Elafin: an elastase-specific inhibitor of human skin. Purification, characterization, and complete amino acid sequence. J Biol Chem *265*, 14791-14795.

Wilkinson, I.B., and Webb, D.J. (2001). Venous occlusion plethysmography in cardiovascular research: methodology and clinical applications. Br J Clin Pharmacol *52*, 631-646.

Williams, M., Zhou, A., Summers, C., Halsall, D., and Menon, D. (2009). Cortisol-binding globulin cleavage at sites of inflammation in critically ill patients. Critical Care *13*, P58.

Williams, S.E., Brown, T.I., Roghanian, A., and Sallenave, J.M. (2006). SLPI and elafin: one glove, many fingers. Clin Sci (Lond) *110*, 21-35.

Wochnik, G.M., Rüegg, J., Abel, G.A., Schmidt, U., Holsboer, F., and Rein, T. (2005). FK506-binding proteins 51 and 52 differentially regulate dynein interaction and nuclear translocation of the glucocorticoid receptor in mammalian cells. J Biol Chem *280*, 4609-4616.

Wolfe, R.R., and Chinkes, D.L. (2005). Isotope Tracers in Metabolic Research: Principles and Practice of Kinetic Analysis, 2nd Edition. (Hoboken, New Jersey: John Wiley & Sons Inc).

Yamamoto, S., and Ohsawa, N. (1976). Effects of dexamethasone on the levels of plasma corticosteroid binding globulin in rats and monkeys. Biochem Biophys Res Commun *72*, 489-498.

Yanovski, J.A., Yanovski, S.Z., Gold, P.W., and Chrousos, G.P. (1997). Differences in corticotropin-releasing hormone-stimulated adrenocorticotropin and cortisol before and after weight loss. J Clin Endocrinol Metab *82*, 1874-1878.

Young, E.A., Lopez, J.F., Murphy-Weinberg, V., Watson, S.J., and Akil, H. (1998). The role of mineralocorticoid receptors in hypothalamic-pituitary-adrenal axis regulation in humans. J Clin Endocrinol Metab *83*, 3339-3345.

Zani, M.L., Nobar, S.M., Lacour, S.A., Lemoine, S., Boudier, C., Bieth, J.G., and Moreau, T. (2004). Kinetics of the inhibition of neutrophil proteinases by recombinant elafin and pre-elafin (trappin-2) expressed in Pichia pastoris. Eur J Biochem *271*, 2370-2378.

Zeiher, B.G., Artigas, A., Vincent, J.L., Dmitrienko, A., Jackson, K., Thompson, B.T., and Bernard, G. (2004). Neutrophil elastase inhibition in acute lung injury: results of the STRIVE study. Crit Care Med *32*, 1695-1702.

Zhao, H., Friedman, R.D., and Fournier, R.E. (2007). The locus control region activates serpin gene expression through recruitment of liver-specific transcription factors and RNA polymerase II. Mol Cell Biol *27*, 5286-5295.

Zhao, X.F., Underhill, D.A., and Hammond, G.L. (1997). Hepatic nuclear proteins that bind cis-regulatory elements in the proximal promoter of the rat corticosteroid-binding globulin gene. Mol Cell Endocrinol *126*, 203-212.

Zhou, A., Wei, Z., Stanley, P.L., Read, R.J., Stein, P.E., and Carrell, R.W. (2008). The S-to-R transition of corticosteroid-binding globulin and the mechanism of hormone release. J Mol Biol *380*, 244-251.

Zouaghi, H., Savu, L., Coulon, A., Nunez, E.A., Guerot, C., Gryman, R., Amamou, R., and Miled, A. (1984). Corticosteroid-binding globulin in various diseases. Clin Chem *30*, 332-333.

Zouaghi, H., Savu, L., Guerot, C., Gryman, R., Coulon, A., and Nunez, E.A. (1985). Total and unbound cortisol-, progesterone-, oestrone- and transcortin-binding activities in sera from patients with myocardial infarction: evidence for differential responses of good and bad prognostic cases. Eur J Clin Invest *15*, 365-370.

Zouaghi, H., Savu, L., Kleinknecht, D., and Nunez, E. (1983). [Decrease in the binding activity of transcortin (CBG) in the serum of chronic hemodialysis patients]. Ann Biol Clin (Paris) *41*, 285-286.